UNIVERSIDAD COMPLUTENSE DE MADRID
FACULTAD DE CIENCIAS QUÍMICAS
Departamento de Ingeniería Química

TESIS DOCTORAL

Supercritical fluid extraction of emulsions to nanoencapsulate liquid lipophilic bioactive compounds: process development and scale up

Extracción supercrítica de emulsiones para nanoencapsular compuestos bioactivos líquidos lipofílicos : desarrollo y cambio de escala del proceso

MEMORIA PARA OPTAR AL GRADO DE DOCTOR

PRESENTADA POR

Cristina Prieto López

Directora

Lourdes Calvo Garrido

Madrid, 2018

UNIVERSIDAD COMPLUTENSE DE MADRID

FACULTAD DE CIENCIAS QUÍMICAS

Departamento de Ingeniería Química

TESIS DOCTORAL

Supercritical fluid extraction of emulsions to nanoencapsulate liquid lipophilic bioactive compounds. Process development and scale-up.

Extracción supercrítica de emulsiones para nanoencapsular compuestos bioactivos líquidos lipofílicos. Desarrollo y cambio de escala del proceso.

MEMORIA PARA OPTAR AL GRADO DE DOCTOR

PRESENTADA POR

Cristina Prieto López

Directora

Dra. Lourdes Calvo Garrido

Madrid, 2017

UNIVERSITY COMPLUTENSE OF MADRID

SCHOOL OF CHEMICAL SCIENCES

Chemical Engineering Department

DOCTORAL THESIS

Supercritical fluid extraction of emulsions to nanoencapsulate liquid lipophilic bioactive compounds. Process development and scale-up.

THESIS SUBMITTED FOR THE DEGREE OF DOCTOR OF PHILOSOPHY

PRESENTED BY

Cristina Prieto López

Supervisor

Dr. Lourdes Calvo Garrido

Madrid, 2017

UNIVERSIDAD COMPLUTENSE
MADRID

LOURDES CALVO GARRIDO, PROFESORA TITULAR DEL DEPARTAMENTO DE INGENIERÍA QUÍMICA DE LA FACULTAD DE CIENCIAS QUÍMICAS DE LA UNIVERSIDAD COMPLUTENSE DE MADRID

CERTIFICA:

Que el presente trabajo de investigación titulado “Supercritical fluid extraction of emulsions to nanoencapsulate liquid lipophilic bioactive compounds. Process development and scale-up”, ha sido realizado bajo su dirección en el Departamento de Ingeniería Química de la Universidad Complutense de Madrid, y constituye la memoria que presenta **Cristina Prieto López** para optar al grado de *Doctora en Ingeniería Química*, que a su juicio, reúne los requisitos de originalidad y rigor científico necesarios para ser presentada como Tesis Doctoral.

Y para que así conste, firma el presente certificado en Madrid a 28 de febrero de 2017.

Prof. Dra. Lourdes Calvo Garrido

Doctoral thesis as a compendium of publications aiming to obtain the European Doctor mention

This dissertation aims to obtain the European Doctorate mention. With this purpose, a research stay of three and a half months was conducted in the ITQB -Instituto de Tecnologia Quimica e Biológica António Xavier- and the IBET -Instituto de Biologia Experimental e Tecnológica- from Universidade Nova de Lisboa, under the supervision of Dr. Catarina M. M. Duarte.

Moreover, this thesis is presented as a compendium of five previously published scientific articles. The complete references of the articles that constitute the body of the thesis are the following:

I. C. Prieto, L. Calvo, Performance of the biocompatible surfactant Tween 80, for the formation of microemulsions suitable for new pharmaceutical processing, Journal of Applied Chemistry 2013 (2013) 930356, http://dx.doi.org/10.1155/2013/930356.

II. C. Prieto, L. Calvo, Supercritical fluid extraction of emulsions to nanoencapsulate vitamin E in polycaprolactone, Journal of Supercritical Fluids 119 (2017) 274-282, http://dx.doi.org/10.1016/j.supflu.2016.10.004. Selected as the Editor-in-Chief's Featured Article, January 2017.

III. C. Prieto, C.M.M. Duarte, L. Calvo, Performance comparison of different supercritical fluid extraction equipments for the production of vitamin E in polycaprolactone nanocapsules by supercritical fluid extraction of emulsions,

Journal of Supercritical Fluids 122 (2017) 70-78, http://dx.doi.org/10.1016/j.supflu.2016.11.015.

IV. C. Prieto, L. Calvo, C.M.M. Duarte, Continuous supercritical fluid extraction of emulsions to produce nanocapsules of vitamin E in polycaprolactone, Journal of Supercritical Fluids 124 (2017) 72-79, http://dx.doi.org/10.1016/j.supflu.2017.01.014.

V. C. Prieto, L. Calvo, The encapsulation of low viscosity omega-3 rich fish oil in polycaprolactone by supercritical fluid extraction of emulsions, submitted for publication.

Acknowledgements

First and foremost, I would like to express my gratitude to Prof. Lourdes Calvo for giving me the opportunity to develop my doctoral thesis in her research group, and for the guidelines transmitted as a professor and researcher. This period has been very enriching both on a professional and personal level.

Secondly, I would like to thank Dr. Catarina Duarte for her warm welcome and for allowing me to perform part of this research in her laboratory.

Additionally, I want to show my gratitude to Profs. Albertina Cabañas and Concha Pando for allowing me to use their SAS equipment, and to Prof. Miguel Ladero for his support on HPLC analysis. As well as, Centro Nacional de Microscopía Electrónica (CNME) and the other UCM Research Aid Centers for their support on particle analyses.

I would like to thank my “supercritical” lab-mates, my colleagues from the department and my colleagues from the lab in Lisbon, for making this period more amusing and rewarding.

I would especially like to thank my family, Pepe and my friends for their support, guidance and encouragement.

Finally, I gratefully acknowledge the financial support of this work by the Ministry of Economy and Competitiveness (project ref. CTQ2013-41781-P) as well as the granting of the UCM predoctoral (BE43/11) and mobility (EB64/15) fellowships of the Complutense University of Madrid.

Table of contents

List of figures

Figures in appendices

List of tables

List of abbreviations

$[AC]_R$	Residual acetone concentration
AC	Acetone
ALA	Alpha-linolenic acid
ASES	Aerosol solvent extraction system
BPR	Back pressure regulator
cGMP	Current Good Manufacturing Practices
CMC	Carboxymethylcellulose
CPF	Concentrated powder form
D	Diameter
DELOS	Depressurization of expanded liquid organic solutions
DHA	Docosahexaenoic acid
EA	Ethyl acetate
EE	Encapsulation efficiency
EPA	Eicosapentaenoic acid
FDA	U.S. Food and Drug Administration
GLY	Glycerol
HETP	Height equivalent to a theoretical stage
HPMC	Hydroxypropyl methylcellulose
HYAFF	Poly-hyaluronic acid
LC	Loading capacity
mp.	Melting point
O/O	Oil in oil emulsion
$[Organic\ solvent]_R$	Residual concentration of organic solvent
O/W	Oil in water
P	Pressure
P_c	Critical pressure
PCL	Polycaprolactone
PdI	Polydispersity index

PEG ..... Polyethylene glycol
PGSS ..... Particles from gas saturated solutions
PHB ..... Polyhydroxy butyric acid
PHBV ..... Poly(hydroxybutyrate-co-hydroxyvalerate)
PLA ..... Poly(lactic acid)
PLG ..... Poly(lactide-co-glycolide)
PLGA ..... Poly(lactic-co-glycolic acid)
PMA ..... Poly(methyl acrylate)
PMMA ..... Poly(methyl methacrylate)
PUFAs ..... Polyunsaturated fatty acids
PVA ..... Polyvinyl alcohol
PVP ..... Polyvinylpyrrolidone
Q ..... Flow rate
Ref. ..... Reference
RESAS ..... Rapid expansion of an aqueous solution
RESOLV ..... Rapid expansion of a supercritical solution into a liquid solvent
RESS ..... Rapid expansion of supercritical solutions
RESSS ..... Rapid expansion from supercritical to surfactant solution
SAILA ..... Supercritical assisted injection in liquid antisolvent
SAS ..... Supercritical antisolvent precipitation
SD ..... Standard deviation
SEDS ..... Solution enhanced dispersion by supercritical fluids
SEM ..... Scanning electron microscopy
SFEE ..... Supercritical fluid extraction of emulsions
SSI ..... Supercritical solvent impregnation
T ..... Temperature
T80 ..... Tween 80
T_c ..... Critical temperature
TEM ..... Transmission electron microscopy
Tg ..... Glass transition temperature

TH ..... Thickener

Vit A ..... Vitamin A

Vit E ..... Vitamin E

W/O/W ..... Water in oil in water emulsion

XG ..... Xanthan gum

ω-3 ..... ω-3 rich fish oil

Summary / Resumen

Summary

1. Introduction

A wide variety of products containing bioactive compounds have been designed to meet the fundamental needs of society in terms of beauty, health and well-being. Nevertheless, these products do not provide the expected health benefit, because of the low water solubility, low chemical or biochemical stability and the high reactivity of these bioactive compounds, reasons why they lose their biological functionality and bioavailability.

Among the different strategies developed to overcome this challenge, biopolymer-based micro- and nanoparticles are the most promising systems to maintain the biological functionality and bioavailability of the bioactive compound and to provide its controlled release in its physiological site of action.

A large number of processes exist for obtaining biopolymer-based micro- and nanoparticles. Nonetheless, companies seek rapid and environmentally-friendly production processes that obtain spherical nanoparticles with core-shell structure, controlled particle size distribution and high encapsulation efficiency, which guarantee the health effect. The increasing demand for new products and the drawbacks of the existing processes are causing a steady research for new technological possibilities.

Supercritical fluid extraction of emulsions (SFEE) is one of the latest technologies developed to fulfill this demand. It consists in the combination of the particle engineering of the emulsion-based encapsulation technologies with the unique properties of supercritical fluids to produce tailored micro- and nanoparticles. The majority of existing research that was conducted in this field involved the encapsulation of solid pharmaceutical compounds. However, this method may also represent a promising technique for encapsulating bioactive compounds for the food industry.

2. Objectives

The main objective of this thesis was to explore the potential of the SFEE technology to nanoencapsulate liquid lipophilic bioactive compounds with application in pharmaceutical or food products. Concretely, the nanoencapsulation of vitamin E and ω-3 rich fish oil in polycaprolactone was envisioned. These two model substances were selected due to their well-known health benefits, and their reduced bioavailability.

It was also an objective of this thesis to develop and scale-up the process. Thus, different configurations were tested and compared in terms of particle characteristics, CO_2 consumption and scalability. The continuous production of particles with reliable characteristics and with low residual organic solvent content was ultimately pursued.

3. A unifying discussion of the results of this thesis

First, a comprehensive analysis of key parameters affecting stability and droplet size of organic solvent-water emulsions formulated with a nonionic, non-toxic and biocompatible surfactant, Tween 80, was performed, which is of fundamental importance for the selection of the emulsion formulation to be subjected to supercritical extraction. Stable emulsions and microemulsions were obtained with high content of surfactant, which could limit its subsequent application and the economical feasibility of the process. However, it was reduced by increasing emulsion temperature. Since Tween 80 has a temperature dependent behavior, slight increments in temperature permitted increasing solubility of the surfactant in the oil phase favoring the expansion of the microemulsion area. Although this work was performed with n-hexane, same guidelines were taken into account when formulating the emulsions with acetone to nanoencapsulate the selected bioactive compounds.

Second, supercritical fluid extraction of emulsions (SFEE) was used to encapsulate vitamin E in polycaprolactone. In first place, an emulsion was developed following the previous guidelines. SFEE process was performed in a bubble column. Operating at 8.0 MPa and 313 K, with a CO_2 flow rate of 7.2 $kg \cdot h^{-1} \cdot kg\ emulsion^{-1}$, a low residual concentration of organic solvent (50 ppm), suitable for food applications, was obtained in 240 min at a CO_2 consumption of 101 kg $CO_2 \cdot kg\ acetone^{-1}$. The

obtained particles from this emulsion exhibited a high encapsulation efficiency of about 90%, and a loading capacity of 42%. They were in the nanometer range (153 nm) with a fairly narrow particle size distribution (polydispersity index of 0.26). However, by fine tuning of the starting emulsion formulation, encapsulation efficiency increased to 96 % and loading capacity to 69 % by increasing the amount of vitamin E. Moreover, particle size could be reduced to 8 nm by using a formulation with smaller colloid size (microemulsion). Regarding morphology, TEM images indicated that the particles were spherical, with a core-shell structure, and non-aggregated. Stability tests indicated that the capsules remained unchanged over long storage periods (6 and 12 months). In comparison to conventional solvent evaporation, although both techniques provided similar particle size, SFEE provided the highest encapsulation efficiency and the lowest residual acetone concentration.

Third, SFEE technology was used for the encapsulation of fish oil rich in ω-3 polyunsaturated fatty acids. Three different emulsion formulations containing stabilizing agents were tested using Tween 80 as a surfactant, polycaprolactone as coating polymer and acetone as organic solvent. Spherical and non-aggregated nanoparticles with sizes ranging from 6 to 73 nm were obtained depending on the starting formulation. The encapsulation efficiency of the particles was around 40%, similar to that generated by conventional solvent evaporation. Operating at 8.0 MPa and 313 K, less than 25 kg CO_2·kg acetone^{-1} were required to reduce the acetone concentration in the nanoparticle suspension to 5000 ppm (pharmaceutical requirements). However, to obtain nanoparticles for use in the food industry (maximum acetone concentration of 50 ppm), CO_2 consumption had to be increased to 127 kg CO_2·kg acetone^{-1}.

The only limitation of SFEE regarding the conventional techniques was its low production capacity. Therefore, in order to increase production capacity, different SFEE installations (a bubble column, a bubble column with gas redistributor, a spray column and a packed column) were compared in terms of organic solvent removal, CO_2 consumption, nanocapsule characteristics (encapsulation efficiency, particle size distribution and morphology) and scalability. Bubble columns provided particles with good characteristics but required a high CO_2 consumption and the production capacities were very low. The gas redistributor allowed decreasing the CO_2 expenditure, but the operation was still discontinuous. Despite the high CO_2 consumption in the spray column, the target acetone removal could not be achieved and particle morphology was negatively affected. The countercurrent operation in a packed column provided high production capacity, maintained good particle quality, and required a low amount of CO_2 to remove the acetone. However, residual organic solvent concentration could not achieve food levels. For this reason, the process was simulated with Aspen Plus in order to test the performance of a taller column. According to the simulations, it would be necessary to increase the packing height by 1.5 m or the CO_2 flow rate to 60 $g \cdot min^{-1}$ in order to get a residual acetone concentration suitable for food applications (50 ppm).

4. Conclusions and further work

SFEE is an efficient new method to nanoencapsulate liquid lipophilic bioactive compounds. To the best of our knowledge, there is no other conventional or emerging technique able of encapsulating such compounds into nanocapsules with core-shell

structure, high encapsulation efficiency, high storage stability in aqueous based systems, and low residual organic solvent concentration as SFEE.

Regarding the process, it was demonstrated that among the operating parameters, the initial emulsion formulation had the biggest impact on nanoparticle characteristics, whereas pressure, temperature and CO_2 flow rate had the most significant influence on the organic solvent removal. The economic feasibility of the process could be compromised due to the high CO_2 consumption and the limited production capacity of the bubble column.

Among the different configurations analyzed, the use of a packed column offered the possibility of a high production capacity with a small volume plant and a lower CO_2 consumption. In addition, the continuous operation in the packed column provided greater product homogeneity by eliminating differences between batches. However, the simulations with Aspen Plus showed that a taller column and higher CO_2 flow rates would be necessary to get a nanoparticle suspension with a residual organic solvent concentration suitable for food application.

In order to commercialize the capsules, it is recommended to continue the research performing *in vitro* stability and release tests under simulated gastric conditions, as well as verifying the bioavailability and beneficial health effects provided by the bioactive compounds by *in vivo* bioassays. In parallel, the design of a pharmaceutical or food product containing such capsules would be envisioned. A safety analysis would be required to get approval to commercialize the final product inside the European Union according to the current European regulation.

Additionally, it would be necessary to optimize the design of the column in terms of height and types of packing in order to reduce the CO_2 consumption. Increasing production capacity to industrial scale would imply, in addition to the scale-up of the packed column, the continuous formation of the emulsion and the implementation a CO_2 regeneration and re-use process.

To evaluate the feasibility of the commercial production, it would be essential to conduct a rigorous economic evaluation and a revision of the intellectual property regarding the SFEE technology.

The industrial development of the process could be addressed in collaboration with any of the engineering firms specialized in supercritical fluids, taking into account the constraints imposed by the food and pharmaceutical industries.

Resumen

1. Introducción

Para satisfacer las necesidades fundamentales de la sociedad en términos de belleza, salud y bienestar, se han desarrollado en los últimos años una gran variedad de productos conteniendo compuestos bioactivos. Sin embargo, estos productos no proporcionan el efecto saludable esperado, debido a la baja solubilidad en agua, la baja estabilidad química o bioquímica y a la elevada reactividad de estos compuestos, razones por las cuales pierden la funcionalidad biológica y la biodisponibilidad.

De las múltiples estrategias desarrolladas para superar este reto, las micro- y nanopartículas basadas en biopolímeros constituyen el sistema más prometedor para mantener la funcionalidad biológica y la biodisponibilidad del compuesto bioactivo, así como para proporcionar su liberación controlada en el lugar fisiológico de acción.

Existe un gran número de procesos para obtener micro- y nanopartículas basadas en biopolímeros. Sin embargo, las compañías buscan procesos de producción rápidos y respetuosos con el medioambiente que obtengan nanopartículas esféricas con estructura núcleo-carcasa, distribución de tamaño de partícula controlada y alta eficiencia de encapsulación, la cuales garanticen el efecto para la salud. La creciente demanda de nuevos productos y las limitaciones de los procesos existentes están causando un aumento en la búsqueda de nuevas posibilidades tecnológicas.

La extracción supercrítica de emulsiones (SFEE) es una de las últimas tecnologías desarrolladas para satisfacer esta demanda. Consiste en la combinación de la ingeniería de partícula de las tecnologías de encapsulación basadas en emulsiones con las propiedades singulares de los fluidos supercríticos para producir micro- y nanopartículas a medida. La mayoría de la investigación realizada hasta el momento en este campo estaba relacionada con la encapsulación de compuestos farmacéuticos sólidos. Sin embargo, este método podría ser una técnica prometedora para encapsular compuestos bioactivos para la industria alimentaria.

2. Objetivos

El principal objetivo de esta tesis fue explorar el potencial de la tecnología SFEE para nanoencapsular compuestos bioactivos lipofílicos líquidos con aplicación en productos alimentarios o farmacéuticos. Concretamente, se abordó la nanoencapsulación de vitamina E y de aceite de pescado rico en ω-3 en policaprolactona. Estas dos sustancias modelo fueron seleccionadas debido a sus conocidos beneficios para la salud y su biodisponibilidad reducida.

También fue un objetivo de esta tesis desarrollar y escalar el proceso. De este modo, se probaron y compararon diferentes instalaciones en términos de características de partículas producidas, consumo de CO_2 y facilidad de escalado. Finalmente, se abordó la producción en continuo de partículas con características reproducibles y con bajo contenido residual de disolvente orgánico.

3. Discusión integradora de los resultados de esta tesis

En primer lugar, se realizó un análisis completo de los parámetros clave que afectan a la estabilidad y al tamaño de gota de emulsiones disolvente orgánico-agua formuladas con un surfactante no-iónico, no-tóxico y biocompatible, Tween 80. Este estudio es fundamental para la selección de la formulación de la emulsión que va a ser sometida a extracción supercrítica. Se obtuvieron emulsiones y microemulsiones estables con elevado contenido de surfactante, el cual podría limitar su posterior aplicación y la viabilidad económica del proceso. Sin embargo, se pudo reducir aumentando la temperatura de la emulsión. Dado que el Tween 80 tiene un comportamiento dependiente de la temperatura, pequeños incrementos de la misma permitieron aumentar la solubilidad del surfactante en la fase orgánica favoreciendo la expansión del área de microemulsión. Aunque este trabajo se realizó con n-hexano, las mismas pautas fueron seguidas al formular las emulsiones con acetona para nanoencapsular los compuestos bioactivos seleccionados.

En segundo lugar, se empleó la extracción supercrítica de emulsiones SFEE para encapsular vitamina E en policaprolactona. Primero, se desarrolló una emulsión estable con estructura O/W siguiendo las pautas anteriores. El proceso SFEE se llevó a cabo en una columna de burbujas operando a 8,0 MPa y 313 K, con un caudal de

CO_2 de 7,2 $kg \cdot h^{-1} \cdot kg$ emulsión^{-1}. Bajo estas condiciones, se obtuvo una baja concentración residual de disolvente orgánico (50 ppm), adecuada para aplicaciones alimentarias, la cual fue obtenida tras 240 min de proceso y con un consumo de CO_2 de 101 kg $CO_2 \cdot kg$ acetona^{-1}. Las partículas obtenidas a partir de esta emulsión mostraron una elevada eficiencia de encapsulación de aproximadamente 90%, y una capacidad de carga del 42%. El tamaño de las partículas producidas estaba en el rango nanométrico (153 nm) con una distribución de tamaño de partícula estrecha (índice de polidispersión de 0,26). Sin embargo, mediante un fino ajuste de la formulación de partida de la emulsión, la eficiencia de encapsulación aumentó hasta el 96% y la capacidad de carga hasta el 69%. Además, el tamaño de partícula se pudo reducir a 8 nm utilizando una formulación con menor tamaño de coloide (microemulsión). Con respecto a la morfología, las imágenes TEM indicaron que las partículas eran esféricas, con estructura núcleo-carcasa, y no agregadas. Los ensayos de estabilidad indicaron que las cápsulas no sufrían cambios incluso bajo largos periodos de almacenamiento (6 y 12 meses). En comparación con las técnicas convencionales de evaporación de disolvente, aunque ambos procesos generaron tamaños de partícula similares, la tecnología SFEE proporcionó la mayor eficiencia de encapsulación y la menor concentración residual de acetona.

En tercer lugar, la tecnología SFEE fue usada para la encapsulación de aceite de pescado rico en ácidos grasos ω-3 poliinsaturados. Se experimentaron tres formulaciones distintas para la emulsión de partida, conteniendo agentes estabilizadores, usando Tween 80 como surfactante, policaprolactona como material recubriente y acetona como disolvente orgánico. Se obtuvieron nanopartículas esféricas no agregadas con tamaños entre 6 y 73 nm dependiendo de la formulación

de partida. La eficiencia de encapsulación de las partículas fue aproximadamente del 40%, similar a la generada mediante el proceso convencional de evaporación de disolvente. Operando a 8,0 MPa y 313 K, menos de 25 kg CO_2·kg acetona^{-1} fueron necesarios para reducir la concentración de acetona en la suspensión de nanopartículas a 5000 ppm (de acuerdo con los requerimientos farmacéuticos). Sin embargo, para obtener nanopartículas de uso en la industria alimentaria (máxima concentración de acetona de 50 ppm), el consumo de CO_2 tuvo que ser aumentado a 127 kg CO_2·kg acetona^{-1}.

La única limitación de SFEE con respecto a las técnicas convencionales fue su baja capacidad de producción. Por lo tanto, con el objetivo de aumentar la capacidad de producción, diferentes instalaciones de SFEE (una columna de burbujas, una columna de burbujas con redistribuidor de gas, una columna de espray, y una columna de relleno) fueron comparadas en términos de eliminación de disolvente orgánico, consumo de CO_2, características de las nanocápsulas obtenidas (eficiencia de encapsulación, distribución de tamaño de partícula y morfología) y escalabilidad. Las columnas de burbujas proporcionaron partículas con buenas características pero requirieron un elevado consumo de CO_2 y la capacidad de producción fue muy baja. El distribuidor de gas permitió disminuir el gasto de CO_2, pero la operación fue todavía discontinua. A pesar del elevado consumo de CO_2 en la columna de espray, un contenido residual de acetona de 50 ppm no pudo ser alcanzado, y la morfología de las partículas fue negativamente afectada. La operación en contracorriente en la columna de relleno proporcionó una elevada capacidad de producción, mantuvo una buena calidad de las partículas, y requirió un bajo consumo de CO_2 para eliminar la acetona. Sin embargo, la concentración residual de disolvente orgánico no alcanzó los

niveles permitidos en la industria alimentaria. Por esta razón, se simuló el proceso en Aspen Plus para comprobar el rendimiento de extracción de una columna de mayor altura. De acuerdo con las simulaciones, sería necesario aumentar la altura de relleno en 1,5 m o aumentar el caudal de CO_2 a 60 $g \cdot min^{-1}$ para conseguir una concentración residual de acetona adecuada para aplicaciones alimentarias (50 ppm).

4. Conclusiones y trabajo futuro

El proceso SFEE es un método nuevo y eficiente para nanoencapsular compuestos bioactivos líquidos lipofílicos. En base a nuestros conocimientos, no hay otra tecnología convencional o emergente capaz de encapsular este tipo de compuestos en nanocápsulas con estructuras núcleo-carcasa, elevada eficiencia de encapsulación, alta estabilidad de almacenamiento en sistemas acuosos, y bajo contenido residual de disolvente orgánico como SFEE.

En lo que atañe al proceso, se demostró que entre los parámetros de operación, la formulación inicial de la emulsión causaba el mayor impacto en las características de las nanopartículas, mientras que la presión, la temperatura y el caudal de CO_2 tenían mayor influencia en la eliminación del disolvente orgánico. Sin embargo, la viabilidad económica del proceso podría verse comprometida debido al elevado consumo de CO_2 y la limitada capacidad de producción de la columna de burbujas.

De entre las diferentes configuraciones analizadas, el uso de la columna de relleno ofreció la posibilidad de una elevada capacidad de producción con una planta de pequeño volumen y un menor consumo de CO_2. Además, la operación en continuo en la columna de relleno proporcionó mayor homogeneidad en el producto al eliminar

las diferencias entre lotes. Sin embargo, las simulaciones con Aspen Plus mostraron que una columna más alta y mayor caudal de CO_2 serían necesarios para obtener una suspensión de nanopartículas con un contenido residual de disolvente orgánico adecuado para aplicaciones alimentarias.

Para comercializar las cápsulas, se recomienda continuar la investigación realizando ensayos *in vitro* de estabilidad y liberación bajo condiciones gástricas simuladas, así como verificando la biodisponibilidad y el efecto saludable proporcionado por el compuesto bioactivo mediante bioensayos *in vivo*. En paralelo, se realizaría el diseño de un producto alimentario o farmacéutico conteniendo dichas capsulas. Para comercializar el producto dentro de la Unión Europea, se requeriría una evaluación de seguridad de acuerdo con las regulaciones europeas actuales.

Además, sería necesario optimizar el diseño de la columna en términos de altura y tipos de relleno con el objetivo de reducir el consumo de CO_2. Aumentar la capacidad de producción a escala industrial implicaría, además del escalado de la columna de relleno, la producción continua de la emulsión y la implementación de un proceso de regeneración y reutilización del CO_2.

Para evaluar la viabilidad de la producción comercial, sería esencial realizar una evaluación económica rigurosa y una revisión de la propiedad intelectual con respecto a la tecnología SFEE.

El desarrollo industrial del proceso podría ser abordado en colaboración con cualquiera de las ingenierías especializadas en fluidos supercríticos, teniendo en cuenta las restricciones impuestas por la industria alimentaria y farmacéutica.

1. Introduction

1. Introduction

Our current health situation is due to the evolution in medicine, as well as in other branches of science susceptible to collaborate with it (chemistry, biology, computer science, engineering, among others), which facilitates the rapid diagnosis and treatment of the disease. But, also thanks to the quality of nutrition and the hygienic measures that help prevent diseases and promote health.

Appearance, health and well-being are conceived as fundamental needs in today's society. In this sense, consumers in the industrialized world are demanding products to address specific health benefits and to improve their appearance [1]. Functional foods, nutraceuticals or nutricosmetics are some of the new products designed to satisfy this demand.

Although the idea of functional food or nutraceuticals seems a modern concept, the importance of dietetics in disease prevention was already known and thus is reflected in the *Corpus Hippocraticum* attributed to Hippocrates of Kos (400 BC) and in the *Treatise on Food* of Avenzoar (12th century) [2].

Historically, plants and animals were the source of all medicinal preparations [3]. The beneficial properties attributed to them were due to certain bioactive compounds, whose main health benefits are shown in Table 1.1 [4].

Table 1.1. Compendium of the main bioactive compounds of animal or plant origin and their potential health benefits.

Bioactive	Examples	Potential health benefits
Vitamins	Lipophilic: A, D, E, K Hydrophilic: B, C	Influence on metabolism Influence on immunity Modulation of oxidative stress
Mineral salts	Ca, Fe, Se, Mg, Zn, K, Mn, Cu	Bone formation Regulation of the heart rhythm Production of hormones
Phytochemicals	Carotenoids (β-carotene, lycopene) Flavonoids (quercetin, catequin) Proanthocyanidins Polyphenols Allicin	Reduction of the risk of: *cardiovascular disease* *cancer* *diabetes* *degenerative diseases*
Polyunsaturated fatty acids (PUFAs)	Alpha-linolenic acid (ALA) Docosahexaenoic acid (DHA) Eicosapentaenoic acid (EPA)	Promotion cardiovascular health
Bioactive peptides	Milk derived peptides	Reduction of blood pressure
Prebiotics	Inulin Oligosaccharides Dietary fiber	Promotion of gut health Modulation of gut microflora
Probiotics	*Lactobacilli* *Bifidobacterium*	Improvement of gut health Immune modulation
Herbs and spices	Essential oils Various herbal preparations	Antimicrobials

Over the last decade, there has been significant research in the areas of bioactive discovery, and in the development of new materials, ingredients, processes and products to meet the fundamental needs of society in terms of beauty, health and well-being [5]. A wide variety of them are already available in the market, including pharmaceuticals, health-care products, cosmetics, and foods [6]. Nevertheless, they do not provide the expected health benefit, mainly because of the low amount of bioactive compound that is absorbed and becomes available at the physiological site of action, i.e. its low bioavailability [7].

This lack of beneficial activity may be due to the fact that these compounds present low water solubility, low chemical or biochemical stability (as a result of their sensitivity to physical or chemical factors such as enzymes, pH, temperature, moisture, light or oxygen), or because they are highly reactive [8, 9]. All these reasons make them lose their biological functionality and bioavailability [10].

Many of these compounds cannot be solubilized in our body fluid systems or lose their biological functionality as they pass through the digestive tract. Nonetheless, the oral mode remains as the preferred administration route due to the improved patient compliance, especially for chronic therapy [11]. Figure 1.1 shows the physiological and physicochemical processes that occur during digestion.

Different strategies were developed to overcome this challenge. For the purpose of solubility enhancement, several approaches may be considered such as size reduction, modification of crystallinity, molecular chemical alteration or solubilization in surfactant micelles, which may increase solubility and thus bioavailability [12]. However, special delivery systems will be required if the

bioactive compound is highly sensitive to chemical and physicochemical factors or highly reactive, in order to protect and stabilize it [4]. Biopolymer-based micro- and nanoparticles, liposomes, solid-lipid nanoparticles, inclusion complexes, foams or films are some of the delivery systems developed so far to fulfill this function [13].

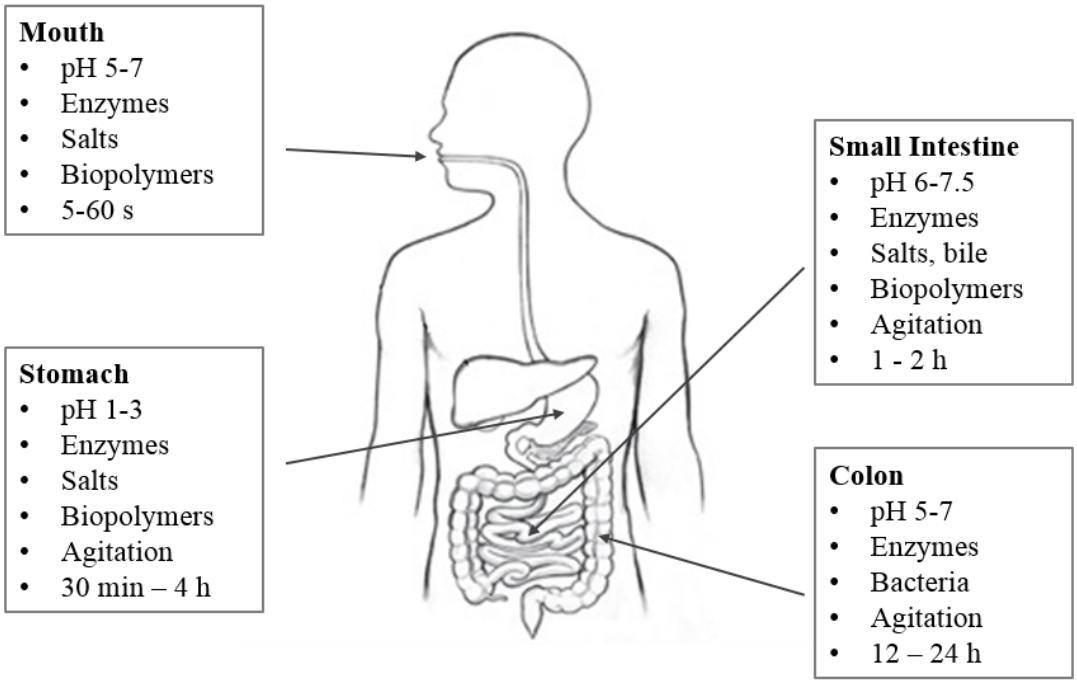

Figure 1.1. Schematic diagram of the physicochemical and physiological processes that may occur through the human gastrointestinal tract [14].

Of the available delivery systems, biopolymer-based micro- and nanoparticles are the most promising systems to maintain the biological functionality and bioavailability of the bioactive compound and provide its controlled release in its physiological site of action [15]. This is why this study focuses on them.

1.1 Biopolymer-based micro- and nanoparticles

Biopolymer-based micro- and nanoparticles are obtained by an encapsulation process, through which the bioactive compound, solid, liquid or gas, is enclosed in an inert shell, which isolates and protects it form the external environment [16]. The bioactive compound to be encapsulated is known as core material and the inert shell has also been referred to as the capsule, coating or wall material [17]. Figure 1.2 shows a scheme of a biopolymer-based particle.

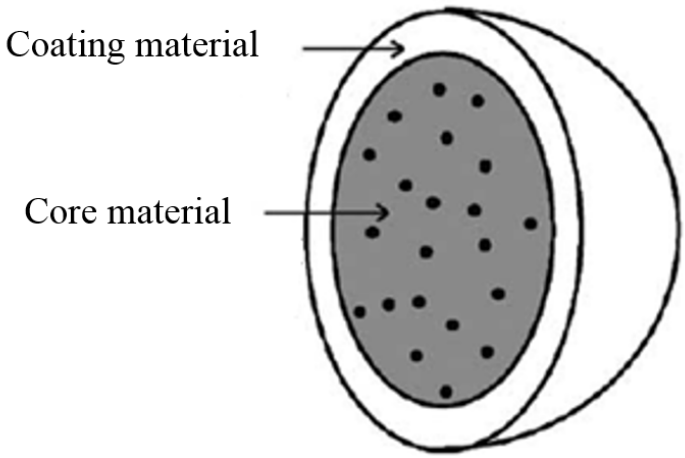

Figure 1.2. Scheme of a biopolymer-based particle.

The encapsulation of a bioactive compound may serve, in addition to protect and stabilize the core and provide its controlled release, to mask undesirable organoleptic properties (color, odor, flavor), avoid adverse effects (gastric irritation), increase shelf-life or provide easier handling (through the conversion of liquid bioactive ingredients into solid forms more easily manipulable and storable) [6, 16, 18]. On the other hand, it has to be compatible with the other components in the system, without altering the qualitative attributes of the final product.

The bioavailability of the bioactive compound and the efficacy of the biopolymer-based particle are often constrained by the type of coating selected, the composition, the encapsulation process and the characteristics of the particles obtained [19]. Therefore, many factors must be taken into account in the design process of biopolymer-based particles. Table 1.2 summarizes this design process.

Table 1.2. A generic approach to the design process of a biopolymer-based particle [4].

I. The core:

Identify the compound and its biological functionality.

Characterize its physical and chemical properties and its stability.

II. The coating material:

Choose the coating.

Characterize its physical and chemical properties and its stability.

III. Formulation:

Design its composition and structure.

Interactions with other components, stability and triggers for release must be taken into account.

IV. Encapsulation process:

Choose the process, its processing parameters and check results.

Costs must be also considered.

V. Product:

Characterize the particle:

- Composition
- Loading capacity
- Encapsulation efficiency
- Morphology
- Size and particle size distribution
- Physical and chemical properties
- Stability and release *in vitro* and *in vivo*

The following lines analyze the available types of coatings, the different types of particles that can be obtained, and the encapsulation processes developed so far, as well as their influence on the efficiency of the delivery system.

1.2 Coating materials

The coating material is one of the key aspects in the design process of a biopolymer-based particle, since the protection and release of the bioactive compound, the type of particle obtained, as well as the characteristics of the resulting particles depend essentially on that.

A suitable coating material needs to fulfil several requirements. First, it needs to be biocompatible or biodegradable. Second, it must be non-toxic and non-immunogenic, and neither its degradation products. Third, it should have the suitable properties (chemical structure, molecular weight, hydrophobicity, viscosity, crystallinity, glass transition temperature, surface charge, biodegradation profile, stability and inertness) to provide protection to the bioactive ingredient, and allow the controlled release of the compound in the physiological site of action, maintaining its concentration within the therapeutic limits [20, 21]. The release of the bioactive can be triggered by a pH change, mechanical stress, temperature, enzymatic activity, time or osmotic force; which provoke the erosion, fragmentation or swelling of the coating wall allowing the diffusion of the bioactive compound [22].

Coating substances can be selected from a wide variety of natural or synthetic polymers. Table 1.3 gives a list of the most widely used. The choice of the wall material depends on a number of factors including nature of the core material, administration route (oral, parenteral, pulmonary, dermic, ocular…), physiological site of action of the bioactive compound, encapsulation process, regulatory issues and economics, among others.

Table 1.3. Coating materials commonly used in encapsulation processes [23, 24, 25].

Type	Coating material	Properties
Natural	Maltodextrins and corn syrup	Low viscosity, hygroscopic, high cost
	Cyclodextrins	Low viscosity, high cost
	Starch	Low solubility in cold water, viscous, low cost, Tg of about 60 - 70ºC
	Sucrose	High solubility in water, non-hygroscopic, low cost
	Sodium alginate	Biodegradable, soluble in water, low cost
	Carragenan	Biodegradable, soluble in hot water, low cost
	Chitosan	Biodegradable and biocompatible, soluble in water at low pH, low cost
	Arabic gum	Biodegradable, high solubility in water, low viscosity, high cost
	Cellulose	Insoluble in water, low cost
	Waxes (beeswax, carnauba wax, paraffin wax)	Insoluble in water, low cost, mp. of about 60 - 70ºC
	Stearic acid	Low solubility in cold water, mp. of about 70ºC
	Monoglycerides, phospholipids and glycolipids	Miscible with water, amphiphilic properties, mp. of about 70ºC
	Fats and oils (milkfat, soybean oil, cocoa butter)	Insoluble in water, low cost, mp. of about 70ºC
	Proteins (albumin, casein, gelatin, zein, peptides)	Biodegradable and biocompatible, low solubility in cold water, high viscosity
Semisynthetic	Methylcellulose, ethylcellulose, carboxymethylcellulose (CMC), hydroxypropyl methylcellulose (HPMC)	Biodegradable and biocompatible, approved by FDA for pharmaceutical application, soluble in water, viscous, low cost, mp. of about 135ºC
Synthetic	Poly(lactic acid) (PLA) Poly(lactic-co-glycolic acid) (PLGA) Poly(lactide-co-glycolide) (PLG)	Biodegradable and biocompatible, insoluble in water, mp. of about 150 - 180ºC, Tg of about 40 - 65ºC
	Polycaprolactone (PCL)	Fully biodegradable, approved by FDA, insoluble in water, low viscosity, mp. of about 58 - 60ºC, Tg of about -60ºC
	Polyhydroxy butyric acid (PHB) and derivatives	Slower degradation rate than polylactic polymers, insoluble in water, mp. of about 150 - 180ºC, Tg of about -5 - 20ºC
	Polyethylene glycol (PEG)	Biocompatible, water soluble, mp. of about 61 - 66ºC, Tg of about 50ºC
	Poly-hyaluronic acid (HYAFF)	Biodegradable and biocompatible, soluble in water
	Poly(methyl methacrylate) (PMMA)	Non-degradable but biocompatible, approved by FDA, water soluble depending on pH, low cost, mp. of about 160ºC, Tg of about 105ºC

The polymers commonly used in controlled release are biodegradable polyesters, especially PCL, PLA, PLGA or PMMA (also known by its commercial name Eudragit), because of their high purity, greater control over the release of the bioactive compound and the better reproducibility than natural polymers [26].

1.3 Types of particles

Particle size and morphology are important aspects, since they can condition the amount of polymer required, the protection efficacy, the release rate, as well as the appearance (particle size over 100 nm provoke turbid suspensions [27]), rheology and mouthfeel of the final product (particle size of 20 μm are detectable by the tongue [28]). Figure 1.3 shows the classification in terms of size, shape and structure. They are called macroparticles if their size is bigger than 1000 μm, microparticles if their size is between 3 and 800 μm, and nanoparticles if their size is less than one micron. Spheres, spheroids, needles, fibers, films or irregular particles are the different possible shapes. Regarding structure, particles can be homogeneous, when the coating is intimately mixed with the bioactive compound; matrix, when the bioactive compound is dispersed as small particles within the coating material; or capsules, when the bioactive compound is confined within a cavity (core-shell or mononuclear) or multiple cavities (polynuclear) surrounded by a thin film of the coating material. If the particle possesses several coatings, it is called multishell [17, 18].

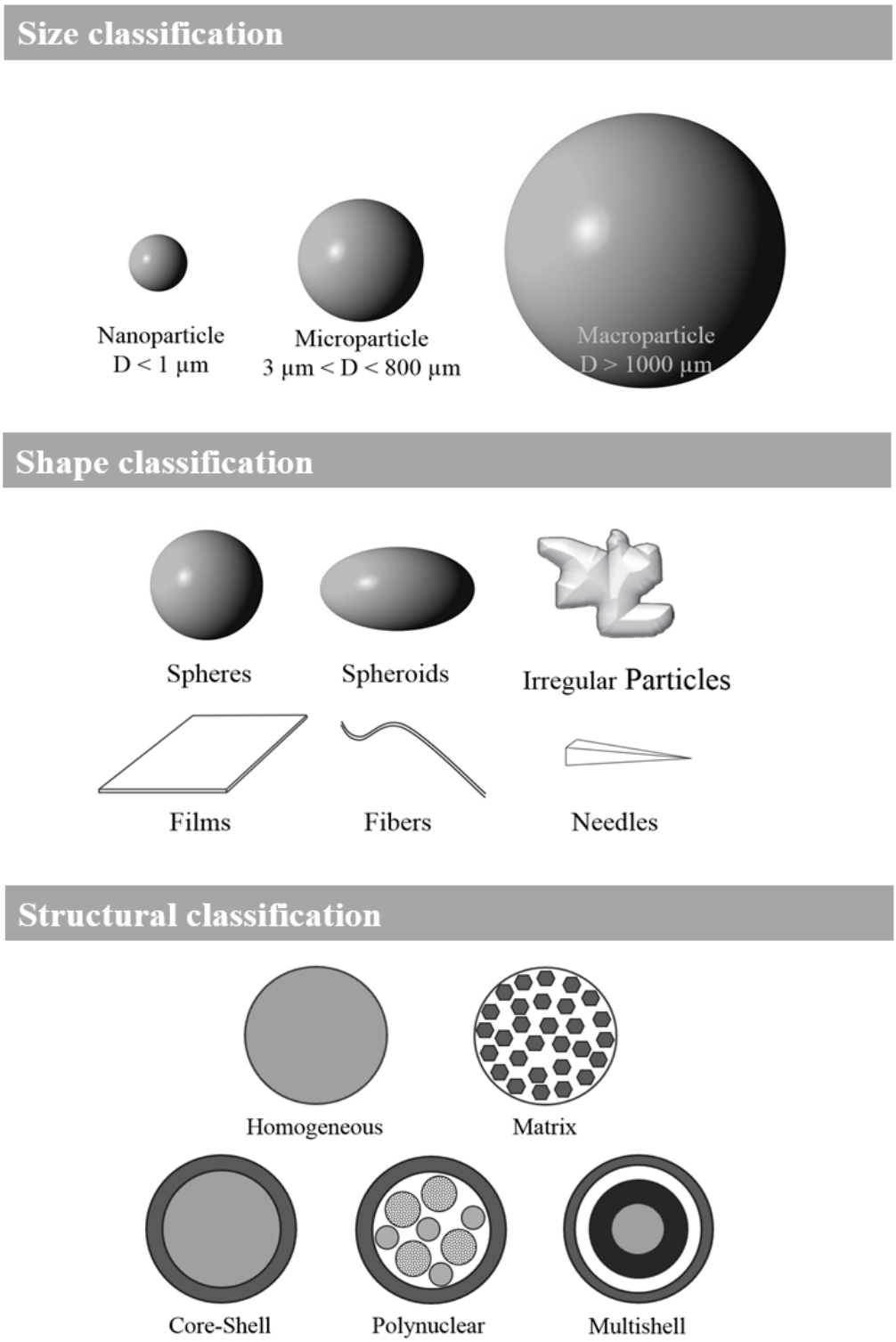

Figure 1.3. Particle classification.

Each type of particle has its own specific advantages and disadvantages for protection and delivery of functional ingredients; however, the most valued type is the spherical nanocapsule. The size in the nanoscale allows relatively higher intracellular uptake, greater stability and better controlled release rate; and together with the spherical shape have a lower effect on the rheology and organoleptic properties of the product. On the other hand, the core-shell structure requires lower polymer content, while providing greater protection [7, 26]. Nevertheless, the selection of a particle type depends on the physicochemical properties of the active ingredient and the coating material, the physiological site of action, the regulatory status, and the cost of the production process [6, 17, 18].

1.4 Encapsulation processes

A large number of processes exist for obtaining biopolymer-based micro- and nanoparticles. The selection of a particular technique depends on the physicochemical properties of the core, the coating used, the type of particle desired, as well as the production scale and costs. Table 1.4 summarizes the advantages and limitations of the main conventional techniques. Fundamentals of each technique can be found in Appendix A.

From the encapsulation technologies available, interfacial polymerization and coacervation have not received much attention from the pharmaceutical and food industries, despite the good characteristics of the particles obtained, mainly due to the presence of toxic chemical agents. However, both techniques have been well received in other sectors such as the agrochemical, for the encapsulation of pesticides or fertilizers [18].

Regarding the emulsion-based technologies, i.e. solvent evaporation, solvent diffusion, nanoprecipitation and salting out, they allow obtaining particles in the nanoscale with narrow size distribution, core-shell structure, and high retention of the bioactive compound [21]. The main drawbacks of these technologies are the use of organic solvents and the requirement of a purification step. On the other hand, these techniques are discontinuous operations that cause differences between batches affecting production quality and are difficult to scale-up.

Spray drying, spray cooling, freeze drying, coextrusion, ionic gelation and fluid bed coating are the most used techniques in the food industry. Most of them are economic processes that are already developed to commercial scale [18]. However, their use for the production of controlled release particles is limited by the use of high temperatures, the difficulty of controlling particle size, and the high porosity of the particle, that promotes burst release. With respect to electrospinning, it is an emerging technology used in the food industry for the manufacture of new packaging materials, which may also be used to obtain spherical particles with application in controlled release; however, the electrical charge and the mechanical stress may affect the functionality of the bioactive compound [29].

Table 1.4. Advantages and limitations of some encapsulation methods and characteristics of the particles produced (adapted from Zuidam *et al*. [30]).

Technology	Advantages	Limitations	Particle shape	Particle structure	Particle size (µm)	Examples
		Chemical methods				
Interfacial polymerization [18, 21]	Narrow size distribution High retention	Non-biodegradable polymer Difficult control of the capsules formation Necessity of purification (organic solvents, monomers, initiators)	Spheres	Capsule	0.2-30	Vitamin C in polyamide [31] Vitamin E in polyurethane [32]
		Physicochemical methods				
Coacervation [18, 33]	High retention Low processing temperature Efficient method	Use of toxic chemical agents Necessity of purification Requirement of a drying process to generate powder High processing costs Complex method	Spheres	Capsule	0.1-800	Capsaicin in gelatin-acacia gum [34] Fish oil in chitosan [35]
Solvent evaporation [21, 36]	Narrow size distribution High retention	Use of organic solvents High energy requirement in homogenization Requirement of a drying process to generate powder	Spheres	Matrix	0.1	Quercetin in PLA [37] Curcumin in PLGA [38]

Table 1.4. (Continued)

Technology	Advantages	Limitations	Particle shape	Particle structure	Particle size (μm)	Examples
Solvent diffusion [21, 26, 39]	Narrow size distribution High retention	Use of organic solvents High volumes of water to be eliminated from the suspension Requirement of an additional drying process to generate powder	Spheres	Capsule or matrix	< 0.5	Fish oil in PCL [40] Capsicum oleoresin in PCL [41]
Nanoprecipitation [21, 26, 42]	Narrow size distribution High retention	Use of organic solvents Requirement of an additional drying process to generate powder	Spheres	Capsule or matrix	< 0.3	β-carotene in PLGA or PLA [43] Caprylic/capric triglycerides in PCL [44]
Salting out [21, 39]	High retention	Extensive washing steps	Spheres	Capsule or matrix	< 1	Ovoalbumin in Eudragit S100 [45]
Ionic gelation [18, 30, 46]	Extreme conditions (temperature and pH) are avoided No use of organic solvents	High porosity promotes burst release Mainly used on a laboratory scale	Spheres	Matrix or capsule	200-5000	Catechin in chitosan [47] Lactic acid bacteria in alginate [48]
		Physicomechanical methods				
Spray drying [9, 18]	High retention Economical process Large-scale production in continuous mode	Degradation of highly temperature-sensitive compounds High porosity promotes burst release Difficult control of the particle size	Spheres or fibers	Matrix	10-400	Fish oil in Hi-Cap 100 [49] d-Limonene in maltodextrin [50]

Table 1.4. (Continued)

Technology	Advantages	Limitations	Particle shape	Particle structure	Particle size (μm)	Examples
Spray cooling/chilling [18, 51]	Low processing temperature Economical Continuous process	Presence of the bioactive on the particle surface Difficult control of the particle size Special handling and storage conditions	Spheres or fibers	Matrix	20-200	Isoflavone in medium chain triglyceride [52] Fe:iodine:Vit A in hydrogenated palm oil [53]
Freeze drying [54, 36]	High retention of volatiles Low processing temperature	High porosity which promotes burst release Long processing time High processing costs Special handling and storage conditions	Irregular	Matrix	20-5000	Capsicum oleoresin oil in PCL in gelatin [55] *Lactobacilli* in disaccharides [56]
Fluid bed coating [16, 18, 46]	Secondary coating Economical process	Degradation of highly temperature-sensitive compounds Requirement of solid particles to start with Batch process	Spheres or irregular	Capsule	5-5000	Ascorbic acid in PMA [57]
Coextrusion [58]	High retention Continuous process	Difficulty to obtain capsules in extremely viscous carrier material melts	Spheres	Capsule	150-8000	Citrus oils in corn syrup [17]
Electrospinning [29, 59, 60]	Low processing temperature Continuous process	Use of organic solvents Electric charge or the mechanical stress may affect functionality	Fibers or spheres	Various	0.04-2	*Bifidobacterium* in pullulan [61]

Nowadays, companies are more and more urged to develop rapid and simple production processes to obtain particles with controlled size and high encapsulation efficiency, with very low environmental impact (reducing the use of volatile organic compounds [62]), as well as easily scalable. The increasing demand for new products and the drawbacks of the existing processes are causing a steady research for new technological possibilities. Since the early 1980s, technologies based on supercritical fluids have created great expectations due to their environmental friendliness and their peculiar properties [63].

1.4.1 Encapsulation processes based on supercritical fluids

Supercritical fluids are defined as substances for which both pressure and temperature are above the critical values. The phase diagram of a pure substance illustrating the supercritical region is depicted in Figure 1.4. In this region, the liquid and gaseous phases are indistinguishable and the thermophysical properties exhibit very high rates of change in response to small temperature and/or pressure modifications. The special combination of gas-like viscosity and liquid-like density makes the supercritical fluid an excellent solvent for various applications, such as extraction, chromatography or particle generation [64]. Among this new generation of green solvents, carbon dioxide is the most widely used for pharmaceutical and food technology applications. It is non-toxic, non-flammable, readily available and cost-effective. It has a relatively low critical point (T_c=304 K and P_c=7.4 MPa) and gaseous state under ambient conditions. Due to its low viscosity and high diffusivity, it reveals a very fast mass transfer with respect to liquid solvents. Further, the solvating power can be controlled by adjusting both pressure and temperature. It has the ability to provide a non-degrading and non-

oxidizing environment for sensitive compounds [65]. Its high evaporation rate allows being quickly extracted from the product without leaving any residue. An additional benefit is that they provide a sterile environment suitable for current good manufacturing practices (cGMP) [66]. Additionally, it can be easily recovered and recycled after use.

These properties allow innovative processing applications that can overcome some technical problems and limitations characterizing conventional encapsulation processes. In this sense, supercritical fluids have been used to extract the residual solvent [67] from particles prepared by conventional techniques such as spray-drying [68], solvent-evaporation [69] or solvent-diffusion [70], among others.

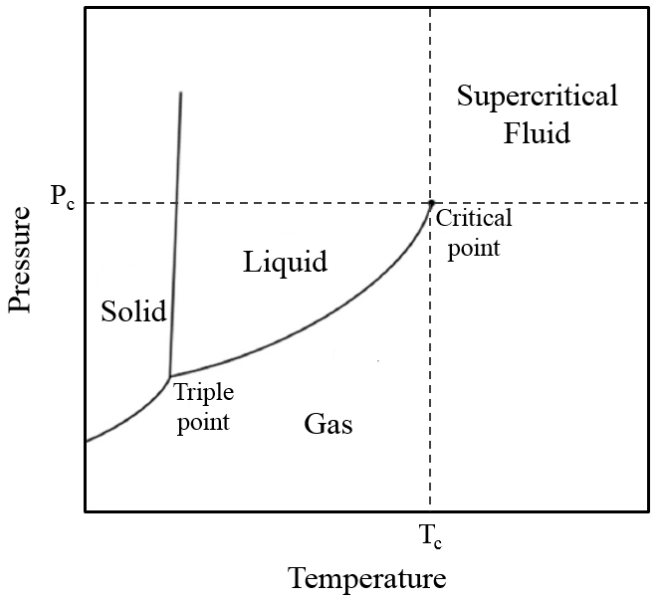

Figure 1.4. Pressure-temperature phase diagram of a pure component indicating the supercritical region.

Several encapsulation processes based on supercritical fluids were also developed. These processes have been an adaptation of the many precipitation processes available with supercritical fluids [71, 72]. Rapid Expansion of

Supercritical Solutions (RESS), Rapid Expansion of a Supercritical Solution into a Liquid Solvent (RESOLV), Rapid Expansion of an Aqueous Solution (RESAS), Supercritical Antisolvent Precipitation (SAS), Aerosol Solvent Extraction System (ASES), Solution Enhanced Dispersion by Supercritical Fluids (SEDS), Particles from Gas Saturated Solutions (PGSS), Depressurization of Expanded Liquid Organic Solutions (DELOS), Concentrated Powder Form (CPF), and Supercritical Solvent Impregnation (SSI) have been used so far for encapsulation purposes [15, 25, 73, 74]. Fundamentals of the main processes are explained in Appendix B. Table 1.5 summarizes the main advantages and limitations of these processes.

The RESS process is a simple and attractive technique, as it does not require the use of organic solvents. However, its application in encapsulation is limited due to the low solubility of the coating and core materials in supercritical CO_2 [25]. In addition, although particles with controlled size can be obtained, it is difficult to control the morphology and particle agglomeration is frequent [72].

In the SAS process, the solubility of the coating and core materials in CO_2 are not necessary since CO_2 acts as an antisolvent and not as a solvent [72]. However, the use of the organic solvent may affect the quality of the final product; consequently, a subsequent washing or purification step is normally required. Micro- and nanoparticles can be obtained with controlled size; however, the morphology depends on the operating conditions [25]. Both techniques have a high consumption of CO_2, which should be purified and recycled to make the process economically feasible at large scale. This purification process can be difficult depending on the compound. In addition, the use of nozzles or capillaries to atomize the solution makes it difficult to scale-up these processes [73].

Table 1.5. Comparison of different supercritical processes for encapsulation purposes [15, 25, 73, 74].

Technology	Advantages	Limitations	Particle shape	Particle structure	Particle size (μm)	Examples
RESS	Narrow particle size distribution Particle size easily controlled No need of organic solvent Simple process	Control of morphology Control of loading Particle agglomeration Bioactive solubility in CO_2 Polymer solubility in CO_2 Use of high pressure and sometimes temperature High CO_2 consumption Difficult CO_2 purification and recycle Difficult to scale-up	Spheres, needles or fibers	Capsules or matrix	0.1-10	Flavones in Eudragit-100 or PEG 6000 [73]
SAS	Nano- and microparticles can be obtained Particle size easily controlled Moderate pressure and temperature Bioactive solubility in CO_2 not required Polymer solubility in CO_2 not required	Use of organic solvents Requirement of a purification process/washing period Difficult organic solvent - CO_2 separation Difficult CO_2 purification and recycle High CO_2 consumption Difficult to scale-up	Spheres, needles or fibers	Capsules or matrix	0.25-10	β-carotene and lutein in PEG [75] Quercetin in poloxamers [76]

Table 1.5. (Continued)

Technology	Advantages	Limitations	Particle shape	Particle structure	Particle size (μm)	Examples
PGSS	Applicable to liquid bioactive compounds Narrow size distribution No need of organic solvent Bioactive solubility in CO_2 not required Polymer solubility in CO_2 not required Use of moderate pressure Low CO_2 consumption Versatile process Continuous process Easy to scale-up	Difficulty in producing submicron particles Solid has to be melted	Various	Matrix	2-400	β-carotene in PCL [77] Lavandin oil in PCL [78]
CPF	High loading Applicable to liquid bioactive compounds Continuous process Easy to scale-up	Use of moderate to high pressures	Various	Matrix	5-2000	Riboflavine in maltodextrin [79]
Impregnation	Applicable to liquid bioactive compounds Polymer solubility in CO_2 not required	Bioactive solubility in CO_2 Requirement of a porous solid Difficult CO_2 purification and recycle	Various	Matrix	Various	Quercetin and thymol in chitosan-agarose [80]

The PGSS process is a versatile process available at commercial scale [74], which can be applied to liquid bioactive compounds. In this process, CO_2 acts as a solute facilitating the formation of the spray [28], so CO_2 consumption is low. PGSS does not require the use of organic solvents; however, it is difficult to obtain submicron particles, and the compounds have to be melted which may affect the thermal stability of the bioactive compound.

CPF is a continuous process also available at commercial scale, which is applied for the encapsulation of liquid compounds [73]. This technology forms agglomerates of particles, with high retention capacity [28]. However, its application in controlled release is limited by the lack of control in size and particle morphology.

Finally, the process of impregnation with supercritical fluids allows the encapsulation of bioactive compounds into porous polymer matrices. However, as in RESS, the process is limited by the solubility of the compound in CO_2 [25]. The characteristics of the particles depend mainly on the porous solid substrate; matrix-like structures are obtained, so the bioactive is not fully protected and the loading obtained depends on the operating conditions.

In summary, the supercritical fluid techniques discussed above can be used to encapsulate bioactive compounds. However, the principal shortcoming of all these methods lies in the lack of particle size control, being difficult to produce particles below the micrometer range, and the lack of control of the morphology (shape and structure) [81]. Consequently, a new process was developed to overcome these limitations.

1.4.2 Supercritical Fluid Extraction of Emulsions (SFEE)

From conventional techniques, emulsion-based encapsulation technologies offered the greatest control of particle size, as it depended on the size of the droplets of the dispersed phase, in which the bioactive and the polymer were dissolved [72]. However, these techniques require large quantities of organic solvents, and their removal involve additional separation techniques and the use of high temperatures or vacuum. In this sense, supercritical fluids present very efficient removal of organic solvents in absence of mechanical or thermal stresses. However, it is difficult to produce particles in the submicron range with controlled morphology. For this reason, the combination of the flexibility of emulsion-based encapsulation technology with the efficiency of the extraction using supercritical fluids could overcome these limitations to produce tailored micro- and nanospheres. Based on this idea, Ferro Corporation patented in 2004 a new technology under the name of Supercritical Fluid Extraction of Emulsions (SFEE) [82, 83].

The basis of the SFEE process relies on the use of supercritical CO_2 to rapidly extract the organic phase of an emulsion, in which a bioactive compound and its coating polymer have been previously dissolved. By removing the solvent, both compounds precipitate, generating a suspension of particles in water. The produced particles have controlled size and morphology [84], due to the use of the emulsion and to the fast kinetics of the supercritical CO_2 extraction. Particle agglomeration in the aqueous phase is avoided since the particles are stabilized by a surfactant. In addition, this technology is very versatile. It is possible to encapsulate hydrophilic and lipophilic compounds by changing the starting emulsion. Oil in water (O/W) emulsions, water-free emulsions (O/O), different multiple emulsions (W/O/W) or

suspensions, can be used to encapsulate bioactive compounds [81]. Figure 1.5 shows the schematic mechanism of the SFEE process starting from an O/W emulsion to encapsulate a hydrophobic bioactive compound.

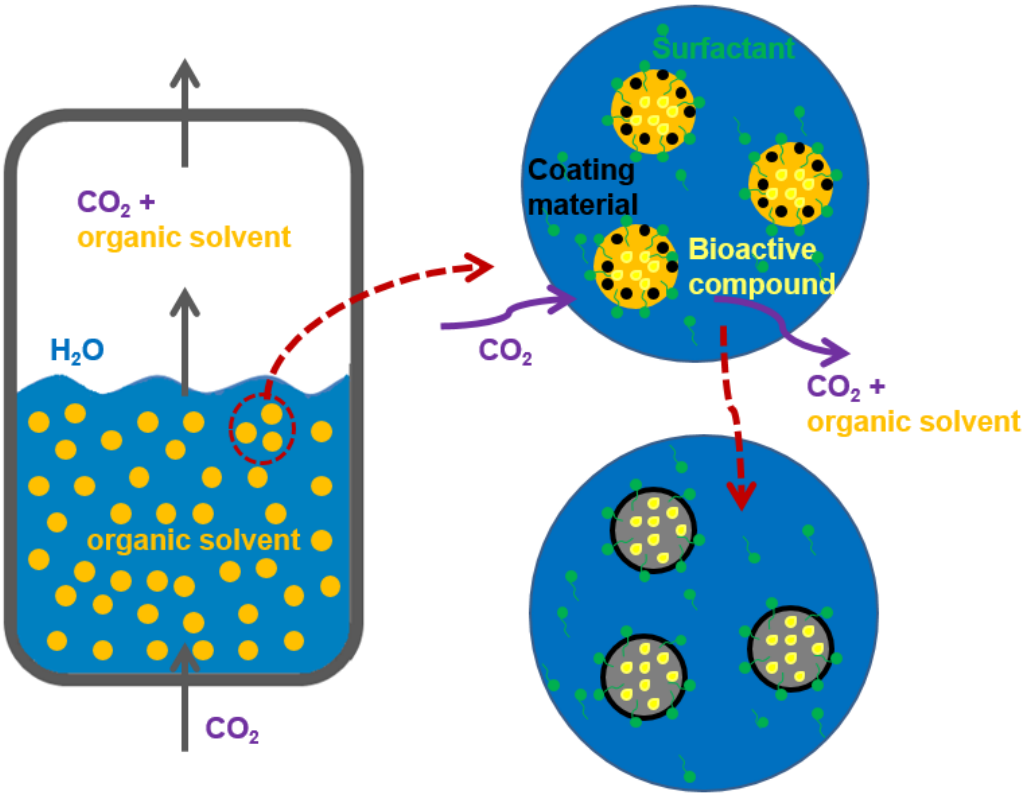

Figure 1.5. Schematic mechanism of the supercritical fluid extraction of emulsions (SFEE) process.

Since the disperse phase of the emulsion acts as a particle template, special attention must be paid to the emulsion formulation (selection of components, composition, preparation method) as it must provide an adequate droplet size, structure and stability. Other important variables of the process are the operating pressure and temperature, and the operating flow rates. They are key parameters since they condition mass transfer as demonstrated by the works of Mattea *et al.* [85, 86]

and Lévai *et al*. [87] analyzing the mass transfer in the SFEE process. However, when selecting the operating conditions several factors must be taken into account since pressure and temperature can also affect the thermal stability of the bioactive compound, the emulsion stability and the final nanoparticle characteristics.

Operating flow rates must be selected according hydrodynamics of the equipment used to maximize the organic solvent extraction. Different supercritical fluid extraction installations were used to carry out the SFEE process. Bubble [88, 89] or spray columns with co-current and countercurrent flowing phases [84, 90] were initially employed. Recently, Della Porta *et al*. [91] demonstrated that the process is easily scalable by means of a countercurrent column; however, more work is still necessary on the design of the column and on the optimization of the operating variables. Although this process produces an aqueous suspension of particles in water, if required, dry powders could be produced by coupling in-line high-pressure filtration, CO_2 lyophilization or PGSS-drying processes [81, 92].

This technology was used for micronization and encapsulation processes. Table 1.6 shows a list of the published papers dealing with SFEE up to our knowledge. The majority of existing research that was conducted in this field involved the encapsulation of pharmaceutical compounds in PLGA. However, this method may represent a promising technique for encapsulating nutraceuticals for the food industry.

Table 1.6. Reported applications of supercritical fluid extraction of emulsions (SFEE). Where EE means Encapsulation Efficiency and $[Organic\ solvent]_R$ means Residual Concentration of Organic Solvent.

Core material	Coating	Surfactant	Organic solvent	Particle size (nm)	EE (%)	$[Organic\ solvent]_R$ (ppm)	Ref.
			Polymers				
	Hi-Cap 100		Ethyl acetate				[93]
	PCL & PLGA	Tween 80 & Span 80	Acetone	160		50	[94]
	PLGA	PVA	Ethyl acetate	1000-3000		40-50	[95]
	PLA, PLGA, PCL	PVA	Acetone	300		< 500	[96]
			Pharmaceutical compounds				
Indomethacin Ketoprofen	PLGA, Eudragit RS	PVA	Ethyl acetate	100-2000		< 50	[84]
Cholesterol acetate Griseofulvin Megestrol acetate	PLGA	Pluronics, Span 80, Tween 80, lecithin, PVA, PVP	Ethyl acetate, toluene, dichloromethane	100-1000	85-99	< 50	[97]
Indomethacin Ketoprofen		Soy lecithin	Chloroform	30	80-90	20	[98]
Piroxicam	PLGA	PVA	Ethyl acetate	1000-3000	90-95	40	[88]
Ibuprofen	PLGA	PVA	Ethyl acetate	100-300	< 50		[99]
Ketoprofen	PLGA	PVA	Ethyl acetate				[100]
Diclophenac sodium Piroxicam	PLGA	PVA	Ethyl acetate	1000-3000	88-96	< 50	[101]
Ketoprofen	PLGA	PVA	Ethyl acetate	100-200			[102]
Retinyl acetate	PLGA	PVA	Acetone	3300-4500	80-90	1000	[91]
Phenanthrene		PVA	Ethyl acetate	3000-5000			[103]

Table 1.6. (Continued)

Core material	Coating	Surfactant	Organic solvent	Particle size (nm)	EE (%)	[Organic solvent]$_R$ (ppm)	Ref.
Hydrocortisone acetate	PLGA	PVA	Ethyl acetate	800-5400	31-80	500	[104]
Rhodamine	PLA-hollow gold nanoshells	Tween 80	Ethyl acetate	250			[105]
Osthole	PLGA	PVA	Dichloromethane		64		[106]
Medroxyprogesterone acetate	PHBV	PVA	Dichloromethane	183-850	70		[107]
Teriparatide and gentamicin sulfate	PLGA / hydroxyapatite / chitosan	PVA, Tween 80	Ethyl acetate	1400-2200	90		[108]
Lipophilic bioactive compounds							
β-carotene	OSA-modified starch	Tween 20 & Span 20	Dichloromethane	400		10	[85]
β-carotene Lycopene	OSA-modified starch		Dichloromethane	350	45	10	[109]
Astaxanthin	Hi-Cap 100		Dichloromethane	800	93		[110]
β-carotene	PCL	PVA	Dichloromethane	300			[111]
Quercetin		Pluronic L64 or lecithin	Ethyl acetate	13000	66	< 100	[87, 89, 112]
Palmitoyethanolamide		PVA	Chloroform	1480			[113]
Pepper oleoresin	Hi-Cap 100		Ethyl acetate	150	20-40	5900	[114]
Hydrophilic bioactive compounds							
Lysozyme	PLGA	PVA	Ethyl acetate	100	48		[90]
DNA	PLGA	PVA	Ethyl acetate	250	1	< 50	[115]
Lactobacillus acidophilus	PLGA	PVA	Ethyl acetate	20000-50000	0.8	< 50	[116]

Table 1.6. (Continued)

Core material	Coating	Surfactant	Organic solvent	Particle size (nm)	EE (%)	[Organic solvent]$_R$ (ppm)	Ref.
Bovine serum albumin Insulin like growth factor	PLGA or PLA	Tween 80 & PVA	Ethyl acetate	300-2600			[117]
Insulin	PLGA	PVA	Ethyl acetate	1800-3400	63-71	300-600	[118]
Insulin	PLGA	PVA	Ethyl acetate	3000-5000	58-60		[119]
Metallic particles							
Magnetic nanocrystals	PLGA	PVA	Dichloromethane	140-230			[120]
Titanium oxide	PLA	Tween 80	Ethyl acetate	200	85-97		[121]

Hitherto, all compounds that were treated by SFEE were solid. The complexity of the encapsulation process is more severe if the core material is a liquid [122]. Therefore, one of the aims of this research was to explore the potential of this technology to encapsulate liquid lipophilic compounds.

Consequently, two liquid bioactive compounds with different viscosities were selected as model substances, concretely vitamin E and ω-3 rich fish oil. Both are important functional ingredients in food, pharmaceutical products and cosmetic preparations, due to their documented health benefits. Whilst vitamin E presents a high antioxidant activity, and the potential to modulate oxidative stress [123], ω-3 rich fish oil can reduce the risk of certain chronic diseases, such as cardiovascular disease, immune response disorders, mental disorders and poor infant development [124]. However, these compounds are highly sensitive to heat and oxygen, exhibit poor water solubility and consequently low bioavailability [123, 124, 125, 126]. Hence, the development of special delivery systems is needed to overcome these challenges.

Tables 1.7 and 1.8 show the biopolymer-based particles developed for these compounds until now. A large number of published works dealing with fish oil encapsulation were found, most of them with great similarity in their results; for this reason, Table 1.8 only shows the most representative ones from our point of view.

Most of the works showed high encapsulation efficiencies, generally higher than 70%. However, their potential as delivery systems is doubtful.

Table 1.7. Biopolymer-based particles encapsulating vitamin E developed so far.

Biopolymer-based particles	Technique	Particle size	EE (%)	Ref.
Conventional techniques				
Vitamin E in polyurethanes, polyurea or polyamide	Interfacial polycondensation	230-370 nm	67-92	[32]
Vitamin E in polyurethanes	Interfacial polycondensation	218-615 nm	85-92	[127]
Vitamin E in polyacrilate resin	Heat and photo polymerization	> 1 mm	80-97	[128]
Vitamin E in gelatin and pectin	Complex coacervation	176 nm	91	[129]
Vitamin E in PCL	Solvent evaporation	368 nm	91	[130]
Vitamin E in PEG-PCL	Solvent evaporation	154 nm	87	[131]
Vitamin E in PLGA	Solvent evaporation	57 nm	89-95	[132]
Vitamin E in Tween 20	Solvent evaporation	56 -103 nm		[133]
Vitamin E acetate in PLA	Solvent evaporation	13 µm		[134]
	Solvent diffusion	276-643 nm		
	Nanoprecipitation	137-169 nm		
Vitamin E in PCL	Nanoprecipitation	165 nm	98	[135]
Vitamin E in PCL	Nanoprecipitation	185 nm	99	[136]
Vitamin E in wheat gliadin	Desolvation method + solvent evaporation	900 nm	77	[137]
Vitamin E in sodium alginate	Ionic gelation	41 µm		[138]
Vitamin E in Pea protein, CMC and maltodextrin	Spray drying	7 µm	78-97	[139]
Vitamin E in inulin	Spray drying		86	[140]
Vitamin E in soy protein isolate	Spray drying	5 - 9 µm	39-95	[141]
Vitamin E in sunflower protein	Spray drying	7 – 27 µm	62-100	[142]
Vitamin E acetate in chitosan	Spray drying	9 µm	91	[143]
Vitamin E acetate in PEG 4000, stearyl alcohol or carnauba wax	Spray congealing	2 µm	79-97	[144]
Vitamin E in maltodextrin and gelatin	Freeze drying		85	[145]
Supercritical fluids				
Vitamin E	SAILA	220-330 nm		[146]
Vitamin E acetate in silica	Supercritical impregnation			[147]

Table 1.8. Biopolymer-based particles encapsulating fish oil developed so far.

Biopolymer-based particles	Technique	Particle size	EE (%)	Ref.
Conventional techniques				
Fish oil in gelatin	Coacervation	30 µm		[148]
Fish oil in gelatin and acacia gum	Coacervation	10 µm	60	[149]
Fish oil in low methoxyamidated pectin	Coacervation	10 µm		[150]
Fish oil in chitosan	Coacervation			[35]
Fish oil in sugar beet pectin and zein	Solvent evaporation + gelation	83 nm		[151]
Fish oil in Eudragit L-100	Solvent diffusion	460-630 nm	16-81	[152]
Fish oil in PCL	Solvent diffusion	90 nm		[153]
Fish oil in PCL	Solvent diffusion	1 µm	99	[154]
Fish oil in PCL	Solvent diffusion	260-350 nm	60-80	[40]
Fish oil in calcium caseinate + whey proteins	Spray drying		50-82	[155]
Fish oil in OSA-starch	Spray drying	10 µm		[156]
Fish oil in methylcellulose or maltodextrin	Spray drying	27 µm	85	[157]
Fish oil in OSA-starch	Spray drying	20 µm	74-92	[158]
Fish oil in OSA-starch	Spray drying	20 µm	90-60	[159]
Fish oil in Hi-Cap 100	Spray drying	1-30 µm	90	[49]
Fish oil in whey protein isolate or corn fiber	Spray drying	130 nm	97	[160]
Fish oil in whey protein isolate	Spray drying	100 µm	70	[161]
Fish oil in maltodextrin or soy bean soluble polysaccharide	Spray drying	50-150 µm	83	[162]
	Freeze drying	100-200 µm	50	
Fish oil in zein	Electrospinning	200-300 nm	91	[60]
Supercritical fluids				
Mackerel oil in PEG 8000	PGSS	100-130 µm	97	[163]
Fish oil in chitosan and maltodextrin	PGSS-drying	30-100 µm	low	[164]

The techniques used in the food industry (spray drying, spray cooling, freeze drying or ionic gelation) generate large particles that could affect the organoleptic properties of the final product as well as the release rate of the compound. In addition, spray drying and spray cooling use high temperatures or high air flow rates that could contribute to the oxidation or loss of the biological functionality. On the other hand, the polymers used in these techniques are water soluble, have high water and oxygen permeability or lack the sufficient mechanical strength [18, 165], whereby an early release may occur, deprotecting the bioactive compound.

The emulsion-based techniques (solvent evaporation, emulsion diffusion or nanoprecipitation) provide particles at the nanometer scale and employ synthetic polymers that are not water-soluble and have a greater control over the bioactive release [26]. However, one of the main disadvantages of these techniques is the residual organic solvent concentration. The publications showed in Tables 1.7 and 1.8 did not report such data, but it is generally higher than the levels allowed in food, and therefore would condition its subsequent use.

The use of toxic chemical agents may also prevent the incorporation of particles produced by interfacial polycondensation or coacervation into food and pharmaceutical products.

Techniques with supercritical fluids provided large particles and lack of control of the morphology (shape and structure), which would affect the rheological properties of the final product and the efficiency of the delivery system.

Then, the particles obtained so far did not possess the proper characteristics to protect these bioactive compounds and deliver them to the intestinal tract, where they are absorbed [165].

In case of fish oil, consumers have reported a lack of odor and taste masking, as well as the occurrence of a disgusting fishy eructation after consuming soft-gel capsules based on natural polymers [4].

To produce particles that retain intact the biological functionality of the bioactive compound to its site of absorption, it is necessary to produce core-shell structures, since they provide the highest degree of protection with the lowest biopolymer content. Likewise, the coating should be non-water soluble and allow the release of the compound into the intestine. Among all the coatings available, synthetic ones provide enhanced protection as well as greater control over release. In this sense, the particles obtained should have nanometric size and narrow size distribution in order to have a greater control over the release and not to affect the organoleptic characteristics of the final product.

Based on the previous works on the SFEE technology, it is possible to consider this technique as an alternative to the previous conventional processes to achieve these characteristics, for the encapsulation of these bioactive compounds.

References

[1] L. Sagalowicz, M.E. Leser, Delivery systems for liquid food products, Current Opinion in Colloid & Interface Science 15 (2010) 61-72, http://dx.doi.org/10.1016/j.cocis.2009.12.003.

[2] J. Salas-Salvadó, M.D. Huetos-Solano, P. García-Lorda, M. Bulló, Diet and dietetics in al-Andalus, British Journal of Nutrition 96 (2006) S100-S104, http://dx.doi.org/10.1079/BJN20061710.

[3] A.L. Harvey, R.A. Edrada-Ebel, R.J. Quinn, The re-emergence of natural products for drug discovery in the genomics era, Nature Reviews Drug Discovery 14 (2015) 111-129, http://dx.doi.org/10.1038/nrd4510.

[4] M.A. Augustin, L. Sanguansri, Challenges in developing delivery systems for food additives, nutraceuticals and dietary supplements, in: N. Garti, D.J. McClements, Encapsulation Technologies and Delivery Systems for Food Ingredients and Nutraceuticals, Woodhead Publishing Limited, Cambridge, 2012, pp. 19-48.

[5] L. Sanguansri, M.A. Augustin, Microencapsulation in functional food product development, in: J. Smith, E. Charter (Eds.) Functional Food Product Development, Wiley-Blackwell Publishing, Oxford, 2010, pp. 3-23, http://dx.doi.org/10.1002/9781444323351.ch1.

[6] J. Weiss, P. Takhistov, D.J. McClements, Functional materials in food nanotechnology, Journal of Food Science 71 (2006) R107-R116, http://dx.doi.org/10.1111/j.1750-3841.2006.00195.x.

[7] U. Lesmes, D.J. McClements, Structure-function relationships to guide rational design and fabrication of particulate food delivery systems, Trends in Food

Science & Technology 20 (2009) 448-457, http://dx.doi.org/10.1016/j.tifs.2009.05.006.

[8] S. Dima, C. Dima, G. Iordăchescu, Encapsulation of functional lipophilic food and drug biocomponents, Food Engineering Reviews 7 (2015) 417-438, http://dx.doi.org/10.1007/s12393-015-9115-1.

[9] Z. Fang, B. Bhandari, Spray drying, freeze drying and related processes for food ingredient and nutraceutical encapsulation, in: N. Garti, D.J. McClements, Encapsulation Technologies and Delivery Systems for Food Ingredients and Nutraceuticals, Woodhead Publishing Limited, Cambridge, 2012, pp. 73-109.

[10] J. Ubbink, J. Krüger, Physical approaches for the delivery of active ingredients in foods, Trends in Food Science & Technology 17 (2006) 244-254, http://dx.doi.org/10.1016/j.tifs.2006.01.007.

[11] G. Gaucher, P. Satturwar, M.C. Jones, A. Furtos, J.C. Leroux, Polymeric micelles for oral drug delivery, European Journal of Pharmaceutics and Biopharmaceutics 76 (2010) 147-158, http://dx.doi.org/10.1016/j.ejpb.2010.06.007.

[12] K. Margulis-Goshen, Shlomo Magdassi, Formation of simvastatin nanoparticles from microemulsions, Nanomedicine: Nanotechnology, Biology, and Medicine 5 (2009) 274-281, http://dx.doi.org/10.1016/j.nano.2008.11.004.

[13] N. Bandi, C.B. Roberts, R.B. Gupta, U.B. Kompella, Formulation of controlled-release drug delivery systems, in: P. York, U.B. Kompella, B.Y. Shekunov (Eds.), Supercritical Fluid Technology for Drug Product Development, Marcel Dekker, New York, 2004, pp. 367-409.

[14] D.J. McClements, E.A. Decker, Y. Park, Controlling lipid bioavailability through physicochemical and structural approaches, Critical Reviews in Food Science and Nutrition 49 (2008) 48-67, http://dx.doi.org/10.1080/10408390701764245.

[15] R. Campardelli, L. Baldino, E. Reverchon, Supercritical fluids applications in nanomedicine, Journal of Supercritical Fluids 101 (2015) 193-214, http://dx.doi.org/10.1016/j.supflu.2015.01.030.

[16] N. Venkata Naga Jyothi, P. Muthu Prasanna, Suhas Narayan Sakarkar, K. Surya Prabha, P. Seetha Ramaiah, G.Y. Srawan, Microencapsulation techniques, factors influencing encapsulation efficiency, Journal of Microencapsulation 27 (2010) 187-197, http://dx.doi.org/10.3109/02652040903131301.

[17] B.F. Gibbs, S. Kermasha, I. Alli, C.N. Mulligan, Encapsulation in the food industry: a review, International Journal of Food Sciences and Nutrition 50 (1999) 213-224, http://dx.doi.org/10.1080/096374899101256.

[18] C. Remuñán López, M.J. Alonso Fernández, Microencapsulación de medicamentos, in: J.L. Vila Jato, Tecnología Farmacéutica vol. 1: Aspectos Fundamentales de los Sistemas Farmacéuticos y Operaciones Básicas, Editorial Síntesis, Madrid, 2008, pp. 577-608.

[19] M. Mukhopadhyay, Phase equilibrium in solid-liquid-supercritical fluid systems, in: P. York, U.B. Kompella, B.Y. Shekunov (Eds.), Supercritical Fluid Technology for Drug Product Development, Marcel Dekker, New York, 2004, pp. 27-90.

[20] C. Vauthier, K. Bouchemal, Methods for the preparation and manufacture of polymeric nanoparticles, Pharmaceutical Research 26 (2009) 1025-1058, http://dx.doi.org/ 10.1007/s11095-008-9800-3.

[21] C. Pinto Reis, R.J. Neufeld, A.J. Ribeiro, F. Veiga, Nanoencapsulation I. Methods for preparation of drug-loaded polymeric nanoparticles, Nanomedicine: Nanotechnology, Biology, and Medicine 2 (2006) 8-21, http://dx.doi.org/10.1016/j.nano.2005.12.003.

[22] A. Matalanis, O. Griffith Jones, D.J. McClements, Structured biopolymer-based delivery systems for encapsulation, protection, and release of lipophilic compounds, Food Hydrocolloids 25 (2011) 1865-1880, http://dx.doi.org/10.1016/j.foodhyd.2011.04.014.

[23] F. Shahidi, X.-Q. Han, Encapsulation of food ingredients, Critical Reviews in Food Science and Nutrition 33 (1993) 501-547, http://dx.doi.org/10.1080/10408399309527645.

[24] M. Li, O. Rouaud, D. Poncelet, Microencapsulation by solvent evaporation: State of the art for process engineering approaches, International Journal of Pharmaceutics 363 (2008) 26-39, http://dx.doi.org/10.1016/j.ijpharm.2008.07.018.

[25] M.J. Cocero, A. Martín, F. Mattea, S. Varona, Encapsulation and co-precipitation processes with supercritical fluids: Fundamentals and applications, Journal of Supercritical Fluids 47 (2009) 546-555, http://dx.doi.org/10.1016/j.supflu.2008.08.015.

[26] C.E. Mora-Huertas, H. Fessi, A. Elaissari, Polymer-based nanocapsules for drug delivery, International Journal of Pharmaceutics 385 (2010) 113-142, http://dx.doi.org/10.1016/j.ijpharm.2009.10.018.

[27] D.J. McClements, Particle characteristics and their impact on physicochemical properties of delivery systems, in: D.J. McClements, Nanoparticle- and Microparticle-based Delivery Systems. Encapsulation, Protection and Release of Active Compounds, CRC Press, Boca Raton, 2014, pp. 79-122, http://dx.doi.org/ 10.1201/b17280-4.

[28] E. Weidner, High pressure micronization for food applications, Journal of Supercritical Fluids 47 (2009) 556-565, http://dx.doi.org/10.1016/j.supflu.2008.11.009.

[29] R. Pérez-Mariá, M.J. Fabra, J.M. Lagarón, A. López-Rubio, Use of electrospinning for encapsulation, in: V. Mittal (Ed.), Encapsulation Nanotechnologies, John Wiley & Sons, Hoboken, (2013) pp. 107-135, http://dx.doi.org/10.1002/9781118729175.ch4.

[30] N.J. Zuidam, E. Shimoni, Overview of microcapsulates for use in food products or processes and methods to make them, in: N.J. Zuidam, V.A. Nedovic (Eds.), Encapsulation Technologies for Active Food Ingredients and Food Processing, Springer, New York, 2010, pp. 3-29, http://dx.doi.org/10.1007/ 978-1-4419-1008-0_2.

[31] L. Ripoll, Y. Clement, Polyamide microparticles containing vitamin C by interfacial polymerization: An approach by design of experimentation, Cosmetics 3 (2016) 38, http://dx.doi.org/10.3390/cosmetics3040038.

[32] K. Bouchemal, S. Briançon, H. Fessi, Y. Chevalier, I. Bonner, E. Perrier, Simultaneous emulsification and interfacial polycondensation for the preparation of colloidal suspensions of nanocapsules, Materials Science and Engineering C 26 (2006) 472-480, http://dx.doi.org/10.1016/j.msec.2005.10.022.

[33] M.A. Augustin, Y. Hemar, Nano- and micro-structured assemblies for encapsulation of food ingredients, Chemical Society Reviews 38 (2009) 902-912, http://dx.doi.org/10.1039/b801739p.

[34] F. Xing, G. Cheng, K. Yi, L. Ma, Nanoencapsulation of capsaicin by complex coacervation of gelatin, acacia, and tannins, Journal of Applied Polymer Science 96 (2005) 2225-2229, http://dx.doi.org/10.1002/app.21698.

[35] S. Chatterjee, Z.M.A. Judeh, Impact of encapsulation on the physicochemical properties and gastrointestinal stability of fish oil, LWT- Food Science and Technology 65 (2016) 206-213, http://dx.doi.org/10.1016/j.lwt.2015.08.010.

[36] P.N. Ezhilarasi, P. Karthik, N. Chhanwal, C. Anandharamakrishnan, Nanoencapsulation techniques for food bioactive components: A review, Food and Bioprocess Technology 6 (2013) 628-647, http://dx.doi.org/10.1007/s11947-012-0944-0.

[37] A. Kumari, S. Kumar Yadav, Y.B. Pakade, B. Singh, S. Chandra Yadav, Development of biodegradable nanoparticles for delivery of quercetin, Colloids and Surfaces B: Biointerfaces 80 (2010) 184-192, http://dx.doi.org/10.1016/j.colsurfb.2010.06.002.

[38] A. Mukerjee, J.K. Vishwanatha, Formulation, characterization and evaluation of curcumin-loaded PLGA nanospheres for cancer therapy, Anticancer Research 29 (2009) 3867-3876.

[39] D. Quintanar-Guerrero, E. Allémann, H. Fessi, E. Doelker, Preparation techniques and mechanisms of formation of biodegradable nanoparticles from preformed polymers, Drug Development and Industrial Pharmacy 24 (1998) 1113-1128, http://dx.doi.org/10.3109/03639049809108571

[40] P. Bejrapha, S.G. Min, S. Surassmo, M.J. Choi, Physicothermal properties of freeze-dried fish oil nanocapsules frozen under different conditions, Drying Technology 28 (2010) 481-489, http://dx.doi.org/10.1080/07373931003613684.

[41] S. Surassmo, S.G. Min, P. Bejrapha, M.J. Choi, Effects of surfactants on the physical properties of capsicum oleoresin-loaded nanocapsules formulated through the emulsion-diffusion method, Food Research International 43 (2010) 8-17, http://dx.doi.org/10.1016/j.foodres.2009.07.008.

[42] U. Bilati, E. Allémann, E. Doelker, Development of a nanoprecipitation method intended for the entrapment of hydrophilic drugs into nanoparticles, European Journal of Pharmaceutical Sciences 24 (2005) 67-75, http://dx.doi.org/10.1016/j.ejps.2004.09.011.

[43] H.S. Ribeiro, B.S. Chu, S. Ichikawa, M. Nakajima, Preparation of nanodispersions containing β-carotene by solvent displacement method, Food Hydrocolloids 22 (2008) 12-17, http://dx.doi.org/10.1016/j.foodhyd.2007.04.009.

[44] C.E. Mora-Huertas, O. Garrigues, H. Fessi, A. Elaissari, Nanocapsules prepared via nanoprecipitation and emulsification-diffusion methods: Comparative study, European Journal of Pharmaceutics and Biopharmaceutics 80 (2012) 235-239, http://dx.doi.org/10.1016/j.ejpb.2011.09.013.

[45] E. González Álvarez, R. Castro Ríos, H.A. Luna Olvera, A. González Horta, S.A. Galindo Rodríguez, A. Chávez Montes, Polymeric microparticles containing protein prepared using a controllable combination of diffusion and emulsification steps as part of the salting out procedure, African Journal of Pharmacy and Pharmacology 7 (2013) 2849-2858, http://dx.doi.org/10.5897/AJPP2013.3463.

[46] S. Gouin, Microencapsulation: industrial appraisal of existing technologies and trends, Trends in Food Science & Technology 15 (2004) 330-347, http://dx.doi.org/10.1016/j.tifs.2003.10.005.

[47] A. Dube, K. Ng, J.A. Nicolazzo, I. Larson, Effective use of reducing agents and nanoparticle encapsulation in stabilizing catechins in alkaline solution, Food Chemistry 122 (2010) 662-667, http://dx.doi.org/10.1016/j.foodchem.2010.03.027.

[48] A.R. Donthidi, R.F. Tester, K.E. Aidoo, Effect of lecithin and starch on alginate-encapsulated probiotic bacteria, Journal of Microencapsulation 27 (2010) 67-77, http://dx.doi.org/10.3109/02652040902982183.

[49] S.M. Jafari, E. Assadpoor, B. Bhandari, Y. He, Nanoparticle encapsulation of fish oil by spray drying, Food Research International 41 (2008) 172-183, http://dx.doi.org/10.1016/j.foodres.2007.11.002.

[50] S.M. Jafari, Y. He, B. Bhandari, Encapsulation of nanoparticles of d-limonene by spray drying: Role of emulsifiers and emulsifying techniques, Drying Technology 25 (2007) 1079-1089, http://dx.doi.org/10.1080/07373930701396758.

[51] J.D. Oxley, Spray cooling and spray chilling for food ingredient and nutraceutical encapsulation, in: N. Garti, D.J. McClements, Encapsulation Technologies and Delivery Systems for Food Ingredients and Nutraceuticals, Woodhead Publishing Limited, Cambridge, 2012, pp. 110-130.

[52] B.J. Jeon, N.C. Kim, E.M. Han, H.S. Kwak, Application of microencapsulated isoflavone into milk, Archives of Pharmacal Research 28 (2005) 859-865.

[53] R. Wegmüller, M.B. Zimmermann, V.G. Bühr, E.J. Windhab, R.E. Hurrell, Development, stability, and sensory testing of microcapsules containing iron, iodine, and vitamin A for use in food fortification, Journal of Food Science 71 (2006) S181-S187, http://dx.doi.org/10.1111/j.1365-2621.2006.tb08923.x.

[54] G. Bonat Celli, A. Ghanem, M. Su-Ling Brooks, Bioactive encapsulated powders for functional foods - A review of methods and current limitations, Food and Bioprocess Technology 8 (2015) 1825-1837, http://dx.doi.org/10.1007/s11947-015-1559-z.

[55] K. Nakagawa, S. Surassmo, S.G. Min, M.J. Choi, Dispersibility of freeze-dried poly(epsilon-caprolactone) nanocapsules stabilized by gelatin and the effect of freezing, Journal of Food Engineering 102 (2011) 177-188, http://dx.doi.org/10.1016/j.jfoodeng.2010.08.017.

[56] S. Miao, S. Mills, C. Stanton, G.F. Fitzgerald, Y. Roos, R.P. Ross, Effect of disaccharides on survival during storage of freeze dried probiotics, Dairy

Science & Technology 88 (2008) 19-30, http://dx.doi.org/10.1051/dst:2007003.

[57] Z. Knezevic, D. Gosak, M. Hraste, I. Jalsenjak, Fluid-bed microencapsulation of ascorbic acid, Journal of Microencapsulation 15 (1998) 237-352, http://dx.doi.org/10.3109/02652049809006853.

[58] J.D. Oxley, Coextrusion for food ingredients and nutraceutical encapsulation: principles and technology, in: N. Garti, D.J. McClements, Encapsulation Technologies and Delivery Systems for Food Ingredients and Nutraceuticals, Woodhead Publishing Limited, Cambridge, 2012, pp. 131-150.

[59] L.T. Lim, Encapsulation of bioactive compounds using electrospinning and electrospraying technologies, in: C.M. Sabliov, H. Chen, R.Y. Yada, Nanotechnology and Functional Foods: Effective Delivery of Bioactive Ingredients, John Wiley & Sons, Chichester, 2015, pp. 297-317, http://dx.doi.org/10.1002/9781118462157.ch18.

[60] K. Moomand, L.T. Lim, Effects of solvent and n-3 rich fish oil on physicochemical properties of electrospun zein fibres, Food Hydrocolloids 46 (2015) 191-200, http://dx.doi.org/10.1016/j.foodhyd.2014.12.014.

[61] A. López-Rubio, E. Sanchez, S. Wilkanowicz, Y. Sanz, J.M. Lagaron, Electrospinning as a useful technique for the encapsulation of living *bifidobacteria* in food hydrocolloids, Food Hydrocolloids 28 (2012) 159-167, http://dx.doi.org/10.1016/j.foodhyd.2011.12.008.

[62] C. Jiménez-González, P. Poechlauer, Q.B. Broxterman, B.S. Yang, D.A. Ende, J. Baird, C. Bertsch, R.E. Hannah, P. Dell'Orco, H. Noorman, S. Yee, R. Reintjens, A. Wells, V. Massonneau, J. Manley, Key green engineering

research areas for sustainable manufacturing: A perspective from pharmaceutical and fine chemicals manufacturers, Organic Process Research & Development 15 (2011) 900-911, http://dx.doi.org/10.1021/op100327d.

[63] A. Bertucco, Precipitation and crystallization techniques, in: P.G. Jessop, W. Leitner (Eds.), Chemical Synthesis Using Supercritical Fluids, Wiley-VCH Verlarg GmbH, Weinheim, 1999, pp. 108-126, http://dx.doi.org/10.1002/9783527613687.ch6.

[64] A.S. Mayo, U.B. Kompella, Supercritical fluid technology in pharmaceutical research, in: J. Swarbrick (Ed.) Encyclopedia of Pharmaceutical Technology, Third Edition, Taylor and Francis, New York, 2007, pp. 3568-3582, http://dx.doi.org/10.1081/E-EPT3-120012011.

[65] M. Kalani, R. Yunus, Application of supercritical antisolvent method in drug encapsulation: a review, International Journal of Nanomedicine 6 (2011) 1429-1442, http://dx.doi.org/10.2147/IJN.S19021.

[66] J.Y. Clavier, M. Perrut, Scale-up issues for supercritical fluid processing in compliance with GMP, in: P. York, U.B. Kompella, B.Y. Shekunov (Eds.), Supercritical Fluid Technology for Drug Product Development, Marcel Dekker, New York, 2004, pp. 615-651.

[67] O.R. Davies, A.L. Lewis, M.J. Whitaker, H. Tai, K.M. Shakesheff, S.M. Howdle, Applications of supercritical CO_2 in the fabrication of polymer systems for drug delivery and tissue engineering, Advanced Drug Delivery Reviews 60 (2008) 373-387, http://dx.doi.org/10.1016/j.addr.2006.12.001.

[68] J. Herberger, K. Murphy, L. Munyakazi, J. Cordia, E. Westhaus, Carbon dioxide extraction of residual solvents in poly(lactide-co-glycolide)

microparticles, Journal of Controlled Release 90 (2003) 181-195, http://dx.doi.org/10.1016 /S0168-3659(03)00152-4.

[69] K. Koushik, U.B. Kompella, Preparation of large porous deslorelin-PLGA microparticles with reduced residual solvent and cellular uptake using a supercritical carbon dioxide process, Pharmaceutical Research 21 (2004) 524-535, http://dx.doi.org/10.1023/B:PHAM.0000019308.25479.a4.

[70] R. Campardelli, M. Cherain, C. Perfetti, C. Iorio, M. Scognamiglio, E. Reverchon, G. Della Porta, Lipid nanoparticles production by supercritical fluid assisted emulsion-diffusion, Journal of Supercritical Fluids 82 (2013) 34-40, http://dx.doi.org/10.1016/j.supflu.2013.05.020.

[71] P. Sheth, H. Sandhu, D. Singhal, W. Malick, N. Shah, M.S. Kislalioglu, Nanoparticles in the pharmaceutical industry and the use of supercritical fluid technologies for nanoparticle production, Current Drug Delivery 9 (2012) 269-284, https://doi.org/10.2174/156720112800389052.

[72] A. Martín, M.J. Cocero, Precipitation processes with supercritical fluids: patents review, Recent Patents on Engineering 2 (2008) 9-20, https://doi.org/10.2174/187221208783478561.

[73] J. Jung, M. Perrut, Particle design using supercritical fluids: Literature and patent survey, Journal of Supercritical Fluids 20 (2001) 179-219, http://dx.doi.org/10.1016/S0896-8446(01)00064-X.

[74] M. Bahrami, S. Ranjbarian, Production of micro- and nano-composite particles by supercritical carbon dioxide, Journal of Supercritical Fluids 40 (2007) 263-283, http://dx.doi.org/10.1016/j.supflu.2006.05.006.

[75] A. Martín, F. Mattea, I. Gutiérrez, F. Miguel, M.J. Cocero, Co-precipitation of carotenoids and bio-polymers with the supercritical anti-solvent process, Journal of Supercritical Fluids 41 (2007) 138-147, http://dx.doi.org/10.1016/j.supflu.2006.08.009.

[76] M. Fraile, R. Buratto, B. Gómez, A. Martín, M.J. Cocero, Enhanced delivery of quercetin by encapsulation in poloxamers by supercritical antisolvent process, Industrial & Engineering Chemistry Research 53 (2014) 4318-4327, http://dx.doi.org/10.1021/ie5001136.

[77] E. de Paz, A. Martín, C.M.M. Duarte, M.J. Cocero, Formulation of β-carotene with poly-(Ɛ-caprolactones) by PGSS process, Powder Technology 217 (2012) 77-83, http://dx.doi.org/10.1016/j.powtec.2011.10.011.

[78] S. Varona, A. Martín, M.J. Cocero, C.M.M. Duarte, Encapsulation of lavandin essential oil in poly-(Ɛ-caprolactones) by PGSS process, Chemical & Engineering Technology 36 (2013) 1187-1192, http://dx.doi.org/10.1002/ceat.201200592.

[79] F. Otto, S. Grüner, B. Weinreich, Design of powders with controlled release properties using CPF-technology, Proceedings of the 6th International Symposium on Supercritical Fluids, Vol. 3, Versailles, France, April 28-30, 2003, pp. 1707-1712.

[80] A.M.A. Dias, M.E.M. Braga, I.J. Seabra, P. Ferreira, M.H. Gil, H.C. Sousa, Development of natural-based wound dressings impregnated with bioactive compounds and using supercritical carbon dioxide, International Journal of Pharmaceutics 408 (2011) 9-19, http://dx.doi.org/10.1016/j.ijpharm.2011.01.063.

[81] B.Y. Shekunov, P. Chattopadhyay, J. Seitzinger, Engineering of composite particles for drug delivery using supercritical fluid technology, in: S. Svenson (Ed.), Polymeric Drug Delivery II. Polymeric Matrices and Drug Particle Engineering, ACS Symposium Series, Vol. 924, 2006, pp. 234-249, http://dx.doi.org/10.1021/bk-2006-0924.ch015.

[82] P. Chattopadhyay, B.Y. Shekunov, J.S. Seitzinger, R.W. Huff, Particles from supercritical fluid extraction of emulsions, U.S. Patent 2004026319 (A1), February 12, 2004.

[83] P. Chattopadhyay, B.Y. Shekunov, J.S. Seitzinger, R.W. Huff, Compoisite particles and method for preparing, U.S. Patent 2004071781 (A1), April 15, 2004.

[84] P. Chattopadhyay, R. Huff, B.Y. Shekunov, Drug encapsulation using supercritical fluid extraction of emulsions, Journal of Pharmaceutical Sciences 95 (2006) 667-679, http://dx.doi.org/10.1002/jps.20555.

[85] F. Mattea, A. Martín, A. Matías-Gago, M.J. Cocero, Supercritical antisolvent precipitation from an emulsion: β-Carotene nanoparticle formation, Journal of Supercritical Fluids 51 (2009) 238-247, http://dx.doi.org/10.1016/j.supflu.2009.08.013.

[86] F. Mattea, A. Martín, C. Schulz, P. Jaeger, R. Eggers, M.J. Cocero, Behavior of an organic solvent drop during the supercritical extraction of emulsions, AIChE Journal 56 (2010) 1184-1195, http://dx.doi.org/10.1002/aic.12061.

[87] G. Lévai, A. Martín, S. Rodríguez Rojo, M.J. Cocero, T.M. Fieback, Measurement and modelling of mass transport properties during the

supercritical fluid extraction of emulsions, Journal of Supercritical Fluids (2017), http://dx.doi.org/10.1016/j.supflu.2017.01.015.

[88] G. Della Porta, E. Reverchon, Nanostructured microspheres produced by supercritical fluid extraction of emulsions, Biotechnology and Bioengineering 100 (2008) 1020-1033, http://dx.doi.org/10.1002/bit.21845.

[89] G Lévai, A. Martín, E. de Paz, S. Rodríguez-Rojo, M.J. Cocero, Production of stabilized quercetin aqueous suspensions by supercritical fluid extraction of emulsions, Journal of Supercritical Fluids 100 (2015) 34-45, http://dx.doi.org/10.1016/j.supflu.2015.02.019.

[90] J. Kluge, F. Fusaro, N. Casas, M. Mazzotti, G. Muhrer, Production of PLGA micro- and nanocomposites by supercritical fluid extraction of emulsions: I. Encapsulation of lysozyme, Journal of Supercritical Fluids 50 (2009) 327-335, http://dx.doi.org/10.1016/j.supflu.2009.05.010.

[91] G. Della Porta, R. Campardelli, N. Falco, E. Reverchon, PLGA microdevices for retinoids sustained release produced by supercritical emulsion extraction: continuous versus batch operation layouts, Journal of Pharmaceutical Sciences 100 (2011) 4357-4367, http://dx.doi.org/10.1002/jps.22647.

[92] G. Lévai, Bioproducts processing by SFEE: application for liquid and solid quercetin formulations, Dissertation, Universidad de Valladolid, Valladolid, 2016.

[93] S.K. Luther, A. Braeuer, High-pressure microfluidics for the investigation into multi-phase systems using the supercritical fluid extraction of emulsions (SFEE), Journal of Supercritical Fluids 65 (2012) 78-86, http://dx.doi.org/10.1016/j.supflu.2012.02.029.

[94] R. Campardelli, G. Della Porta, E. Reverchon, Solvent elimination from polymer nanoparticle suspensions by continuous supercritical extraction, Journal of Supercritical Fluids 70 (2012) 100-105, http://dx.doi.org/10.1016/j.supflu.2012.06.005.

[95] G. Della Porta, N. Falco, E. Reverchon, Continuous supercritical emulsions extraction: A new technology for biopolymer microparticles production, Biotechnology and Bioengineering 108 (2011) 676-686, http://dx.doi.org/10.1002/bit.22972.

[96] G. Della Porta, R. Campardelli, E. Reverchon, Monodisperse biopolymer nanoparticles by Continuous Supercritical Emulsion Extraction, Journal of Supercritical Fluids 76 (2013) 67-73, http://dx.doi.org/10.1016/j.supflu.2013.01.009.

[97] B.Y. Shekunov, P. Chattopadhyay, J. Seitzinger, R. Huff, Nanoparticles of poorly water-soluble drugs prepared by supercritical fluid extraction of emulsions, Pharmaceutical Research 23 (2006) 196-204, http://dx.doi.org/10.1007/s11095-005-8635-4.

[98] P. Chattopadhyay, B.Y. Shekunov, D. Yim, D. Cipolla, B. Boyd, S. Farr, Production of solid lipid nanoparticle suspensions using supercritical fluid extraction of emulsions (SFEE) for pulmonary delivery using the AERx system, Advanced Drug Delivery Reviews 59 (2007) 444-453, http://dx.doi.org/10.1016/j.addr.2007.04.010.

[99] C.S. Lin, J.J. Xu, K.M. Ng, Encapsulation of a low aqueous solubility substance in a biodegradable polymer using supercritical fluid extraction of emulsion,

Industrial & Engineering Chemistry Research 52 (2013) 134-141, http://dx.doi.org/10.1021/ie300612r.

[100] J. Kluge, M. Mazzotti, G. Muhrer, Solubility of Ketoprofen in colloidal PLGA, International Journal of Pharmaceutics 399 (2010) 163-172, http://dx.doi.org/10.1016/j.ijpharm.2010.08.016.

[101] G. Della Porta, N. Falco, E. Reverchon, NSAID drugs release from injectable microspheres produced by supercritical fluid emulsion extraction, Journal of Pharmaceutical Sciences 99 (2010) 1484-1499, http://dx.doi.org/10.1002/jps.21920.

[102] J. Kluge, F. Fusaro, M. Mazzotti, G. Muhrer, Production of PLGA micro- and nanocomposites by supercritical fluid extraction of emulsions: II. Encapsulation of Ketoprofen, Journal of Supercritical Fluids 50 (2009) 336-343, http://dx.doi.org/10.1016/j.supflu.2009.05.002.

[103] J. Kluge, L. Joss, S. Viereck, M. Mazzotti, Emulsion crystallization of phenanthrene by supercritical fluid extraction of emulsions, Chemical Engineering Science 77 (2012) 249-258, http://dx.doi.org/10.1016/j.ces.2011.12.008.

[104] N. Falco, E. Reverchon, G. Della Porta, Injectable PLGA/hydrocortisone formulation produced by continuous supercritical emulsion extraction, International Journal of Pharmaceutics 441 (2013) 589-597, http://dx.doi.org/10.1016/j.ijpharm.2012.10.039.

[105] R. Campardelli, G. Della Porta, L. Gomez, S. Irusta, E. Reverchon, J. Santamaria, Au-PLA nanocomposites for photothermally controlled drug

delivery, Journal of Materials Chemistry B 2 (2014) 409-417, http://dx.doi.org/10.1039/C3TB21099E.

[106] B. Liu, Y. Wu, Y. Chang, Optimization of process parameters of osthole-loaded PLGA microparticles prepared using emulsification-solvent extraction, Journal of Dispersion Science and Technology 35 (2014) 1247-1254, http://dx.doi.org/10.1080/01932691.2013.838680.

[107] W. Machado Giufrida, V. Ferreira Cabral, L. Cardoso-Filho, D. Dos Santos Conti, V.E.B. de Campos, S.R.P. da Rocha, Medroxyprogesterone-encapsulated poly(3-hydroxybutirate-co-3-hydroxyvalerate) nanoparticles using supercritical fluid extraction of emulsions, Journal of Supercritical Fluids 118 (2016) 79-88, http://dx.doi.org/10.1016/j.supflu.2016.07.026.

[108] G. Della Porta, R. Campardelli, V. Cricchio, F. Oliva, N. Maffulli, E. Reverchon, Injectable PLGA/hydroxyapatite/chitosan microcapsules produced by supercritical emulsion extraction technology: an in vitro study on teriparatide/gentamicin controlled release, Journal of Pharmaceutical Sciences 105 (2016) 2164-2172, http://dx.doi.org/10.1016/j.xphs.2016.05.002.

[109] D.T. Santos, A. Martín, M.A.A. Meireles, M.J. Cocero, Production of stabilized sub-micrometric particles of carotenoids using supercritical fluid extraction of emulsions, Journal of Supercritical Fluids 61 (2012) 167-174, http://dx.doi.org/10.1016/j.supflu.2011.09.011.

[110] N. Mezzomo, E. de Paz, M. Maraschin, A. Martín, M.J. Cocero, S.R.S Ferreira, Supercritical anti-solvent precipitation of carotenoid fraction from pink shrimp residue: Effect of operational conditions on encapsulation efficiency, Journal

of Supercritical Fluids 66 (2012) 342-349, http://dx.doi.org/10.1016/j.supflu.2011.08.006.

[111] E. de Paz, S. Rodríguez, J. Kluge, A. Martín, M. Mazzotti, M.J. Cocero, Solubility of β-carotene in poly-(Ɛ-caprolactone) particles produced in colloidal state by Supercritical Fluid Extraction of Emulsions (SFEE), Journal of Supercritical Fluids 84 (2013) 105-112, http://dx.doi.org/10.1016/j.supflu.2013.09.017.

[112] G. Lévai, J.Q. Albarelli, D.T. Santos, M.A.A. Meireles, A. Martín, S. Rodríguez-Rojo, M.J. Cocero, Quercetin loaded particles production by means of supercritical fluid extraction of emulsions: Process scale-up study and thermo-economic evaluation, Food and Bioproducts Processing 103 (2017) 27-38, http://dx.doi.org/10.1016/j.fbp.2017.02.008.

[113] E. Reverchon, R. Adami, R. Campardelli, G. Della Porta, I. De Marco, M. Scognamiglio, Supercritical fluids based techniques to process pharmaceutical products difficult to micronize: Palmitoyethanolamide, Journal of Supercritical Fluids 102 (2015) 24-31, http://dx.doi.org/10.1016/j.supflu.2015.04.00.

[114] A.C. de Aguiar, L.P. Sales Silva, C.A. de Rezende, G. Fernandez Barbero, J. Martínez, Encapsulation of pepper oleoresin by supercritical fluid extraction of emulsions, Journal of Supercritical Fluids 112 (2016) 37-43, http://dx.doi.org/10.1016/j.supflu.2016.02.009.

[115] A.S. Mayo, B.K. Ambati, U.B. Kompella, Gene delivery nanoparticles fabricated by supercritical fluid extraction of emulsions, International Journal of Pharmaceutics 387 (2010) 278-285, http://dx.doi.org/10.1016/j.ijpharm.2009.12.024.

[116] G. Della Porta, F. Castaldo, M. Scognamiglio, L. Paciello, P. Parascandola, E. Reverchon, Bacteria microencapsulation in PLGA microdevices by supercritical emulsion extraction, Journal of Supercritical Fluids 63 (2012) 1-7, http://dx.doi.org/10.1016/j.supflu.2011.12.020.

[117] R. Campardelli, E. Reverchon, G. Della Porta, Biopolymer particles for proteins and peptides sustained release produced by supercritical emulsion extraction, Procedia Engineering 42 (2012) 239-246, http://dx.doi.org/10.1016/j.proeng.2012.07.415.

[118] N. Falco, E. Reverchon, G. Della Porta, Continuous supercritical emulsions extraction: Packed tower characterization and application to poly(lactic-co-glycolic acid) + insulin microspheres production, Industrial & Engineering Chemistry Research 51 (2012) 8616-8623, http://dx.doi.org/10.1021/ie300482n.

[119] G. Della Porta, N. Falco, E. Giordano, E. Reverchon, PLGA microspheres by supercritical emulsion extraction: a study on insulin release in myoblast culture, Journal of Biomaterials Science, Polymer Edition, 24 (2013) 1831-1847, http://dx.doi.org/10.1080/09205063.2013.807457.

[120] M. Furlan, J. Kluge, M. Mazzotti, M. Lattuada, Preparation of biocompatible magnetite-PLGA composite nanoparticles using supercritical fluid extraction of emulsions, Journal of Supercritical Fluids 54 (2010) 348-356, http://dx.doi.org/10.1016/j.supflu.2010.05.010.

[121] R. Campardelli, G. Della Porta, V. Gomez, S. Irusta, E. Reverchon, J. Santamaria, Encapsulation of titanium dioxide nanoparticles in PLA microspheres using supercritical emulsion extraction to produce bactericidal

nanocomposites, Journal of Nanoparticles Research 15 (2013) 1987, http://dx.doi.org/10.1007/s11051-013-1987-5.

[122] C. Thies, A survey of microencapsulation processes, in: S. Benita (Ed.), Microencapsulation. Methods and industrial applications, Vol. 73, Marcel Dekker, New York, 1996, pp. 1-19.

[123] C.M. Sabliov, C.E. Astete, Encapsulation and controlled release of antioxidants and vitamins, in: N. Garti (Ed.), Delivery and Controlled release of bioactives in foods and nutraceuticals, Woodhead Publishing Limited, Cambridge, 2008, pp. 297-330, doi:10.1016/B978-1-84569-145-5.50020-2.

[124] A. Gulotta, A.H. Saberi, M.C. Nicoli, D.J. McClements, Nanoemulsion-based delivery systems for polyunsaturated (ω-3) oils: formation using a spontaneous emulsification method, Journal of Agricultural and Food Chemistry 62 (2014) 1720-1725, http://dx.doi.org/10.1021/jf4054808.

[125] A.H. Saberi, Y. Fang, D.J. McClements, Fabrication of vitamin E-enriched nanoemulsions: Factors affecting particle size using spontaneous emulsification, Journal of Colloid and Interface Science 391 (2013) 95-102, doi:10.1016/j.jcis.2012.08.069.

[126] J. Rodríguez, M.J. Martín, M.A. Ruíz, B. Clares, Current encapsulation strategies for bioactive oils: From alimentary to pharmaceutical perspectives, Food Research International 83 (2016) 41-59, http://dx.doi.org/10.1016/j.foodres.2016.01.032.

[127] K. Bouchemal, S. Briançon, E. Perrier, H. Fessi, I. Bonnet, N. Zydowicz, Synthesis and characterization of polyurethane and poly(ether urethane) nanocapsules using a new technique of interfacial polycondensation combined

to spontaneous emulsification, International Journal of Pharmaceutics 269 (2004) 89-100, http://dx.doi.org/10.1016/j.ijpharm.2003.09.025.

[128] T. Takei, K. Terazono, K. Araki, Y. Ozuno, G. Hayase, K. Kanamori, K. Nakanishi, M. Yoshida, Encapsulation of hydrophobic ingredients in hard resin capsules with ultrahigh efficiency using a superoleophobic material, Polymeric Bulletin 73 (2016) 409-417, http://dx.doi.org/10.1007/s00289-015-1497-y.

[129] F. Sharifi, F. Hadizadeh, F. Sadeghi, M.T. Hamed Mosavian, C. Zarei, Process optimization, physical properties and environmental stability of an α-tocopherol nanocapsule preparation using complex coacervation method and full factorial design, Chemical Engineering Communications 203 (2016) 64-74, http://dx.doi.org/10.1080/00986445.2014.973941.

[130] Y. Byun, J.B. Hwang, S.H. Bang, D. Darby, K. Cooksey, P.L. Dawson, H.J. Park, S. Whiteside, Formulation and characterization of α-tocopherol loaded poly Ɛ-caprolactone (PCL) nanoparticles, LWT - Food Science and Technology 44 (2011) 24-28, http://dx.doi.org/10.1016/j.lwt.2010.06.032.

[131] A. Laouini, K.P. Koutromanis, C. Charcosset, S. Georgiadou, H. Fessi, R.G. Holdich, G.T. Vladisavljević, pH-Sensitive micelles for targeted drug delivery prepared using a novel membrane contactor method, ACS Applied Materials & Interfaces 5 (2013) 8939-8947, http://dx.doi.org/10.1021/am4018237.

[132] I.G. Zigoneanu, C.E. Astete, C.M. Sabliov, Nanoparticles with entrapped α-tocopherol: synthesis, characterization, and controlled release, Nanotechnology 19 (2008) 105606, http://dx.doi.org/10.1088/0957-4484/19/10/105606.

[133] N. Anarjan, N. Jaberi, S. Yeganeh-Zare, E. Banafshehchin, A. Rahimirad, H. Jafarizadeh-Malmiri, Optimization of mixing parameters for α-tocopherol

nanodispersions prepared using solvent displacement method, Journal of the American Oil Chemists' Society 91 (2014) 1397-1405, http://dx.doi.org/10.1007/s11746-014-2482-6.

[134] J.P. Anais, N. Razzouq, M. Carvalho, C. Fernandez, A. Astier, M. Paul, A. Astier, H. Fessi, A.M. Lorino, Development of α-tocopherol acetate nanoparticles: Influence of preparative processes, Drug Development and Industrial Pharmacy 35 (2009) 216-223, http://dx.doi.org/10.1080/03639040802248798.

[135] N. Khayata, W. Abdelwahed, M.F. Chehna, C. Charcosset, H. Fessi, Preparation of vitamin E loaded nanocapsules by the nanoprecipitation method: From laboratory scale to large scale using a membrane contactor, International Journal of Pharmaceutics 43 (2012) 419-427, http://dx.doi.org/10.1016/j.ijpharm.2011.12.016.

[136] C. Montanheiro Noronha, A. Ferreira Granada, S. Matos de Carvalho, R. Calegari Llino, M.V. de O.B. Maciel, P.L. Manique Barreto, Optimization of α-tocopherol loaded nanocapsules by the nanoprecipitation method, Industrial Crops and Products 50 (2013) 896-906, http://dx.doi.org/10.1016/j.indcrop.2013.08.015.

[137] C. Duclainoir, A.M. Orecchioni, P. Depraetere, E. Nakache, α-Tocopherol encapsulation and *in vitro* release from wheat gliadin nanoparticles, Journal of Microencapsulation 19 (2002) 53-60, http://dx.doi.org/10.1080/02652040110055207.

[138] A. Dalmoro, A.A. Barba, M. d'Amore, G. Lamberti, Single-pot semicontinuous bench scale apparatus to produce microparticles, Industrial & Engineering

Chemistry Research 53 (2014) 2771-2780, http://dx.doi.org/10.1021/ie403308q.

[139] A.P.T.R. Pierucci, L.R. Andrade, M. Farina, C. Pedrosa, M.H. M. Rocha-Leão, Comparison of α-tocopherol microparticles produced with different wall materials: pea protein a new interesting alternative, Journal of Microencapsulation 24 (2007) 201- 213, http://dx.doi.org/10.1080/02652040701281167.

[140] P. García, J. Vega, P. Jimenez, J. Santos, P. Robert, Alpha-tocopherol microspheres with cross-linked and acetylated inulin and their release profile in a hydrophilic model, European Journal of Lipid Science and Technology 115 (2013) 811-819, http://dx.doi.org/10.1002/ejlt.201200109.

[141] A. Nesterenko, I. Alric, F. Silvestre, V. Durrieu, Influence of soy protein's structural modifications on their microencapsulation properties: α-Tocopherol microparticle preparation, Food Research International 48 (2012) 387-396, http://dx.doi.org/10.1016/j.foodres.2012.04.023.

[142] A. Nesterenko, I. Alric, F. Violleau, F. Silvestre, V. Durrieu, A new way of valorizing biomaterials: The use of sunflower protein for α-tocopherol microencapsulation, Food Research International 53 (2013) 115-124, http://dx.doi.org/10.1016/j.foodres.2013.04.020.

[143] G. Garrastazu Pereira, C. Britto Detoni, T. Lima da Silva, L. Marques Colomé, A. Raffin Pohlmann, S. Stanisçuaski Guterres, α-Tocopherol acetate-loaded chitosan microparticles: Stability during spray drying process, photostability and swelling evaluation, Journal of Drug Delivery Science and Technology 30 (2015) 220-224, http://dx.doi.org/10.1016/j.jddst.2015.10.018.

[144] B. Albertini, N. Passerini, F. Pattarino, L. Rodriguez, New spray congealing atomizer for the microencapsulation of highly concentrated solid and liquid substances, European Journal of Pharmaceutics and Biopharmaceutics 69 (2008) 348-357, http://dx.doi.org/10.1016/j.ejpb.2007.09.011.

[145] M. Campagnaro Farias, M. Leite Moura, L. Andrade, M.H. Miguez Rocha Leão, Encapsulation of the alpha-tocopherol in a glassy food model matrix, Materials Research 10 (2007) 57-62, http://dx.doi.org/10.1590/S1516-14392007000100013.

[146] R. Campardelli, E. Reverchon, α-Tocopherol nanosuspensions produced using a supercritical assisted process, Journal of Food Engineering 149 (2015) 131-136, http://dx.doi.org/10.1016/j.jfoodeng.2014.10.015.

[147] F. Belhadj-Ahmed, E. Badens, P. Llewellyn, R. Denoyel, G. Charbit, Impregnation of vitamin E acetate on silica mesoporous phases using supercritical carbon dioxide, Journal of Supercritical Fluids 51 (2009) 278-286, http://dx.doi.org/10.1016/j.supflu.2009.07.012.

[148] C.J. Barrow, C. Nolan, B.J. Holub, Bioequivalence of encapsulated and microencapsulated fish-oil supplementation, Journal of Functional Foods I (2009) 38-43, http://dx.doi.org/10.1016/j.jff.2008.09.006.

[149] F. Tamjidi, A. Nasirpour, M. Shahedi, Mixture design approach for evaluation of fish oil microencapsulation in gelatin-acacia gum coacervates, International Journal of Polymeric Materials and Polymeric Biomaterials 62 (2013) 444-449, http://dx.doi.org/10.1080/00914037.2012.719138.

[150] Z. Zhang, E.A. Decker, D.J. McClements, Encapsulation, protection, and release of polyunsaturated lipids using biopolymer-based hydrogel particles,

Food Research International 64 (2014) 520-526, http://dx.doi.org/10.1016/j.foodres.2014.07.020.

[151] S. Soltani, A. Madadlou, Gelation characteristics of the sugar beet pectin solution charged with fish oil-loaded zein nanoparticles, Food Hydrocolloids 43 (2015) 664-669, http://dx.doi.org/10.1016/j.foodhyd.2014.07.030.

[152] E. Averina, E. Allémann, Encapsulation of alimentary bioactive oils of the Baikal Lake area into pH-sensitive micro- and nanoparticles, LWT- Food Science and Technology 53 (2013) 271-277, http://dx.doi.org/10.1016/j.lwt.2013.01.020.

[153] M.J. Choi, U. Ruktanonchai, A. Soottitantawat, S.G. Min, Morphological characterization of encapsulated fish oil with β-cyclodextrin and polycaprolactone, Food Research International 42 (2009) 989-997, http://dx.doi.org/10.1016/j.foodres.2009.04.019.

[154] M.J. Choi, U. Ruktanonchai, S.G. Min, J.Y. Chun, A. Soottitantawat, Physical characteristics of fish oil encapsulated by β-cyclodextrin using an aggregation method or polycaprolactone using and emulsion-diffusion method, Food Chemistry 119 (2010) 1694-1703, http://dx.doi.org/10.1016/j.foodchem.2009.09.052.

[155] M.K. Keogh, B.T. O'Kennedy, J. Kelly, M.A. Auty, P.M. Kelly, A. Fureby, A.M. Haahr, Stability to oxidation of spray-dried fish oil powder microencapsulated using milk ingredients, Journal of Food Science 66 (2001) 217-224, http://dx.doi.org/10.1111/j.1365-2621.2001.tb11320.x.

[156] S. Drusch, Y. Serfert, K. Schwarz, Microencapsulation of fish oil with n-octenylsuccinate-derivatised starch: Flow properties and oxidative stability,

European Journal of Lipid Science and Technology 108 (2006) 501-512, http://dx.doi.org/10.1002/ejlt.200500312.

[157] W. Kolanowski, M. Ziolkowski, J. Weiβbrodt, B. Kunz, G, Laufenberg, Microencapsulation of fish oil by spray drying-impact on oxidative stability. Part 1, European Food Research and Technology 222 (2006) 336-342, http://dx.doi.org/10.1007/s00217-005-0111-1.

[158] S. Drusch, Y. Serfert, M. Scampicchio, B. Schmidt-Hansber, K. Schwarz, Impact of physicochemical characteristics on the oxidative stability of fish oil microencapsulated by spray-drying, Journal of Agricultural and Food Chemistry 55 (2007) 11044-11051, http://dx.doi.org/10.1021/jf072536a.

[159] S. Drusch, S. Berg, Extractable oil in microcapsules prepared by spray-drying: Localisation, determination and impact on oxidative stability, Food Chemistry 109 (2008) 17-24, http://dx.doi.org/10.1016/j.foodchem.2007.12.016.

[160] Q. Chen, F. Zhong, J. Wen, D. McGillivray, S.Y. Quek, Properties and stability of spray-dried and freeze-dried microcapsules co-encapsulated with fish oil, phytosterol esters, and limonene, Drying Technology 31 (2013) 707-716, http://dx.doi.org/10.1080/07373937.2012.755541.

[161] Y. Wang, W. Liu, X.D. Chen, C. Selomulya, Micro-encapsulation and stabilization of DHA containing fish oil in protein-based emulsion through mono-disperse droplet spray dryer, Journal of Food Engineering 175 (2016) 74-84, http://dx.doi.org/10.1016/j.jfoodeng.2015.12.007.

[162] S.H. Anwar, B. Kunz, The influence of drying methods on the stabilization of fish oil microcapsules: Comparison of spray granulation, spray drying, and

freeze drying, Journal of Food Engineering 105 (2011) 367-378, http://dx.doi.org/10.1016/j.jfoodeng.2011.02.047.

[163] A.S.M. Tanbirul Haque, B.S. Chun, Particle formation and characterization of mackerel reaction oil by gas saturated solution process, Journal Food Science and Technology 53 (2016) 293-303, http://dx.doi.org/10.1007/s13197-015-2000-3.

[164] K. Dubbert, N. Rubio-Rodríguez, S. Kareth, S. Beltrán, M. Petermann, Encapsulation of fish oil in biodegradable polymers by the PGSS process, in: Institut National Polytechnique de Lorraine (Ed.), Proceedings of the 13th European Meeting on Supercritical Fluids, The Hague, 2011, p. 176.

[165] Z. Zhang, R. Zhang, L. Chen, Q. Tong, D.J. McClements, Designing hydrogel particles for controlled or targeted release of lipophilic bioactive agents in the gastrointestinal tract, European Polymer Journal 72 (2015) 698-716, http://dx.doi.org/10.1016/j.eurpolymj.2015.01.013.

2. Objectives

2. Objectives

The objective of this thesis was to explore the potential of the supercritical fluid extraction of emulsions technology to nanoencapsulate liquid lipophilic bioactive compounds with application in pharmaceutical or food products. Concretely, the nanoencapsulation of vitamin E and ω-3 rich fish oil in polycaprolactone was envisioned. These two model substances were perfect candidates, since they provide well-known health benefits, but present very low water solubility and are highly sensitive to suffer an oxidation reaction losing their biological functionality. On the other hand, they have different viscosity, which was a key parameter for the starting emulsion formulation, directly affecting the retention capacity of the particle.

Polycaprolactone was selected as the coating material since, due to its physicochemical properties, it is ideally suited when a targeted delivery to the

intestinal tract is intended [1]. An emulsion made up of acetone (O), water (W), and Tween 80 as a surfactant was used. Acetone was selected as the organic solvent because of its low toxic potential, which is in line with the ICH guidelines [2]. Tween 80 was selected because it is a particularly attractive non-ionic surfactant that is non-toxic, environmentally-friendly and biocompatible. It is commercially inexpensive and approved for pharmaceutical and food use [3]. The best formulation was sought to produce the desired particles.

It was also an objective of this thesis project to develop and scale-up the process. Thus, different configurations were tested and compared in terms of particle characteristics, CO_2 consumption and scalability. The continuous production of particles with reliable characteristics and with a low residual organic solvent content was ultimately pursued.

This document includes an initial section with the unifying discussion of the main results, gathering the content of five published papers that are attached in the Publications Section of this manuscript. Their objectives were:

In a first publication: "Performance of the biocompatible surfactant Tween 80, for the formation of microemulsions suitable for new pharmaceutical processing" (J. Appl. Chem. 2013 (2013) 930356), the phase behavior and structure of organic solvent-water emulsions based on Tween 80 were studied. The effect of the amount of surfactant on colloid size was first explored. Since Tween 80 shows a temperature dependent behavior, the influence of temperature on emulsion stability was further investigated. Finally, the possibility of using additives, to reduce the amount of surfactant required to form microemulsions was addressed.

In a second publication: "Supercritical fluid extraction of emulsions to nanoencapsulate vitamin E in polycaprolactone" (J. Supercrit. Fluids 119 (2017) 274-282), SFEE was used to nanoencapsulate vitamin E. Firstly, the development of the emulsion formulation, which provided stability, adequate droplet size and O/W structure was done. Secondly, the influence of the operating parameters on the effectiveness of the organic solvent removal was examined. Thirdly, the initial formulation was varied to enhance the encapsulation efficiency, particle size distribution and morphology of the nanocapsules. Finally, a comparison with particles produced by conventional solvent evaporation was made in order to evaluate the potential benefits of the supercritical technology.

In a third publication: "Performance comparison of different supercritical fluid extraction equipments for the production of vitamin E in polycaprolactone nanocapsules by the supercritical fluid extraction of emulsions" (J. Supercrit. Fluids 122 (2017) 70-78), the encapsulation of vitamin E in polycaprolactone was done using four SFEE installations: A) a bubble column, B) a bubble column with gas redistributor, C) a spray column and D) a packed column. Performance of each installation was compared in terms of organic solvent removal, CO_2 consumption and nanocapsule characteristics (encapsulation efficiency, particle size distribution and morphology).

In a fourth publication: "Continuous supercritical fluid extraction of emulsions to produce nanocapsules of vitamin E in polycaprolactone" (J. Supercrit. Fluids 124 (2017) 72-79), vitamin E in polycaprolactone nanoparticles were continuously produced by means of a high-pressure packed column. First, hydrodynamics of the column was studied as well as its dependence on the density difference between

phases, and on the solvent to feed ratio. Secondly, the best operating conditions were determined in order to maximize acetone extraction. The produced nanoparticles were studied in terms of encapsulation efficiency, particle size distribution, residual acetone concentration and morphology, and compared to the characteristics of the particles obtained in the bubble column operating in batch. Finally, the process was modeled with a commercial process simulator, Aspen Plus, in order to determine the size of the column to achieve an organic solvent removal acceptable for food applications.

In a fifth publication: "The encapsulation of low viscosity omega-3 rich fish oil in polycaprolactone by supercritical fluid extraction of emulsions" (submitted for publication), SFEE was applied to nanoencapsulate fish oil with a high content in ω- 3 PUFAs in polycaprolactone. Several formulations to prepare fish oil enriched emulsions were first studied. The best formulations were subjected to SFEE and the obtained nanoparticles were compared in terms of encapsulation efficiency, particle size distribution and morphology. A comparison with the particles produced by conventional solvent evaporation was also made to analyze the potential improvements generated by the use of the supercritical technology.

References

[1] V.R. Sinha, K. Bansal, R. Kaushik, R. Kumria, A. Trehan, Poly-ε-caprolactone microspheres and nanospheres: an overview, International Journal of Pharmaceutics 278 (2004) 1-23, http://dx.doi.org/10.1016/j.ijpharm.2004.01.044.

[2] Guidance for Industry Q3C- Tables and List, U.S. Department of Health and Human Services, Food and Drug Administration Center for Drug Evaluation and Research (CDER), Center for Biologics Evaluation and Research (CBER), ICH, Revision 2, 2012.

[3] B.A. Kerwin, Polysorbates 20 and 80 used in the formulation of protein biotherapeutics: structure and degradation pathways, Journal of Pharmaceutical Sciences 97 (2008) 2924-2935, http://dx.doi.org/10.1002/jps.21190.

3. A unifying discussion the results

3. A unifying discussion of the results of this thesis

This chapter summarizes the most relevant results obtained in the research conducted during the present doctoral thesis. They were already published in five papers that are attached in the Publications Section of this document. They include detailed information on experimental and analytical procedures, as well as the totality of the results.

This chapter is structured in four main experimental blocks:

- Background on emulsion formulation (Publication I).
- Nanoencapsulation of vitamin E in PCL by SFEE (Publication II).
- Nanoencapsulation of ω-3 rich fish oil in PCL by SFEE (Publication V).
- Scale-up and continuous production of vitamin E nanocapsules (Publications III and IV).

3.1 Background on emulsion formulation

A comprehensive analysis of the key parameters affecting the stability and droplet size of emulsions formulated with a biocompatible surfactant, Tween 80, was initially performed (Publication I). This type of in-depth analysis is of fundamental importance for the selection of the emulsion formulation to be subjected to supercritical extraction.

Emulsions are mixtures of water, organic solvent and surfactant, optically opaque since they contain relatively large droplets (>0.1 μm); although not thermodynamically stable, may be kinetically stable for long periods. In contrast, microemulsions are optically transparent, thermodynamically stable, isotropic mixtures [1], with disperse phase droplets ranging from 2 to 50 nm in diameter [2]. Due to these characteristics, microemulsions have received great attention from the food, pharmaceutical and cosmetic industries [3]. Thereby, they could be used as colloidal nanocarriers, improving drug delivery or skin penetration; as nanoparticle templates, as well as for biotechnological reactions. Nonetheless, their use in these industries requires biocompatible systems. Hence, the interest of producing microemulsions with a biocompatible surfactant as Tween 80.

In this work, the phase behavior of the Tween 80 / water / n-hexane emulsions were investigated by visual observation of each sample, which allowed its classification according to its turbidity into emulsions and microemulsions. Thus, microemulsions were identified as transparent samples, whereas turbid samples were emulsions. Highly viscous samples were also observed and identified as gel-like. All information was gathered and represented in phase maps. Since the amount of

surfactant can affect the economy of the process and the emulsion subsequent application, the aim of this work was to obtain microemulsions with the minimum amount of surfactant by varying temperature or using additives.

Tween 80 shows a temperature dependent behavior, its surfactive character can be modified towards more lipophilic with slight increases of temperature (always below the cloud point). The phase prism in Figure 3.1 reflects the behavior for the Tween 80 / water / n-hexane system with temperature. Thus, at 303 K this system showed a large emulsion region (area with light grey shading). However, when increasing temperature to 313 K, the microemulsion region (area without shading) increased, due to the reduction of the hydrophilic character of the surfactant favoring the organic solvent dissolution. At 323 K, the microemulsion region increased only on the right side of the diagram because of the increase in the lipophilic character of the surfactant, favoring the dissolution of a bigger amount of organic solvent. Finally, at 333 K, the emulsion region increased again as a result of reaching the cloud point (phase separation temperature) [4]. Therefore, by increasing temperature from 303 K to 323 K, the required amount of surfactant to form microemulsions could be reduced from 80% to 20%.

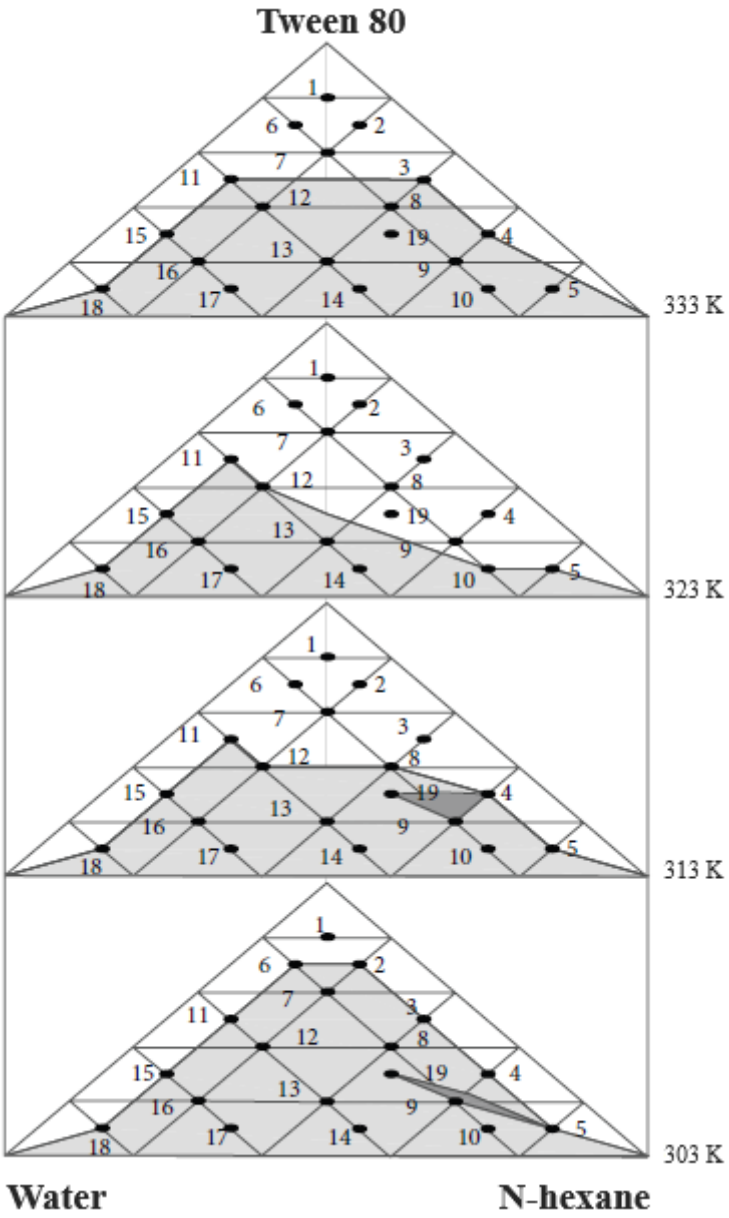

Figure 3.1. Phase prism corresponding with the Tween 80 / water / n-hexane system. The system exhibited three behaviors: microemulsions are shown in white; emulsions corresponds to the light grey shading area; and gel-like to the dark grey shading area.

Although this work was performed with n-hexane, same guidelines were taken into account when formulating the emulsions with acetone to nanoencapsulate the selected bioactive compounds.

3.2 Nanoencapsulation of vitamin E in PCL by SFEE

This research focused on the formation of vitamin E nanocapsules by means of the SFEE process using a bubble column (Publication II). First, the selection of the starting emulsion formulation was made following the principles described earlier. Second, the influence of the extraction parameters (pressure, temperature, CO_2 flow rate and extraction time) was studied because these factors have an impact on the technical and economic viability of the process, as well as on the characteristics of the final product. Then, the effect of the initial formulation was evaluated in terms of encapsulation efficiency, particle size, particle size distribution, and morphology. Finally, a comparison was made between the particles produced by conventional solvent evaporation and those obtained by SFEE.

3.2.1 Selection of the starting formulation

Vitamin E was encapsulated in PCL using an emulsion, consisting of acetone as the organic solvent, Tween 80 as surfactant and water. Although acetone is completely miscible with water, the presence of vitamin E increased the viscosity of the organic phase, allowing the formation of emulsions. When PCL was present in the organic phase, the slow diffusion of the acetone to the water phase initiated PCL precipitation. However, particles were not adequately formed until the supercritical extraction of the acetone.

A study of the phase behavior of the system Tween 80 / water / acetone + vitamin E + PCL at atmospheric pressure and ambient temperature was executed in

order to select the compositions that would be subjected to SFEE. Twenty compositions were considered as shown in Figure 3.2.

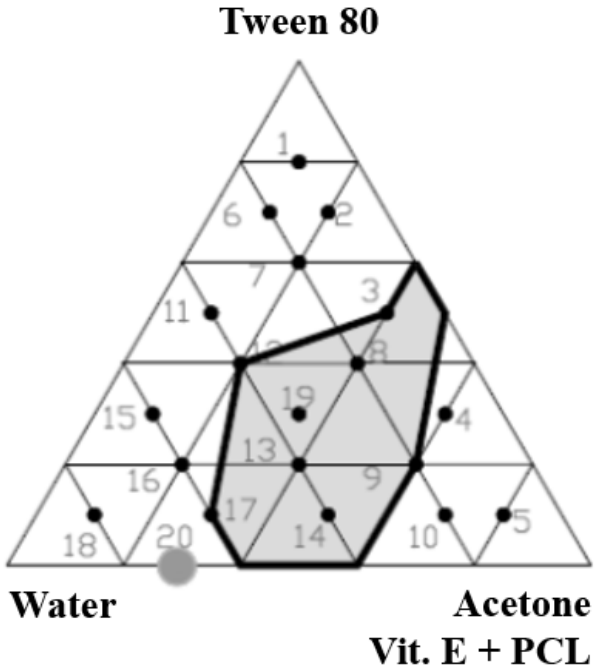

Figure 3.2. Phase map of the system Tween 80 / water / acetone + vitamin E (0.51% by mass) + PCL (0.63% by mass). The system exhibited three behaviors: the transparent samples are shown in white; PCL separated as a solid phase within the light shaded area; formulation 20 was turbid.

Since the colloid acts as a template, it must provide an adequate size and an O/W structure, which is required to encapsulate lipophilic compounds. These requirements were fulfilled by formulations 18 and 20, whose compositions are summarized in Table 3.1. Whilst formulation 18 was transparent, formulation 20 was turbid. This difference in turbidity was indicative of a different colloid size [2], being smaller for the transparent one. However, formulation 18 required a higher concentration of surfactant, which could condition the subsequent application of the nanoparticles.

Table 3.1. Composition and appearance of the two formulations selected in this study.

Formulation	Water (g)	Tween 80 (g)	Acetone (g)	PCL (g)	Vitamin E (g)	Appearance
18	4.000	0.500	0.500	0.009	0.007	Transparent
20	3.580	0.004	1.420	0.009	0.007	Turbid

3.2.2 Influence of the operating conditions

Attention must be paid in the selection of the operating temperature and pressure since, besides affecting mass transfer; they may affect the thermal stability of the bioactive compound, the stability of the emulsion (as explained in section 3.1), and the final nanoparticle characteristics. Initially, pressure and temperature were selected such that they favored the maximum extraction rate of the organic solvent without extracting the bioactive compound while avoiding the use of high temperatures. According to the high-pressure phase equilibrium diagram of the CO_2-acetone mixture [5], at 8.0 MPa and 313 K, miscibility between carbon dioxide and acetone was complete. In these conditions, the solubility of vitamin E in supercritical CO_2 was quite low (0.3 mg vitamin E·g CO_2) [6], not being significantly improved by the presence of the acetone as no vitamin E was collected on the CO_2 outlet stream after many runs.

The SFEE apparatus used for the encapsulation of vitamin E consisted of a 10 mL cylindrical stainless steel bubble column with a length-to-diameter (L/D) ratio of nine. This equipment consists of a vertical vessel partially filled with liquid into which supercritical CO_2 is bubbled [7]. Thereby, five grams of the freshly prepared starting emulsion were placed inside the vessel, and CO_2 was bubbled at the selected operating pressure and temperature until the desired operation time was reached. After

slow depressurization, the suspension of nanoparticles in water was recovered. A scheme of this installation is shown in Figure 3.3.

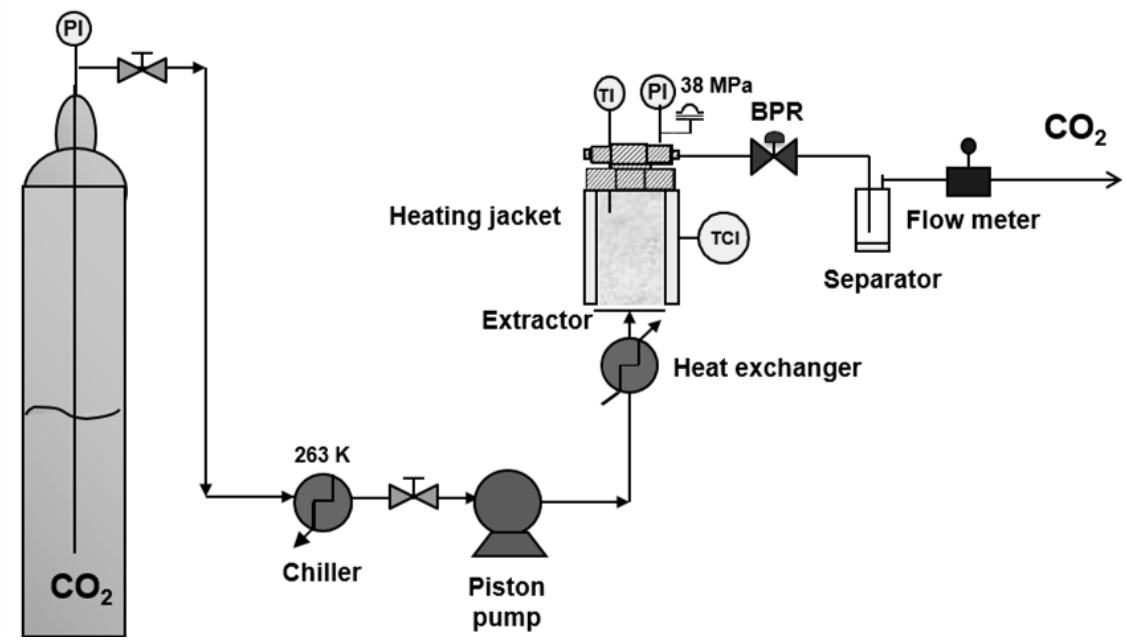

Figure 3.3. Scheme of the equipment used for supercritical fluid extraction of emulsions (SFEE).

The CO_2 flow rate used in the bubble column was studied with the intention of maximizing the extraction of the organic solvent. Several CO_2 flow rates were tested trying to avoid the entrainment of the emulsion. An increase in CO_2 flow rate from 1 to 3 $mL \cdot min^{-1}$ led to a higher acetone extraction rate. However, the removal rate was at a maximum when the system operated at 2 $mL \cdot min^{-1}$ (7.2 $kg \cdot h^{-1} \cdot kg$ $emulsion^{-1}$). Larger flow rates benefited turbulence and external mass transfer but reduced contact time.

The residual acetone concentration versus the required amount of CO_2 under these operating conditions is shown in Figure 3.4. The extraction of the acetone was initially very fast because high amounts of acetone were available. However, as the

acetone concentration decreased and particles were formed, the extraction rate rapidly decreased. Some of the acetone was entrapped inside the particles and the internal diffusion and transport through the polymer wall controlled the overall rate of extraction. Consequently, high CO_2/acetone ratios and long operation times were required to reduce the residual acetone concentration to pharmaceutical and food accepted levels. Thus, 21 kg CO_2·kg acetone^{-1} were required to achieve 5000 ppm (maximum acetone concentration permitted in pharmaceutics [8]), whereas 101 kg CO_2·kg acetone^{-1} were needed to get the maximum acetone concentration permitted in food (50 ppm) [9]. Even at this point, acetone content in the interior of the particles was about 5 ppm.

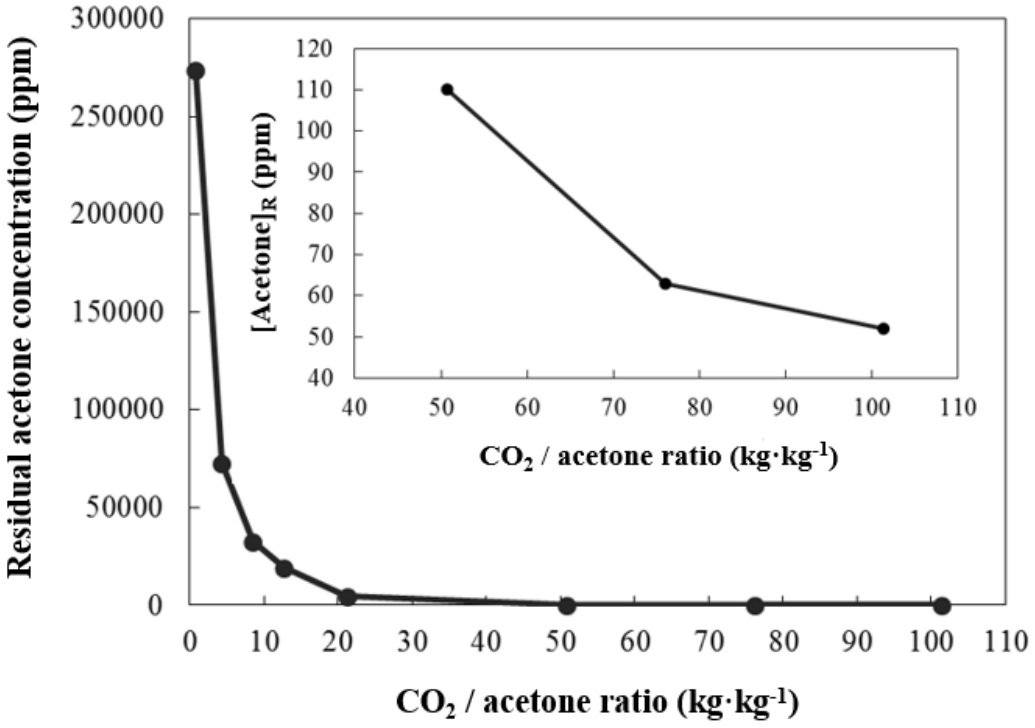

Figure 3.4. Extraction curve of acetone from an emulsion in the SFEE process at a CO_2 flow rate of 2 mL·min^{-1} (7.2 kg·h^{-1}·kg emulsion^{-1}), operating at 8.0 MPa and 313 K.

3.2.3 Influence of the composition on the characteristics of the particles

The nanoparticles obtained from the formulation 20 exhibited a high encapsulation efficiency of about 90%, and a loading capacity of 42%. In terms of particle size, they were in the nanometer range (153 nm) with a fairly narrow particle size distribution (polydispersity index of 0.26). Despite these good characteristics, the effect of the variation of the amount of vitamin E, PCL, acetone and Tween 80, on the nanoparticle characteristics (particle size distribution, encapsulation efficiency, and morphology) was studied with respect to formulation 20. Each effect was analyzed separately. In addition, the particles obtained from formulation 18 (smaller colloid size) were also compared in terms of particle size distribution and morphology. A table with the compositions of all the variations tested, as well as the characteristics of the nanoparticles obtained from them is shown in Publication II.

The main parameter affecting encapsulation efficiency was the amount of vitamin E, which increased, as did the vitamin E concentration from 90% to 96%. This phenomenon can be related to the higher initial amount of vitamin E, and to its lipophilicity [10] and viscosity [11], which prevented its leakage to the water phase. However, the augmentation in encapsulation efficiency with increasing amount of vitamin E was limited due to the loss of emulsion stability, as evidenced the appearance of separate vitamin E droplets.

Regarding loading capacity, it was possible to increase it from 40% to 69% by increasing the amount of vitamin E, since more vitamin E was encapsulated, or by reducing the amount of PCL.

Increasing the amount of vitamin E or reducing the amount of acetone contributed to a small reduction in particle size. Nevertheless, formulation 18 with a smaller colloid size allowed reducing particle size to 8 nm.

Regarding morphology, TEM images showed non-agglomerated spherical particles with sizes that correlated well with data from photon correlation spectroscopy. Figure 3.5 shows the nanoparticles obtained from formulations 18 and 20. Analysis of the internal morphology showed that there was a hole in the interior of the nanoparticle, confirming that nanocapsules were obtained [12].

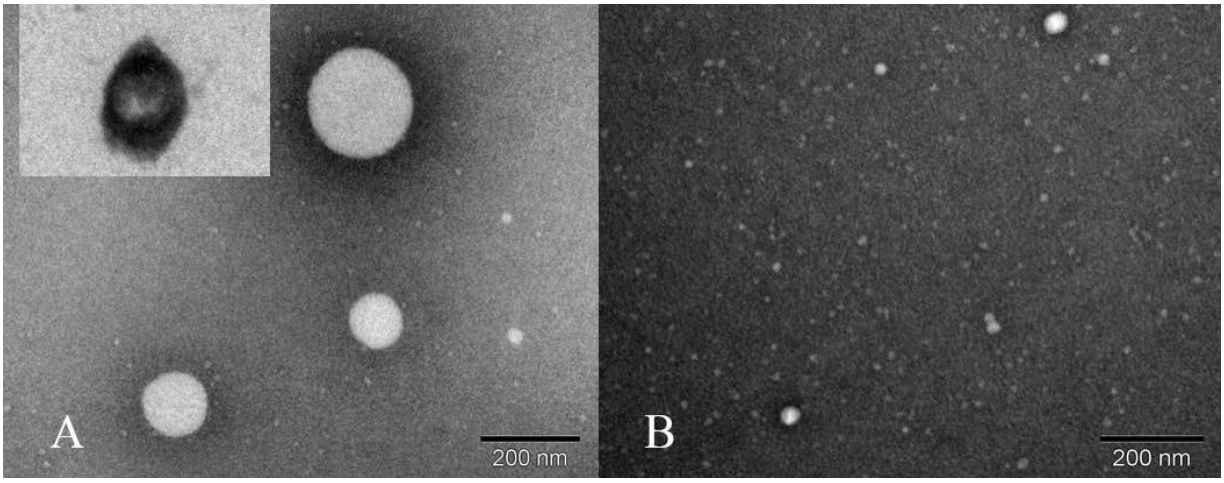

Figure 3.5. TEM images of vitamin E loaded nanocapsules. Image A: nanoparticles obtained from formulation 20, an ultrathin section of vitamin E nanoparticles is shown in the upper left corner. Image B: nanoparticles obtained from formulation 18.

Stability tests indicated that the encapsulation efficiency and particle size distribution remained unchanged after 6 and 12 months. This significant stability could be related to the hardness and semicrystalline character of the PCL, and to the high viscosity of vitamin E, which prevented its leakage through the PCL wall.

3.2.4 Formation of nanoparticles through conventional solvent evaporation

Acetone was extracted from the sample using two variations of the conventional solvent evaporation process: 1) under vacuum pressure using a rotating evaporator, and 2) at atmospheric pressure using a hotplate with temperature and stirring control. Table 3.2 shows a comparison between the operating conditions and results obtained by SFEE and the two conventional solvent evaporation processes.

Table 3.2. A comparison between the operation conditions and results obtained by SFEE and solvent evaporation at vacuum pressure or atmospheric pressure.

	SFEE	**Solvent evaporation at vacuum**	**Solvent evaporation at atmospheric pressure**
Pressure (kPa)	$8 \cdot 10^3$	30 + 6	100
Operation time (min)	240	30 + 30	240
Temperature (K)	313	323	313
Sample amount (g)	5	75	100
Residual acetone concentration ± SD (ppm)	52 ± 7	235 ± 63	157 ± 31
Encapsulation efficiency ± SD (%)	90.5 ± 1.1	86.0 ± 1.0	78.0 ± 1.0
Loading capacity ± SD (%)	42.0 ± 0.3	40.2 ± 0.1	37.7 ± 0.3
Mean particle size ± SD (nm)	153 ± 33	115 ± 15	123 ± 51
Polydispersity index ± SD	0.26 ± 0.02	0.63 ± 0.09	0.18 ± 0.02

SFEE and conventional solvent evaporation provided similar particle size; however, polydispersity index increased in solvent evaporation at vacuum maybe due to the acetone boiling bubbles inside the droplet, as Li *et al.* [11] stated. SFEE provided the highest encapsulation efficiency (90%) and the lowest residual acetone concentration (52 ppm). The residual acetone concentration in solvent evaporation at atmospheric pressure was slightly higher (157 ppm) than in SFEE after the same

operation time (4 h). It is important to take into account the fact that mass transfer between the water-air interface was improved using the fume hood. The production capacity of the bubble column used for SFEE was very low (5 g) in comparison with the conventional solvent evaporation technique. Hence, the following assays were performed to increase the production capacity (section 3.4).

3.3 Nanoencapsulation of ω-3 rich fish oil in PCL by SFEE

The purpose of this part of the research was the encapsulation of fish oil with high content in ω-3 polyunsaturated fatty acids (PUFAs), such as eicosapentaenoic acid (EPA, C20:5) and docosahexaenoic acid (DHA, C22:6). The fatty acid profile of this oil is shown in Table 3.3. First, the best emulsion formulation to be subjected to SFEE was sought using the Tween 80 / water / acetone system. Second, CO_2 consumption to obtain nanoparticles with a residual organic solvent concentration suitable for the pharmaceutical and food industries was studied. Third, the effect of the initial formulation was evaluated in terms of encapsulation efficiency, particle size, particle size distribution, and morphology. Finally, nanoparticles obtained by SFEE were compared with those generated by solvent evaporation in terms of nanoparticle characteristics and residual acetone concentration.

Table 3.3. Fatty acid profile of the fish oil used provided by Biomega Natural Nutrients.

Fatty acids	Proportion (%)
C14:0	2.70 ± 0.04
C15:0	0.61 ± 0.01
C16:0	16.06 ± 0.09
C16:1	4.23 ± 0.04
C17:0	1.39 ± 0.00
C17:1	0.65 ± 0.00
C18:0	4.34 ± 0.01
C18:1	20.00 ± 0.08
C18:2	0.82 ± 0.00
C18:3	0.29 ± 0.00
C18:4	0.40 ± 0.00
C20:0	0.19 ± 0.00
C20:1	7.08 ± 0.07
C20:4	1.65 ± 0.01
C20:5	4.50 ± 0.02
C22:5	2.29 ± 0.01
C22:6	20.98 ± 0.03
PUFAs	30.94 ± 0.04
EPA+DHA	25.49 ± 0.04

3.3.1 Selection of the starting emulsion formulation

The system used for the encapsulation of fish oil consisted of acetone, water, Tween 80 and PCL, due to the good characteristics of the vitamin E nanoparticles generated with this system by SFEE (Publication II). However, it was not possible to obtain a stable O/W emulsion with the fish oil because of its low viscosity. Therefore, the incorporation of glycerol, xanthan gum and vitamin E was considered to improve the emulsion stability [13]. Publication V shows the composition of all the emulsions tested, as well as their characteristics in terms of turbidity, phase separation, PCL precipitation and odor masking. Three different formulations (I, O, R) fulfilled the requirements of O/W structure, adequate colloid size, and stability, avoiding fishy smell. Table 3.4 shows the composition of these samples.

Table 3.4. Formulations selected for the encapsulation of ω-3 rich fish oil in polycaprolactone by SFEE. TH means thickener; T80, Tween 80; AC, acetone; PCL, polycaprolactone; ω-3, ω-3 rich fish oil; Vit E, vitamin E.

Sample	TH	M H_2O+ TH (g)	[TH] (%)	M T80 (g)	M AC (g)	M PCL (g)	M ω-3 (g)	M Vit E (g)
I	Glycerol	3.580	70	0.360	1.420	0.009	0.007	0.014
O	Xanthan Gum	3.580	0.25	0.360	1.420	0.009	0.007	0.014
R	-	3.580	-	0.004	1.420	0.009	0.007	0.014

While formulation I was transparent, O and R were turbid. All of them included vitamin E as weighting agent; however, they differentiated in the thickening agent of the aqueous phase. Formulation I used glycerol, and O used xanthan gum. One of the advantages of using xanthan gum instead of glycerol could be the low amount required to get the same stabilizing effect (only 0.25% by mass in comparison with the 70% of glycerol), in addition to its antioxidant activity [14]. Nonetheless, formulation R required much lower amount of surfactant (only 4 mg in comparison with 360 mg of formulations O and I). Moreover, no thickening agent was used in this formulation.

3.3.2 Nanoparticle formation by SFEE

Operating conditions were selected to reach complete acetone extraction without extracting the fish oil. Therefore, according to the high-pressure phase equilibrium diagram of the CO_2-acetone mixture [5], temperature and pressure were set at 313 K and 8.0 MPa, respectively. Under these conditions, supercritical CO_2 and acetone were completely miscible and fish oil solubility in supercritical CO_2 was rather low (0.73 mg fish oil·g CO_2^{-1}) [15].

Nanoparticles of ω-3 rich fish oil in PCL were produced in the same bubble column used for vitamin E. As occurred for vitamin E, the best CO_2 flow rate to maximize acetone extraction, avoiding entrainment of the emulsion, was 2 $mL \cdot min^{-1}$. Similarly, extraction of acetone was very fast initially, but as nanoparticles formed and the amount of acetone decreased, extraction rate rapidly diminished. The extraction rate was also slowed down by the presence of the thickeners. This is in agreement with the observations made by Lévai *et al*. [16] on the mass transfer in the SFEE process. They concluded that the extraction process was controlled by the dissolution of CO_2 in the emulsion. Thus, 127 kg $CO_2 \cdot$kg $acetone^{-1}$ were required for formulation I and O to achieve the legally permitted level of acetone in food (50 ppm) [9], whilst only 101 kg $CO_2 \cdot$kg $acetone^{-1}$ were required for formulation R.

The characteristics of the nanoparticles obtained from formulations I, O and R are summarized in Table 3.5. Formulations I and R achieved encapsulation efficiencies of around 40%, while formulation O only achieved around 10%. Similar efficiencies were obtained in the encapsulation of bioactive oils with other supercritical fluid technologies [17, 18]. These low values could be due to the fish oil solubility in supercritical CO_2, or more probably to the loss of stability of the emulsion during SFEE treatment.

Table 3.5. Characteristics of the fish oil loaded nanoparticles produced in the bubble column using formulations I, O and R. EE means Encapsulation Efficiency; PdI, Polydispersity Index; LC, Loading Capacity, $[AR]_R$, Residual Acetone Concentration.

Formulation	EE ± SD (%)	Mean diameter ± SD (nm)	PdI ± SD	LC ± SD (%)	$[AC]_R$ ± SD (ppm)
I	38 ± 5	8 ± 1	0.29 ± 0.02	10 ± 1	30 ± 3
O	12 ± 1	6 ± 1	0.44 ± 0.09	3 ± 1	63 ± 14
R	43 ± 12	73 ± 1	0.40 ± 0.03	15 ± 6	54 ± 5

All formulations provided spherical and non-aggregated nanoparticles as shown in Figure 3.6. The clustered appearance of the nanoparticles obtained from formulation I could be due to the high amount of glycerol used. Whilst formulations I and O generated particles with a size under 10 nm, formulation R produced particles with an average size of 73 nm. This difference in size could be explained by the presence of the thickener, which could decrease droplet size [19, 20]. Greater size variability was observed in formulations R and O, which was also confirmed by photon correlation spectroscopy analysis.

Compared to other supercritical fluid techniques, the nanoparticle size achieved was much lower than that obtained using techniques such as PGSS or PGSS-drying. Only nanoparticle sizes smaller than 1 μm were reported in research conducted with SEDS [21] or RESSS [22] in oil encapsulation. Conventional techniques generated particles with sizes around 20 μm [23]. Lower sizes of particles encapsulating fish oil were only achieved by the emulsion diffusion technique (90 nm) [24].

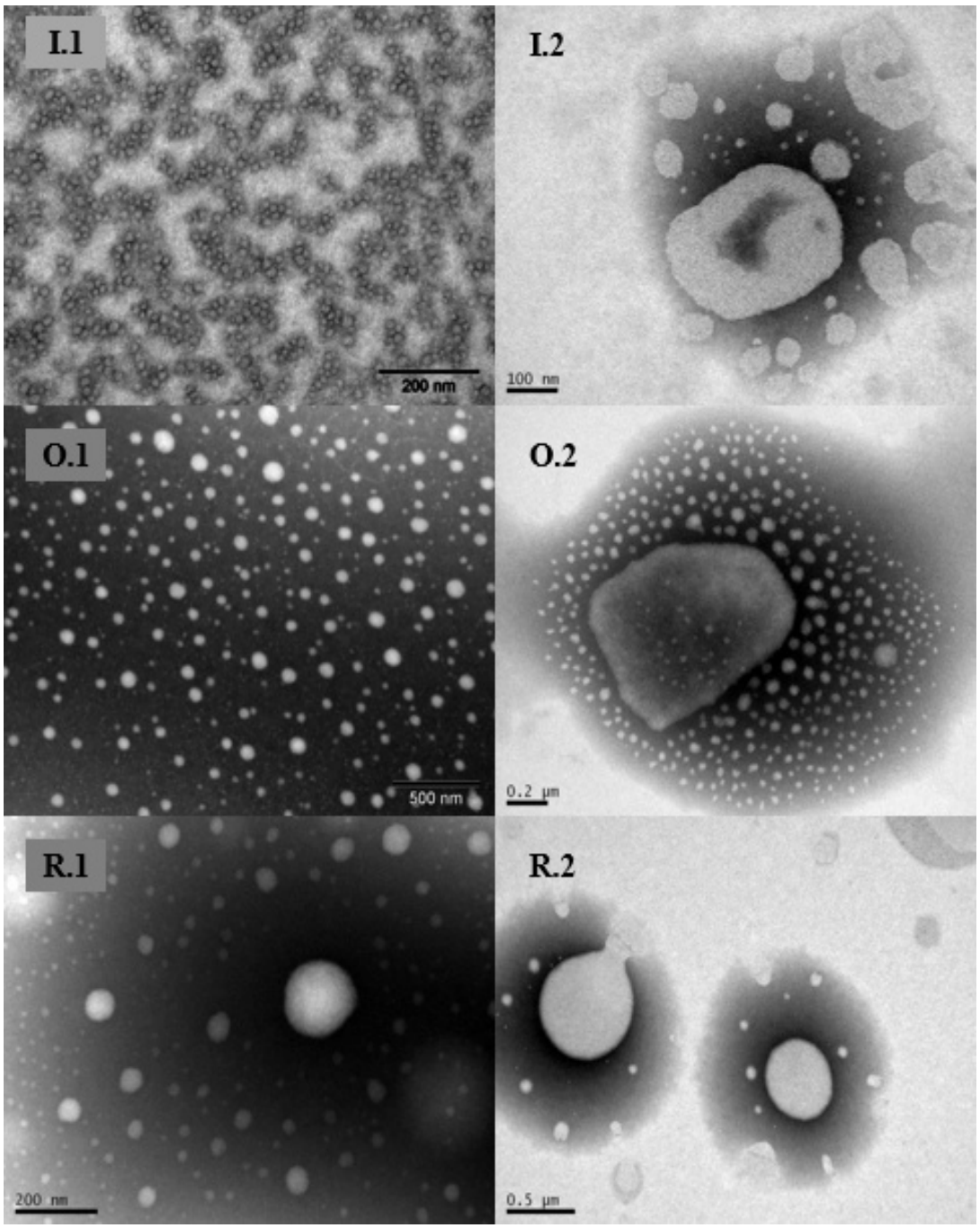

Figure 3.6. TEM images of fish oil loaded nanoparticles obtained by SFEE (left) and conventional solvent evaporation (right) from formulations I, O and R.

3.3.3 Formation of nanoparticles through conventional solvent evaporation

The three selected formulations were treated by solvent evaporation at atmospheric pressure using a hotplate with temperature and stirring control at 313 K for 8 h inside a fume hood. The characteristics of the particles obtained by this method are shown in Table 3.6. These particles presented worse characteristics than those obtained by SFEE. The nanoparticles produced from formulation R had much lower encapsulation efficiency and a strong fishy smell. As for those obtained from formulation O, they had a residual concentration of acetone higher than the allowed in the pharmaceutical industry [8], and the particles were aggregated (Figure 3.6). Finally, the particles obtained from formulation I had a residual acetone concentration higher than that accepted in the food industry [9], and they presented a strong fish odor after the extraction process and were aggregated. These results could be caused by the loss of emulsion stability, the mechanical stress caused by the magnetic stirrer, the process temperature or the contact with air.

Table 3.6. Characteristics of the fish oil loaded nanoparticles produced by solvent evaporation from formulations I, O and R. EE means Encapsulation Efficiency; LC, Loading Capacity; $[Acetone]_R$, Residual Acetone Concentration.

Formulation	EE ± SD (%)	LC ± SD (%)	$[Acetone]_R$ ± SD (ppm)	Fishy smell
I	49 ± 7	13 ± 2	758 ± 101	Strong
O	19 ± 12	5 ± 4	6295 ± 804	Weak
R	10 ± 5	3 ± 1	34 ± 4	Strong

Consequently, the good characteristics obtained in the particles by means of SFEE make this technology an alternative for the encapsulation of liquid lipophilic compounds. However, to achieve its commercial exploitation it is necessary to reduce CO_2 consumption and increase production capacity.

3.4. Scale-up and continuous production of vitamin E nanocapsules

The encapsulation of vitamin E in PCL was done using four SFEE installations: A) a bubble column, B) a bubble column with gas redistributor, C) a spray column and D) a packed column. Table 3.7 summarizes the characteristics of each extraction equipment. Details of each installation can be found in Publication III. Performance of each installation was compared in terms of organic solvent removal, CO_2 consumption and nanocapsule characteristics (encapsulation efficiency, particle size distribution and morphology).

Table 3.7. Summary of the characteristics of the extraction equipment used. L/D means length to diameter ratio; V, volume; Q CO_2, CO_2 flow rate.

Equipment	L/D	V (mL)	Q CO_2 ($g \cdot min^{-1}$)	Amount of emulsion treated	Operation mode
Bubble column	9	10	0.3-0.9	5 g	Discontinuous
Bubble column + gas redistributor	4	500	3.0	40 g	Discontinuous
Spray column	4	500	15.0	1-3 $mL \cdot min^{-1}$	Continuous & co-current flow
Packed column	67	1765	10.0-30.0	1-4 $mL \cdot min^{-1}$	Continuous & counter-current flow

3.4.1 Comparison of the effect of the different configurations on acetone removal and CO_2 consumption.

In order to make such comparison, same emulsion formulation was used (formulation 20), as well as same pressure and temperature conditions, 8.0 MPa and 313 K. CO_2 flow rate was chosen to maximize acetone extraction according to hydrodynamics of each installation. Operation was maintained until 50 ppm of residual acetone concentration was reached (in batch experiments) or until a certain amount of

emulsion was treated (in continuous experiments). Figure 3.7 shows the acetone removal versus the CO_2/acetone ratio in the four extraction installations used.

The first apparatus selected for the nanoencapsulation of vitamin E in polycaprolactone was a bubble column (configuration A). Only one or two theoretical stages can be achieved in this equipment [7]; however, they are widely used as multiphase contactors in the chemical, petrochemical and biochemical industries, since they have excellent heat and mass transfer characteristics and require little maintenance and low operating costs [25].

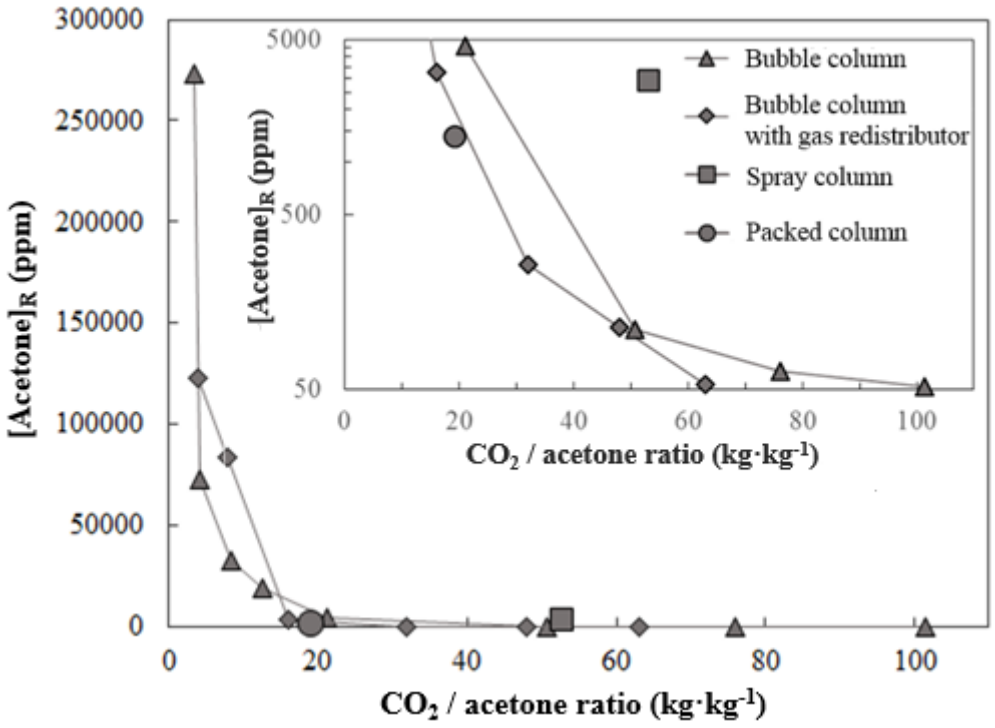

Figure 3.7. Comparison of the acetone removal in four supercritical extraction installations.

In this equipment, as it was aforementioned and can be seen in Figure 3.7, 50 min and a CO_2/acetone mass ratio of 21 kg CO_2·kg acetone^{-1} were required to achieve the maximum acetone concentration permitted in pharmaceutics (5000 ppm) [8]. Operating time and CO_2/acetone mass ratio had to be increased to 240 min and 101 kg CO_2·kg acetone^{-1}, respectively, in order to achieve the maximum acetone concentration of 50 ppm required in food production [9]. Similar CO_2 consumption was required by Lévai *et al*. [45] in the encapsulation of quercetin in lecithin.

The following equipment used was a larger bubble column with a gas redistributor (configuration B). This equipment consisted of a 500 mL cylindrical stainless steel vessel with a length to diameter (L/D) ratio of four. CO_2 entered in the vessel through a porous plate distributor to improve the contact between the CO_2 and the emulsion. Porous plate distributors affect bubble size, bubble velocity, and gas hold-up [27]. Forty grams of the freshly prepared starting emulsion were placed inside the vessel and CO_2 was bubbled through until the selected operating time was reached. After slow depressurization, a suspension of nanoparticles in water was recovered.

Experiments were done at the highest CO_2 flow rate, avoiding entrainment of the emulsion, which was 3 g·min^{-1} (4.5 kg CO_2·h^{-1}·kg emulsion^{-1}). The extraction curves in both bubble columns (A and B) are compared in Figure 3.7. Again, two distinct periods were detected, i.e., a first period where acetone removal was rapid, and a second period where the extraction rate slowed down due to the lower driving force and internal diffusion control. However, in configuration B, acetone removal proceeded faster; therefore, a lower amount of CO_2 was required. 63 kg CO_2·kg acetone^{-1} were required to achieve a residual organic solvent concentration of about

50 ppm, which is almost half the amount required in configuration A. Therefore, the presence of the porous plate distributor and the increase in the CO_2 flow rate improved mass transfer. Della Porta el al. [28] obtained a residual acetone concentration of 4000 ppm in the nanoparticle suspension when they encapsulated retinyl acetate in PLGA by SFEE. As similar CO_2/acetone ratio was used, the difference could be due to a lower operating temperature (309 K) and a higher CO_2 flow rate (7 $g \cdot min^{-1}$), which provided less contact time, as well as to the presence of glycerol in the aqueous phase, which could also affect mass transfer.

The comparison of the published works done on SFEE in bubble columns with gas redistributors showed that ethyl acetate is more readily extractable than acetone, since it required a lower amount of CO_2 and consequently less operating time. This could be justified by the difference between the distribution coefficient for the systems acetone-water-CO_2 and ethyl acetate-water-CO_2 at similar pressure and temperature conditions [29, 30, 31].

Further experiments were carried out in a spray column, which corresponds to configuration C. It consists of an empty vessel in which a continuous gas phase contacts an atomized liquid phase usually generated in a nozzle [7]. The spray column used was a cylindrical stainless steel vessel of 500 mL with an L/D of four, in which the freshly prepared starting emulsion was sprayed through a stainless steel nozzle, and CO_2 was introduced co-currently in the chamber through another inlet port, next to the nozzle. A 100 mL stainless steel vessel (L/D=6) after the BPR was used to continuously separate the gas phase from the nanocapsule suspension. The operation was considered complete once the desired amount of emulsion was processed. The arrangement of the spray column is shown in Figure 3.8.

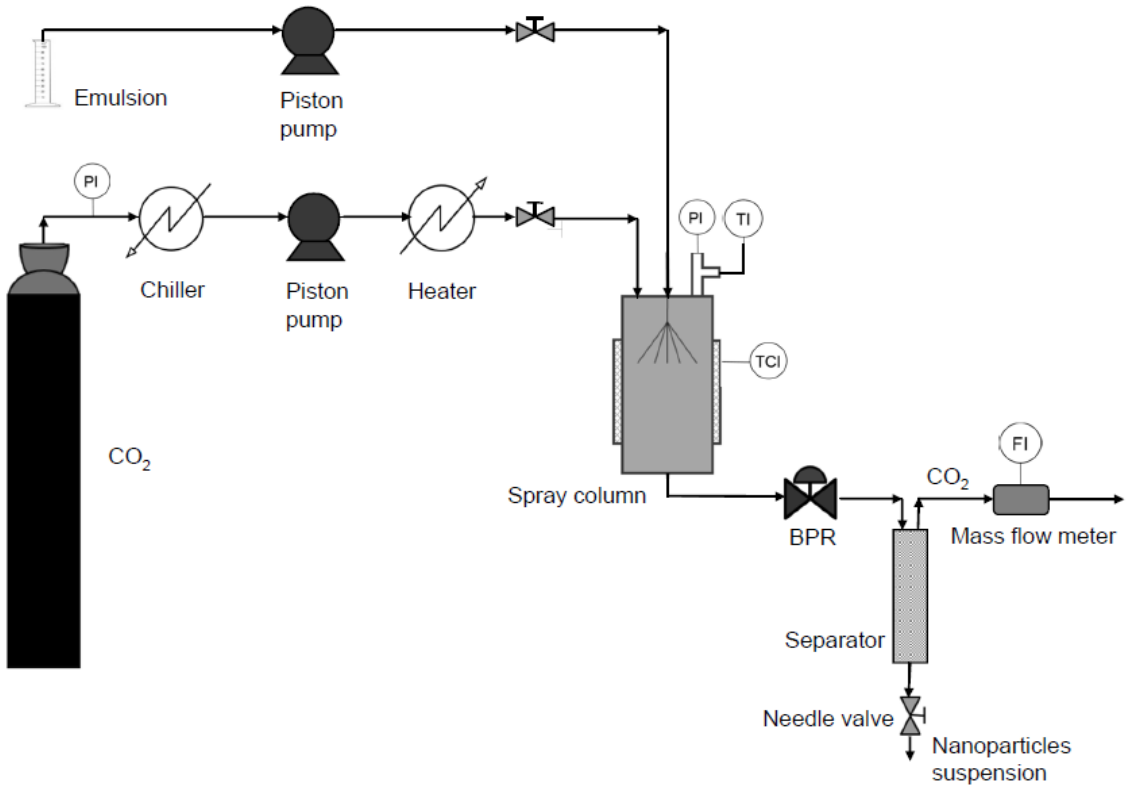

Figure 3.8. Scheme of the spray column configuration used for continuous SFEE.

This equipment is used when only one or two stages and a very low pressure drop are required, and when the solute is very soluble in the solvent [7]. Mass transfer in this installation is conditioned by the design of the spray system [32] and the hydrodynamics of the vessel [33]. However, neither the flow rate of the emulsion nor the diameter of the nozzle had a significant effect on acetone removal. Nozzle diameter did not affect particle diameter either. Santos *et al*. [34] also did not observe any influence of process parameters on particle size for the encapsulation of β - carotene and lycopene in n-OSA starch by SFEE in a spray column.

A CO_2 flow rate of 15 $g \cdot min^{-1}$ was used in the spray column operating in continuous mode, which was the highest possible rate. An increase in the solvent ratio notably increased acetone extraction, achieving the lowest residual acetone

concentration of around 3000 ppm with a CO_2/acetone mass ratio of 53 kg CO_2·kg acetone^{-1}. However, residual acetone concentrations lower than that could not be obtained with this installation. It is noteworthy that same acetone concentration could be obtained in the bubble column using a lower CO_2/acetone ratio, but the operation was discontinuous.

Other authors obtained lower residual organic solvent concentrations using a further extraction step [34, 35]. The aqueous suspension of the particles was bubbled with more CO_2 to completely remove the organic solvent, similar to what is done in the SAS process. This washing step allowed decreasing the organic solvent content in the suspension; however, it increased CO_2 consumption and the total process time.

Another possibility for increasing contact time in spray columns and accordingly decreasing the organic solvent concentration is to increase the length of the spray column. Chattopadhyay *et al*. [36] proposed in their patent the combination of the spray column with the use of internal packing and countercurrent operation in order to maximize contact between the emulsion and supercritical CO_2.

The fourth equipment used for the production of vitamin E nanocapsules was a high-pressure packed column (configuration D). This apparatus consisted of a 3 m long column with an internal diameter of 0.03 m, packed with a random stainless steel packing, Propak. The starting emulsion and fresh supercritical CO_2 were delivered to the column countercurrently. CO_2 and the extract were depressurized down to atmospheric pressure in a separator and the gas stream was vented in the hood. CO_2 was not recycled. The nanoparticle suspension was recovered by opening a needle valve at the bottom of the column. A scheme of this installation is shown in Figure 3.9.

In this equipment, the countercurrently flowing phases come into contact with each other on the packing surface, promoting rapid mass transfer. Packed columns are preferred when corrosion or foaming may occur, or even when the pressure drop must be low. These are possible scenarios when working with emulsions and supercritical fluids.

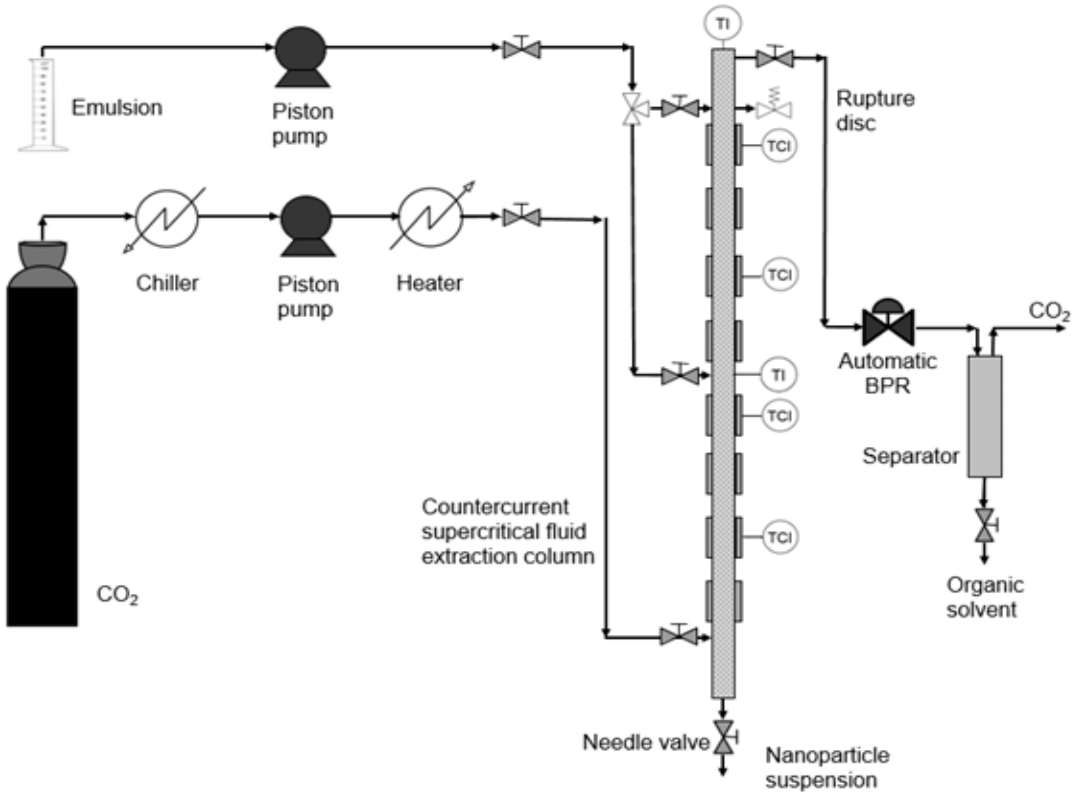

Figure 3.9. Scheme of the packed column configuration used for continuous SFEE.

A key factor is the hydrodynamic behavior of the packed column (flooding, pressure drop and liquid hold-up) which conditions mass transfer. Consequently, the hydrodynamic behavior of the column was first studied. Flow in a gravity driven column depends on the density difference between the phases. With a liquid phase density of 930 $kg \cdot m^{-3}$, CO_2 densities higher than 500 $kg \cdot m^{-3}$ provoked column flooding. However, at CO_2 densities lower than 500 $kg \cdot m^{-3}$, column flooding was not

observed at liquid flow rates between 1 and 5 $mL \cdot min^{-1}$ and CO_2 flow rates between 10 and 30 $g \cdot min^{-1}$. These experimental results were corroborated by the flooding correlations of Sherwood [37], Brunner [38] and Lobo [39] at gas to liquid ratios between 2 and 30 $kg \cdot kg^{-1}$ and CO_2 density of 280 $kg \cdot m^{-3}$, which indicate that CO_2 flow rate should be much higher (400 $g \cdot min^{-1}$) to provoke flooding in this column. On the other hand, liquid flow rates lower than 10 $mL \cdot min^{-1}$ did not provoke the entrainment of the dense phase at any CO_2 flow rates.

Then, time required to reach steady state was studied. It was considered that the system achieved steady state when the residual acetone concentration in the raffinate remained unchanged. For this column, it was necessary to wait 3 h. High stabilization times were also reported by other authors for the separation of organic compounds from aqueous solutions [40, 41].

Subsequently, the effects of liquid and CO_2 flow rates on acetone removal were also studied. At a CO_2 flow rate of 20 $g \cdot min^{-1}$and a liquid flow rate of 4 $mL \cdot min^{-1}$, the highest extraction yields were achieved, probably due to a better wetting of the packing.

Although the presence of solids is not recommended in packed columns due to the blockage of the packing, no problem was observed, maybe due to the small size of the solid particles and to the presence of the surfactant in the aqueous particle suspension, which prevented the particles from sticking on the packing surface. Additionally, foaming was not observed at surfactant concentrations up to 10%. According to Della Porta *et al*. [28] emulsions containing thickening agents did not cause problems either.

Formulations 18 and 20 were treated in the column; however, only results for formulation 20 are shown here. Results for formulation 18 could be found in Publication IV. Under the best operating conditions, the obtained nanoparticles had a residual acetone concentration of 1410 ± 310 ppm, using for that a CO_2/acetone mass ratio of 19 kg CO_2·kg acetone^{-1}. This residual acetone concentration was much lower than 5000 ppm, so they were suitable for use in the pharmaceutical industry [8]. However, a residual concentration of 50 ppm required for food applications [9] could not be reached with this column.

When compared with all other configurations (Figure 3.7), it is clear that this configuration provided the highest acetone removal efficiency. As it can be seen in Table 3.8, to achieve such acetone concentration in the nanoparticle suspension, between 25 and 45 kg CO_2·kg acetone^{-1} in the bubble columns and > 60 kg CO_2·kg acetone^{-1} in the spray column were necessary.

Table 3.8. Comparison of the different configurations tested in acetone removal.

Equipment	**Operation mode**	**$[Acetone]_R$ = 1410 ± 310 ppm**	
		Contact time (min)	**CO_2/acetone ratio (kg·kg^{-1})**
Bubble column	Discontinuous	100	42
Bubble column + gas redistributor	Discontinuous	97	26
Spray column	Continuous	< 1	> 60
Packed column	Continuous	≈ 10	19

Therefore, in order to enhance the extraction yield, it would be advisable to study taller columns and other packing types. Although this study could not be performed in an experimental column, the possibility of using taller columns was studied by process simulation in Aspen Plus (section 3.4.3).

3.4.2 Comparison of the effect of the different configurations on nanoparticle characteristics.

The different configurations not only affected acetone extraction but also nanoparticle characteristics as can be seen in Table 3.9. Whilst configurations A and B provided particles with the same characteristics, C and D produced particles with a much smaller particle size, higher polydispersity index and lower encapsulation efficiency. Apart from the important difference in the operating mode and the hydrodynamics of continuous versus batch operation, the difference in the state and amount of CO_2 during the first contact with the emulsion could explain these results. In the tests performed in the bubble columns (A and B configurations), CO_2 was introduced at 6.0 MPa during temperature adjustment to 313 K, and then pressure was increased to 8.0 MPa; while in the tests performed in the spray and packed columns (C and D configurations), CO_2 and the emulsion come into contact at 8.0 MPa and 313 K. Precipitation in the supercritical region usually generates smaller and amorphous particles because of a fast expansion of the liquid phase upon contact with CO_2 [42, 43]. This fact could also explain the lower encapsulation efficiency obtained in configurations C and D.

Table 3.9. Comparison of the nanoparticle characteristics obtained by different supercritical fluid extraction equipment. EE means Encapsulation Efficiency; PdI, Polydispersity Index; $[Acetone]_R$, Residual Acetone Concentration.

Configuration	EE ± SD (%)	Mean size ± SD (nm)	PdI ± SD	$[Acetone]_R$ ± SD (ppm)
A) Bubble column	90.5 ± 1.1	153 ± 33	0.26 ± 0.02	52 ± 7
B) Bubble column + gas redistributor	89.1 ± 1.4	144 ± 2	0.19 ± 0.01	53 ± 14
C) Spray column	71.7 ± 4.5	60 ± 15	0.34 ± 0.06	2950 ± 850
D) Packed column	72.6 ± 2.6	84 ± 1	0.42 ± 0.10	1410 ± 340

The comparison between the morphology of the nanoparticles obtained in the four configurations was studied through TEM images, and it is shown in Figure 3.10. It seems that the operating mode and the hydrodynamics also affected nanoparticle morphology. Therefore, configuration A produced non-aggregated spherical nanocapsules. As turbulence increased, as in configuration B, the shape of the particles lost some sphericity, becoming more similar to an ellipsoid, which could be caused by particle aggregation. Regarding configuration C, besides the aforementioned size reduction, a greater presence of angular particles was observed. This could also be related to the fast expansion of the liquid phase, as well as to a high degree of turbulence in the nozzle. Particles obtained in configuration D, not being perfect spheres, were rounder than those obtained in configuration C, probably due to the lower degree of turbulence generated by the packing.

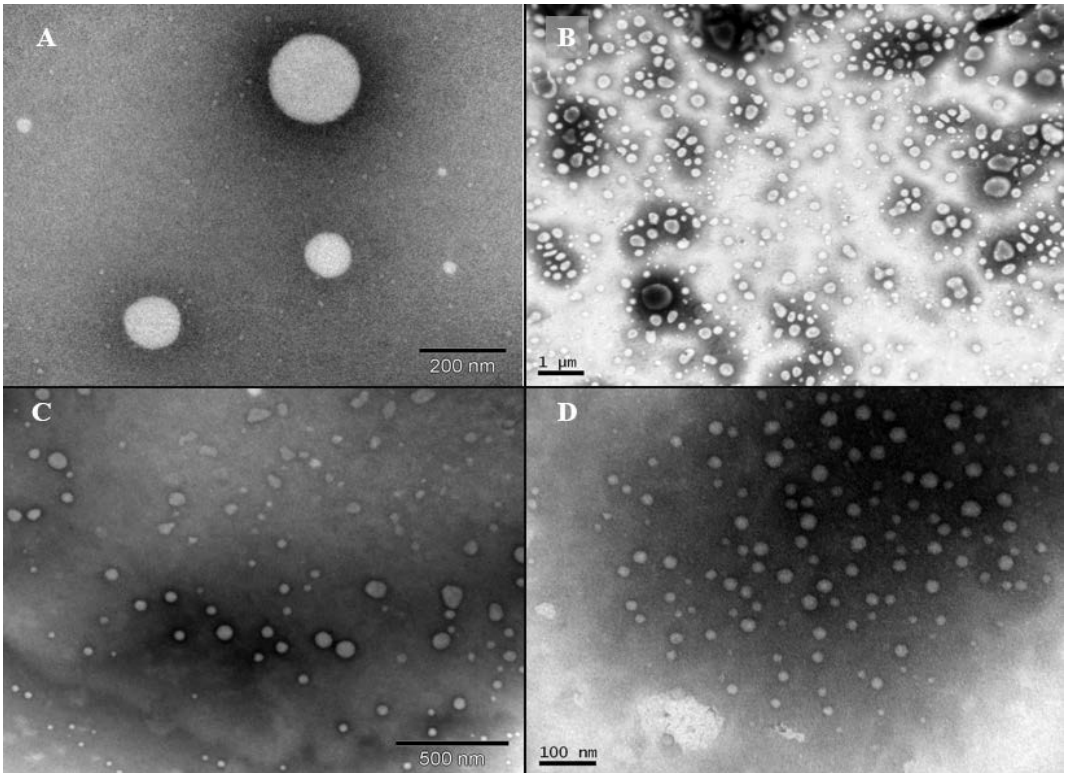

Figure 3.10. Morphological comparison of the nanocapsules obtained by SFEE in different supercritical fluid extraction equipment. Image A: bubble column; B: bubble column with as redistributor; C: spray column; and D: packed column.

3.4.3 Column simulation.

The performance of a taller high-pressure packed column on acetone removal was evaluated by means of process simulation with Aspen Plus. To simulate the acetone extraction from the emulsion by supercritical CO_2, only the three major components of the system: carbon dioxide, acetone and water, were used. The CO_2-acetone-water system shows a peculiar phase behavior, since CO_2 has a salting out effect in the acetone-water mixture [44, 45]. In order to select the thermodynamic model, a comparison was made between the available experimental phase equilibrium data in the two-phase region over the upper critical solution pressure at 313 K [30, 31] and that provided by the simulation software using the implemented thermodynamic models. Thereby, the best models were SR-Polar and PSRK. Of the two, SR-Polar represented the literature data slightly better than PSRK did. Figure 3.11 shows a comparison between the available phase equilibrium data and data generated by Aspen Plus with the SR-Polar thermodynamic model. At molar fractions of acetone below 12% the fitting was good, and it is in this range of low concentrations of acetone where the column operated.

The high-pressure packed column was modeled with the help of the Extract block. The column was operated in countercurrent flow without reflux. Pressure in the column was kept constant at 8.0 MPa. Estimated temperature in the first stage was 318 K. The input conditions supplied to the program for formulation 20 are summarized in Table 3.10. In Publication IV can be also found results for formulation 18.

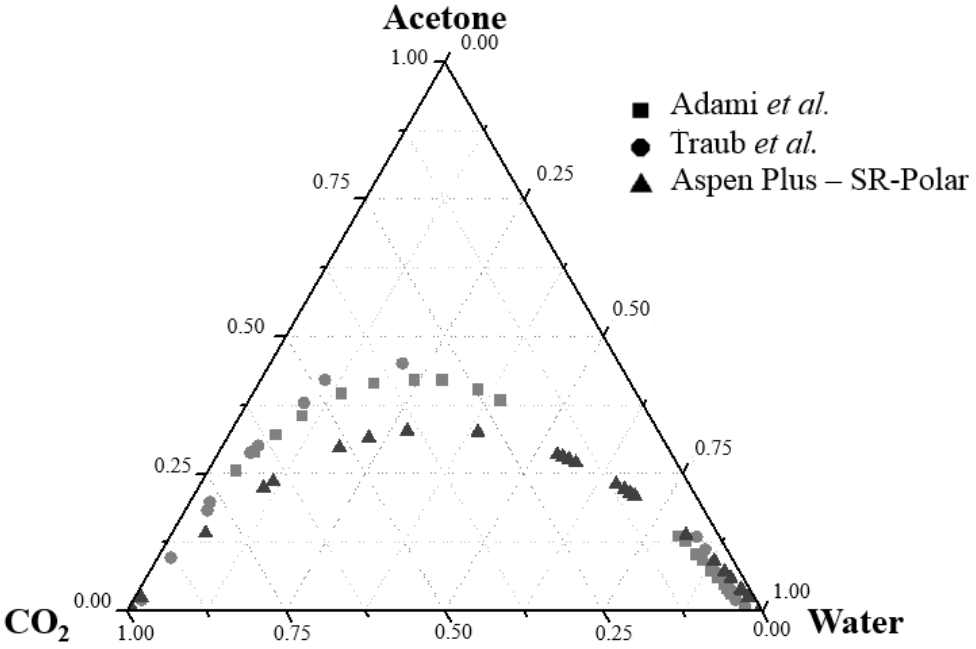

Figure 3.11. Comparison of the CO_2 / acetone / water phase equilibrium data from Adami *et al*. [31], Traub *et al*. [30] and the data provided by Aspen Plus using the model SR-Polar, at 10.0 MPa and 313 K.

The number of theoretical stages was determined iteratively in order to find the value that reproduced the experimental results. When the composition of the Feed stream was formulation 20, four theoretical stages were required to obtain a residual acetone concentration in the Raffinate stream close to the experimental value of 1410 ± 340 ppm. Two theoretical stages produced a Raffinate stream of 15000 ppm; this value was consistent with the experimental residual acetone concentration in the Raffinate stream (15400 ± 310 ppm) obtained when the emulsion was introduced at the second inlet of the column where only 1 m of packing height was used.

The height equivalent to a theoretical stage (HETP) could be estimated through the comparison between the simulation and the experimental data. It varied between 0.4-0.5 m depending on the composition of the Feed stream. These values are

consistent with those reported in the literature for aqueous mixtures [46]. Budich *et al*. [40] obtained HETP between 0.25 and 1 m for the supercritical fluid extraction of ethanol from aqueous solutions using Sulzer CY packing.

Table 3.10. Simulation results of the SFEE column using Aspen Plus with the SR-Polar model and the Extract block with four theoretical stages.

	CO_2	**Feed**	**Extract**	**Raffinate**
T (K)	313	313	320	312
P (MPa)	8.5	8.0	8.0	8.0
Flow rate (g·min^{-1})	20.0	3.7	21.1	2.6
Composition (by mass):				
CO_2	100%	0	946923 ppm	10589 ppm
Acetone	0	28.4%	49704 ppm	936 ppm
Water	0	71.6%	3373 ppm	988475 ppm

In order to reach the residual acetone concentration of 50 ppm required for food applications [9] at these operating conditions, it was necessary to increase the number of theoretical stages. Figure 3.12 shows the evolution of the residual acetone concentration in the Raffinate stream with the number of theoretical stages. Seven theoretical stages were required to reach an acetone concentration in the Raffinate stream below 50 ppm. Therefore, it would be necessary to increase the packing height to 3.5 m.

A sensitivity analysis was also performed studying the variation of the Raffinate composition with the number of stages at different solvent to feed ratios. The calculation was carried out at a constant feed flow rate of 4 mL·min^{-1} and with various CO_2 flow rates. Results are shown in Figure 3.13. By increasing the solvent to feed ratio, acetone extraction increased and consequently it would be possible to reduce the required number of theoretical stages. Indeed, by increasing the CO_2 flow

rate to 60 g·min^{-1}, it would be feasible to obtain a residual acetone concentration in the Raffinate stream lower than 50 ppm using the same column.

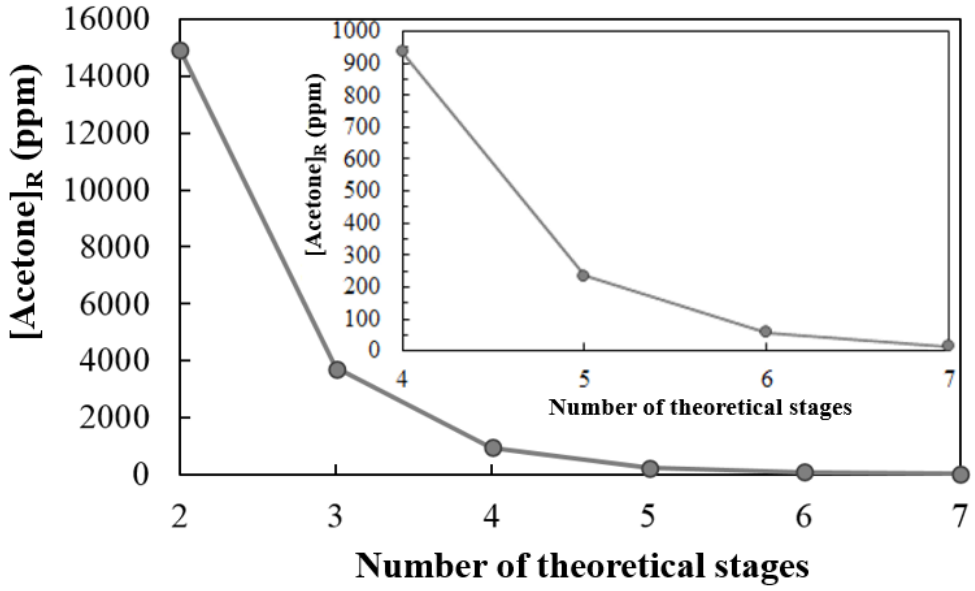

Figure 3.12. Dependence of the composition of the Raffinate stream on the number of theoretical stages.

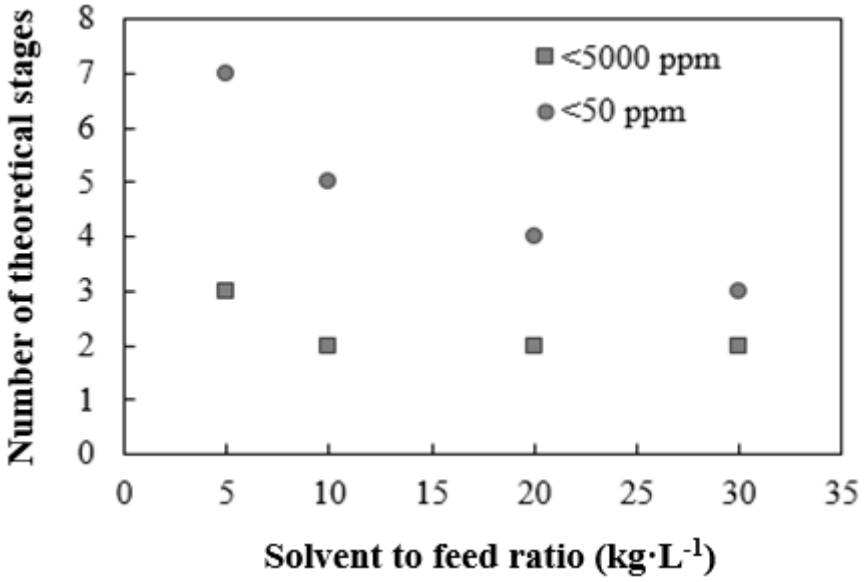

Figure 3.13. Influence of the solvent to feed ratio on the required number of theoretical stages for a desired residual acetone concentration in the nanoparticle suspension.

By means of simulation with Aspen Plus, it was determined that it is possible to obtain a suspension of nanoparticles with a residual acetone concentration suitable for the food industry. However, it would be interesting to test it experimentally with a column that fulfilled those conditions and even to try other types of packing materials that improve the contact between phases.

References

[1] K. Shinoda, B. Lindman, Organized surfactant systems: microemulsions, Langmuir 3 (1987) 135-149, http://dx.doi.org/10.1021/la00074a001.

[2] D.J. McClements, Particle characteristics and their impact on physicochemical properties of delivery systems, in: D.J. McClements, Nanoparticle- and Microparticle-based Delivery Systems. Encapsulation, Protection and Release of Active Compounds, CRC Press, Boca Raton, 2014, pp. 79-122, http://dx.doi.org/ 10.1201/b17280-4.

[3] S.P. Moulik, A.K. Rakshit, Physicochemistry and applications of microemulsions, Journal of Surface Science and Technology 22 (2006) 159-186.

[4] B.A. Kerwin, Polysorbates 20 and 80 used in the formulation of protein biotherapeutics: structure and degradation pathways, Journal of Pharmaceutical Sciences 97 (2008) 2924-2935, http://dx.doi.org/10.1002/jps.21190.

[5] H.Y. Chiu, M.J. Lee, H.M. Lin, Vapor-liquid phase boundaries of binary mixtures of carbon dioxide with ethanol and acetone, Journal of Chemical Engineering Data 53 (2008) 2393-2402, http://dx.doi.org/10.1021/je800371a.

[6] J. Chrastil, Solubility of solids and liquids in supercritical gases, Journal of Physical Chemistry 86 (1982) 3016-3021, http://dx.doi.org/10.1021/j100212a041.

[7] J.D. Seader, E.J. Henley, D.K. Roper, Separation Process Principles, 3rd ed. John Wiley & Sons, New York, 2010, pp. 207-213.

[8] Guidance for Industry Q3C- Tables and List, U.S. Department of Health and Human Services, Food and Drug Administration Center for Drug Evaluation

and Research (CDER), Center for Biologics Evaluation and Research (CBER), ICH, Revision 2, 2012.

[9] Spain 2011. Real Decreto 1101/2011, de 22 de Julio, por el que se aprueba la lista positiva de los disolventes de extracción que se pueden utilizar en la fabricación de productos alimenticios y de sus ingredientes. Boletín Oficial del Estado, 30 de Agosto de 2011, 208, 94132-94137.

[10] N. Khayata, W. Abdelwahed, M.F. Chehna, C. Charcosset, H. Fessi, Preparation of vitamin E loaded nanocapsules by the nanoprecipitation method: From laboratory scale to large scale using a membrane contactor, International Journal of Pharmaceutics 423 (2012) 419-427, http://dx.doi.org/10.1016/j.ijpharm.2011.12.016.

[11] M. Li, O. Rouaud, D. Poncelet, Microencapsulation by solvent evaporation: State of the art for process engineering approaches, International Journal of Pharmaceutics 363 (2008) 26-39, http://dx.doi.org/10.1016/j.ijpharm.2008.07.018.

[12] S. Begum, I.P. Jones, C. Jiao, D.E. Lynch, J.A. Preece, Characterisation of hollow Russian doll microspheres, Journal of Materials Science 45 (2010) 3697-3706, http://dx.doi.org/10.1007/s10853-010-4479-3.

[13] E. Dickinson, Hydrocolloids at interfaces and the influence on the properties of dispersed systems, Food Hydrocolloids 17 (2003) 25-39, http://dx.doi.org/ 10.1016/S0268-005X(01)00120-5.

[14] D.J. McClements, E.A. Decker, Lipid oxidation in oil-in-water emulsions: impact of molecular environment on chemical reactions in heterogeneous Food

Systems, Journal of Food Science 65 (2000) 1270-1282, http://dx.doi.org/10.1111/j.1365-2621.2000.tb10596.x.

[15] C. Borch-Jensen, J. Mollerup, Phase equilibria of fish oil in sub- and supercritical carbon dioxide, Fluid Phase Equilibria 138 (1997) 179-211, http://dx.doi.org/10.1016/S0378-3812(97)00155-6.

[16] G. Lévai, A. Martín, S. Rodríguez Rojo, M.J. Cocero, T.M. Fieback, Measurement and modelling of mass transport properties during the supercritical fluid extraction of emulsions, Journal of Supercritical Fluids (2017) http://dx.doi.org/10.1016/j.supflu.2017.01.015.

[17] K. Dubbert, N. Rubio-Rodríguez, S. Kareth, S. Beltrán, M. Petermann, Encapsulation of fish oil in biodegradable polymers by the PGSS process, in: Institut National Polytechnique de Lorraine (Ed.), Proceedings of the 13th European Meeting on Supercritical Fluids, The Hague, 2011, p. 176.

[18] S. Varona, A. Martín, M.J. Cocero, C.M.M. Duarte, Encapsulation of lavandin essential oil in poly-(ε-caprolactone) by PGSS process, Chemical Engineering & Technology 36 (2013) 1187-1192, http://dx.doi.org/10.1002/ceat.201200592.

[19] A. Gulotta, A.H. Saberi, M.C. Nicoli, D.J. McClements, Nanoemulsion-based delivery systems for polyunsaturated (ω-3) oils: formation using a spontaneous emulsification method, Journal of Agricultural and Food Chemistry 62 (2014) 1720-1725, http://dx.doi.org/10.1021/jf4054808.

[20] V. Krtonošić, L. Dokić, P. Dokić, T. Dapčević, Effects of xanthan gum on physicochemical properties and stability of corn oil-in-water emulsions

stabilized by polyoxyethylene (20) sorbitan monooleate, Food Hydrocolloids 23 (2009) 2212-2218, http://dx.doi.org/10.1016/j.foodhyd.2009.05.003.

[21] D.L. Boschetto, I. Dalmolin, A.M. de Cesaro, A.A. Rigo, S.R.S. Ferreira, M.A.A. Meireles, E.A.C. Batista, J. Vladimir Oliveira, Phase behavior and process parameters effect on grape seed extract encapsulation by SEDS technique, Industrial Crops and Products 50 (2013) 352-360, http://dx.doi.org/10.1016/j.indcrop.2013.07.044.

[22] Z. Wen, B. Liu, Z. Zheng, X. You, Y. Pu, Q. Li, Preparation of liposomes entrapping essential oil from *Atractylodes Macrocephala Koidz* by modified RESS technique, Chemical Engineering Research and Design 88 (2010) 1102-1107, http://dx.doi.org/10.1016/j.cherd.2010.01.020.

[23] J. Rodríguez, M.J. Martín, M.A. Ruíz, B. Clares, Current encapsulation strategies for bioactive oils: From alimentary to pharmaceutical perspectives, Food Research International 83 (2016) 41-59, http://dx.doi.org/10.1016/j.foodres.2016.01.032.

[24] M.J. Choi, U. Ruktanonchai, A. Soottitantawat, S.G. Min, Morphological characterization of encapsulated fish oil with β-cyclodextrin and polycaprolactone, Food Research International 42 (2009) 989-997, http://dx.doi.org/10.1016/j.foodres.2009.04.019.

[25] N. Kantarci, F. Borak, K.O. Ulgen, Bubble column reactors, Process Biochemistry 40 (2005) 2263-2283, http://dx.doi.org/10.1016/j.procbio.2004.10.004.

[26] G. Lévai, A. Martín, E. de Paz, S. Rodríguez-Rojo, M.J. Cocero, Production of stabilized quercetin aqueous suspensions by supercritical fluid extraction of

emulsions, Journal of Supercritical Fluids 100 (2015) 34-45, http://dx.doi.org/10.1016/j.supflu.2015.02.019.

[27] R. Lau, W.S. Beverly Sim, R. Mo, Effect of gas distributor on hydrodynamics in shallow bubble column reactors, The Canadian Journal of Chemical Engineering 87 (2009) 847-854, http://dx.doi.org/10.1002/cjce.20224.

[28] G. Della Porta, R. Campardelli, N. Falco, E. Reverchon, PLGA microdevices for retinoids sustained release produced by supercritical emulsions extraction: continuous versus batch operation layouts, Journal of Pharmaceutical Sciences 100 (2011) 4357-4367, http://dx.doi.org/10.1002/jps.22647.

[29] S. Klaus Luther, J.J. Schuster, A. Leipertz, A. Braeuer, Non-invasive quantification of phase equilibria of ternary mixtures composed of carbon dioxide, organic solvent and water, Journal of Supercritical Fluids 84 (2013) 146-154, http://dx.doi.org/10.1016/j.supflu.2013.09.012.

[30] P. Traub, K. Stephan, High-pressure phase equilibria of the system CO_2-water-acetone measured with a new apparatus, Chemical Engineering Science 45 (1990) 751-758, http://dx.doi.org/10.1016/0009-2509(90)87016-L.

[31] R. Adami, J. Schuster, S. Liparoti, E. Reverchon, A. Leipertz, A. Braeuer, A Raman spectroscopic method for the determination of high pressure vapour liquid equilibria, Fluid Phase Equilibria 300 (2013) 265-273, http://dx.doi.org/10.1016/j.fluid.2013.09.046.

[32] C. Vemavarapu, M.J. Mollan, M. Lodaya, T.E. Needham, Design and process aspects of laboratory scale SCF particle formation systems, International Journal of Pharmaceutics 292 (2005) 1-16, http://dx.doi.org/10.1016/j.ijpharm.2004.07.021.

[33] R. Thiering, F. Dehghani, N.R. Foster, Current issues relating to anti-solvent micronisation techniques and their extension to industrial scales, Journal of Supercritical Fluids 21 (2001) 159-177, http://dx.doi.org/10.1016/S0896-8446(01)00090-0.

[34] D.T. Santos, A. Martín, M.A.A. Meireles, M.J. Cocero, Production of stabilized sub-micrometric particles of carotenoids using supercritical fluid extraction of emulsions, Journal of Supercritical Fluids 61 (2012) 167-174, http://dx.doi.org/10.1016/j.supflu.2011.09.011.

[35] F. Mattea, A. Martín, A. Matías-Gago, M.J. Cocero, Supercritical antisolvent precipitation from an emulsion: β-Carotene nanoparticle formation, Journal of Supercritical Fluids 51 (2009) 238-247, http://dx.doi.org/10.1016/j.supflu.2009.08.013.

[36] P. Chattopadhyay, B.Y. Shekunov, J.S. Seitzinger, Method and apparatus for continuous particle production using supercritical fluids, US Patent 20040156911A1.

[37] T.K. Sherwood, G.H. Shipley, F.A.L. Holloway, Flooding velocities in packed columns, Industrial and Engineering Chemistry 30 (1938) 765-769, http://dx.doi.org/10.1021/ie50343a008.

[38] R. Stockfleth, G. Brunner, Film thickness, flow regimes, and flooding in countercurrent annular flow of a falling film at high pressures, Industrial & Engineering Chemistry Research 40 (2001) 6014-6020, http://dx.doi.org/10.1021/ie0100885.

[39] W.E. Lobo, L. Friend, F. Hashmall, F. Zenz, Limiting capacity of dumped tower packings, Transactions of the American Institute of Chemical Engineers 41 (1945) 693.

[40] M. Budich, G. Brunner, Supercritical fluid extraction of ethanol from aqueous solutions, Journal of Supercritical Fluids 25 (2003) 45-55, http://dx.doi.org/10.1016/S0896-8446(02)00091-8.

[41] J.S. Lim, Y.W. Lee, J.D. Kim, Y.Y. Lee, H.S. Chun, Mass-transfer and hydraulic characteristics in spray and packed extraction columns for supercritical carbon dioxide-ethanol-water system, Journal of Supercritical Fluids 8 (1995) 127-137, http://dx.doi.org/10.1016/0896-8446(95)90025-X.

[42] E. Reverchon, I. De Marco, Mechanisms controlling supercritical antisolvent precipitate morphology, Chemical Engineering Journal 169 (2011) 358-370, http://dx.doi.org/10.1016/j.cej.2011.02.064.

[43] E. Reverchon, Supercritical antisolvent precipitation of micro- and nano-particles, Journal of Supercritical Fluids 15 (1999) 1-21, http://dx.doi.org/10.1016/S0896-8446(98)00129-6.

[44] M. Wendland, H. Hasse, G. Maurer, Multiphase high-pressure equilibria of carbon dioxide-water-acetone, Journal of Supercritical Fluids 7 (1994) 245-250, http://dx.doi.org/10.1016/0896-8446(94)90011-6.

[45] A.Z. Panagiotopoulos and R.C. Reid, High-pressure phase equilibria in ternary fluid mixtures with a supercritical component, in: T. Squires, M.E. Paulatis (Eds.), Supercritical Fluids. Chemical and Engineering Principles and Applications, ACS Symposium Series, American Chemical Society,

Washington, 1987, pp. 115-129, http://dx.doi.org/10.1021/bk-1987-0329.ch010.

[46] G. Brunner, Counter-current separations, Journal of Supercritical Fluids 47 (2009) 574-582, http://dx.doi.org/10.1016/j.supflu.2008.09.022.

4. Conclusions and further work

4. Conclusions and further work

This doctoral thesis aimed to explore the potential of the supercritical fluid extraction of emulsions (SFEE) technology to nanoencapsulate liquid lipophilic bioactive compounds with application in pharmaceutical or food products. According to the aforementioned goal, the main conclusions of this research work are summarized hereafter.

SFEE is an efficient new method to nanoencapsulate liquid lipophilic bioactive compounds, which was demonstrated through the nanoencapsulation of two model substances of different viscosity, concretely vitamin E and ω-3 rich fish oil. The particles obtained for both systems via this process exhibited a high encapsulation efficiency, narrow particle size distribution and high storage stability in aqueous-based systems. The morphological analyses confirmed that spherical, core-shell and

non-aggregated nanocapsules were produced. Moreover, residual organic solvent concentrations suitable for application of these capsules in food and pharmaceutical products were achieved. Besides that, the use of a synthetic polymer, non-water soluble and with a slow degradation profile, would allow the controlled release of the bioactive compound.

When the nanoparticles obtained by SFEE were compared to those obtained by conventional solvent evaporation, SFEE nanoparticles showed better characteristics in terms of encapsulation efficiency and residual acetone concentration. In addition, they were produced in a shorter operating time, under a CO_2 inert atmosphere and at low temperatures, which would avoid degradation of the bioactive compound.

The use of organic solvents, the necessity of formulating an emulsion for each product and the low particle production per volume of treated emulsion are the main limitations of this new technology. Nonetheless, to the best our knowledge, there is no other conventional or emerging technique able of encapsulating liquid lipophilic bioactive compounds into nanoparticles with core-shell structure, high encapsulation efficiency, high storage stability and low residual organic solvent concentration as SFEE.

Regarding the process, it was demonstrated that among the operating parameters, the initial emulsion formulation had the biggest impact on nanoparticle characteristics. In contrast, pressure, temperature and CO_2 flow rate had the most significant influence on the organic solvent removal. The economic feasibility of the process could be compromised due to the high CO_2 consumption required for the

removal of the organic solvent and the limited production capacity in the bubble column. For these reason, the scale-up of the process was investigated using different SFEE installations. Among the different configurations analyzed, the use of a packed column offered the possibility of a high production capacity with a small volume plant and a lower CO_2 consumption. In fact, production capacity was increased from 15 mg·batch^{-1} in the bubble column to 0.67 g·h^{-1} in the packed column, and CO_2 consumption was reduced from 101 kg CO_2·kg acetone^{-1} to 19 kg CO_2·kg acetone^{-1}, which is very convenient from the economic point of view. In addition, the continuous operation in the packed column provided greater product homogeneity by eliminating differences between batches.

However, optimization in the design of the packed column is required since a moderate decrease in encapsulation efficiency and particle size was observed with respect to the particles obtained with the bubble column, due to the different operation mode. Moreover, the simulations with Aspen Plus showed that a taller column and higher CO_2 flow rates would be necessary to get a nanoparticle suspension with the residual organic solvent concentration suitable for food application.

Further work

In order to commercialize the technology and the capsules produced, it is recommended to continue the research dealing with the following aspects:

First, it would be necessary to optimize the column design, verifying the results obtained by Aspen Plus simulations in an experimental column, as well as

evaluating the performance of other types of packings, which could provide better contact between phases, and therefore a reduction in CO_2 consumption.

In view of the commercialization, it would be interesting to evaluate different bioactive compounds and coatings in order to establish a niche of products suitable for SFEE processing. Besides, it would be desirable to try to increase the ratio of particles produced per volume of treated emulsion by testing different emulsion formulations.

When particles are used with controlled delivery purposes, it would be necessary to perform *in vitro* stability and release tests under simulated gastric conditions. Furthermore, it would be convenient to verify the bioavailability and beneficial health effects provided by the bioactive compound. Nowadays, *in vivo* bioassays are required for the pharmaceutical industry to get approval for commercialization a new product; however, new European regulations could require these tests also for the food industry.

In parallel, the design of a pharmaceutical or food product containing such capsules would be envisioned. In this sense, capsules should resist the required processing steps and storage conditions of the final product, as well as not affect its organoleptic properties. A safety analysis would be certainly required in order to get approval to commercialize the final product inside the European Union, since products containing nanoparticles appear under the auspices of novel foods, according to the current European regulation (EC) 2015/2283.

Increasing production capacity to industrial scale (about tens of kilograms per day in the pharmaceutical industry and 1 $ton \cdot day^{-1}$ in non-pharmaceutical

applications) would imply, in addition to the scale-up of the packed column, the continuous formation of the emulsion, which could be done via membrane emulsification and/or high-pressure homogenization. Additionally, due to the high CO_2 consumption, it will be necessary to implement a CO_2 regeneration and re-use process for economic and environmental reasons. From the available alternatives to accomplish the CO_2 regeneration (depressurization, temperature change, distillation, absorption, adsorption, chromatography or membranes), it would be convenient to perform it at constant pressure (membrane or adsorption on activated carbon), given that recompression would increase production costs.

It would be possible to couple a drying process for the capsules if they were required in powder form, i.e. high-pressure filtration, CO_2 lyophilization, or PGSS-drying. Furthermore, an integrated processing strategy based on supercritical fluids, including extraction, encapsulation, drying and sterilization, could be developed.

To evaluate the feasibility of the commercial production, it would be essential to conduct a rigorous economic evaluation. Moreover, it would be required to make a revision of the intellectual property regarding the SFEE technology, since several patents were filed and are still valid.

There is technological maturity for the fractionation of liquid streams in packed columns, so the whole process could be rapidly developed in collaboration with any of the engineering firms specialized in supercritical fluids (Natex, Feyecon, Uhde-HPT, among others), taking into account the constraints imposed by the food and pharmaceutical industries (traceability, GMP, sterility, etc.).

Publications

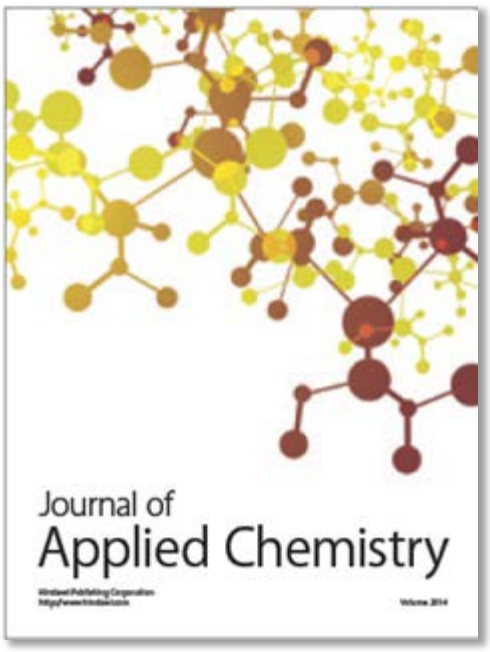

Publication I:

"*Performance of the biocompatible surfactant Tween 80, for the formation of microemulsions suitable for new pharmaceutical processing*"

Cristina Prieto, Lourdes Calvo

Journal of Applied Chemistry 2013 (2013) 930356,

http://dx.doi.org/10.1155/2013/930356.

Impact Factor (2013): -

Citations: 12

Hindawi Publishing Corporation
Journal of Applied Chemistry
Volume 2013, Article ID 930356, 10 pages
http://dx.doi.org/10.1155/2013/930356

Research Article

Performance of the Biocompatible Surfactant Tween 80, for the Formation of Microemulsions Suitable for New Pharmaceutical Processing

Cristina Prieto and Lourdes Calvo

Departamento de Ingeniería Química, Facultad de Ciencias Químicas, Universidad Complutense de Madrid, Avenue Complutense s/n, 28040 Madrid, Spain

Correspondence should be addressed to Lourdes Calvo; lcalvo@quim.ucm.es

Received 30 April 2013; Accepted 24 June 2013

Academic Editor: Rassoul Dinarvand

The aim of this work was to investigate the phase behaviour and the structure of the n-hexane/water emulsions based on a nonionic, nontoxic and biocompatible surfactant, Tween 80. This system is of interest for new pharmaceutical techniques based on supercritical fluids to form nano- and encapsulated particles. However, it showed a lack of stability denoted by large areas of macroemulsion. For this reason, the effect of additives (alcohols and brine) and external variables (temperature) were explored. The replacement of water by brine caused negligible impact due to the nonionic character of Tween 80. On the contrary, the presence of an alcohol (ethanol or 1-butanol) enhanced the solubility of the surfactant in the oil phase and decreased the mixture viscosity, resulting in improved surface activity. Similar results were obtained by raising the temperature until the cloud point was reached (60°C). With these modifications, microemulsions at relatively low concentrations of surfactant (around 30%) and within a broad interval of compositions could be obtained, widening their possible use in pharmaceuticals manufacturing (such as controlled drug delivery, enzymatic reactions, or excipient processing). The understanding of the surfactant performance could be further used to substitute the n-hexane by a greener solvent, such as supercritical CO_2.

1. Introduction

Under the principles of sustainable development and being environmentally friendly, a new field, called green chemistry, has been developed based on waste minimisation, energy efficiency, nonhazardous raw materials, solvents or products, inherently safe chemicals processes, and on renewable feedstocks [1]. In this sense, the global pharmaceutical corporations have encouraged the integration of green chemistry and green engineering into the pharmaceutical industry [2]. Between the key research areas for sustainable manufacturing, emulsions have generated a lot of interest, due to the fact that many pharmaceutical processes include direct or indirect contact with some kinds of emulsions in some of their innumerable applications.

The term emulsion designates a system composed of two immiscible liquids, one dispersed in the other, in a more or less stable way [3]. It is possible to make these two liquids compatible so that the mixture could be manipulated, administered, and used without breaking.

The general structure of emulsions comprises one phase formed by water or a water solution and another phase formed by an organic solvent insoluble in water, which is known as oil. Such emulsions are usually of two classes: oil in water (O/W) or water in oil (W/O), where the first liquid comprises the dispersed phase and the second one the continuous phase.

They can be classified into macroemulsions (which generally are called emulsions) and microemulsions. Although terminology suggests that colloid size is the determining factor, there are important differences in properties, which make their separate study interesting.

Microemulsions are optically transparent, thermodynamically stable, isotropic mixtures of water, organic solvent, and surfactant [4] and typically consist of disperse phase droplets from 2 to 50 nm in diameter. In contrast

to microemulsions, macroemulsions contain relatively large droplets (>0.1 μm) that are opaque and, although no longer thermodynamically stable, may be kinetically stable for long periods. Furthermore, macroemulsions may be formed with higher interfacial tensions between water and oil than in the case of microemulsions and, thus, with lower values of surfactant adsorption at the interface. Therefore, macroemulsions may be formed for a wider variety of surfactants than microemulsions, and with lower surfactant concentrations. This becomes especially important when dealing with expensive surfactants.

An influential factor on emulsion formation and stability is the surfactant, and its action depends on its structure and nature of the two phases. These agents could be classified according to the chemical group of the hydrophilic head into ionic, which could be further divided into anionic and cationic, nonionic, and zwitterionic.

The design of new functional surfactants exhibiting additional chemical and biological functionalities attracts a large interest nowadays, due to new potential applications [5]. The selected agent to carry out this study was Tween 80, an especially attractive nonionic surfactant, non-toxic, environmental friendly, biocompatible, and commercially inexpensive [6].

In recent years, a great amount of theoretical and experimental work has been developed devoted to different kinds of emulsions to try to expand the knowledge of these systems with regard to their molecular structure and formation process [7]. Since technical applications of these systems in pharmacy, cosmetics, and nutraceutics among others increasingly require more systematic optimisation of system properties, a complete revolution in the conception, design, production, and characterization of the emulsions in a variety of chemical and industrial processes has been made [8, 9]. However, very little work has focused on researching the formation, phase behaviour, and structure of both emulsions and microemulsions from completely non-toxic and safe materials, and consequently the widespread pharmaceutical use of microemulsions has been limited, by the requirement for pharmaceutically acceptable ingredients.

We have selected n-hexane, thinking of the multiple possibilities of the system. First, this system is very useful for nanoparticles formation, either by conventional techniques, such as solvent evaporation or spray drying, or by new techniques using supercritical fluids, such as (supercritical fluid extraction of emulsions) SFEE and (concentrated powder form) technology CPF. These techniques are based on the extraction of the organic solvent, leading to the formation of the nanoparticles, which can be even encapsulated during the same process. The use of a microemulsion supposes a better control of nanoparticle size and morphology, because it acts as a template. Despite being an organic solvent, the use of n-hexane is permitted in this kind of extractions, even in the food industry. Second, the study of this system provides us with the needed knowledge to substitute the organic solvent by a supercritical fluid, since at supercritical conditions, the CO_2 has a very similar density to the n-hexane. Microemulsions with supercritical fluids were formed by fluorinated surfactants up to now [10]. Nonetheless, their use in pharmaceutical industry requires biocompatible systems, which could be used to synthesize nanoparticles, as well as for biotechnological reactions [11].

The aim of this paper was to study comprehensively the n-hexane/water emulsions, using Tween 80, a non-toxic and biocompatible surfactant. The use of additives (alcohols and brine) and the variation of external variables (temperature) were investigated to modify the stability. This type of in-depth analysis with a biocompatible surfactant was not made up to our knowledge; nevertheless, it is of fundamental importance for the selection of operational conditions for further research as well as the development of new applications.

2. Experimental Section

2.1. Materials. Tween 80 (polyoxyethylene (20) sorbitan monooleate $[C_{24}H_{46}O_6 \cdot [C_2H_4O]_{w+x+y+z}$ for $w + x + y + z = 20]$), n-hexane (≥99% (GC)), 1-butanol (99.9%), ethanol (99.5%), and sodium chloride were all from Sigma Aldrich and used as received. Millipore water was used throughout the study.

2.2. Sample Preparation. The Tween 80/water/n-hexane mixtures were prepared using screw-cap tubes. Nineteen compositions in mass were chosen to cover the whole ternary phase map, with a final sample mass of 5 g. For each of the experiments, a table of experiments was built similarly to Table 1.

Two types of additives were used: alcohols (1-butanol and ethanol) and brine. In order to study the influence of alcohols, a mixture of alcohol and surfactant was made in proportion 1 : 1 in volume; for example, in sample 1, the 80% of surfactant in this case represents 80% of mixture surfactant + cosurfactant. In the case of brine, instead of using Millipore water, 2% NaCl brine was used.

To prepare the emulsions, the following steps were carried out.

(1) Addition of the adequate quantity of oil.

(2) Addition of the adequate quantity of surfactant and cosurfactant (if it was necessary).

(3) Mechanical shaking for 1 min on the vortex.

(4) Addition of the adequate quantity of water.

(5) Vigorous mechanical shaking for 5 min on the vortex, due to the high viscosity of the surfactant in order to guarantee a homogeneous dispersion.

(6) Control of temperature by placing the tube within a thermostatic water bath.

(7) Left at rest during 24 h before analysis.

Experiments were developed between room temperature and boiling point of n-hexane, concretely at 25, 30, 40, 50, and 60°C.

2.3. Determination of Phase Behaviour. In order to study the behaviour of Tween 80/water/n-hexane emulsions, visual observation and UV-Vis spectroscopy tests were carried out.

Table 1: Table of experiments built for each system.

Number of the sample	Composition (mass %)		
	Water	n-hexane	Surfactant
1	10	10	80
2	10	20	70
3	10	40	50
4	10	60	30
5	10	80	10
6	20	10	70
7	20	20	60
8	20	40	40
9	20	60	20
10	20	70	10
11	40	10	50
12	40	20	40
13	40	40	20
14	40	50	10
15	60	10	30
16	60	20	20
17	60	30	10
18	80	10	10
19	35	35	30

All samples were measured in triplicate, and therefore the result shown is a mean value. With all this information, phase maps were constructed for all samples and in all operational conditions studied.

2.3.1. Visual Observations. The first step for determining the phase behaviour, once the emulsion was created, was to make a visual inspection. Different results were obtained in colour and in texture as well as in transparency. Microemulsions were identified as transparent samples, whilst showing phase separation (Winsor I, II, or III); in the same way, samples with at least one turbid phase were considered macroemulsions, and they were stable over several days. In both, macroemulsion and microemulsions, there were cases of phase separation of the component in excess. Highly viscous samples were also observed and classified as gel-like.

2.3.2. UV-Vis Spectroscopy. Observations made by naked eye were corroborated by absorbance measurements. Absorbance of each sample was measured in an MRC UV 1800 spectrophotometer at 340 nm [12], taking the n-hexane as the (white) reference solution.

A calibration curve of surfactant water was created to establish a correlation between absorbance and concentration of surfactant. So when absorbance of the sample coincided with the calibration curve, this indicated that it was a transparent microemulsion. On the contrary, macroemulsions were obtained with a high absorbance value. For each one of the systems and each temperature, a graphic similar to Figure 1 was created. Represented data were the average of three measurements. The standard deviation, analysed over a sample measured six times, was ±0.030.

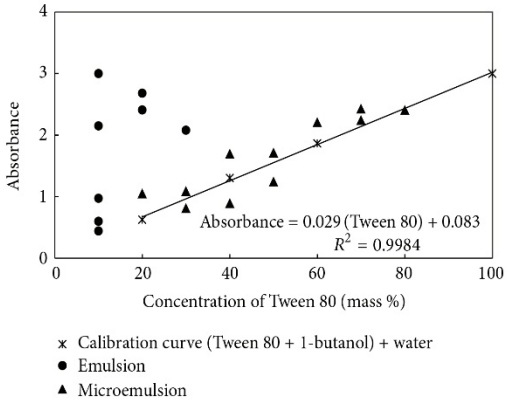

Figure 1: Absorbance measurements for the system: Tween 80 + 1-butanol/water/n-hexane at 30°C.

2.3.3. Construction of Phase Maps. Ternary mixtures were represented on the triangular phase map in terms of mass percentages of the components, where the apex designates 100% of each component, sides represent binary mixtures, and points inside the triangle represent ternary mixtures.

If the system had four components with related concentrations, a quaternary representation was needed [13], but it was simplified by taking the constant ratio between two components, generating a pseudoternary map. Therefore mass-pseudoternary phase maps were used when a cosurfactant, 1-butanol or ethanol, was added, in both cases in a proportion of 1 : 1 in volume to Tween 80.

To show the evolution of the map as a function of the temperature, a prism of phases was constructed by the superposition of the ternary phase maps at each one of the temperatures studied. All the presented observations were confirmed by at least three samples.

2.4. Determination of the Emulsions Structure by Conductimetry. The structure and composition of one emulsion are highly related; however, the excess of the solvents is indicative but not determinative of the emulsion structure. Conductimetry measurements were then performed to conclude the structure of the emulsion. This simple technique allows classification of the emulsion structure into O/W, bicontinuous, or W/O.

A Eutech Instruments CON510 conductivity was used to measure the conductance, which is defined as the ability to conduct electrical current between two points. In this case, it measured the conductance of a solution enclosed in a cube of 1 cm^3. Electrical conductance measurements in emulsions with nonionic surfactants had to be done in the presence of a solved electrolyte, which gives the electric charge needed for transport. Due to Tween 80 not being conductive, 2% brine was used instead of the aqueous phase.

The conductivity of O/W emulsions had the same order of magnitude as the aqueous phase conductivity, around several mS/cm, due to sodium and chloride ions moving along the water channel, showing the conducting nature of

the emulsion, whilst W/O emulsion conductivity was usually around 100 or 1000 times smaller, since the mobility of ions was restricted due to surrounding strong insulating oil which disconnects the water network. Bicontinuous phase displayed high or low conductivity depending on what the external phase was, water or oil.

3. Results and Discussion

This research focused on the formation and stability of Tween 80/water/n-hexane emulsions; therefore, the first step was the determination of the phase behaviour through techniques such as visual observation and UV-Vis spectroscopy, which allowed classification of the systems into macro- and microemulsions. All the information was gathered and represented in phase maps, at all studied conditions. Additives (alcohols and brine) and external variables (temperature) were used in order to modify the original phase map according to the potential requirements of the different applications. The final step was the determination of the emulsion structure, using conductimetry measurements.

3.1. Determination of Phase Behaviour. The phase behaviour of the Tween 80/water/n-hexane system was obtained by visual observation and absorbance measurements of each sample. With all this information, a ternary phase map was constructed. An example at 25°C is shown in Figure 2.

The system shows three regions represented with different shadings: area without shading or microemulsion, corresponding with sample 1; area with a light grey shading or macroemulsion; a third area with dark grey shading or gel-like area, corresponding to samples 3, 4, 5, 9, and 19. The latter area was mainly provoked by the high viscosity of Tween 80 at room temperature. Additives and temperature differences were used to correct this negative effect.

3.1.1. Effect of Additives. Temperature, salinity, and type of alcohol are the common variables used to manipulate phase behaviour and emulsion structure, because these parameters modify the interactions between components with the polar head of the surfactant [14]. Pressure provides a completely different mechanism of control of the emulsion, due to the main effect being created on the hydrophobic tail [15]; however, the effect of pressure is weak compared with that of temperature, so it is usually kept constant [16].

Effect of an Added Alcohol. Some surfactants need the presence of other active surface agents, which are called cosurfactants, to generate microemulsions [2, 17]. These compounds often belong to the group of components able to form hydrogen bonds and/or which have a strong attraction to the surfactant. Such additives can be long chain amines, amides, fatty acids, ethoxylates, chloroform, and so forth, but frequently oil or water-soluble alcohols are used.

For the system Tween 80/water/n-hexane, two alcohols were selected: 1-Butanol and ethanol. 1-butanol is frequently used as an additive and ethanol was tested because it is less toxic for pharmaceutical and food applications. First of all, the power of both alcohols as emulsifying agents by themselves was investigated, resulting in the finding that they were not capable of stabilising the water/n-hexane system, so the emulsion broke down when the shaking was stopped. However, when used as cosurfactants of Tween 80 in the ratio of 1 : 1 v/v, a better solubilisation between phases and a decrease of the mixture viscosity were reached, achieving a higher stabilisation of the system. Indeed, the emulsion region diminished, increasing the microemulsion one, and the gel-like region disappeared, as the base of the phase prisms in Figures 4 and 5 showd. When comparing both cosurfactants, 1-butanol proved to be more efficient at room temperature.

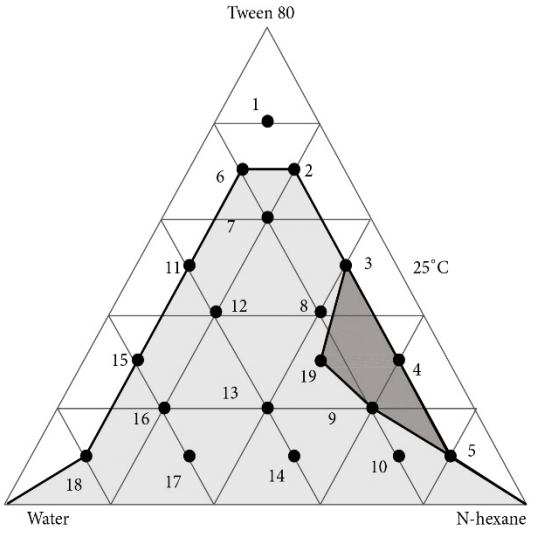

FIGURE 2: Ternary phase map of the system: Tween 80/water/n-hexane at 25°C.

It is believed that the alcohol joins the interface of the micelle, placing itself among surfactant heads, creating an increase of the dielectric constant and the ionisation degree [18]. The penetration of the alcohol into the interfacial film reduces the repulsion of the long hydrophobic tails of the surfactant at the interface, favouring its dissolution in the oil phase. Consequently, an increase in the length of the cosurfactant hydrocarbon chain increases the superficial activity (Traube's rule) [18] so that the micelle reaches a greater degree of stabilisation. At the molecular level, this effect could be explained as follows: the chain length of the surfactant must be equal to the sum of the cosurfactant chain length and the oil chain length in order to minimise disruption in the interfacial region. When chain lengths are not the same, the resulting monolayer film is disrupted easily. Consequently, microemulsion stability should be higher for 1-butanol than for ethanol, as indeed observed.

The presence of the alcohol also affects the physical properties of the water. The alcohol disrupts the water structure, creating an increase in the lipophilic character of the Tween 80 [19]. Furthermore, the alcohol provokes a decrease in the mixture viscosity [20]; therefore, the big

molecules such as Tween 80 can reach the interface faster. However, the presence of the alcohol in the mixture also promotes a decrease in the cloud point of the surfactant (see temperature effect).

Despite the many advantages of the use of alcohol as a cosurfactant, traces of it will be present on the final product and depending on the application; this presence may or may not be acceptable. According to the European laws (Directive 2009/32/CE, April 23, 2009), 1-butanol can be present in the final food product with a maximum quantity of 1 mg/kg. On the contrary, ethanol is non-toxic and so can be used more safely in food [21] and pharmaceutical applications.

Effect of Brine. If an electrolyte, NaCl, is added to the surfactant/water/organic solvent system, a system of four components is generated; however, it is possible to assume that the salt is confined to the aqueous domain [22], and consequently the quaternary map can be simplified to a pseudoternary one. Thus the substitution of water by 2% brine was investigated at different temperatures. The only difference observed was produced by the combination of the effect of the salt and temperature. At 40˚C, the emulsion area and gel-like region slightly increased with respect to the same system using water (results not shown).

This negative effect could be primarily attributed to two actions: a decrease in the superficial activity or a decrease of the CMC (critical micelle concentration), although both effects are usually negligible for non-ionic surfactants. Therefore, the action of the salt in the system should be explained by other reasons.

In the first place, the addition of an electrolyte (NaCl) tends to decrease the hydrophilicity of the surfactant [23], so the system becomes more sensitive to the temperature, decreasing the cloud point (salting out) [24].

Secondly, the presence of ions disrupts the water structure, which affects the number of water molecules available for solvation [25].

Moreover, the presence of salt also modifies physical properties of the system such as the viscosity. This last effect is related to the growth of the micelles: electrolytes which cause the salting out tend to promote growth [26]. The larger the micelle size, the greater the viscosity of the mixture, promoting the growth of the emulsion area and the gel-like appearance. This effect was also observed by other authors who reported that the replacement of water by brine provoked the appearance of gel-like structures in the low emulsifier and higher oil proportion domain [27].

3.1.2. Effect of Temperature. In order to study the temperature effect of each system, a phase prism was built. Temperature effect depends on the type of surfactant, which is able to affect the action over the interface and/or the mutual solubility of the phases. Related to both actions, non-ionic surfactants, such as Tween 80, are known to show a temperature-dependent behaviour. With increasing temperature, dehydratation of the oxyethylene head groups of the surfactant molecule occurs and as a consequence the surfactant loses its hydrophilic character, becoming more lipophilic. The phase

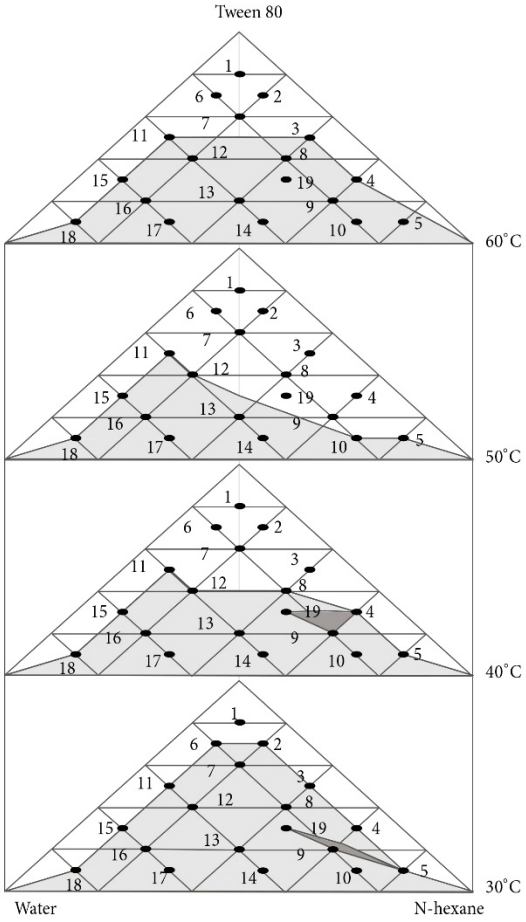

Figure 3: Phase prism corresponding with the Tween 80/water/n-hexane system.

prism for the Tween 80/water/n-hexane system reflects this behaviour in Figure 3.

It was noted that when temperature was raised from 25˚C to 30˚C, the gel-like region decreased as a result of a reduction in viscosity.

From 30˚C to 40˚C, the microemulsion region increased as expected, due to the reduction of the hydrophilic character of the surfactant favouring the oil dissolution. However, at 40˚C the gel-like region increased. The only explanation found for this unexpected result was that polyoxyethylene chains increased in length when the temperature rose above a point called the (phase inversion temperature) PIT [14], resulting in an increase of the micelle size and consequently in an increase of the viscosity.

From 40 to 50˚C, the gel-like region disappeared due to a viscosity reduction as an effect of the increase of temperature, and the emulsion region diminished. Moreover, the emulsion region shifted to the left as a consequence of the increase in the lipophilic character of the surfactant when high temperatures were reached. Therefore, more quantity

of oil was dissolved, which favoured the formation of W/O structures (see determination of the emulsions structure section) [18].

Finally, from 50 to 60°C, the emulsion region increased as a result of reaching the cloud point (phase separation temperature) [6], as occurred in samples 3, 4, 9, and 19, which became turbid. This critical temperature is attained when the dehydratation of the oxyethylene head groups of the surfactant reaches a maximum, causing the micellar aqueous solution of the surfactant to demix into a surfactant-rich phase and a water-rich phase. The cloud point depends on the molecular structure of the non-ionic surfactant, more specifically on the hydrophobic chain length and the number of oxyethylene units. However, this phenomenon was reversible: the solution became transparent when the temperature fell again to 50°C.

When 1-butanol was added to the system (see Figure 4), it gained stability at room temperature as explained earlier; however, when temperature increased, this benefit was partially lost. For temperatures over 30°C, turbidity increased as the temperature increased at the same time that the macroemulsion region shifted to the left. For example, at 40°C samples 11, 12, and 15 became turbid. This was an indication that in the presence of 1-butanol, the cloud point was reached at lower temperature than for the system without alcohol. This effect was also observed by other authors over a similar system [28]. On the other hand, sample 5 at 50°C became transparent as a result of an increase of the W/O structures, as explained earlier.

The behaviour of the Tween 80 + ethanol/water/n-hexane system is shown in Figure 5. The phase behaviour kept the same tendencies outlined thus far. As temperature increased, emulsion region diminished. Similarly, at high temperatures the emulsion region shifted to the left; however, cloud point was not detected on the range of temperatures studied.

The difference between this system to the one with 1-butanol was that the lowest temperature to obtain the ternary phase map was 30°C; under this temperature phases were not miscible. It is explained in terms of the effect that temperature had on the surfactant action, as well as on the surfactant dissolution in phases [29]. As a result, a range of temperature is defined (lower critical temperature (T_{lc}) and upper critical temperature (T_{uc})), outside of which the three components of the system are not totally soluble. In this case, T_{lc} for the Tween 80 + ethanol/water/n-hexane system was 30°C, below which it was impossible to achieve solvation between phases. It is worth noting that for the system without alcohol and the system with 1-butanol this temperature was under 25°C. The reason why this temperature for the system with ethanol was lower than that for the system without alcohol is that the amount of surfactant was lower and the ethanol was unable to stabilise the system at this temperature by itself.

3.1.3. Selection of Conditions for Further Applications. A comparison of the results produced by each parameter was made with the objective of carrying out an easier selection of the operational conditions, in a pharmaceutical potential application of this type of systems. Figure 6 shows a summary

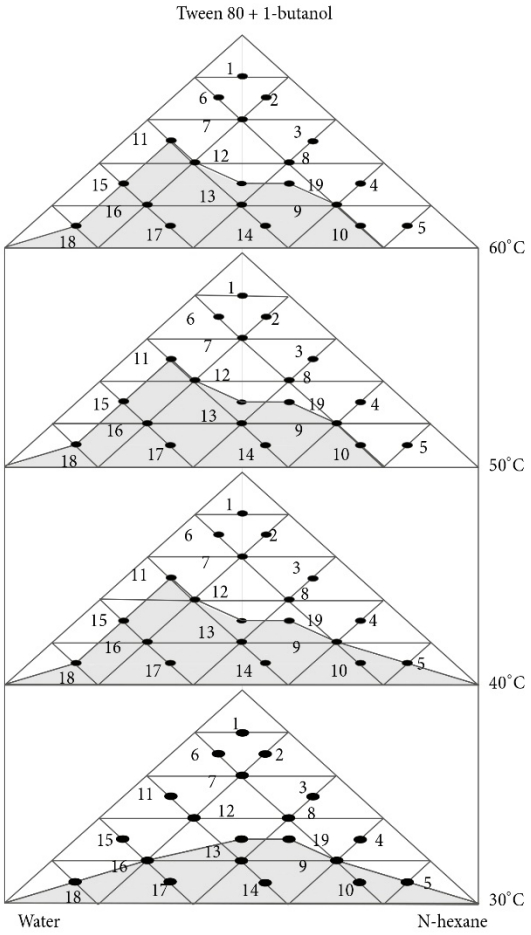

FIGURE 4: Phase prism corresponding with the Tween 80 + 1-butanol/water/n-hexane system.

of the foregoing purposes, detailing the extension of each region and the minimum amount of surfactant needed to get microemulsions. The gel-like region was not considered.

The basic case of reference is the system without additives at room temperature (25°C). This system showed a lack of stability, which is reflected by the high extension of macroemulsion region, around 65%. Just one sample of microemulsion was obtained, for which it was necessary to add 80% of surfactant.

The effect of temperature is represented by the second and third columns. The second one shows the effect of the temperature under the cloud point (60°C). The microemulsion area increased to about 60%, needing only 40% of surfactant. When temperature exceeded the cloud point (third column), turbidity increased to almost 60%.

The fourth column demonstrates the benefits achieved by adding an alcohol as cosurfactant, in this case 1-butanol, which can be summarised in an increase of the microemulsion area (67%), a decrease in the macroemulsion area, and

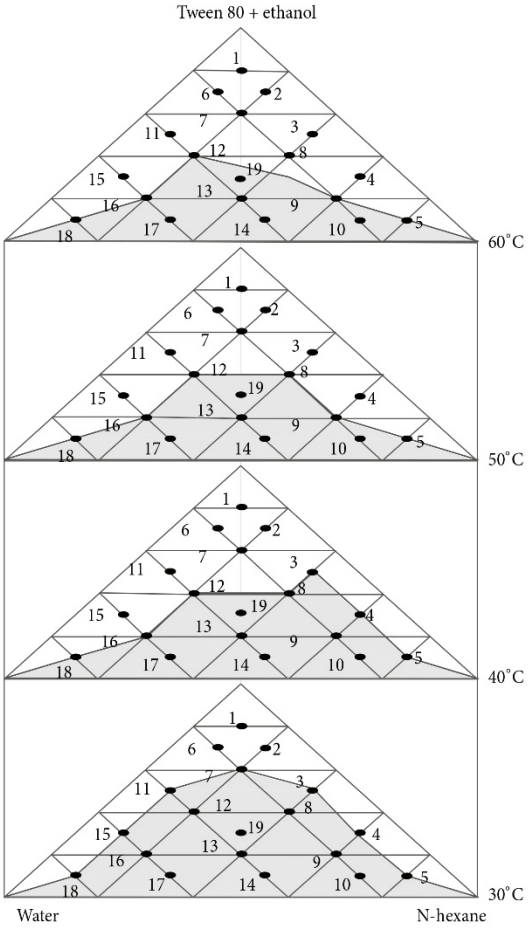

FIGURE 5: Phase prism for the Tween 80 + ethanol/water/n-hexane system.

disappearance of the gel-like region. All of it achieved with only 30% of surfactant. The reasons could be attributed to an improvement of the solubility of the surfactant in the oil phase and to several physical effects that ended up enhancing the superficial activity of the surfactant at the interface.

However, these benefits are only possible in a narrow interval of temperatures since the cloud point of the surfactant was diminished to 40°C, as shown in the fifth column. Thus, turbidity increased again as well as the amount of surfactant needed to get transparent microemulsions. It is worth noting that when ethanol was used, the cloud point was not detected under 60°C, showing larger areas of microemulsion at high temperatures (around 63%) with only 30% of surfactant. Therefore, depending on the working temperature, a different alcohol could be required to stabilise the system.

Thus, according to the final application, all these variables have to be counterbalanced to obtain the specific characteristic of the required type of emulsion.

Frequently, it is preferable to work with macroemulsions since they are several times cheaper than microemulsions,

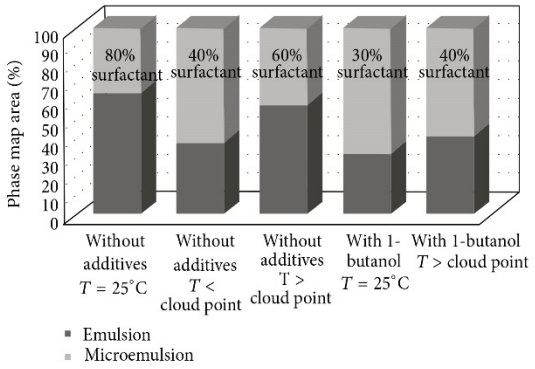

FIGURE 6: Comparison between the effects on the extension of emulsion and microemulsion region and the minimum amount of surfactant needed for each case.

and they have a wide range of operational conditions for obtainment processes. However, microemulsions provide the product with high stability, and also, for example, in pharmaceutics, better drug delivery [30, 31] and in cosmetics, better skin penetration [32, 33]. For the studied system, the best combination for obtaining microemulsions depends on the temperatures allowed for process and product: at room temperature the most advisable would be to include 1-butanol; between 40 to 60°C, it might be advisable not to use cosurfactant and to just play with the temperature. If high temperatures (around 60°C) are required, then the choice should be to add ethanol. On the other hand, if surfactant concentration is kept low (less than 1%) macroemulsions would be favoured.

3.2. Determination of the Emulsions Structure. Emulsion formation and stability depend on many factors, among which the structure is of great importance. This term refers to the type of phase: W/O, bicontinuous, or O/W; they are very important, because the structure together with micelle size affects hydrodynamics and interfacial science and even determines the applications. Definition of the structure of an emulsion is sometimes difficult to predict from solvent ratio, especially at close solvent proportions. Thus, other techniques such as conductimetry have to be used.

The type of emulsion can be deducted from the conductivity value. Since neither the organic phase nor the non-ionic surfactant is conductive, an electrolyte had to be added to the aqueous solution to provide electrical charge to the mixture. Thus, water was replaced in conductivity measurements by 2% brine (NaCl). As shown earlier, the areas of the microdomains remained the same when this replacement was done.

The resulting structures at 25°C for the systems Tween 80 + 1-butanol/brine/n-hexane and Tween 80 + ethanol/brine/n-hexane are shown in Figures 7 and 8.

In both systems, there is a predominance of O/W over bicontinuous and W/O structures. According to Bancroft's rule, O/W emulsions are produced by emulsifying agents that are more soluble in the "water" than in the "oil" phase,

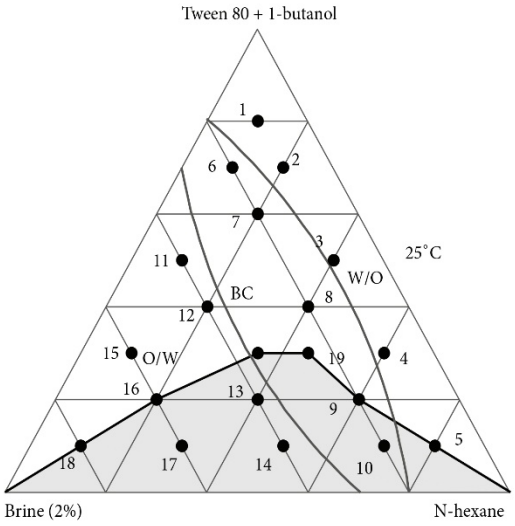

FIGURE 7: Structural classification for the system: Tween 80 + 1-butanol/brine/n-hexane.

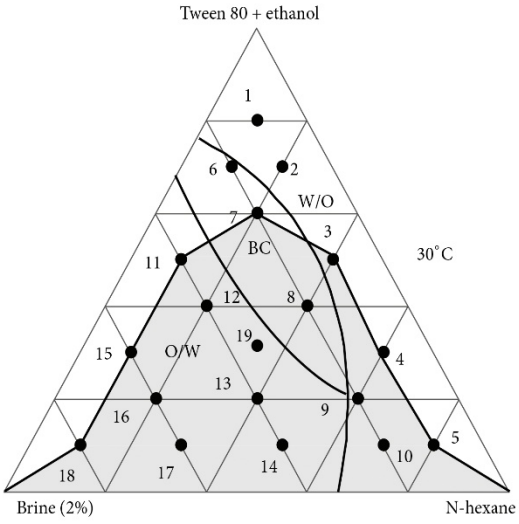

FIGURE 8: Structural classification for the Tween 80 + ethanol/brine/n-hexane system.

whereas W/O emulsions are produced by emulsifier agents that are more soluble in "oil" than in "water." Therefore, as the Tween 80 is a water-soluble compound, it tends to form O/W emulsion. This conclusion could also be obtained by using the HLB concept. According to this parameter, HLB values between 3.5 and 6 promote the formation of W/O emulsions and values between 8 and 18, O/W [34]. Since Tween 80 has an HLB of 15, O/W emulsions predominated in both systems.

The same tendency was observed by other authors using Tween 80 + 1-butanol in a ratio of 2 : 1, where O/W structures predominated and the bicontinuous region on average started at around 12% of water [35].

As stated before, an increase in temperature should provoke an increase in the W/O region, but with our equipment it was impossible to corroborate this.

The structural classification for systems using 1-butanol and ethanol was very similar and the main differences were found on the extension of the bicontinuous region. This could be caused by the difference in chain length. In this sense, the fact that ethanol has a shorter chain provides a lower capacity than 1-butanol to improve the solubility of Tween 80 in the oil phase according to Traube's rule. Consequently, the bicontinuous region, for being an unstable transition structure, became smaller.

4. Conclusion

The water/n-hexane system with the non-toxic, biodegradable, and non-ionic surfactant, Tween 80, was studied according to phase behaviour and structure, broadening previous researches made in a similar system, which were concentrated in temperature effect and molecular structure, respectively [27, 35]. In our study concretely, the effect of additives such as alcohols (1-butanol and ethanol) and brine was considered as well as their combined influence with temperature. In addition, emulsions structure was analyzed.

The aim of the variations over the original system was always the same: to increase the stability. In the first attempt, alcohols enhanced the solubility of the surfactant in the oil phase and decreased the mixture viscosity. As a result and in accordance with the basic principles of fluid dynamics and interfacial science, the superficial activity of the surfactant increased. However, the cosurfactant action of the alcohols depended on their carbon chain length according to Traube's rule [18]; thus, 1-butanol was more effective at room temperature.

On the other hand, taking into account the influence of thermodynamics over our colloidal system [16], the solubility of the surfactant in the oil phase could be increased by an augment of temperature favouring the expansion of the microemulsion area. Nevertheless, this effect was lost when the cloud point was reached at 60°C, because the surfactant solubility in the aqueous phase decreased, destabilizing the system and thus increasing the turbidity. It is important to note that the presence of 1-butanol decreased this temperature to 40°C but for ethanol the cloud point was not detected up to 60°C.

The structure was directly dependent on the surfactant solubility in both phases according to Bancroft's rule [34]. Due to the greater solubility of the Tween 80 in the water phase the predominant structure at room temperature was O/W, although W/O microemulsions could be obtained by increasing the temperature as a consequence of the enhanced surfactant solubility in the oil phase.

This comprehensive analysis of the system allows the establishment of the best formulation and operational conditions at the lowest possible surfactant concentration (to reduce costs) for potential pharmaceutical applications. In this system, microemulsions could be favoured at relatively

low surfactant concentration (around 30%) by addition of an alcohol or by increasing temperature. Evidently, this selection must be done according to the final application which will provide some restrictions to the system. In this sense, when microemulsions are used as colloidal nanocarriers, the drug to be delivered may condition the system composition, the temperature or even limit the use of the alcohol. Similar argumentations are valid if the microemulsions are to be used for enzymatic reactions or excipient processing.

References

[1] M. Lancaster, "Principles of sustainable and green chemistry," in *Handbook of Green Chemistry and Technology*, J. Clark and D. Macquarrie, Eds., pp. 10–27, Blackwell Science, Oxford, UK, 2002.

[2] D. J. C. Constable, P. J. Dunn, J. D. Hayler et al., "Key green chemistry research areas—a perspective from pharmaceutical manufacturers," *Green Chemistry*, vol. 9, no. 5, pp. 411–420, 2007.

[3] G. Barnes and I. Gentle, *Interfacial Science: An Introduction*, Oxford University Press, 2005.

[4] K. Shinoda and B. Lindman, "Organized surfactant systems: microemulsions," *Langmuir*, vol. 3, no. 2, pp. 135–149, 1987.

[5] Y.-Y. Luk and N. L. Abbott, "Applications of functional surfactants," *Current Opinion in Colloid and Interface Science*, vol. 7, no. 5-6, pp. 267–275, 2002.

[6] B. A. Kerwin, "Polysorbates 20 and 80 used in the formulation of protein biotherapeutics: structure and degradation pathways," *Journal of Pharmaceutical Sciences*, vol. 97, no. 8, pp. 2924–2935, 2008.

[7] B. K. Paul and S. P. Moulik, "Microemulsioins: an overview," *Journal of Dispersion Science and Technology*, vol. 18, no. 4, pp. 301–367, 1997.

[8] S. P. Moulik and B. K. Paul, "Structure, dynamics and transport properties of micro emulsions," *Advances in Colloid and Interface Science*, vol. 78, no. 2, pp. 99–195, 1998.

[9] S. P. Moulik and A. K. Rakshit, "Physicochemisty and applications of microemulsions," *Journal of Surface Science and Technology*, vol. 22, no. 3-4, pp. 159–186, 2006.

[10] C. T. Lee Jr., W. Ryoo, P. G. Smith Jr. et al., "Carbon dioxide-in-water microemulsions," *Journal of the American Chemical Society*, vol. 125, no. 10, pp. 3181–3189, 2003.

[11] M. Haruki, K. Matsuura, Y. Kaida, S.-I. Kihara, and S. Takishima, "Microscopic phase behavior of supercritical carbon dioxide + non-ionic surfactant + water systems at elevated pressures," *Fluid Phase Equilibria*, vol. 289, no. 1, pp. 1–5, 2010.

[12] W. Peter Wuelfing, K. Kosuda, A. C. Templeton, A. Harman, M. D. Mowery, and R. A. Reed, "Polysorbate 80 UV/vis spectral and chromatographic characteristics—defining boundary conditions for use of the surfactant in dissolution analysis," *Journal of Pharmaceutical and Biomedical Analysis*, vol. 41, no. 3, pp. 774–782, 2006.

[13] H. Kahl, K. Quitzsch, and E. H. Stenby, "Phase equilibria of microemulsion forming system n-decyl-β-D-glucopyranoside/water/n-octane/1-butanol," *Fluid Phase Equilibria*, vol. 139, no. 1-2, pp. 295–309, 1997.

[14] J. L. Salager, L. Márquez, I. Mira, A. Peña, E. Tyrode, and N. B. Zambrano, "Principles of emulsion formulation engineering," in *Adsorption and Aggregation of Surfactants in Solution*, K. L. Mittal and D. O. Shah, Eds., vol. 109 of *Surfactant Science Series*, pp. 501–524, Marcel Dekker, New York, NY, USA, 2002.

[15] D. G. Peck and K. P. Johnston, "Theory of the pressure effect on the curvature and phase behavior of AOT/propane/brine water-in-oil microemulsions," *Journal of Physical Chemistry*, vol. 95, no. 23, pp. 9549–9556, 1991.

[16] M. Kahlweit, R. Strey, and G. Busse, "Microemulsions: a qualitative thermodynamic approach," *Journal of Physical Chemistry*, vol. 94, no. 10, pp. 3881–3894, 1990.

[17] M. Porras, C. Solans, C. González, A. Martínez, A. Guinart, and J. M. Gutiérrez, "Studies of formation of W/O nano-emulsions," *Colloids and Surfaces A*, vol. 249, pp. 115–118, 2004.

[18] D. Attwood and A. T. Florence, *Surfactant Systems. Their Chemistry, Pharmacy and Biology*, Chapman and Hall, New York, NY, USA, 1983.

[19] S. Reekmans, H. Luo, M. Van Der Auweraer, and F. C. De Schryver, "Influence of alcohols and alkanes on the aggregation behavior of ionic surfactants in water," *Langmuir*, vol. 6, no. 3, pp. 628–637, 1990.

[20] Y. Bayrak and M. Iscan, "Studies on the phase behavior of the system non-ionic surfactant/alcohol/ alkane/H_2O," *Colloids and Surfaces A*, vol. 268, no. 1–3, pp. 99–103, 2005.

[21] A. Yaghmur, A. Aserin, and N. Garti, "Phase behavior of microemulsions based on food-grade nonionic surfactants: effect of polyols and short-chain alcohols," *Colloids and Surfaces A*, vol. 209, no. 1, pp. 71–81, 2002.

[22] J. Sjöblom, R. Lindberg, and S. E. Friberg, "Microemulsions—phase equilibria characterization, structures, applications and chemical reactions," *Advances in Colloid and Interface Science*, vol. 65, pp. 125–287, 1996.

[23] W. Warisnoicharoen, A. B. Lansley, and M. J. Lawrence, "Non-ionic oil-in-water microemulsions: the effect of oil type on phase behaviour," *International Journal of Pharmaceutics*, vol. 198, no. 1, pp. 7–27, 2000.

[24] S. Ajith and A. K. Rakshit, "Effect of NaCl on a nonionic surfactant microemulsion system," *Langmuir*, vol. 11, no. 4, pp. 1122–1126, 1995.

[25] H. Coulombeau, F. Testard, T. Zemb, and C. Larpent, "Effect of recognized and unrecognized salt on the self-assembly of new thermosensitive metal-chelating surfactants," *Langmuir*, vol. 20, no. 12, pp. 4840–4850, 2004.

[26] H. Schott, "Salting in of nonionic surfactants by complexation with inorganic salts," *Journal of Colloid And Interface Science*, vol. 43, no. 1, pp. 150–155, 1973.

[27] P. Mukherjee, S. K. Padhan, S. Dash, S. Patel, P. K. Mohapatra, and B. K. Mishra, "Effect of temperature on pseudoternary system Tween-80-butanol-hexane-water," *Journal of Colloid and Interface Science*, vol. 355, no. 1, pp. 157–163, 2011.

[28] S. Y. Shiao, V. Chhabra, A. Patist et al., "Chain length compatibility effects in mixed surfactant systems for technological applications," *Advances in Colloid and Interface Science*, vol. 74, no. 1–3, pp. 1–29, 1998.

[29] J. L. Salager, "Phase transformation and emulsion inversion on the basis of catastrophe theory," in *Encyclopedia of Emulsion Technology*, P. Becker, Ed., vol. 3 of *Basic Theory Measurement Applications*, pp. 79–134, Marcel Dekker, New York, NY, USA, 1988.

[30] F. Podlogar, M. Gašperlin, M. Tomšič, A. Jamnik, and M. B. Rogač, "Structural characterisation of water-Tween 40/Imwitor 308-isopropyl myristate microemulsions using different experimental methods," *International Journal of Pharmaceutics*, vol. 276, no. 1-2, pp. 115–128, 2004.

[31] P.-C. Wu, Y.-H. Lin, J.-S. Chang, Y.-B. Huang, and Y.-H. Tsai, "The effect of component of microemulsion for transdermal delivery of nicardipine hydrochloride," *Drug Development and Industrial Pharmacy*, vol. 36, no. 12, pp. 1398–1403, 2010.

[32] S. Hoeller, A. Sperger, and C. Valenta, "Lecithin based nanoemulsions: a comparative study of the influence of non-ionic surfactants and the cationic phytosphingosine on physicochemical behaviour and skin permeation," *International Journal of Pharmaceutics*, vol. 370, no. 1-2, pp. 181–186, 2009.

[33] A. Azeem, Z. I. Khan, M. Aqil, F. J. Ahmad, R. K. Khar, and S. Talegaonkar, "Microemulsions as a surrogate carrier for dermal drug delivery," *Drug Development and Industrial Pharmacy*, vol. 35, no. 5, pp. 525–547, 2009.

[34] K. Holmberg, B. Jönsson, B. Kronberg, and B. Lindman, *Surfactants and Polymers in Aqueous Solution*, John Wiley & Sons, 2002.

[35] H. P. Mishra, N. Jyotish, S. Panigrahi, and P. K. Misra, "Organization of amphiphiles, part IX: effect of molecular structure of cosurfactants and oils on the phase behavior of tween-80: alkanol-oil-water systems," *Journal of Dispersion Science and Technology*, vol. 30, no. 4, pp. 564–574, 2009.

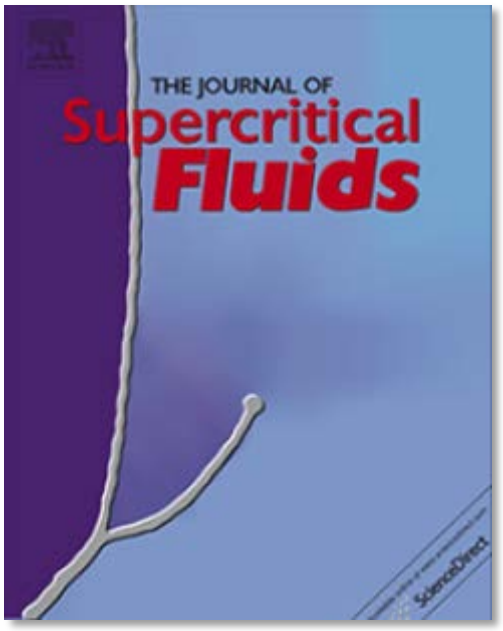

Publication II:

"***Supercritical fluid extraction of emulsions to nanoencapsulate vitamin E in polycaprolactone***"

Cristina Prieto, Lourdes Calvo

Journal of Supercritical Fluids 119 (2017) 274-282,

http://dx.doi.org/10.1016/j.supflu.2016.10.004.

Impact Factor (2015): 2.579

Citations: 2

Editor-in-Chief's Featured Article, January 2017.

J. of Supercritical Fluids 119 (2017) 274–282

Contents lists available at ScienceDirect

The Journal of Supercritical Fluids

journal homepage: www.elsevier.com/locate/supflu

Supercritical fluid extraction of emulsions to nanoencapsulate vitamin E in polycaprolactone

Cristina Prieto, Lourdes Calvo*

Departamento de Ingeniería Química, Facultad de Ciencias Químicas, Universidad Complutense de Madrid, Av. Complutense s/n, 28040 Madrid, Spain

ARTICLE INFO

Article history:
Received 22 June 2016
Received in revised form 6 October 2016
Accepted 7 October 2016
Available online 8 October 2016

Keywords:
Supercritical fluid extraction of emulsions
Vitamin E
Polycaprolactone
Encapsulation
Nanocapsules

ABSTRACT

Supercritical fluid extraction of emulsions (SFEE) was used to encapsulate a liquid lipophilic compound, concretely vitamin E in polycaprolactone. The influence of the initial formulation on the characteristics of the nanoparticles (encapsulation efficiency, particle size distribution, and morphology) was studied. The obtained particles exhibited a high encapsulation efficiency (around 90%), narrow particle size distribution (polydispersity index between 0.24 and 0.54), and nanoscale particle sizes (between 8 and 276 nm). The morphological analysis indicated that the particles were spherical, with a core-shell structure, and non-aggregated. Operating at 8 MPa and 313 K, with a CO_2 flow rate of 7.2 kg h^{-1} kg emulsion^{-1}, a low residual concentration of organic solvent (50 ppm) was obtained in 240 min at a CO_2 consumption of 101 kg CO_2 kg acetone^{-1}. Stability tests indicated that the capsules remained unchanged over long storage periods (6 and 12 months).

1. Introduction

Vitamin E is a fat-soluble compound that exists naturally in eight different isomers including the α, β, γ and δ derivatives of tocopherol and tocotrienol [1]. Among these isomers, α-tocopherol is the most naturally abundant. It can be found in many natural sources such as wheat germ oil, sunflower seed, almond, and cereals, among others. In addition, α-tocopherol is the most important biologically active form of vitamin E, and it has exhibited antioxidant activity and the potential to modulate oxidative stress [2]. Due to its recognized virtues, α-tocopherol is widely used as a functional ingredient in food, pharmaceutical products and cosmetic preparations. However, the use of α-tocopherol is not without challenges because it is sensitive to heat and oxygen and it exhibits poor water solubility and low bioavailability [3]. A number of different α-tocopherol delivery systems have been investigated [4] as a potential means of overcoming the problems these challenge create during the processing, storage, and utilization of commercial products. These delivery systems include emulsions and nanoemulsions [3], solid-lipid nanoparticles [5], liposomes [6], and biopolymer-based micro and nanoparticles [7–9].

Of the various delivery systems that are available, biopolymer-based micro and nanoparticles can be designed to transport the bioactive to a specific site of action with minimal degradation. The bioactive is then released in a controlled and predictable manner through a controlled degradation profile of the polymer triggered by environmental conditions such as temperature, pH, enzymes, or ionic strength [2]. An important consideration in the design of a delivery system is the need to ensure that the system effectively encapsulates the bioactive in a form that does not adversely affect product quality; for example, by altering appearance, taste, texture or stability.

Multiple processes have been developed for the formation of biopolymeric-based micro and nanoparticles [10,11]. Some of these methods use an emulsion to produce the subsequent nanoparticles. This emulsion acts as a template that facilitates the production of particles that have a narrower particle size distribution, which is very interesting in order to have a higher degree of control over the bioactive release. However, the emulsion-based nanoparticle production processes that are currently in common use, such as solvent evaporation or solvent extraction, do not typically produce solvent-free nanoparticles [12,13] in the submicro or nano size range that exhibit a controlled size distribution and good encapsu-

Abbreviations: BPR, back pressure regulator; CPF, concentrated powder form; EE, encapsulation efficiency; FDA, food and drug administration; F_E, free vitamin E concentration; O/W, oil in water emulsion; PCL, polycaprolactone; PdI, polydispersity index; PGSS, particles from gas saturated solutions; PLGA, poly(lactic-co-glycolic acid); PVA, poly(vinyl alcohol); SFEE, supercritical fluid extraction of emulsions; T_E, total vitamin E concentration; TEM, transmission electron microscopy; W/O/W, water in oil in water emulsion.

* Corresponding author.
E-mail addresses: crisprie@ucm.es (C. Prieto), lcalvo@ucm.es (L. Calvo).

http://dx.doi.org/10.1016/j.supflu.2016.10.004
0896-8446/

lation efficiency. In addition, these techniques are difficult to scale [14].

Supercritical fluid encapsulation techniques promote the effective elimination of solvents thanks to the high solubility of small organic molecules on these fluids and to the fast mass transfer at low temperature and moderate pressure. Of the various supercritical fluid techniques that have been employed [15,16], some can be used to load liquids on powders, concretely Concentrated Powder Form (CPF) and Particles from Gas Saturated Solutions (PGSS) [17]. In the case of CPF, microagglomerates with sizes of between 5 μm and 2 mm and a high liquid retention (≤90%) can be obtained [18]. CPF technology has been developed on an industrial scale and commercialized by the consortium of Natex, VTP, Raps and Yara. One commercialized product that uses CPF technology is FLAVOCAPS, which consists of different flavors encapsulated in carriers such as sugar, cellulose or starch, among others. Liquid-polymer microagglomerates can be produced via the PGSS process. One example is the work of Varona et al. [19], who encapsulated lavadin oil in poly-(ε-caprolactone). Particles with sizes of between 10 and 50 μm and an encapsulation efficiency of up to 50% were obtained. However, none of these techniques have been successfully employed to produce real nanocapsules (core-shell structure).

Supercritical fluid extraction of emulsions (SFEE) is a novel encapsulation technology [20,21] that combines conventional emulsion processes with the unique properties of supercritical fluids to produce tailored micro- and nanoparticles. The basis of this process relies on the use of supercritical CO_2 to rapidly extract the organic phase of an emulsion, in which a bioactive compound and its coating polymer have been previously dissolved. By removing the solvent, both compounds precipitate, generating a suspension of particles in water. The produced particles have controlled size and morphology [22], due to the use of the emulsion and to the fast kinetics of the supercritical CO_2 extraction. Particle agglomeration in the aqueous phase is avoided since the particles are stabilized by a surfactant. In addition, this technology is very versatile. It is possible to encapsulate hydrophilic and lipophilic compounds by changing the starting emulsion. An oil in water (O/W) emulsion can be used to encapsulate lipophilic compounds, while a water in oil in water (W/O/W) emulsion can be used to encapsulate hydrophilic compounds. Previous studies have demonstrated that this process is easily scalable by means of a countercurrent column [23,24]; however, more work should still be done on the design and optimization of the operation variables. The majority of existing research that has been conducted in this field involved the encapsulation of solid pharmaceutical compounds in poly(lactic-co-glycolic acid) (PLGA). However, this method may also represent a promising technique for encapsulating nutraceuticals for the food industry. For example, Santos et al. [25] encapsulated β-carotene and lycopene in *n*-octenyl succinic anhydride (OSA)-modified starch to be used as colorants and antioxidants in the food industry.

The current study involved the use of SFEE to encapsulate vitamin E in polycaprolactone. The system for the encapsulation of this compound consisted of acetone (O) and water (W); Tween 80 was used as a surfactant, and polycaprolactone (PCL) as the encapsulating polymer. PCL is a synthetic, biocompatible, and fully biodegradable polymer, which has a semicrystalline nature (glass transition temperature of 213 K). It is approved by the FDA (Food and Drug Administration) for drug delivery. It has high hydrophobicity, high in vitro stability and is low cost. Due to its slow degradation, PCL is ideally suited for long-term delivery, or when a targeted delivery to the intestinal tract is intended [26].

The solvents used in SFEE form an emulsion with water in the presence of a surfactant but are also highly soluble in supercritical CO_2 at moderate pressure and temperatures. Prior to this study, previous research has examined the use of ethyl acetate [22,24], dichloromethane [25], and acetone [23] solvents in SFEE. Acetone was selected as the organic solvent because of its low toxic potential (Class 3) which is in the line with the ICH guidelines [27].

Tween 80 was selected as the surfactant because it is a particularly attractive non-ionic surfactant that is non-toxic, environmentally friendly and biocompatible. It is commercially inexpensive and is fully approved for pharmaceutical and food use.

The aim of the current study was to examine the influence that the operational variables had on the effectiveness of the organic solvent removal. In addition, the effect of the initial formulation was assessed in order to enhance the encapsulation efficiency, particle size distribution, and morphology of the final product. Finally, the particles obtained by SFEE were compared with those obtained by conventional techniques, specifically by solvent evaporation, to evaluate the potential benefits of the use of the supercritical technology.

2. Materials and methods

2.1. Materials

Vitamin E (α-tocopherol, ≥95%), polycaprolactone (PCL) (MW of 10,000), Tween 80 (polyoxyethylene (20) sorbitan monooleate), acetone (≥99.5% (GC)), absolute ethanol (99.5%), sodium hydroxide (≥98%), and sodium dihydrogen phosphate monohydrate (≥98%) were all from Sigma Aldrich (Spain). Paraformaldehyde (16%), glutaraldehyde (25%), osmium tetroxide (2%), and Spurr resin were all from Electron Microscopy Sciences (USA). Uranyl acetate solution (2%) and sodium phosphotungstic acid solution (1%) were from Panreac (Spain). Acetonitrile (gradient 240 nm/far UV HPLC grade) was from Scharlab (Spain). Carbon dioxide (>99.5%) was from Carburos Metálicos (Air Products, Spain). All materials were used as received. Millipore water was used throughout the study.

2.2. Preparation of the starting emulsions

PCL and vitamin E were dissolved in acetone. The aqueous phase was prepared by dissolving the Tween 80 in water. The organic phase was added to the aqueous phase, drop by drop, and stirred on the vortex (Heidolph REAX top) for 5 min to guarantee a homogeneous dispersion.

2.3. Determination of phase behavior

The first step in determining the phase behavior involved visually inspecting the samples. Samples in the whole range of composition were classified into transparent or turbid, since turbidity of colloidal dispersions is an indicator of the size of the colloid. In general terms, samples with colloids that range from 2 to 50 nm in diameter are transparent, while samples with colloid larger than 100 nm are opaque [28,29]. All samples were analyzed in triplicate.

2.4. SFEE nanoparticles formation

The SFEE apparatus consisted of a 10 ml cylindrical stainless steel extractor with a length-to-diameter (L/D) ratio of nine. Liquid chilled CO_2 at 263 K was delivered using a head cooled piston pump (Jasco, PU-2080). The temperature in the extractor was regulated by a heating jacket and recorded within ±0.1 K through the use of a type T thermocouple that was positioned inside the vessel. The pressure inside the extractor was regulated by a backpressure regulator (BPR, TESCOM) and read via a digital internal pump manometer within ±0.1 MPa and via an external online Bourbon manometer. A mass flow meter (AlicatScientific, M-10SLPM-D) was used to measure the total amount of CO_2 employed. The arrangement of the equipment is shown in Fig. 1.

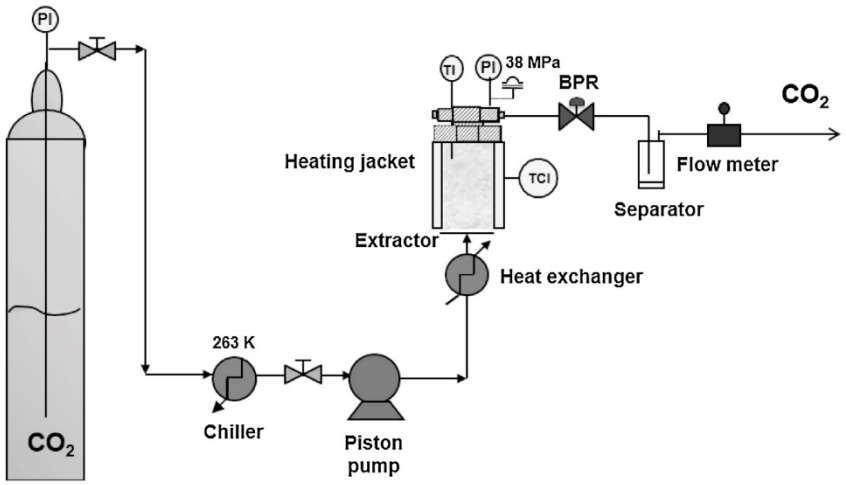

Fig. 1. Scheme of the equipment used for supercritical fluid extraction of emulsions (SFEE).

In order to carry out the process, five grams of the freshly prepared starting formulation were placed inside the extractor before the vessel was closed. CO_2 was added, and the temperature was adjusted. The vessel was then pressurized to 8 MPa. Finally, the BPR was opened and the flow adjusted. The operation was deemed to be complete when the selected operation time was reached. The vessel was then slowly depressurized. A suspension of nanoparticles in water was recovered and stored in screw cap glass vials in the refrigerator until the time of analysis.

2.5. Formation of nanoparticles through conventional solvent evaporation

Acetone was extracted from the sample using two variations of the conventional solvent evaporation process. In the first, the acetone was evaporated using a mild vacuum (30 kPa) in a rotating evaporator (Rotavapor R-210, Buchi) at 323 K for 30 min, followed by a further 30 min at 6 kPa in order to concentrate the nanoparticle suspension. In the second approach, the acetone was eliminated using a hotplate with temperature control (MST Digital, Yellow Line-IKA) at 313 K for 8 h inside a fume hood under constant magnetic agitation (400 rpm).

2.6. Encapsulation efficiency

The encapsulation efficiency (EE) was determined as the percentage of vitamin E entrapped in the particle. It was calculated following Eq. (1).

$$\textit{Encapsulation efficiency}\,(\%) = \frac{T_E - F_E}{T_E} \cdot 100 \qquad (1)$$

The total vitamin E concentration (T_E) was determined after dissolving 1 ml of nanoparticles suspension in 10 ml of acetonitrile at 313 K overnight.

Free vitamin E concentration (F_E) was determined in the aqueous supernatant after the particles were separated by centrifugation (Digicen 21, Orto Arlesa) at 15,000 rpm for 10 min.

Quantitative measurements of vitamin E (as α-tocopherol) was performed with an HPLC chromatograph equipped with a diode array detector (Jasco MD 2015) at λ = 285 nm using a silica gel column (Mediterranean Sea-18, Teknokroma) as stationary phase and methanol as mobile phase at 1 ml min^{-1}. The measurements were performed at 303 K. The calibration of the peak area versus concentration of α-tocopherol were linear in the concentration range of 0.175–3.500 mg ml^{-1} (R^2 = 0.9996).

The loading capacity was calculated as the mass percentage ratio between the encapsulated vitamin E and the mass of the encapsulated vitamin E plus the amount of polymer.

2.7. Residual concentration of organic solvent

The amount of acetone in the nanoparticle suspension was measured using headspace gas chromatography. In order to perform the headspace, 2 ml of nanoparticle suspension were introduced into a 20 ml vial, and stabilized for 1 h at 333 K. At this temperature, the polymer melts and acetone is enriched in the vapor phase. Then, 0.5 ml of the vapor phase of this vial were extracted with a gas tight syringe and injected manually into a gas chromatograph (Shimazdu GC-2010-Plus) that was connected to a flame ionization detector. Acetone was separated using a fused-silica capillary column: 20 m long, 0.18 mm internal diameter and 0.18 μm film thickness (Zebron-ZB-1HT inferno). The oven temperature was set to 313 K for 6 min. The injector temperature was maintained at 453 K in split mode (ratio 19.5) and nitrogen was employed as carrier, at 7 ml min^{-1} at 40.9 kPa. Each sample was measured in triplicate.

The residual concentration of acetone in the nanoparticles after the SFEE process was also measured. The aqueous suspension was centrifuged (Digicen 21, Orto Arlesa) at 15,000 rpm for 10 min, to separate the pellet and the supernatant. The pellet was dried in the oven (Digitheat, Selecta) at 308 K until reaching constant weight. The dried particles were resuspended in 2 ml of milli-q water and analyzed by headspace gas chromatography following the preceding procedure.

2.8. Particle size distribution

Particle size distribution was measured by photon correlation spectroscopy using a Zetasizer Nano Zs (Malvern). A dilution of the sample with milli-q water was required to achieve a suitable optical density. All measurements were performed at 298 K.

2.9. Nanoparticles morphology

Aqueous suspensions of nanoparticles were centrifuged at 15,000 rpm for 10 min. After that, the 70% of the supernatant was

removed. A drop of concentrated aqueous suspension was negatively stained for 60 s with a 1% sodium phosphotungstic acid solution, and placed on a carbon-coated copper grid. Transmission Electron Microscopy (TEM) pictures were taken using a JEOL JEM 1010.

The internal morphology of the nanoparticles was studied by TEM using the same microscope. Samples were washed with milli-q water three times before being prepared for TEM. This procedure was performed in an Eppendorf tube, which acted as a mold. The sample preparation process [30] consisted of fixation with Karnosvky solution, washing with phosphate buffer, staining with osmium tetroxide, dehydration with absolute ethanol and inclusion in Spurr resin. After polymerization, ultrathin section of samples were cut using an ultramicrotome before being stained with uranyl salts and deposited over the TEM grid.

2.10. Statistical analysis

The experiments were repeated three times. Analyses were performed in duplicate for each replicate ($n = 3 \times 2$). Means and standard deviations were calculated for all data.

3. Results and discussion

This research focused on the formation of vitamin E nanocapsules using the SFEE process. First, the influence of the extraction parameters (pressure, temperature, CO_2 flow rate, and extraction time) was studied because these properties affect the rate at which the acetone is removed and influence the characteristics of the product. As such, these parameters impact the technical and economic viability of the process. Then, the effect of the initial formulation was evaluated in terms of encapsulation efficiency, particle size, particle size distribution, and morphology.

3.1. Selection of the starting formulation

A study of the phase behavior of the system Tween 80/water/acetone + vitamin E + PCL at atmospheric pressure and ambient temperature was executed in order to select the composition that would be subjected to SFEE. Since the system had five components, data were plotted in a pseudoternary phase diagram, where composition of the organic phase was maintained constant (0.51% and 0.63% by mass of vitamin E and PCL, respectively). Twenty compositions that completely covered the pseudoternary phase diagram were selected. A visual observation of each sample resulted in the triangular diagram depicted in Fig. 2. At high surfactant concentration (>10%), samples were transparent (shown in white) possibly due to the formation of nanosize colloids. PCL separated as a solid phase within the light shaded area.

Only formulation 20 was turbid. Acetone is completely miscible with water; however, the presence of the vitamin E increased the viscosity of the organic phase, allowing the formation of emulsions. These emulsions were stable for days (results not shown). When the PCL was present in the organic phase, the slow diffusion of the acetone to the water initiated PCL precipitation, due to its low solubility in acetone and insolubility in vitamin E. Thus, the turbidity of the formulation 20 was also due to the presence of the incipient particles. However, TEM images of this sample showed that particles were not completely formed at this stage and consequently they broke and aggregated as shown in Fig. 3. Only after the supercritical extraction of the acetone, the particles were adequately formed as described later.

Since the colloid acts as a template, it must provide an adequate size and an O/W structure, which is required to encapsulate a lipophilic compound. These requirements were fulfilled by formulation 20, which had a composition of 71.57% of water, 28.35% of acetone, and 0.08% of Tween 80 by mass. In addition, the low concentration of surfactant in formulation 20 may favor its potential applications. This composition was also selected by Khayata et al. [31] to encapsulate vitamin E using the nanoprecipitation method coupled with solvent evaporation. This coincidence allowed us to compare the results from both techniques. Another starting mixture was selected, in this case, a transparent dispersion that corresponded with formulation 18 (80% of water, 10% of acetone and 10% of Tween 80). Compared to formulation 20, this sample had a smaller colloid size; however, the concentration of surfactant was higher, which could condition the subsequent application of the nanoparticles.

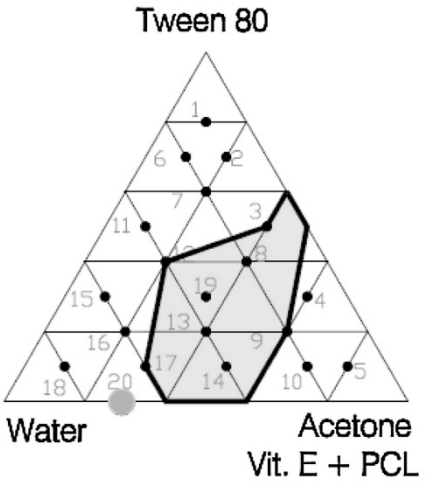

Fig. 2. Phase map of the system Tween 80/water/acetone + vitamin E (0.51% by mass) + PCL (0.63% by mass). The system exhibited three behaviors: the transparent samples are shown in white; PCL separated as a solid phase within the light shaded area; formulation 20 was turbid.

3.2. Influence of the operating conditions

Pressure and temperature have a significant effect on the emulsion characteristics and, consequently, on the produced nanoparticles. Temperature can provoke a change in the hydrophilic character of the surfactant, or even the loss of its surfactive character, if it reaches the cloud point [32].

The organic solvent should not be heated to boiling point [13] because the formation of bubbles can destroy the drops of the organic phase, affecting encapsulation efficiency, particle size, and the porosity of the polymeric wall. At atmospheric pressure, the boiling temperature of acetone is 323 K. It is also important that the glass transition temperature and the melting point of the polymer are taken into consideration because these factors can affect drug retention. Polycaprolactone is a semicrystalline polymer that has a very low glass transition temperature (213 K) and a melting point of 333 K. In addition, pressure and temperature affect the CO_2 density, vapor pressure of the acetone, the critical locus of the mixture CO_2-acetone, and the degradation of the active compound. Thus, their impact is complex and difficult to predict.

Initially, the pressure and temperature were selected such that they favored the maximum extraction rate of the organic solvent without extracting the bioactive compound while avoiding the use of high temperatures. According to the high pressure vapor-liquid equilibrium diagram of the CO_2-acetone mixture [33], at 8 MPa and 313 K, respectively, miscibility between carbon dioxide and acetone was complete. In these conditions, the solubility of vitamin E in supercritical CO_2 was quite low (0.3 mg vitamin E per g CO_2) [34]

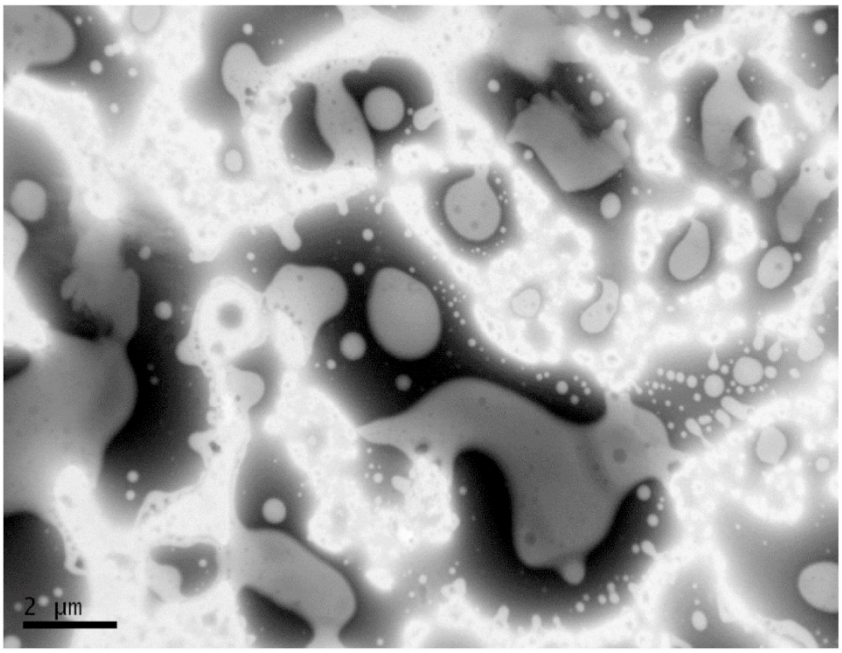

Fig. 3. TEM image of the formulation 20 before being subjected to SFEE.

not being significantly improved by the presence of the acetone as no vitamin E was collected on the CO_2 outlet stream after many runs.

Next, the CO_2 flow rate was studied with the intention of maximize the extraction of the organic solvent. Several CO_2 flow rates were tested trying to avoid the entrainment of the sample. Table 1 shows the outcomes of CO_2 flow rates that varied from 1 to 3 ml min^{-1}. As the results indicate, an increase in CO_2 flow rate led to a higher acetone extraction rate. However, the removal rate was at a maximum when the system operated at 2 ml min^{-1} (7.2 kg h^{-1} kg $emulsion^{-1}$). This can be attributed to the competing effects that arise when the CO_2 flow rate is augmented. On the one hand, larger flow rates enhanced Reynolds numbers and superficial solvent velocity, which benefited turbulence and external mass transfer. On the other hand, larger flow rates reduced contact time for acetone extraction.

The residual concentration of acetone versus the required amount of CO_2 when operating at 2 ml min^{-1} is shown in Fig. 4. The extraction of the acetone was initially very fast because high amounts of acetone were available. Thus, with 12 g of CO_2, corresponding to a CO_2/acetone mass ratio of 8 kg kg^{-1}, the concentration of acetone decreased from 283,500 ppm to 32,607 ppm (corresponding to an extraction yield of 88%) in the first 20 min. However, as the acetone concentration decreased and particles were formed, the extraction rate rapidly decreased. Some of the acetone was entrapped inside the particles and the internal diffusion and transport through the polymer wall controlled the overall rate of extraction. Consequently, higher CO_2 ratios and longer operation times were required to reduce the acetone concentration below 30,000 ppm. For example, 50 min and a CO_2/acetone ratio of 21 kg kg^{-1} were required to achieve a residual solvent concentration of 5000 ppm, which is the maximum acetone concentration permitted in pharmaceutics [27]. Operation time and CO_2/acetone ratio should be increased to 240 min and 101 kg kg^{-1} respectively in order to achieve the maximum acetone concentration of 50 ppm required in food production [35]. At this point, acetone content in the interior of the particles was about 5 ppm. Similar extraction curve shapes were reported in [22].

3.3. Influence of the composition on the characteristics of the particles

The impact of the initial composition (amount of vitamin E, PCL, Tween 80, and acetone) on the characteristics of the nanoparticles (particle size distribution, encapsulation efficiency, and morphology) was further investigated. This stage of the research involved

Table 1
Influence of the CO_2 flow rate on the residual concentration of acetone. Formulation 20 had an initial acetone concentration of 28.35% by mass (283,500 ppm).

Time (min)	CO_2 Flow rate (ml min^{-1})	CO_2/Acetone Ratio (kg CO_2 kg $acetone^{-1}$)	Residual Concentration of Acetone (ppm)
60	1	13	12,380 ± 1437
120	1	25	4067 ± 941
180	1	38	2834 ± 667
30	2	13	19,278 ± 1333
120	2	51	110 ± 22
180	2	76	63 ± 2
240	2	101	52 ± 7
30	3	19	12,691 ± 1490
45	3	28	3427 ± 540
120	3	76	2066 ± 104

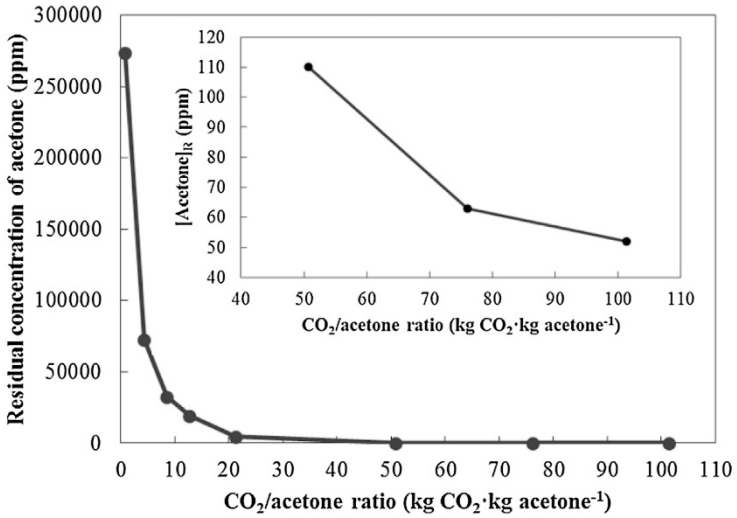

Fig. 4. Extraction curve of acetone from formulation 20 in the SFEE process at a CO_2 flow rate of 2 ml min^{-1} (7.2 kg h^{-1} kg emulsion^{-1}), operating at 8 MPa and 313 K.

nine samples (A–I) that varied in respect to the amount of vitamin E, PCL, Tween 80, and acetone contained within formulation 20, which corresponds to letter A. Each effect was studied separately while the other components of the system remained constant. The nanoparticles obtained from a turbid (A) and a transparent (J) samples were compared in terms of particle size distribution and morphology. A summary of the composition of the samples (A–J) is presented in Table 2, and the influence of the composition on the nanoparticle characteristics is shown in Table 3.

As it can be observed in Table 3, the nanoparticles obtained from these formulations exhibited high encapsulation efficiency of around 90%, and a loading capacity of between 40% and 70%. In terms of particle size, they were in the nanometer range, with mean size that varied between 8 and 276 nm. In addition, they showed a fairly narrow particle size distribution, with polydispersity index (PdI) around 0.26, which increased to 0.40 or 0.54 in some samples.

Table 2
Composition of the samples. Sample A corresponded to the formulation 20. Sample J corresponded to the formulation 18.

Sample	Water (g)	Tween 80 (g)	Acetone (g)	PCL (g)	Vitamin E (g)
A	3.580	0.004	1.420	0.009	0.007
B	3.580	0.004	1.420	0.009	0.014
C	3.580	0.004	1.420	0.009	0.021
D	3.580	0.004	1.420	0.003	0.007
E	3.580	0.004	1.420	0.007	0.007
F	4.500	0.004	0.500	0.009	0.007
G	4.000	0.004	1.000	0.009	0.007
H	3.580	0.002	1.420	0.009	0.007
I	3.580	0.050	1.420	0.009	0.007
J	4.000	0.500	0.500	0.009	0.007

The amount of vitamin E and PCL were the two formulation parameters that influenced encapsulation efficiency and consequently loading capacity. Both parameters increased as did the

Table 3
Influence of the composition on the characteristics of the nanoparticles. The variation in the amount of the compound is represented as a percentage of the total amount of starting emulsion.

Sample	Amount (%)	Mean diameter ± SD (nm)	PdI ± SD	EE ± SD (%)	Loading capacity ± SD (%)
			Effect of the Amount of Vitamin E		
A	0.14	153 ± 33	0.26 ± 0.02	90.5 ± 1.1	42.0 ± 0.3
B	0.28	113 ± 51	0.30 ± 0.05	95.6 ± 2.6	60.1 ± 0.7
C	0.42	90 ± 18	0.40 ± 0.06	96.1 ± 6.4	69.4 ± 0.8
			Effect of the Amount of PCL		
D	0.06	129 ± 27	0.24 ± 0.10	95.6 ± 7.0	69.6 ± 1.6
E	0.14	156 ± 19	0.26 ± 0.04	91.6 ± 6.9	48.5 ± 1.5
A	0.18	153 ± 33	0.26 ± 0.02	90.5 ± 1.1	42.0 ± 0.3
			Effect of the Amount of Acetone		
F	9.96	66 ± 9	0.26 ± 0.01	n.m.[a]	n.m.
G	19.92	90 ± 12	0.30 ± 0.07	n.m.	n.m.
A	28.28	153 ± 33	0.26 ± 0.02	90.5 ± 1.1	42.0 ± 0.3
			Effect of the Amount of Tween 80		
H	0.04	110 ± 27	0.32 ± 0.06	n.m.	n.m.
A	0.08	153 ± 33	0.26 ± 0.02	90.5 ± 1.1	42.0 ± 0.3
I	1.00	276 ± 10	0.34 ± 0.11	n.m.	n.m.
			Effect of the Initial Colloid Size		
A	0.08	153 ± 33	0.26 ± 0.02	90.5 ± 1.1	42.0 ± 0.3
J	10.00	8 ± 1	0.54 ± 0.07	n.m.	n.m.

[a] n.m. Not measured.

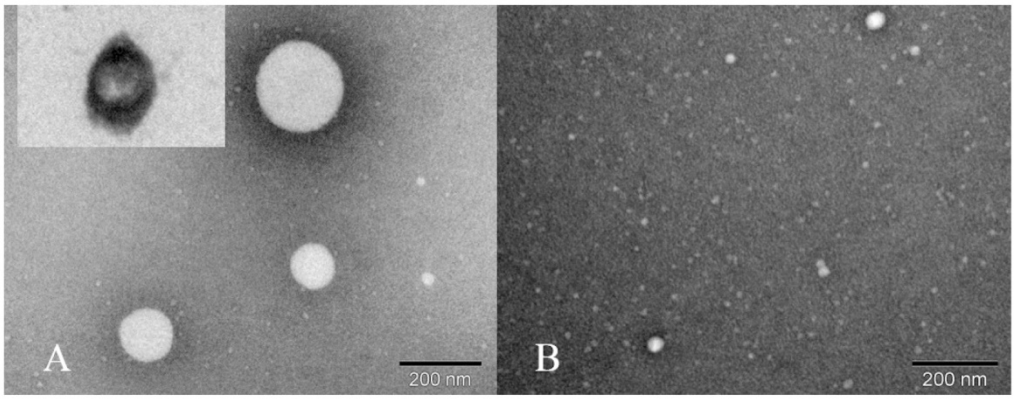

Fig. 5. TEM image of vitamin E loaded nanocapsules. Image A: nanoparticles obtained from a formulation 20, an ultrathin section of vitamin E nanoparticles is shown in the upper left corner. Image B: nanoparticles obtained from formulation 18.

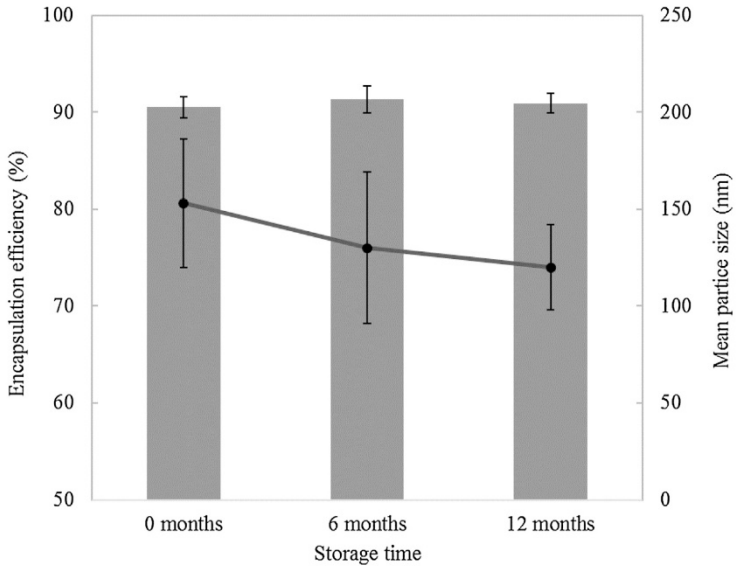

Fig. 6. Evolution of encapsulation efficiency and mean particle size of the particles obtained from formulation 20 with storage time. The columns indicate the encapsulation efficiency while the points depict the mean particle size.

amount of vitamin E. This can be related to the higher initial amount of vitamin E, and to its lipophilicity [31] and viscosity [13], which prevented its leakage to the water phase. In the same way, André-Abrant et al. [36] observed that the encapsulation efficiency increased as did the drug amount for the microencapsulation of ethybenzoate in ethylcellulose by solvent evaporation. The reason of this behaviour was attributed to the increase of the organic phase viscosity, which reduced the mass transfer resistance between phases. However, the augmentation in encapsulation efficiency with increasing the amount of vitamin E is limited by the loss of stability, by pore formation or due to the insufficient thickness of the polymeric wall to protect the core [13]. For this system, the amount of vitamin E could not be further increased because the emulsion lost its stability, as evidenced by the appearance of separate vitamin E droplets.

The reduction in the amount of PCL in the range considered did not have a significant effect on encapsulation efficiency; however, loading capacity increased because of the reduction in the amount of polymer. Moreover, excessive amounts of polymer provoked a loss in stability, since phase separation and PCL precipitation were observed (results not shown). This stability loss could be linked to the low solubility of PCL in acetone. Therefore, the main parameter affecting encapsulation efficiency was the amount of vitamin E.

It is well known that viscosities of the dispersed and continuous phases together with flow-mechanic factors (agitation device, agitation intensity, time) are the most relevant parameters that affect particle size [13]. In the current study, the amount of each component was varied while the starting emulsion preparation procedure remained constant. The viscosity of the dispersed phase can be theoretically increased by rising the amount of vitamin E, PCL or reducing the amount of acetone. Surprisingly, the results in Table 3 do not respond to this tendency. In the current study, the particle size decreased as the amount of vitamin E increased, while PdI increased. Similarly, Saberi et al. [3] observed that droplet size and PdI were dependent on the amount of vitamin E acetate in an emulsion composed of vitamin E acetate, medium chain triglyc-

Table 4
A comparison between the operation conditions and results obtained by SFEE and solvent evaporation at vacuum pressure or atmospheric pressure.

	SFEE	Solvent Evaporation at Vacuum	Solvent Evaporation at Atmospheric Pressure
Pressure (kPa)	$8{\cdot}10^3$	30+6	100
Operation time (min)	240	30+30	240
Temperature (K)	313	323	313
Sample amount (g)	5	75	100
		Residual amount of acetone	
±SD (ppm)	52 ± 7	235 ± 63	157 ± 31
		Encapsulation efficiency	
±SD (%)	90.5 ± 1.1	86.0 ± 1.0	78.0 ± 1.0
Loading capacity ± SD (%)	42.0 ± 0.3	40.2 ± 0.1	37.7 ± 0.3
Mean particle size ± SD (nm)	153 ± 33	115 ± 15	123 ± 51
Polydispersity index ± SD	0.26 ± 0.02	0.63 ± 0.09	0.18 ± 0.02

eride oil, Tween 80, and water. Thus, they observed that the droplet size decreased with respect to the amount of vitamin E acetate until it reached a minimum level and then subsequently increased. With respect to PCL, it was expected that the particle size should be larger when a higher amount of PCL was used. However, no significant changes were observed in the studied range. Khayata et al. [31] obtained the same results for the same system when using nanoprecipitation coupled with solvent evaporation. Likewise, Moinard-Checot et al. [37] did not observe any significant influence of the amount of polymer in particle size when encapsulating caprylic and capric fatty acids in PCL by emulsion-diffusion.

On the other hand, the particle size decreased as did the acetone concentration even though the viscosity of the organic dispersed phase increased. This could be due to a smaller initial colloid size caused by a lower amount of the organic phase.

A further factor that can influence particle size is the amount of surfactant. A slight increase in the amount of Tween 80 resulted in a larger particle size (compare the mean diameter of particles of samples H, A and I). The same results were obtained by Moinard-Chécot et al. [37] for the system caprylic and capric fatty acids, PCL, ethyl acetate, PVA (poly(vinyl alcohol) and water, in which the particle size increased as the concentration of PVA increased.

However, when sample J was subjected to SFEE, nanoparticles with a mean particle diameter of 8 nm were obtained; thus, particle size was highly reduced by starting from a colloid of smaller size. The increase in PdI is also noteworthy.

3.4. Morphology

The morphology of the nanoparticles was studied by TEM. Particles obtained from the formulation 20 after the SFEE procedure, are shown in Fig. 5A. These particles were spherical and had a size of around 200 nm. This data correlated well with the size measured by photon correlation spectroscopy shown in Table 3. No particle agglomeration was observed.

The internal morphology of these particles was studied by cutting the nanoparticles. A cut nanoparticle of vitamin E in polycaprolactone is shown in the upper left corner of Fig. 5A. As can be observed in the image, there was a hole in the interior of the nanoparticle [38] because there was no polymer inside the nanoparticle. This confirms that nanocapsules were obtained. This result can be linked to the high surface activity of the PCL, which tends to transition to the particle surface [39], generating true core-shell nanoparticles.

A TEM image of vitamin E-loaded nanoparticules obtained from the formulation 18 is shown in Fig. 5B. As can be observed, by changing the starting colloid size, nanoparticle size can be highly reduced, up to 8 nm as revealed by photon correlation spectroscopy. Particles were not aggregated.

3.5. Storage stability tests

Nanoparticle suspensions obtained during these experiments were stored at 277 K in the refrigerator for 6 and 12 months. After this time, particles were reanalyzed in terms of encapsulation efficiency and particle size distribution. No significant changes were observed. The encapsulation efficiency remained constant after one year, as can be observed in Fig. 6. The same phenomenon could be observed in terms of particle size distribution and polydispersity index. This significant stability could be related to the hardness and semicrystalline character of the PCL. Furthermore, it could be associated with the fact that the high viscosity of vitamin E prevented its leakage through the pores of the PCL.

3.6. Formation of nanoparticles through conventional solvent evaporation

The vitamin E nanoparticles were formed by conventional solvent evaporation using the formulation 20 in order to compare results with those particles obtained by SFEE. The results are shown in Table 4.

The characteristics of the particles obtained by conventional solvent evaporation were similar to those obtained by SFEE when the rotatory evaporator was used at vacuum pressure; however, the residual concentration of acetone was higher (235 ppm) and the encapsulation efficiency was slightly lower (86%). The increase in the polydispersity index could be due to the acetone boiling bubbles inside the droplet, as Li et al. [13] stated. In terms of solvent evaporation at atmospheric pressure, the residual concentration of acetone was slightly higher (157 ppm) than that observed for the SFEE procedure after the same operation time (4 h). It is important to take into account the fact that mass transfer between the water-air interface was improved using the fume hood. The characteristics of the particles were similar to those observed for the other two processes.

It is obvious that SFEE required a longer operation time than the other techniques to obtain a small sample. However, it is possible to increase the production capacity by running a continuous operation in a spray or a packed column [25,23].

4. Conclusions

This research demonstrated that SFEE is a viable new method of producing nanocapsules of liquid lipophilic compounds. The particles obtained via this process exhibited a high encapsulation efficiency, narrow particle size distribution, and high storage stability. A morphological analysis confirmed that spherical, core-shell and non-aggregated nanocapsules were produced. Of the operation parameters, initial formulation had the biggest impact on nanoparticle characteristics. In contrast, the operation variables of the SFEE process had the most significant influence on the organic solvent

removal. By fine tuning the pressure, temperature, and CO_2 flow rate, it was possible to obtain the residual solvent concentration required for food applications. Nonetheless, more work is required in this area to reduce the production costs of this approach; i.e., to reduce the operation time and CO_2 consumption required for the removal of the organic solvent. Above all else, it is necessary to improve the internal mass transfer that controls the overall extraction rate. However, there is little margin for improvement in terms of the manipulation of the pressure and temperature, and the properties of the dispersed phase. Therefore, the best opportunity for this supercritical technology, involves increasing the contact time by using a packed column of adequate length, run in counter-current mode. A continuous operation would also be beneficial because it will increase the capacity of the procedure while consuming less CO_2, which is the most important benefit of the technology versus the conventional solvent evaporation techniques, which are difficult to scale. Furthermore, SFEE can be performed at low temperatures. This is advantageous because it is suitable for use with heat sensitive materials. Thus, future work should focus on the scale-up of the SFEE technology.

Acknowledgments

Authors acknowledge prof. Miguel Ladero for his support on HPLC analysis, and Centro Nacional de Microscopía Electrónica (CNME) for its support on TEM analysis. Cristina Prieto thanks the Complutense University of Madrid for an UCM predoctoral grant.

References

[1] P.M. Bramley, I. Elmadfa, A. Kafatos, F.J. Kelly, Y. Manios, H.E. Roxborough, W. Schuch, P.J.A. Sheehy, K.H. Wagner, Vitamin E, J. Sci. Food Agric. 80 (2000) 913–938, http://dx.doi.org/10.1002/(SICI)1097-0010(20000515)80:7<913:AID-JSFA600>3.0.CO;2-3.

[2] C.M. Sabliov, C.E. Astete, Encapsulation and controlled release of antioxidants and vitamins, in: N. Garti (Ed.), Delivery and Controlled Release of Bioactives in Foods and Nutraceuticals, Woodhead Publishing Limited, Cambridge, 2008, pp. 297–330, http://dx.doi.org/10.1016/B978-1-84569-145-5.50020-2.

[3] A.H. Saberi, Y. Fang, D.J. McClements, Fabrication of vitamin E-enriched nanoemulsions: factors affecting particle size using spontaneous emulsification, J. Colloid Interface Sci. 391 (2013) 95–102, http://dx.doi.org/10.1016/j.jcis.2012.08.069.

[4] M. Gonnet, L. Lethuaut, F. Boury, New trends in encapsulation of liposoluble vitamins, J. Control. Release 146 (2010) 276–290, http://dx.doi.org/10.1016/j.jconrel.2010.01.037.

[5] A. Dingler, R.P. Blum, H. Niehus, R.H. Müller, S. Gohla, Solid lipid nanoparticles (SLNTM/LipopearlsTM)- a pharmaceutical and cosmetic carrier for the application of vitamin E in dermal products, J. Microencapsul. 16 (1999) 751–767, http://dx.doi.org/10.1080/026520499288690.

[6] M.N. Padamwar, V.B. Pokharkar, Development of vitamin loaded topical liposomal formulation using factorial design approach: drug deposition and stability, Int. J. Pharm. 320 (2006) 37–44, http://dx.doi.org/10.1016/j.ijpharm.2006.04.001.

[7] M. Otadi, F. Zabihi, Vitamin E microencapsulation by ethylcellulose through emulsion solvent evaporation technique; an operational condition study, World Appl. Sci. J. 14 (2011) 20–25.

[8] C.C. Chen, G. Wagner, Vitamin E nanoparticle for beverage applications, Chem. Eng. Res. Des. 82 (2004) 1432–1437, http://dx.doi.org/10.1205/cerd.82.11.1432.52034.

[9] B. Albertini, N. Passerini, F. Pattarino, L. Rodríguez, New spray congealing atomizer for the microencapsulation of highly concentrated solid and liquid substances, Eur. J. Pharm. Biopharm. 69 (2008) 348–357, http://dx.doi.org/10.1016/j.ejpb.2007.09.011.

[10] N.V.N. Jyothy, P.M. Prasanna, S.N. Sakarkar, K.S. Prabha, P.S. Ramaiah, G.Y. Srawan, Microencapsulation techniques, factors influencing encapsulation efficiency, J. Microencapsul. 27 (2010) 187–197, http://dx.doi.org/10.3109/02652040903131301.

[11] C.E. Mora-Huertas, H. Fessi, A. Elaissari, Polymer-based nanocapsules for drug delivery, Int. J. Pharm. 385 (2010) 113–142, http://dx.doi.org/10.1016/j.ijpharm.2009.10.018.

[12] S. Freitas, H.P. Merkle, B. Gander, Microencapsulation by solvent extraction/evaporation: reviewing the state of the art of microsphere preparation process technology, J. Control. Release 102 (2005) 313–332, http://dx.doi.org/10.1016/j.jconrel.2004.10.015.

[13] M. Li, O. Rouaud, D. Poncelet, Microencapsulation by solvent evaporation: state of the art for process engineering approaches, Int. J. Pharm. 363 (2008) 26–39, http://dx.doi.org/10.1016/j.ijpharm.2008.07.018.

[14] N. Falco, E. Reverchon, G. Della Porta, Continuous supercritical emulsions extraction: packed tower characterization and application to poly(lactic-co-glycolic acid) + insulin microspheres production, Ind. Eng. Chem. Res. 51 (2012) 8616–8623, http://dx.doi.org/10.1021/ie300482n.

[15] M. Perrut, J. Jung, F. Leboeuf, Enhancement of dissolution rate of poorly soluble active ingredients by supercritical fluid processes part II: preparation of composite particles, Int. J. Pharm. 288 (2005) 11–16, http://dx.doi.org/10.1016/j.ijpharm.2004.09.008.

[16] M.J. Cocero, A. Martín, F. Mattea, S. Varona, Encapsulation and co-precipitation processes with supercritical fluids: fundamentals and applications, J. Supercrit. Fluids 47 (2009) 546–555, http://dx.doi.org/10.1016/j.supflu.2008.08.015.

[17] E. Weidner, High pressure micronization for food applications, J. Supercrit. Fluids 47 (2009) 556–565, http://dx.doi.org/10.1016/j.supflu.2008.11.009.

[18] Natex Prozesstechnologie Austria, Powder Plants, http://www.natex.at/Processdescriptionpow.html, 2016 (accessed 18.03.16).

[19] S. Varona, A. Martín, M.J. Cocero, C.M.M. Duarte, Encapsulation of lavandin essential oil in poly-(ε-caprolactones) by PGSS process, Chem. Eng. Technol. 36 (2013) 1187–1192, http://dx.doi.org/10.1002/ceat.201200592.

[20] P. Chattopadhyay, B.Y. Shekunov, J.S. Seitzinger, R.W. Huff, Particles from supercritical fluid extraction of emulsion, U.S. Patent 2004026319 (A1), February 12, 2004.

[21] P. Chattopadhyay, B.Y. Shekunov, J.S. Seitzinger, R.W. Huff, Composite Particles and Method for Preparing, U.S. Patent 2004071781 (A1), April 15, 2004.

[22] P. Chattopadhyay, R. Huff, B.Y. Shekunov, Drug encapsulation using supercritical fluid extraction of emulsions, J. Pharm. Sci. 95 (2006) 667–679, http://dx.doi.org/10.1002/jps.20555.

[23] G. Della Porta, R. Campardelli, N. Falco, E. Reverchon, PLGA microdevices for retinoids sustained release produced by supercritical emulsions extraction: continuous versus batch operation layouts, J. Pharm. Sci. 100 (2011) 4357–4367, http://dx.doi.org/10.1002/jps.22647.

[24] G. Della Porta, N. Falco, E. Reverchon, Continuous supercritical emulsions extraction: a new technology for biopolymer microparticles production, Biotechnol. Bioeng. 108 (2011) 676–686, http://dx.doi.org/10.1002/bit.22972.

[25] D.T. Santos, A. Martín, M.A.A. Meireles, M.J. Cocero, Production of stabilized sub-micrometric particles of carotenoids using supercritical fluid extraction of emulsions, J. Supercrit. Fluids 61 (2012) 167–174, http://dx.doi.org/10.1016/j.supflu.2011.09.011.

[26] V.R. Sinha, K. Bansal, R. Kaushik, R. Kumria, A. Trehan, Poly-ε-caprolactone microspheres and nanospheres: an overview, Int. J. Pharm. 278 (2004) 1–23, http://dx.doi.org/10.1016/j.ijpharm.2004.01.044.

[27] Guidance for Industry QC3- Tables and List, U.S. Department of Health and Human Services, Food and Drug Administration Center for Drug Evaluation and Research (CDER), Center for Biologics Evaluation and Research (CBER), ICH, Revision 2, 2012.

[28] D.J. McClements, Nanoparticle- and Microparticle Based Delivery Systems. Encapsulation, Protection and Release of Active Compounds, CRC, Press, Boca Raton, 2015, pp. 103–105, http://dx.doi.org/10.1201/b17280-4.

[29] J. Lyklema, Fundamentals of Interface and Colloid Science, Volume 4 Particulate Colloids, Elsevier, London, 2005, pp. 2.39–2.43.

[30] J. Ayache, L. Beaunier, J. Boumendil, G. Ehret, D. Laub, Sample Preparation Handbook for Transmission Electron Microscopy. Techniques, Springer, New York, 2010, http://dx.doi.org/10.1007/978-1-4419-5975-1.

[31] N. Khayata, W. Abdelwahed, M.F. Chehna, C. Charcosset, H. Fessi, Preparation of vitamin E loaded nanocapsules by the nanoprecipitation method: from laboratory scale to large scale using a membrane contactor, Int. J. Pharm. 423 (2012) 419–427, http://dx.doi.org/10.1016/j.ijpharm.2011.12.016.

[32] C. Prieto, L. Calvo, Performance of the biocompatible surfactant tween 80, for the formation of microemulsions suitable for new pharmaceutical processing, J. Appl. Chem. 2013 (2013), 930356 10, http://dx.doi.org/10.1155/2013/930356.

[33] H.Y. Chiu, M.J. Lee, H.M. Lin, Vapor-liquid phase boundaries of binary mixtures of carbon dioxide with ethanol and acetone, J. Chem. Eng. Data 53 (2008) 2393–2402, http://dx.doi.org/10.1021/je800371a.

[34] J. Chrastil, Solubility of solids and liquids in supercritical gases, J. Phys. Chem. 86 (1982) 3016–3021, http://dx.doi.org/10.1021/j100212a041.

[35] Spain 2011. Real Decreto 1101/2011, de 22 de Julio, por el que se aprueba la lista positiva de los disolventes de extracción que se pueden utilizar en la fabricación de productos alimenticios y de sus ingredientes. Boletín Oficial del Estado, 30 de Agosto de 2011, 208, 94132–94137.

[36] A. André-Abrant, J.L. Taverdet, J. Jay, Microencapsulation par évaporation de solvent, Eur. Polym. J. 37 (2001) 955–963, http://dx.doi.org/10.1016/S0014-3057(00)00197-X.

[37] D. Moinard-Chécot, Y. Chevalier, S. Briançon, L. Beney, H. Fessi, Mechanism of nanocapsules formation by the emulsion-diffusion process, J. Colloid Interface Sci. 317 (2008) 458–468, http://dx.doi.org/10.1016/j.jcis.2007.09.081.

[38] S. Begum, I.P. Jones, C. Jiao, D.E. Lynch, J.A. Preece, Characterisation of hollow Russial doll microspheres, J. Mater. Sci. 45 (2010) 3697–3706, http://dx.doi.org/10.1007/s10853-010-4479-3.

[39] Z.G. Tang, R.A. Black, J.M. Curran, J.A. Hunt, N.P. Rhodes, D.F. Williams, Surface properties and biocompatibility of solvent-cast poly[ε - caprolactone] films, Biomaterials 25 (2004) 4741–4748, http://dx.doi.org/10.1016/j.biomaterials.2003.12.003.

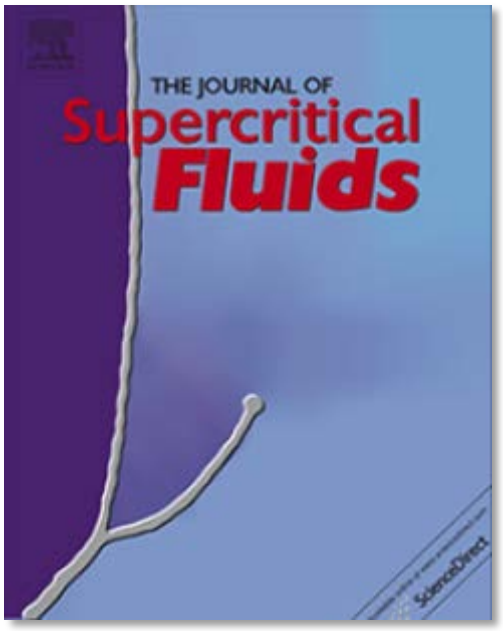

Publication III:

"***Performance comparison of different supercritical fluid extraction equipments for the production of vitamin E in polycaprolactone nanocapsules by supercritical fluid extraction of emulsions***"

Cristina Prieto, Catarina M.M. Duarte, Lourdes Calvo

Journal of Supercritical Fluids 122 (2017) 70-78,

http://dx.doi.org/10.1016/j.supflu.2016.11.015.

Impact Factor (2015): 2.579

Citations: 0

J. of Supercritical Fluids 122 (2017) 70–78

Contents lists available at ScienceDirect

The Journal of Supercritical Fluids

journal homepage: www.elsevier.com/locate/supflu

Performance comparison of different supercritical fluid extraction equipments for the production of vitamin E in polycaprolactone nanocapsules by supercritical fluid extraction of emulsionsc

Cristina Prieto[a], Catarina M.M. Duarte[b,c], Lourdes Calvo[a,*]

[a] *Departamento de Ingeniería Química, Facultad de Ciencias Químicas, Universidad Complutense de Madrid, Av. Complutense s/n, 28040 Madrid, Spain*
[b] *IBET– Instituto de Biología Experimental e Tecnológica, Av. República, Qta. Do Marquês, Estação Agronómica Nacional, apartado 12, 2780-157, Oeiras, Portugal*
[c] *ITQB – Instituto de Tecnologia Química e Biológica António Xavier, Universidade Nova de Lisboa, Av. da República, 2780-157, Oeiras, Portugal*

ARTICLE INFO

Article history:
Received 22 November 2016
Accepted 23 November 2016
Available online 24 November 2016

Keywords:
Supercritical fluid extraction of emulsions
Bubble column
Spray column
Packed column
Scale-up

ABSTRACT

The encapsulation of vitamin E in polycaprolactone was done using four SFEE installations: A) a bubble column, B) a bubble column with gas redistributor, C) a spray column and D) a packed column. Performance of each installation was compared in terms of organic solvent removal, CO_2 consumption and nanocapsule characteristics (encapsulation efficiency, particle size distribution and morphology). Bubble columns provided particles with good characteristics but required a high CO_2 consumption and the production capacity were very low. The gas redistributor allowed decreasing the CO_2 expenditure, but the operation was still discontinuous. Despite the high CO_2 consumption in the spray column, the target acetone removal could not be achieved and particle morphology was negatively affected. The countercurrent operation in a packed column provided high production capacity, maintained good particle quality, and required a low amount of CO_2 to remove the acetone.

1. Introduction

Multiple processes have been developed for the formation of biopolymer-based micro- and nanoparticles [1,2], the most important being spray drying, coacervation, fluid bed coating, interfacial polymerization, and solvent evaporation, among others. Some of these methods, such as solvent evaporation, solvent extraction or solvent diffusion, use an emulsion for the subsequent production of nanoparticles, since the emulsion acts as a template, which allows obtaining particles with a narrower particle size distribution.

Current emulsion-based nanoparticle production processes have difficulties in producing solvent-free nanoparticles with good encapsulation efficiency [3,4]. In these processes, the organic solvent is removed by solvent evaporation or solvent extraction; however, residual organic solvent concentration is high, compromising product safety and applicability [5]. The alternative to conventional processes is to use supercritical fluid extraction.

Supercritical fluids are a new generation of green solvents. Among them, carbon dioxide is the most widely used for pharmaceutical and food technology applications. It is non-toxic, non-inflammable, relatively cheap and has mild critical conditions (T_c = 304 K and P_c = 7.4 MPa). In addition, some supercritical CO_2 properties, such as density, dielectric constant, diffusion coefficient, and solvent power can be modified changing pressure and temperature, especially near the critical region. Secondly, it can be easily recovered and recycled after use.

Supercritical Fluid Extraction of Emulsions (SFEE) is a novel encapsulation technology [6] that combines conventional emulsion processes with the unique properties of supercritical fluids to produce tailored micro- and nanoparticles. The basis of this process relies on the use of supercritical CO_2 to rapidly extract the organic phase of an emulsion, in which a bioactive compound and its coating polymer have been previously dissolved. By removing the solvent, both compounds precipitate, generating a suspension of particles in water. The produced particles have controlled size and morphology [6], due to the use of the emulsion and to the fast kinetics of the supercritical CO_2 extraction. Particle agglomeration in the aqueous phase is avoided since the particles are stabilized by a surfactant. In addition, this technology is very versatile. It

* Corresponding author.
E-mail address: lcalvo@ucm.es (L. Calvo).

http://dx.doi.org/10.1016/j.supflu.2016.11.015
0896-8446/

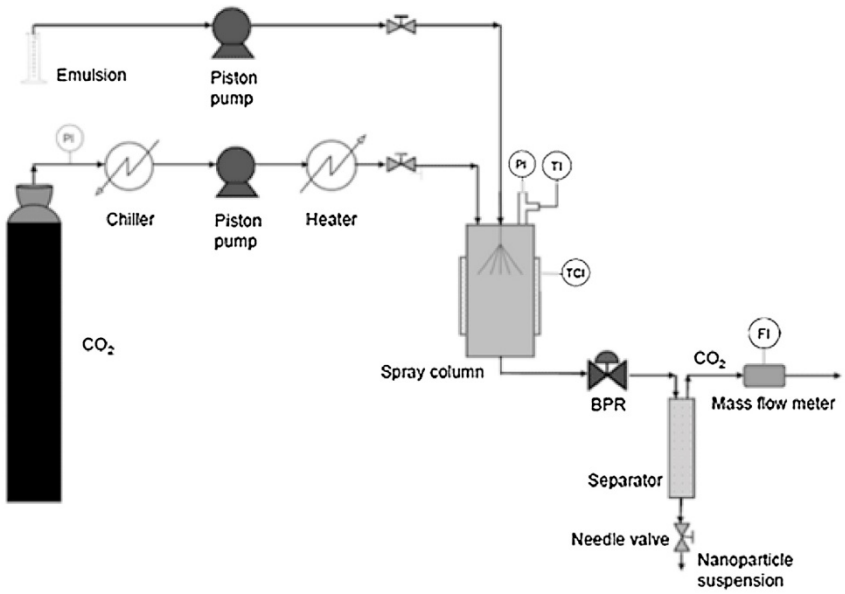

Fig. 1. Scheme of the spray column configuration used for continuous Supercritical Fluid Extraction of Emulsions (SFEE).

is possible to encapsulate hydrophilic and lipophilic compounds by changing the starting emulsion. An oil-in-water (O/W) emulsion can be used to encapsulate lipophilic compounds, while a water-in-oil-in-water (W/O/W) emulsion can be used to encapsulate hydrophilic compounds. Previous studies have demonstrated that this process is easily scalable by means of a countercurrent column [7,8]; however, more work should still be done on the design and optimization of operating variables. In an earlier work, we have investigated the encapsulation of vitamin E in polycaprolactone using this technology [9]. Yielded particles had a very high encapsulation efficiency (around 90%), narrow particle size distribution (polydispersity index was between 0.24 and 0.54) and sizes at the nanoscale (between 8 and 276 nm). Morphology analysis showed that they were true spherical nanocapsules and they were non-aggregated. Stability testing showed that they remained unchangeable even at long storage times (6 and 12 months).

Such promising results made it interesting to scale-up the technology. However, this technology will be only feasible if particles are obtained with an adequate residual organic solvent concentration for the final application, normally in the pharmaceutical or food industries. So far, works have been conducted with solvents such as dichloromethane, toluene, chloroform, ethyl acetate or acetone [7,9–12]. Only acetone and ethyl acetate are solvents allowed in compliance with Good Manufacturing Practices in the food industry, whilst the amount of dichloromethane is limited depending on the food product; toluene and chloroform are not permitted [13]. Moreover, while acetone and ethyl acetate are Class 3 solvents (solvents with low toxic potential, permitted daily exposure of 50 mg day^{-1} or 5000 ppm) following ICH guidelines for pharmaceutical applications [14], dichloromethane, toluene and chloroform are Class 2 (solvents to be limited) and thus the allowed residual concentration is lower, between 890 and 60 ppm.

The aim of this work was to study the efficiency of different supercritical extraction installations on organic solvent removal and the impact on nanocapsule characteristics. The best configuration should provide reduced CO_2 consumption, high production capacity and good particle characteristics.

2. Materials and methods

2.1. Materials

Vitamin E (α-tocopherol, ≥95%), polycaprolactone (PCL) (MW = 10,000), Tween 80 (polyoxyethylene (20) sorbitan monooleate), and acetone (≥99.5% (GC)) were all from Sigma Aldrich. Acetonitrile (gradient 240 nm/far UV HPLC grade) was from Scharlab. Sodium phosphotungstic acid solution (1%) was from Panreac. Carbon dioxide (99.98%) was from Air Liquide. All materials were used as received. Millipore water was used throughout the study.

2.2. Preparation of the starting emulsions

The system for the encapsulation of vitamin E consisted of acetone, water, Tween 80 as a surfactant, and PCL as the encapsulating polymer. PCL (0.51% by mass) and vitamin E (0.63% by mass) were dissolved in acetone. The aqueous phase was prepared by dissolving Tween 80 (0.08% by mass) in water. The organic phase (28.4% by mass) was added dropwise to the aqueous phase and stirred in the vortex (Heildolph Reax Top) for 5 min to guarantee a homogeneous dispersion. When high volumes of starting emulsion were required, a peristaltic pump (Masterflex 7524-10, Cole-Palmer) was used to add the organic phase dropwise, and a high-speed homogenizer (Ultraturrax T-25, IKA) was used instead of the vortex.

Although acetone is completely water-miscible, the presence of vitamin E increased the viscosity of the organic phase, allowing the formation of stable emulsions. When PCL was present in the organic phase, the slow diffusion of acetone into the water initiated PCL precipitation; however, nanoparticles were not formed until acetone was extracted by the supercritical CO_2 [9].

2.3. SFEE nanoparticle formation

Four different extraction apparatus were used for the formation of nanocapsules by SFEE.

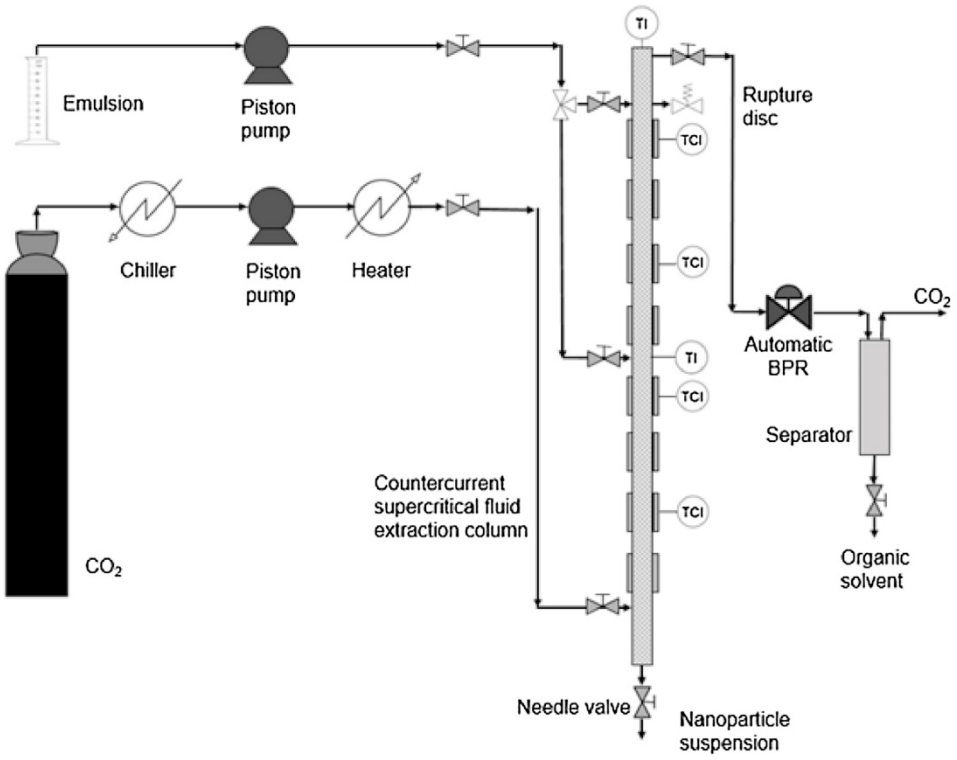

Fig. 2. Scheme of the packed column configuration used for continuous Supercritical Fluid Extraction of Emulsions (SFEE).

2.3.1. Configuration A: bubble column

The SFEE apparatus consisted of a 10 mL cylindrical stainless steel extractor with a length-to-diameter (L/D) ratio of nine. Liquid-cooled CO_2 at 263 K was delivered using a head cooled piston pump (Jasco, PU-2080). Temperature in the extractor was regulated by a heating jacket and recorded within ±0.1 K through the use of a type T thermocouple that was positioned inside the vessel. The pressure inside the extractor was regulated by a backpressure regulator (BPR, TESCOM) and read via a digital internal pump manometer within ± 0.1 MPa and via an external online Bourbon manometer. A mass flow meter (AlicatScientific, M-10SLPM-D) was used to read the flow rate and the total amount of CO_2 employed. A scheme of this configuration can be found in an earlier work [9].

Five grams of the freshly prepared starting emulsion were placed inside the extractor before the vessel was closed. CO_2 was added, and the temperature was adjusted to 313 K (pretreatment). Then, the vessel was pressurized to 8.0 MPa. Finally, the BPR was opened and flow adjusted. The operation was deemed to be complete when the selected operating time was reached. The vessel was slowly depressurized. A suspension of nanoparticles in water was recovered and stored in screw cap glass vials in the refrigerator until the time of analysis.

2.3.2. Configuration B: bubble column with a gas redistributor

Nanoparticle formation was also done in a bubble column with gas redistributor. This equipment consisted of a 500 mL cylindrical stainless steel vessel (Thar-SFC) with a length-to-diameter (L/D) ratio of four. Liquid cooled CO_2 was delivered using a high-pressure pump (Thar SFC CO_2 Pump P-50) entering in the vessel through a porous plate distributor. The temperature in the extractor was regulated by a heating jacket and recorded within ±0.1 K through the use of a type T thermocouple that was positioned inside the vessel. The pressure in the extractor was regulated by an automatic BPR (Thar SFC) and read via a Bourbon manometer and via the control software (Thar SFC) within ± 0.1 MPa.

Forty grams of the freshly prepared starting emulsion were placed inside the extractor before the vessel was closed. CO_2 was added, and the temperature was adjusted to 313 K (pretreatment). The vessel was pressurized to 8.0 MPa. Finally, the BPR was opened and flow adjusted. The operation was deemed to be completed when the selected operating time was reached. The vessel was then slowly depressurized. A suspension of nanoparticles in water was recovered and stored in screw cap test tubes in the refrigerator until the time of analysis.

2.3.3. Configuration C: spray column

The spray column (Thar-SCF) was a stainless steel cylinder vessel of 500 mL with a length-to-diameter (L/D) ratio of four, in which the emulsion was pumped in (Series III pump) and sprayed through a stainless steel nozzle. Two nozzles with different diameters, 100 or 200 μm, were used. Supercritical CO_2 was pumped in (Thar-SCF CO_2 Pump P-50), preheated in a water bath, and introduced cocurrently in the chamber through another inlet port, next to the nozzle. The pressure inside the precipitation chamber was regulated using a BPR (TESCOM) and read via a pressure transducer (Gems Sensors & Controls, 2800 CVD series) within ±0.1 MPa. The temperature was controlled using a heating jacket and recorded within ±0.1 K through the use of a type T thermocouple that was positioned inside the vessel. A 100 mL stainless steel vessel (L/D = 6) after the BPR was used to continuously separate CO_2 from the nanocapsule suspension. A mass flow meter (AlicatScientific, M-10SLPM-D) was used to read the flow rate and the total amount of CO_2 employed. The arrangement of the spray column configuration is shown in Fig. 1.

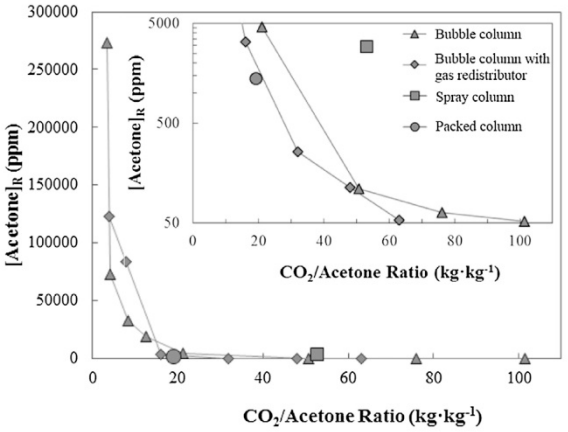

Fig. 3. Acetone removal in different supercritical extraction equipment.

The experiments were performed following two procedures: semicontinuous and continuous. In the semicontinuous mode, the vessel was closed and the precipitation chamber was filled with CO_2. The pressure and temperature were adjusted to 8.0 MPa and 313 K, respectively. The freshly prepared starting emulsion was then sprayed at different flow rates and with different nozzles. When the desired volume of emulsion was introduced, the pump was stopped and the precipitation chamber slowly depressurized. The nanoparticle suspension was recovered in a sample recipient.

In the continuous mode, the vessel was closed and the precipitation chamber was filled with CO_2. The pressure and temperature were adjusted to 8.0 MPa and 313 K, respectively. The BPR was opened and the CO_2 flow rate was adjusted. When the steady state was reached, the freshly prepared starting emulsion was pumped at the selected flow rate. Once the desired amount of emulsion was processed, both pumps were stopped, and the precipitation chamber was slowly depressurized. The nanoparticle suspension was collected at the bottom of the separator and continuously recovered through a needle valve. Samples were stored in the refrigerator until analysis.

2.3.4. Configuration D: packed column

This apparatus consisted of a 3 m long column with an internal diameter of 0.03 m, packed with random stainless steel packing (1889 m^{-1} specific surface, 0.94 of voidage; Propak, Canon Instrument Company). Two high-pressure pumps (Thar-SCF CO_2 Pump P-50) were used to deliver the starting emulsion and fresh supercritical CO_2 to the column, countercurrently. Supercritical CO_2 was preheated in a heat exchanger (Thar SFC) before entering the extraction column from the bottom. The temperature inside the column was controlled by eight heating jackets and recorded within ±0.1 K through the use of two type T thermocouples inside the column. The pressure inside the column was controlled by an automated BPR within ±0.1 MPa and read via the computer control system. CO_2 and the extract were depressurized down to atmospheric pressure in a separator and the gas stream was vented in the hood. CO_2 was not recycled. A scheme of this equipment is shown in Fig. 2.

The column was first preheated. The packing of the column was then wetted with a solution of water and surfactant with the same concentration as the aqueous phase of the starting emulsion, to prevent nanoparticles from sticking to the packing surface. Afterwards, the column was pressurized with CO_2, the BPR was opened and the flow rate was adjusted. Finally, the freshly prepared starting emulsion was pumped in through the upper inlet port of the column, and the supercritical CO_2 entered near the bottom. The extract (CO_2 and acetone) was removed from the top. The nanoparticle suspension was recovered by opening a needle valve at the bottom of the column. Three hours of continuous operation were required to achieve steady state in the product composition. The operation was finished when a sufficient amount of sample was collected. Samples were stored in the refrigerator until analysis.

Table 1
Acetone removal in a bubble column with gas redistributor operating at 8.0 MPa and 313 K with a CO_2 flow rate of 3 g min^{-1}. Initial acetone concentration was 283,500 ppm.

Time (min)	CO_2/Acetone Ratio (kg kg^{-1})	$[Acetone]_R$ (ppm)
15	4	122,000 ± 11,000
30	8	84,000 ± 20,000
60	16	3240 ± 710
120	32	257 ± 44
180	48	113 ± 10
240	63	53 ± 14

2.4. Product characterization

2.4.1. Encapsulation efficiency

The encapsulation efficiency was determined as the percentage of vitamin E entrapped inside the particle. It was calculated following Eq. (1).

$$Encapsulationefficiency\,(\%) = \frac{T_E - F_E}{T_E} \cdot 100 \quad (1)$$

Total vitamin E concentration (T_E) was determined after dissolving 1 mL of nanoparticle suspension in 10 mL of acetonitrile at 313 K overnight.

Free vitamin E concentration (F_E) was determined in the aqueous supernatant after the particles were separated by centrifugation (Digicen 21, Orto Arlesa) at 15,000 rpm for 10 min.

Quantitative measurements of vitamin E (as α-tocopherol) were performed with a Jasco HPLC chromatographer equipped with a diode array detector (Jasco MD 2015) at λ = 285 nm using a silica gel column (Teknokroma, Mediterranean Sea-18) as stationary phase and methanol as mobile phase at 1 mL min^{-1}. Measurements were taken at 303 K. The calibration of the peak area versus α-tocopherol concentration were linear in the concentration range of 0.175–3.500 mg mL^{-1} (R^2 = 0.9996).

2.4.2. Residual organic solvent concentration

The amount of acetone in the nanoparticle suspension was measured using headspace gas chromatography. In order to perform the headspace, 2 mL of nanoparticle suspension were introduced into a 20 mL vial and stabilized for 1 h at 333 K. At this temperature, the polymer melts and acetone is enriched in the vapor phase. Then, 0.5 mL of the vapor phase of this vial were extracted with a gas-tight syringe and injected manually into a gas chromatograph (Shimazdu GC-2010-Plus) that was connected to a flame ionization detector. Acetone was separated using a fused-silica capillary column: 20 m long, 0.18 mm internal diameter and 0.18 μm film thickness (Zebron-ZB-1HT inferno). The oven temperature was set to 313 K, for 6 min. The injector temperature was maintained at 453 K in split mode (ratio 19.5) and nitrogen was employed as the carrier, at 7 mL min^{-1} at 40.9 kPa. Each sample was measured in triplicate.

The residual acetone concentration in the nanoparticles after the SFEE process was also measured. The aqueous suspension was centrifuged (Digicen 21, Orto Arlesa) at 15,000 rpm for 10 min to separate the pellet and the supernatant. The pellet was dried in the oven (Digitheat, Selecta) at 308 K until reaching constant weight.

Table 2
Residual organic solvent concentration and operating conditions used in the published works about the SFEE process in bubble columns with gas redistributor. Where EA means Ethyl Acetate, AC means Acetone, and Q means flow rate.

		Q		Emulsion	Operating	CO_2/Organic	[Organic	
P	T	CO_2	Organic	Composition	Time	Solvent Ratio	solvent]$_R$	
(MPa)	(K)	(g min^{-1})	Solvent	(% by mass)	(min)	(kg kg^{-1})	(ppm)	Ref.
8.5–15.0	311	1–8	EA	20:80	30	4–30	40	[25]
8.0	311	8	EA	20:80	30	30	10	[21]
8.0	309	7	AC	20:80	60	52	4000	[7]
8.0	313	3	AC	28.4:71.6	240	63	53	this work

The dried particles were resuspended in 2 mL of Milli-q water and analyzed by headspace gas chromatography following the preceding procedure.

2.4.3. Particle size distribution

Particle size distribution was determined by photon correlation spectroscopy using a Zetasizer Nano Zs (Malvern). A dilution of the sample with Milli-q water was required to achieve suitable optical density. All measurements were performed at 298 K.

2.4.4. Nanoparticles morphology

Aqueous suspensions of nanoparticles were centrifuged at 15,000 rpm for 10 min. After that, 70% of the supernatant was removed. A drop of concentrated aqueous suspension was negatively stained for 60 s with a 1% sodium phosphotungstic acid solution and placed on a carbon-coated copper grid. TEM pictures were taken using a JEOL JEM 1010.

2.5. Statistical analysis

The experiments were repeated three times. Analyses were performed in duplicate for each replicate ($n = 3 \times 2$). Means and standard deviations were calculated for all data.

3. Results and discussion

The encapsulation of vitamin E in PCL by SFEE was done in four different configurations. The same formulation containing 28.4% by mass of acetone was used in all experiments. Pressure and temperature conditions were selected after the liquid-vapor phase equilibrium data of Chiu et al. [15] in order to guarantee complete miscibility between CO_2 and acetone, without extracting vitamin E [16]. Thus, 8.0 MPa and 313 K were selected. CO_2 flow rate was chosen to maximize acetone extraction according to the hydrodynamics of each installation. Operation was maintained until 50 ppm of residual acetone concentration was reached (in batch experiments) or until a certain amount of emulsion was treated (in continuous experiments).

3.1. Production of vitamin E nanoparticles in a bubble column

The first equipment selected for the nanoencapsulation of vitamin E in polycaprolactone was a bubble column (configuration A). Bubble columns consist of a vertical vessel partially filled with liquid into which supercritical CO_2 is bubbled. Only one or two theoretical stages can be achieved [17]; however, they are widely used as multiphase contactors in the chemical, petrochemical and biochemical industries, since they have excellent heat and mass transfer characteristics and require little maintenance and low operating costs [18].

In this equipment, different CO_2 flow rates were tested in order to maximize the extraction of organic solvent, avoiding entrainment of the liquid phase. Specifically, the acetone extraction rate was highest when CO_2 flow rate was 0.6 g min^{-1} [9]. Residual acetone concentration versus CO_2 consumption at this optimum CO_2 flow rate is shown in Fig. 3.

The extraction of acetone was initially very fast because high amounts of acetone were available. Thus, with 12 g of CO_2, equivalent to a CO_2/acetone mass ratio of 8 kg CO_2·kg acetone^{-1}, the acetone concentration decreased from 283,500 ppm to 32,607 ppm (corresponding to an extraction yield of 88%) in the first 20 min. However, as the acetone concentration decreased and particles were formed, the extraction rate rapidly decreased. Some of the acetone was entrapped inside the particles and the internal diffusion and transport through the polymer wall controlled the overall extraction rate. Consequently, higher CO_2 ratios and longer operating times were required to reduce the acetone concentration below 30000 ppm. For example, 50 min and a CO_2/acetone mass ratio of 21 kg CO_2 kg acetone^{-1} were required to achieve a residual solvent concentration of 5000 ppm, which is the maximum acetone concentration permitted in pharmaceutics [14]. Operating time and CO_2/acetone mass ratio should be increased to 240 min and 101 kg CO_2 kg acetone^{-1}, respectively, in order to achieve the maximum acetone concentration of 50 ppm required in food production [13]. At this point, acetone content in the interior of the particles was about 5 ppm.

Lévai et al. [19] used a bubble column to encapsulate quercetin in lecithin. The extraction process consisted of five extraction cycles lasting for different durations, which ended when CO_2 was saturated with ethyl acetate (EA). The CO_2 was regenerated after each cycle. More than 8 h of operating time were required to reach 100 ppm with a CO_2 consumption of 149 kg CO_2 kg ethyl acetate^{-1}.

3.2. Production of vitamin E nanoparticles in a bubble column with gas redistributor

The equipment used was a larger bubble column with gas redistributor (configuration B) to improve the contact between the CO_2 and the emulsion. Porous plate distributors affect bubble size, bubble velocity and gas hold-up [20]. Experiments were done at the highest CO_2 flow rate, avoiding entrainment of the emulsion, which was 3 g min^{-1} (4.5 kg CO_2 h^{-1} kg emulsion^{-1}). The extraction rate obtained with this equipment is shown in Table 1. The extraction curves in both bubble columns (A and B) are compared in Fig. 3. Again, two distinct periods were detected, i.e., a first period where acetone removal was rapid and a second period where the extraction rate slowed down due to the lower driving force and internal diffusion control. However, in configuration B, acetone removal proceeded faster; therefore, a lower amount of CO_2 was required. For example, 63 kg CO_2 kg acetone^{-1} were required to achieve a residual solvent concentration of about 50 ppm, which is almost half the amount required in configuration A. Therefore, the presence of the porous plate distributor and the increase in the CO_2 flow rate improved mass transfer. With a similar CO_2/acetone ratio, Della Porta et al. [7] obtained a residual acetone concentration of 4000 ppm in the nanoparticle suspension when they encapsulated retinyl acetate in PLGA by SFEE. This difference could be due to a lower operating temperature (309 K) and a higher CO_2 flow rate

Table 3
Effect of the operating parameters on acetone extraction by SFEE in a spray column. Operating pressure and temperature were 8.0 MPa and 313 K 20 g of freshly prepared starting emulsion were pumped in semicontinuous mode while 40 g were used in continuous mode.

Type of contact	CO_2	Emulsion	CO_2/Acetone	Nozzle	
	Flow Rate	Flow Rate	Ratio	Diameter	$[Acetone]_R$
	($g\,min^{-1}$)	($mL\,min^{-1}$)	($kg\,kg^{-1}$)	(μm)	(ppm)
Semicontinuous	–	1.0	26	100	8600 ± 1200
Semicontinuous	–	1.5	26	100	10,700 ± 1500
Semicontinuous	–	2.0	26	100	9300 ± 1500
Semicontinuous	–	2.0	26	200	10,000 ± 1100
Semicontinuous	–	3.0	26	200	10,500 ± 2300
Continuous	15	1.0	53	100	2950 ± 850
Continuous	15	2.0	26	100	9000 ± 1200

Table 4
Residual organic solvent concentration and operating parameters for the published works dealing with SFEE in a packed column. The packing used in all works was Propak. AC means Acetone, EA Ethyl Acetate, and Q flow rate.

	Emulsion	Column	Column			Q	Q	CO_2/Organic	[Organic	
Organic	Composition	Height	Diameter	P	T	CO_2	Emulsion	Solvent Ratio	Solvent]$_R$	
Solvent	(% by mass)	(m)	(cm)	(MPa)	(K)	($g\,min^{-1}$)	($mL\,min^{-1}$)	($kg\,kg^{-1}$)	(ppm)	Ref.
EA	20:80	1.7	1.3	8.0	311	23	2.3	50	300	[8]
EA	1:19:80	1.0	1.3	8.0	311	23	2.3	53	600	[33]
EA	1:19:80	1.7	1.3	8.0	311	23	2.3	53	500	[34]
EA	1:19:80	1.2	1.3	8.0	310	23	2.3	53	500	[35]
AC	20:80	1.0	1.3	8.0	309	23	2.5	46	1075	[7]
AC	28.4:71.6	3.0	3.0	8.0	313	20	4	19	1410	[32]

($7\,g\,min^{-1}$), which provided less contact time, as well as to the presence of glycerol in the aqueous phase which could also affect mass transfer.

Table 2 shows a comparison of the published works done on SFEE in bubble columns with gas redistributors. Della Porta et al. [21] working at operating conditions similar to this work obtained a residual ethyl acetate concentration of 10 ppm with a CO_2/ethyl acetate mass ratio of 30 kg CO_2 kg ethyl acetate^{-1}. Therefore, it seems that ethyl acetate is more readily extractable than acetone, since it required a lower amount of CO_2 and consequently less operating time. Indeed, the distribution coefficient of ethyl acetate for the ethyl acetate-water-carbon dioxide system at 8.5 MPa and 310 K [22] was 37% higher than the distribution coefficient of acetone for the acetone-water-carbon dioxide system at 10 MPa and 313 K [23,24].

3.3. Production of vitamin E nanoparticles in a spray column

Further experiments were carried out in a spray column, which corresponds to configuration C. Mass transfer in the spray column is conditioned by the design of the spray system [26] and the hydrodynamics of the vessel [27]. This equipment is used when only one or two stages and a very low pressure drop are required, and when the solute is very soluble in the solvent [17].

First, semicontinuous experiments were carried out to study the effect of the nozzle diameter and emulsion flow rate. Finally, continuous experiments were done to study the effect of the CO_2 flow rate, using the best conditions obtained previously. Results are shown in Table 3.

Operating conditions along with emulsion flow rate determine the jet mixing regime, which affects mass transfer [28]. An increase in emulsion flow rate from 1 to 3 mL·min^{-1} had no significant effect on the acetone extraction yield. Higher flow rates were not possible due to equipment limitations. The increase in the emulsion flow rate within this interval probably did not provoke a change in the jet mixing regime, and consequently no improvement in acetone removal was observed.

Nozzle diameter had no significant effect on acetone removal either. Moreover, it also seems it did not impact nanoparticle size, since particles obtained with both nozzles were similar in size and polydispersity index (PdI) (results not shown). Santos et al. [10] did not observe any influence of process parameters on particle size for the encapsulation of β-carotene and lycopene in n-OSA starch by SFEE in a spray column, asserting that particle size is only controlled by emulsion properties. In similar fashion, the use of a coaxial nozzle to increase contact between phases had little impact on the removal of ethyl acetate in the encapsulation of pepper oleoresin in Hi-Cap 100 [29]. In this work CO_2/ethyl acetate mass ratios as high as 130 kg CO_2 kg ethyl acetate^{-1} were used, and the ethyl acetate concentration in the final product was 5900 ppm. As nozzle diameter did not show an effect on particle size, the 100 μm nozzle was used for the following experiments.

In continuous mode, the spray comes into contact with the supercritical CO_2 stream cocurrently. A CO_2 flow rate of $15\,g\,min^{-1}$ was used, which was the highest possible rate. An increase in the solvent ratio notably increased acetone extraction, achieving the lowest residual acetone concentration of around 3000 ppm with a CO_2/acetone mass ratio of 53 kg CO_2 kg acetone^{-1}. However, residual acetone concentrations lower than 3000 ppm could not be obtained with this installation. The same acetone concentration was obtained in the bubble column using a CO_2/acetone mass ratio around 31 kg CO_2 kg acetone^{-1}, but the operation was discontinuous.

Other authors obtained lower residual organic solvent concentrations using a further extraction step [10,30]. The aqueous suspension of the particles was bubbled with more CO_2 to completely remove the organic solvent, similar to what is done in the SAS process. Thus, Santos et al. [10] obtained a residual dichloromethane concentration of 10 ppm in the encapsulation of β-carotene and lycopene in *n*-octenyl succinic anhydride (OSA) modified starch with a CO_2 flow rate of $50\,g\,min^{-1}$ and an emulsion flow rate between 2.5 and 5.5 $mL\,min^{-1}$, followed by 10 min of washing time at the same CO_2 flow rate. The washing step allowed decreasing the organic solvent content in the suspension; however, it increased CO_2 consumption and the total process time.

Table 5
Comparison of nanoparticle characteristics obtained by different supercritical fluid extraction equipment. EE means Encapsulation Efficiency; PdI, Polydispersity Index; $[Acetone]_R$, Residual Acetone Concentration.

Configuration	EE ± SD (%)	Mean size ± SD (nm)	PdI ± SD	$[Acetone]_R$ (ppm)
A	90.5 ± 1.1	153 ± 33	0.26 ± 0.02	52 ± 7
B	89.1 ± 1.4	144 ± 2	0.19 ± 0.01	53 ± 14
C	71.7 ± 4.5	60 ± 15	0.34 ± 0.06	2950 ± 850
D	72.6 ± 2.6	84 ± 1	0.42 ± 0.10	1410 ± 340

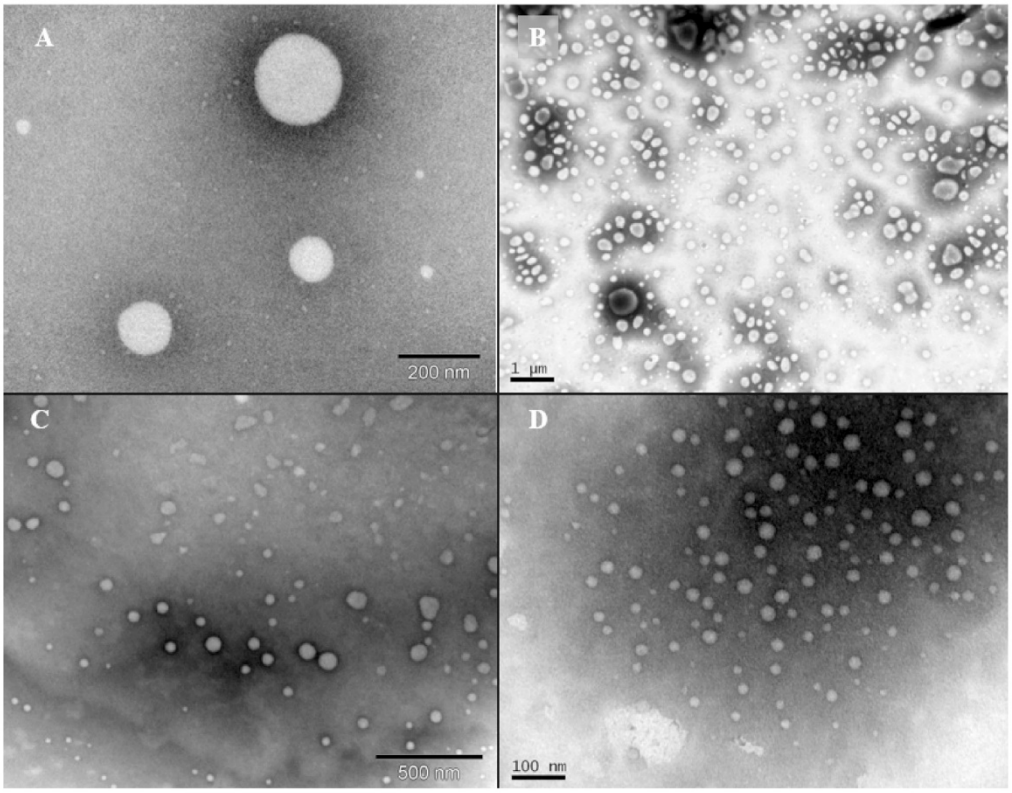

Fig. 4. Morphological comparison of nanocapsules obtained by SFEE in different supercritical fluid extraction equipment. Image A: bubble column; B: bubble column with gas redistributor; C: spray column; and D: packed column.

Another possibility for increasing contact time in spray columns and accordingly decreasing the organic solvent concentration, is to increase the length of the spray column. Effectively, residual amounts around 20 ppm were found with continuous operation in a 1 m long column [11,12]. Chattopadhyay et al. [6] proposed in their patent the combination of the spray column with the use of internal packing and countercurrent operation in order to maximize contact between the emulsion and supercritical CO_2 [31].

3.4. Production of vitamin E nanoparticles in a packed column

The fourth equipment used for the production of vitamin E nanocapsules was a high-pressure packed column (configuration D). Trays or packed columns are commonly used when multiple stages are required [17]. In this equipment, the countercurrently flowing liquid and supercritical fluid come into contact with each other on trays or on the packing surface, promoting rapid mass transfer. Packed columns are preferred when corrosion or foaming may occur, or even when the pressure drop must be low. These are possible scenarios when working with emulsions and supercritical fluids. Among the commercially available types of packing, random packing is preferred when the column diameter is less than 0.6 m and packing height is less than 6 m [17].

Another key factor is the hydrodynamic behavior of the packed column (flooding, pressure drop and liquid hold-up) which conditions column performance. In a previous study, the hydrodynamic behavior of our column was studied [32], and the best operating parameters to maximize acetone extraction were determined. Pressure and temperature of 8.0 MPa and 313 K, and flow rates of 20 g min^{-1} of CO_2 and 4 mL min^{-1} of emulsion (CO_2/acetone mass ratio of 19 kg CO_2 kg $acetone^{-1}$) allowed obtaining an aqueous nanoparticle suspension with a residual acetone concentration of 1410 ± 340 ppm. When compared with all other configurations (Fig. 3), it is clear that this configuration provided the highest acetone removal efficiency. To achieve such acetone concentration in the nanoparticle suspension, between 25 and 40 kg CO_2 kg $acetone^{-1}$ in the bubble columns and >60 kg CO_2 kg $acetone^{-1}$ in the spray column were necessary.

Table 4 shows a summary of the published works dealing with SFEE in countercurrent extraction columns. All of them were devel-

oped under similar operating conditions (packing, pressure and temperature); however, as was observed in the bubble column experiments, there is an appreciable difference in the residual organic solvent concentration depending on the organic solvent used, either ethyl acetate or acetone. In general, higher remaining acetone concentrations were found at equal CO_2 consumption.

Among the works using acetone as organic solvent, Della Porta et al. [7] obtained a residual concentration around 1000 ppm for the encapsulation of retinoids in PLGA (poly(lactic-co-glycolic)acid) using a packing column that is 1 m long and has an internal diameter of 1.3 cm packed with the random stainless steel packing (Propak) and with an average solvent consumption of 40 kg CO_2 kg acetone^{-1}. We obtained a concentration of 1400 ppm with a CO_2/acetone mass ratio of 19 kg CO_2 kg acetone^{-1} but in a higher column measuring 3 m. Therefore, in order to enhance extraction yield, it would be advisable to study higher columns and other packing types. Indeed, by simulation of the SFEE process with Aspen Plus [32], it was determined that it would be necessary to add 1.5 m of packing height to our column to obtain a residual acetone concentration of 50 ppm.

3.5. Comparison of the effect of the different configurations on nanoparticle characteristics

The different configurations not only affected acetone extraction but also nanoparticle characteristics as can be seen in Table 5. Whilst configurations A and B provided particles with the same characteristics, C and D produced particles with a much smaller particle size, higher polydispersity index and lower encapsulation efficiency. Apart from the important difference in the operating mode and the hydrodynamics of continuous versus batch operation, the difference in the state and amount of CO_2 during the first contact with the emulsion could explain these results. In the tests performed in the bubble columns (A and B configurations), CO_2 was introduced at 6.0 MPa during temperature adjustment to 313 K, and then pressure was increased to 8.0 MPa; while in the tests performed in the spray and packed columns (C and D configurations), CO_2 and the emulsion come into contact at 8.0 MPa and 313 K. Precipitation in the supercritical region usually generates smaller and amorphous particles because of a fast expansion of the liquid phase upon contact with CO_2 [36,37]. This fact could also explain the lower encapsulation efficiency obtained in configurations C and D.

The comparison between the morphology of the nanoparticles obtained in the four configurations was studied through TEM images, and it can be seen in Fig. 4. It seems that the operating mode and the hydrodynamics also affected nanoparticle morphology. Therefore, configuration A produced non-aggregated spherical nanocapsules [9]. As turbulence increased, as in configuration B, the shape of the particles lost some sphericity. In this case, the shape of the particles became more similar to an ellipsoid, which could be caused by particle aggregation. Regarding configuration C, besides the aforementioned size reduction, a greater presence of angular particles was observed. This could also be related to the fast expansion of the liquid phase, as well as to a high degree of turbulence in the nozzle. Particles obtained in configuration D, not being perfect spheres, were rounder than those obtained in configuration C, probably due to the lower degree of turbulence generated by the packing.

4. Conclusions

The encapsulation of vitamin E in PCL was done using four different SFEE equipments. The best installation to execute the scale-up must provide good particle characteristics, high production capacity and require a reduced amount of CO_2 for adequate solvent removal. In this sense, configurations A and B generated extraction curves with similar shapes; however, the bubble column with gas redistributor provided better contact between phases, and therefore the CO_2/acetone mass ratio was lower. However, both processes were semicontinuous, which is a disadvantage from the point of view of the scale-up due to the time used for loading and unloading, and the differences between batches. Configuration C and D were continuous; both provided nanoparticle suspensions with a residual acetone concentration adequate for the pharmaceutical industry [14], but too high for the food industry [13]. In order to use these nanoparticles in the food industry, an improvement in equipment design would be needed in both configurations. Nonetheless, configuration D provided a lower residual acetone concentration than configuration C with a lower CO_2/acetone mass ratio, which is very convenient from the economic point of view. In a previous work, it was demonstrated that with a higher packing height in the packing column, it would be possible to obtain the adequate acetone concentration for food applications [32].

Acknowledgments

The authors gratefully acknowledge the financial support of this work by the Ministry of Economy and Competitiveness, project ref CTQ2013-41781-P. The authors would also like to thank to Professor M. Ladero for his support on HPLC analysis, Professors A. Cabañas and C. Pando for their fruitful discussion and for allowing us to use their SAS equipment, and Centro Nacional de Microscopía Electrónica (CNME) for taking the TEM images. Cristina Prieto thanks theUniversidad Complutense de Madrid for a UCM predoctoral grant and a mobility grant (EB64/15).

References

[1] N.V.N. Jyothi, P.M. Prasanna, S.N. Sakarkar, K.S. Prabha, P.S. Ramaiah, G.Y. Srawan, Microencapsulation techniques factors influencing encapsulation efficiency, J. Microencapsul. 27 (2010) 187–197, http://dx.doi.org/10.3109/02652040903131301.
[2] C.E. Mora-Huertas, H. Fessi, A. Elaissari, Polymer-based nanocapsules for drug delivery, Int. J. Pharm. 385 (2010) 113–142, http://dx.doi.org/10.1016/j.ijpharm.2009.10.018.
[3] S. Freitas, H.P. Merkle, B. Gander, Microencapsulation by solvent extraction/evaporation: reviewing the state of the art of microsphere preparation process technology, J. Control. Release 102 (2005) 313–332, http://dx.doi.org/10.1016/j.jconrel.2004.10.015.
[4] M. Li, O. Rouaud, D. Poncelet, Microencapsulation by solvent evaporation: state of the art for process engineering approaches, Int. J. Pharm. 363 (2008) 26–39, http://dx.doi.org/10.1016/j.ijpharm.2008.07.018.
[5] J. Herberger, K. Murphy, L. Munyakazi, J. Cordia, E. Westhaus, Carbon dioxide extraction of residual solvents in poly(lactide-co-glycolide) microparticles, J. Control. Release 90 (2003) 181–195, http://dx.doi.org/10.1016/S0168-3659(03)00152-4.
[6] P. Chattopadhyay, R. Huff, B.Y. Shekunov, Drug encapsulation using supercritical fluid extraction of emulsions, J. Pharm. Sci. 95 (2006) 667–679, http://dx.doi.org/10.1002/jps.20555.
[7] G. Della Porta, R. Campardelli, N. Falco, E. Reverchon, PLGA microdevices for retinoids sustained release produced by supercritical emulsions extraction: continuous versus batch operation layouts, J. Pharm. Sci. 100 (2011) 4357–4367, http://dx.doi.org/10.1002/jps.22647.
[8] G. Della Porta, N. Falco, E. Reverchon, Continuous supercritical emulsions extraction: a new technology for biopolymer microparticles production, Biotechnol. Bioeng. 108 (2011) 676–686, http://dx.doi.org/10.1002/bit.22972.
[9] C. Prieto, L. Calvo, Supercritical fluid extraction of emulsions to nanoencapsulate vitamin E in polycaprolactone, J. Supercrit. Fluids 119 (2017) 274–282, http://dx.doi.org/10.1016/j.supflu.2016.10.004.
[10] D.T. Santos, A. Martín, M.A.A. Meireles, M.J. Cocero, Production of stabilized sub-micrometric particles of carotenoids using supercritical fluid extraction of emulsions, J. Supercrit. Fluids 61 (2012) 167–174, http://dx.doi.org/10.1016/j.supflu.2011.09.011.
[11] B.Y. Shekunov, P. Chattopadhyay, J. Seitzinger, R. Huff, Nanoparticles of poorly water-soluble drugs prepared by supercritical fluid extraction of emulsions, Pharm. Res. 23 (2006) 196–204, http://dx.doi.org/10.1007/s11095-005-8635-4.
[12] P. Chattopadhyay, B.Y. Shekunov, D. Yim, D. Cipolla, B. Byod, S. Farr, Production of solid lipid nanoparticle suspensions using supercritical fluid extraction of emulsions (SFEE) for pulmonary delivery using AERx system,

Adv. Drug Deliv. Rev. 59 (2007) 444–453, http://dx.doi.org/10.1016/j.addr.2007.04.010.
[13] Spain, 2011. Real Decreto 1101/2011, de 22 de Julio, por el que se aprueba la lista positiva de los disolventes de extracción que se pueden utilizar en la fabricación de productos alimenticios y de sus ingredientes. Boletín Oficial del Estado, 30 de Agosto de 2011, 208, 94132–94137.
[14] Guidance for Industry QC3- Tables and List, U.S. Department of Health and Human Services, Food and Drug Administration Center for Drug Evaluation and Research (CDER), Center for Biologics Evaluation and Research (CBER), ICH, Revision 2, 2012.
[15] H.Y. Chiu, M.J. Lee, H.M. Lin, Vapor-liquid phase boundaries of binary mixtures of carbon dioxide with ethanol and acetone, J. Chem. Eng. Data 53 (2008) 2393–2402, http://dx.doi.org/10.1021/je800371a.
[16] J. Chrastil, Solubility of solids and liquids in supercritical gases, J. Phys. Chem. 86 (1982) 3016–3021, http://dx.doi.org/10.1021/j100212a041.
[17] J.D. Seader, E.J. Henley, D.K. Roper, Separation Process Principles, 3rd ed., John Wiley & Sons, New York, 2010, pp. 207–213.
[18] N. Kantarci, F. Borak, K.O. Ulgen, Bubble column reactors, Process Biochem. 40 (2005) 2263–2283, http://dx.doi.org/10.1016/j.procbio.2004.10.004.
[19] G. Lévai, A. Martín, E. de Paz, S. Rodríguez-Rojo, M.J. Cocero, Production of stabilized quercetin aqueous suspensions by supercritical fluid extraction of emulsions, J. Supercrit. Fluids 100 (2015) 34–45, http://dx.doi.org/10.1016/j.supflu.2015.02.019.
[20] R. Lau, W.S. Beverly Sim, R. Mo, Effect of gas distributor on hydrodynamics in shallow bubble column reactors, Can. J. Chem. Eng. 87 (2009) 847–854, http://dx.doi.org/10.1002/cjce.20224.
[21] G. Della Porta, N. Falco, E. Reverchon, NSAID drugs release from injectable microspheres produced by supercritical fluid emulsion extraction, J. Pharm. Sci. 99 (2010) 1484–1499, http://dx.doi.org/10.1002/jps.21920.
[22] S. Klaus Luther, J.J. Schuster, A. Leipertz, A. Braeuer, Non-invasive quantification of phase equilibria of ternary mixtures composed of carbon dioxide, organic solvent and water, J. Supercrit. Fluids 84 (2013) 146–154, http://dx.doi.org/10.1016/j.supflu.2013.09.012.
[23] P. Traub, K. Stephan, High-pressure phase equilibria of the system CO_2-water-acetone measured with a new apparatus, Chem. Eng. Sci. 45 (1990) 751–758, http://dx.doi.org/10.1016/0009-2509(90)87016-L.
[24] R. Adami, J. Schuster, S. Liparoti, E. Reverchon, A. Leipertz, A. Braeuer, A raman spectroscopic method for the determination of high pressure vapour liquid equilibria, Fluid Phase Equilib. 300 (2013) 265–273, http://dx.doi.org/10.1016/j.fluid.2013.09.046.
[25] G. Della Porta, E. Reverchon, Nanostructured microspheres produced by supercritical fluid extraction of emulsions, Biotechnol. Bioeng. 100 (2008) 1020–1033, http://dx.doi.org/10.1002/bit.21845.
[26] C. Vemavarapu, M.J. Mollan, M. Lodaya, T.E. Needham, Design and process aspects of laboratory scale SCF particle formation systems, Int. J. Pharm. 292 (2005) 1–16, http://dx.doi.org/10.1016/j.ijpharm.2004.07.021.
[27] R. Thiering, F. Dehghani, N.R. Foster, Current issues relating to anti-solvent micronisation techniques and their extension to industrial scales, J. Supercrit. Fluids 21 (2001) 159–177, http://dx.doi.org/10.1016/S0896-8446(01)00090-0.
[28] E. Reverchon, E. Torino, S. Dowy, A. Braeuer, A. Leipertz, Interactions of phase equilibria, jet fluid dynamics and mass transfer during supercritical antisolvent micronization, Chem. Eng. J. 156 (2010) 446–458, http://dx.doi.org/10.1016/j.cej.2009.10.052.
[29] A.C. De Aguiar, L.P. Sales Silva, C. Alves de Rezende, G. Fernández Barbero, J. Martínez, Encapsulation of pepper oleoresin by supercritical fluid extraction of emulsions, J. Supercrit. Fluids 112 (2016) 37–43, http://dx.doi.org/10.1016/j.supflu.2016.02.009.
[30] F. Mattea, A. Martín, A. Matías-Gago, M.J. Cocero, Supercritical antisolvent precipitation from an emulsion: β-carotene nanoparticle formation, J. Supercrit. Fluids 51 (2009) 238–247, http://dx.doi.org/10.1016/j.supflu.2009.08.013.
[31] P. Chattopadhyay, B.Y. Shekunov, J.S. Seitzinger, Method and Apparatus for Continuous Particle Production using Supercritical Fluids. US Patent 2004/0156911A1.
[32] C. Prieto, L. Calvo, C.M.M. Duarte, Continuous supercritical fluid extraction of emulsions to produce nanocapsules of vitamin E in polycaprolactone, J. Supercrit. Fluids (2016) (send to publication).
[33] N. Falco, E. Reverchon, G. Della Porta, Continuous supercritical emulsions extraction: packed tower characterization and application to poly(lactic-co-glycolic acid) + insulin microspheres production, Ind. Eng. Chem. Res. 51 (2012) 8616–8623, http://dx.doi.org/10.1021/ie300482n.
[34] N. Falco, E. Reverchon, G. Della Porta, Injectable PLGA/hydrocortisone formulation produced by continuous supercritical emulsion extraction, Int. J. Pharm. 441 (2013) 589–597, http://dx.doi.org/10.1016/j.ijpharm.2012.10.039.
[35] G. Della Porta, N. Falco, E. Giordano, E. Reverchon, PLGA microspheres by supercritical emulsion extraction: a study on insulin release in myoblast culture, J. Biomater. Sci. 24 (2013) 1831–1847, http://dx.doi.org/10.1080/09205063.2013.807457 (Polymer Edition).
[36] E. Reverchon, I. De Marco, Mechanisms controlling supercritical antisolvent precipitate morphology, Chem. Eng. J. 169 (2011) 358–370, http://dx.doi.org/10.1016/j.cej.2011.02.064.
[37] E. Reverchon, Supercritical antisolvent precipitation of micro- and nano-particles, J. Supercrit. Fluids 15 (1999) 1–21, http://dx.doi.org/10.1016/S0896-8446(98)00129-6.

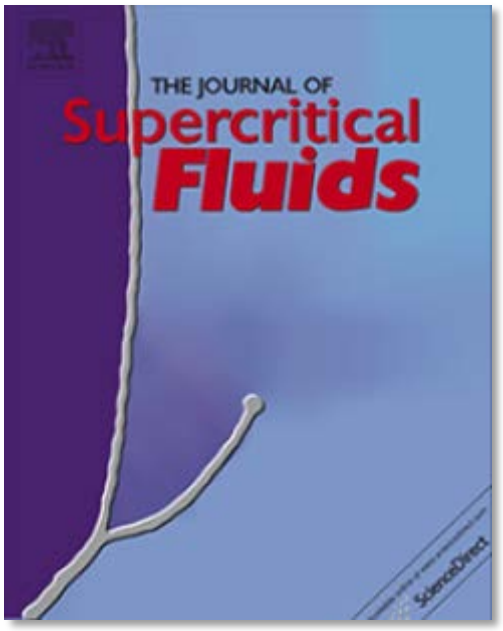

Publication IV:

"***Continuous supercritical fluid extraction of emulsions to produce nanocapsules of vitamin E in polycaprolactone***"

Cristina Prieto, Lourdes Calvo, Catarina M.M. Duarte

Journal of Supercritical Fluids 124 (2017) 72-79,

http://dx.doi.org/10.1016/j.supflu.2017.01.014.

Impact Factor (2015): 2.579

Citations: 1

J. of Supercritical Fluids 124 (2017) 72–79

Contents lists available at ScienceDirect

The Journal of Supercritical Fluids

journal homepage: www.elsevier.com/locate/supflu

Continuous supercritical fluid extraction of emulsions to produce nanocapsules of vitamin E in polycaprolactone

Cristina Prieto [a], Lourdes Calvo [a,*], Catarina M.M. Duarte [b,c]

[a] Departamento de Ingeniería Química, Facultad de Ciencias Químicas, Universidad Complutense de Madrid, Av. Complutense s/n, 28040 Madrid, Spain
[b] IBET – Instituto de Biologia Experimental e Tecnológica, Av. República, Qta. Do Marquês, Estação Agronómica Nacional, apartado 12, 2780-157 Oeiras, Portugal
[c] ITQB – Instituto de Tecnologia Química e Biológica António Xavier, Universidade Nova de Lisboa, Av. da República, 2780-157 Oeiras, Portugal

ARTICLE INFO

Article history:
Received 22 November 2016
Received in revised form 14 January 2017
Accepted 27 January 2017
Available online 30 January 2017

Keywords:
Supercritical fluid extraction of emulsions
Countercurrent packed column
Continuous process
Aspen Plus Simulation
Vitamin E nanocapsules

ABSTRACT

Vitamin E in polycaprolactone nanoparticles was continuously produced by supercritical fluid extraction of emulsions using a high-pressure packing column in countercurrent mode. This operating mode reduces the amount of solvent required, increases production capacity and enables lower residual organic solvent concentrations in the raffinate. At 8.0 MPa and 313 K, with a packing height of 2 m, and a solvent to feed ratio of 5 kg L^{-1}, the residual acetone concentration was 1400 ppm, far below 5000 ppm, and therefore suitable for pharmaceutical applications. The process was also simulated with Aspen Plus. It would be necessary to increase the packing height to 3.5 m or the CO_2 flow rate to 60 g min^{-1} in order to get a residual acetone concentration suitable for food applications (50 ppm). The nanoparticles produced were non-aggregated spheres, which had an encapsulation efficiency higher than 70% and particle size at the nanoscale.

1. Introduction

Supercritical fluid extraction of emulsions (SFEE) is a novel encapsulation technology [1] that combines conventional emulsion processes with the unique properties of supercritical fluids to produce tailored micro- and nanoparticles. The basis of this process relies on the use of supercritical CO_2 to rapidly extract the organic phase of an emulsion in which a bioactive compound and its coating polymer have been previously dissolved. By removing the solvent, both compounds precipitate, generating a suspension of particles in water. The produced particles have controlled size and morphology [1], due to the use of the emulsion and to the fast kinetics of the supercritical CO_2 extraction. Particle agglomeration in the aqueous phase is avoided since the particles are stabilized by a surfactant. In addition, this technology is very versatile. It is possible to encapsulate hydrophilic and lipophilic compounds by changing the starting emulsion. An oil-in-water (O/W) emulsion can be used to encapsulate lipophilic compounds, while a water-in-oil-in-water (W/O/W) emulsion can be used to encapsulate hydrophilic compounds.

In an earlier work, we have investigated the encapsulation of the vitamin E in polycaprolactone using this technology in a batch apparatus at lab scale [2]. Yielded particles had very high encapsulation efficiency (around 90%), narrow particle size distribution (polydispersity index was between 0.24 and 0.54) and sizes at the nanoscale (between 8 and 276 nm). Morphology analysis showed that they were true spherical nanocapsules and they were non-aggregated. Stability testing showed that they remained unchangeable even at long storage times (6 and 12 months).

Such promising results made it interesting to scale-up the technology. Earlier studies have demonstrated that this process is easily scalable by means of a high-pressure packing column operating in countercurrent mode [3,4]. The supercritical extraction process of liquid mixtures in countercurrent packed columns has some resemblance to gas–liquid extraction processes due to the gas-like transport properties of supercritical fluids and to the liquid–liquid extraction processes, because of its liquid-like density [5]. The high-pressure packing column provides certain advantages over other gas–liquid extraction equipment, bubble columns or spray columns, such as the increase in mass transfer efficiency due to the presence of the packing, which provides a tortuous path for the dispersed phase [6]. In addition, the countercurrent operation in a separation device reduces the amount of solvent required, increases production capacity and enables higher extract concentrations in the solvent and lower residual concentrations in the raffinate than a cocurrent or crosscurrent operation does [7].

* Corresponding author.
E-mail address: lcalvo@ucm.es (L. Calvo).

http://dx.doi.org/10.1016/j.supflu.2017.01.014
0896-8446/

Table 1
Composition and density of the two formulations used in the study.

Sample	Water (g)	Tween 80 (g)	Acetone (g)	PCL (g)	Vitamin E (g)	Density (kg m^{-3})
A	716	0.71	284	1.78	1.44	930
B	800	100	100	1.78	1.44	970

There is an extensive knowledge of the fundamentals of the liquid-supercritical fluid extraction in a packed column [8]. However, published data on the performance of packed columns applied to supercritical fluid extraction of liquid mixtures at large scales are limited, although this information is essential for a successful design and operation of such contactors [5]. The design and optimization of operating variables requires fundamental data on phase equilibria, mass transfer and hydrodynamics of the packed column [9].

The aim of this work was to study the SFEE process in continuous operation using a high-pressure packing column to produce nanocapsules of vitamin E in PCL. First, the hydrodynamics of the column were studied as well as its dependence on the density difference between phases, and on the solvent to feed ratio. Secondly, the best operating conditions were determined in order to maximize acetone extraction. Thirdly, nanocapsules of vitamin E were produced using two formulations with different colloid size. Nanoparticle characteristics were studied in terms of encapsulation efficiency, particle size distribution, residual acetone concentration and morphology. Finally, the process was simulated with a commercial process simulator, Aspen Plus, in order to evaluate the performance of supercritical CO_2 extraction on acetone removal.

2. Materials and methods

2.1. Materials

Vitamin E (α-tocopherol, ≥95%), polycaprolactone (PCL) (MW = 10,000), Tween 80 (polyoxyethylene (20) sorbitan monooleate), and acetone (≥99.5% (GC)) were all from Sigma Aldrich. Acetonitrile (gradient 240 nm/far UV HPLC grade) was from Scharlab. Sodium phosphotungstic acid solution (1%) was from Panreac. Carbon dioxide (99.98%) was from Air Liquide. All materials were used as received. Millipore water was used throughout the study.

2.2. Preparation of the starting emulsions

The system for the encapsulation of vitamin E consisted of acetone, water, Tween 80 as a surfactant, and PCL as the encapsulating polymer. PCL and vitamin E were dissolved in acetone. The aqueous phase was prepared by dissolving Tween 80 in water. The organic phase was added dropwise to the aqueous phase using a peristaltic pump (Masterflex 7524-10, Cole-Palmer) and stirred with a high speed homogenizer at 9500 rpm (Ultraturrax T-25, IKA) for 10 min to guarantee a homogeneous dispersion. Two formulations with a different colloid size were used. Compositions of these two formulations are shown in Table 1 and were taken from [2].

Although acetone is completely water-miscible, the presence of vitamin E increased the viscosity of the organic phase, allowing the formation of stable emulsions. When PCL was also present in the organic phase, the slow diffusion of the acetone into the water initiated PCL precipitation; however, particles were not formed until acetone was extracted by the supercritical CO_2 [2].

2.3. Installation description

The apparatus consisted of a 3 m long column with an internal diameter of 0.03 m, packed with random stainless steel packing (1889 m^{-1} specific surface, 0.94 of voidage; Propak, Canon Instrument Company). Two high-pressure pumps (Thar-SCF CO_2 Pump P-50) were used to deliver the aqueous solution and fresh supercritical CO_2 to the column, countercurrently. Supercritical CO_2 was preheated in a heat exchanger (Thar SFC) before entering the extraction column from the bottom. The temperature inside the column was controlled by eight heating jackets and recorded within ±0.1 K through the use of two type T thermocouples inside the column. The pressure inside the column was controlled by an automated BPR within ±0.1 MPa and read via the computer control system. CO_2 and the extract were depressurized down to atmospheric pressure in a separator and the gas stream was vented in the hood. CO_2 was not recycled. A scheme of this equipment is shown in Fig. 1.

2.4. Determination of the hydrodynamic behavior of the column

The maximum flow rate for the light and dense phases was determined as follows. The column was first preheated. The packing of the column was then wetted with a solution of water and surfactant with the same concentrations as the aqueous phase of the starting emulsion. Afterwards, the column was pressurized with CO_2, the BPR was opened and the CO_2 flow rate was adjusted. A synthetic mixture of acetone–water of the same composition as in the starting emulsion was used as the dense phase, since no significant difference was observed between the densities and viscosities of the emulsion and the acetone–water mixture. At a fixed operating pressure and temperature, and CO_2 flow rate, liquid flow rate ranged between 1 and 10 mL min^{-1}. Then, CO_2 flow rate was increased from 10 to 30 g min^{-1}. CO_2 density ranged between 280 and 630 kg m^{-3} by changing the pressure and temperature between 8.0 and 8.5 MPa and between 305.5 and 313 K, respectively. The maximum flow rate that produced entrainment was identified when water was found in the separator. Flooding was identified when no raffinate was withdrawn from the column.

2.5. Nanoparticle production

First, the column was preheated and wetted as explained earlier. Then, operation was carried out in countercurrent mode, with the emulsion entering near the top of the column, and the supercritical carbon dioxide entering near the bottom. The light phase (mainly CO_2 and acetone) was removed from the top. The nanoparticle suspension was recovered by opening a needle valve at the bottom of the column at constant time intervals to keep the level of the dense phase inside the column constant. It was necessary to wait until steady state was reached to take a sample of the nanoparticle suspension. Each experiment ended when a sufficient amount of raffinate had been recovered. Samples were stored in the refrigerator until analysis.

2.6. Product characterization

2.6.1. Encapsulation efficiency

The encapsulation efficiency was determined as the percentage of vitamin E entrapped in the particle. It was calculated by Eq. (1).

$$\text{Encapsulation efficiency } (\%) = \frac{T_E - F_E}{T_E} \times 100 \quad (1)$$

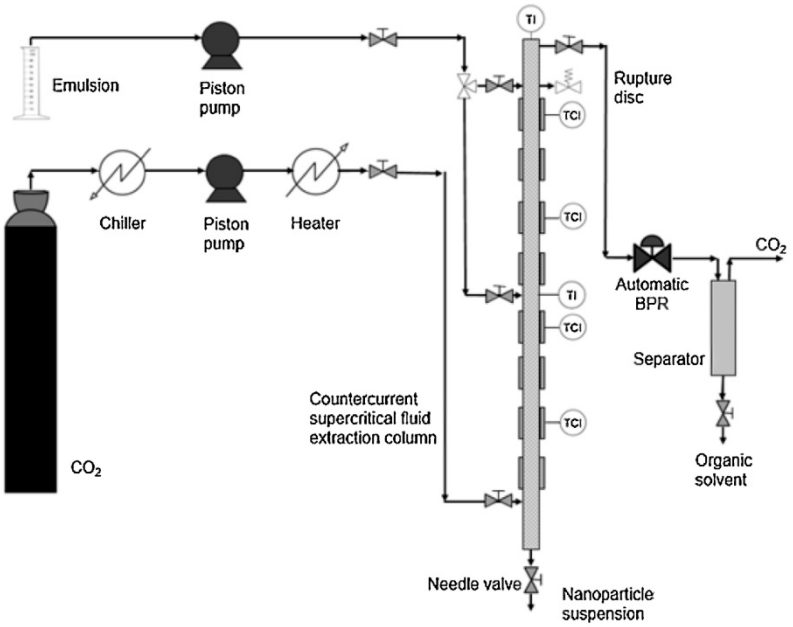

Fig. 1. Schematic diagram for continuous supercritical fluid extraction of emulsions (SFEE) process.

Total vitamin E concentration (T_E) was determined after dissolving 1 mL of nanoparticle suspension in 10 mL of acetonitrile at 313 K overnight.

Free vitamin E concentration (F_E) was determined in the aqueous supernatant after the particles were separated by centrifugation (Digicen 21, Orto Arlesa) at 15,000 rpm for 10 min.

Quantitative measurements of vitamin E (as α-tocopherol) were taken with a Jasco HPLC chromatographer equipped with a diode array detector (Jasco MD 2015) at λ = 285 nm using a silica gel column (Teknokroma, Mediterranean Sea-18) as the stationary phase and methanol as the mobile phase at 1 mL min^{-1}. The measurements were performed at 303 K. The calibration of the peak area versus concentration of α-tocopherol was linear in the concentration range of 0.175–3.500 mg mL^{-1} (R^2 = 0.9996).

2.6.2. Residual organic solvent concentration

The amount of acetone in the nanoparticle suspension was measured using headspace gas chromatography. In order to perform the headspace, 2 mL of nanoparticle suspension were introduced into a 20 mL vial and stabilized for 1 h at 333 K. At this temperature, the polymer melts and acetone is enriched in the vapor phase. Then, 0.5 mL of the vapor phase of this vial were extracted with a gas-tight syringe and injected manually into a gas chromatograph (Shimazdu GC-2010-Plus) that was connected to a flame ionization detector. Acetone was separated using a fused-silica capillary column: 20 m long, 0.18 mm internal diameter and 0.18 μm film thickness (Zebron-ZB-1HT inferno). The oven temperature was set to 313 K, for 6 min. The injector temperature was maintained at 453 K in split mode (ratio 19.5) and nitrogen was employed as a carrier, at 7 mL min^{-1} at 40.9 kPa. Each sample was measured in triplicate.

2.6.3. Particle size distribution

Particle size distribution was determined by photon correlation spectroscopy using a Zetasizer Nano Zs (Malvern). A dilution of the sample with Milli-q water was required to achieve suitable optical density. All measurements were performed at 298 K.

2.6.4. Nanoparticle morphology

Aqueous suspensions of nanoparticles were centrifuged at 15,000 rpm for 10 min. After that, 70% of the supernatant was removed. A drop of concentrated aqueous suspension was negatively stained for 60 s with a 1% sodium phosphotungstic acid solution and placed on a carbon-coated copper grid. TEM pictures were taken using a JEOL JEM 1010.

2.7. Statistical analysis

The experiments were repeated three times. Analyses were performed in duplicate for each replicate ($n = 3 \times 2$). Means and standard deviations were calculated for all data.

2.8. Process simulation

The simulation of acetone extraction from the emulsion by supercritical CO_2 was performed with the aid of Aspen Plus. Only the three major components of the system: carbon dioxide, acetone and water, were used. Thermodynamic models based on the equations of state of Peng Robinson, Redlich-Kwong, Lee-Kesler-Plöker, Schwartzentruber-Renon (SR-Polar) and Perturbed-Chain Statistical Associating Fluid Theory (PC-SAFT) with the available mixing rules (Modified Huron-Vidal, Wong-Sandler and Boston-Mathias) were first tested to describe the ternary equilibrium. In addition, some activity coefficient models were considered, such as NRTL, electrolyte NRTL and Pitzer. The model that more accurately represented the experimental phase equilibrium data was selected for the simulation of the extraction module.

The high-pressure packing column was modeled with the help of the Extract block to explore feasible operating conditions for SFEE. It is a rigorous model to simulate liquid–liquid extractors. For each simulation, it was necessary to specify the conditions of the inlet streams and the operating conditions of the column. Results were compared with a cascade of flash units, modeled with the Flash 2 block.

Sensitivity analysis was done to explore the effect of the number of theoretical stages and solvent flow rate on raffinate purity under different operating conditions. The simulation results were compared to experimental data.

3. Results and discussion

Vitamin E nanocapsules were produced in a packed column by the extraction of the acetone from the starting emulsion. First, it was necessary to study the hydrodynamics of the column in order to define the operating conditions that ensure countercurrent operation. Secondly, operating parameters were studied in order to maximize acetone extraction without extracting vitamin E. Thirdly, vitamin E nanocapsules were produced in the column working under the best operating conditions. Finally, the separation of the acetone–water mixture with supercritical CO_2 was simulated with Aspen Plus.

3.1. Determination of the hydrodynamic behavior of the column

Mass transfer in packed columns depends strongly on hydrodynamics [7]; that is, the type of packing, and on the amounts of the countercurrently flowing phases, as it determines flooding, liquid hold-up and pressure drop.

Flow in a gravity driven column depends on the density difference of the phases. With a liquid phase density of 930 kg m^{-3}, CO_2 densities higher than 500 kg m^{-3} provoked column flooding. At CO_2 densities lower than 500 kg m^{-3}, column flooding was not observed at liquid flow rates between 1 and 5 mL min^{-1} and CO_2 flow rates between 10 and 30 g min^{-1}. These experimental results were corroborated by the flooding correlations of Sherwood [10], Brunner [11] and Lobo [12] at gas to liquid ratios between 2 and 30 kg kg^{-1} and CO_2 density of 280 kg m^{-3}. According to these equations, the CO_2 flow rate should be much higher (400 g min^{-1}) to provoke flooding in this column. Nevertheless, the CO_2 flow rate could not be further increased due to equipment limitations. For the removal of ethyl acetate in an SFEE process performed in a high-pressure column using the same packing (Propak), the difference in density between phases to avoid flooding was slightly lower, of 400 kg m^{-3} [13] at solvent to feed ratios between 3 and 20 kg kg^{-1}.

Entrainment of liquid was only observed when the liquid flow rate was 10 mL min^{-1}, even at low CO_2 flow rates (10 g min^{-1}). Lower liquid flow rates did not provoke the entrainment of the dense phase at any CO_2 flow rates.

No pressure drop was observed in the column. Based on other works done in supercritical extraction packing columns, it is around 0.001 MPa [7,14], a value that is far below the precision of the installation manometers.

3.2. Influence of the operating variables

Initially, the pressure and temperature were selected so that they favored the maximum extraction rate of the organic solvent without extracting the bioactive compound while avoiding the use of high temperatures. According to the high pressure vapor–liquid equilibrium diagram of the CO_2–acetone mixture [15], at 8.0 MPa and temperatures below 313 K, miscibility between carbon dioxide and acetone was complete. In these conditions, the solubility of vitamin E in supercritical CO_2 was quite low (0.3 mg g CO_2^{-1}) [16], not being significantly improved by the presence of the acetone as no detectable vitamin E was collected on the separator. Moreover, under these conditions the solubility of the water in the supercritical CO_2 was very low and could be neglected [17]. As pressure affected vitamin E solubility in supercritical CO_2, pressure could not be greatly increased to improve acetone extraction; therefore it was fixed at 8.0 MPa.

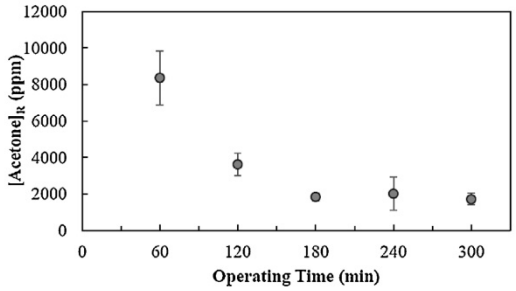

Fig. 2. Evolution of residual acetone concentration with operating time.

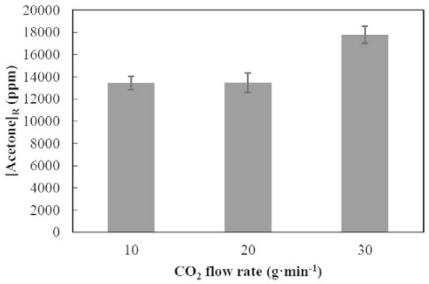

Fig. 3. Effect of the CO_2 flow rate on acetone removal. Liquid flow rate was kept constant at 1 mL min^{-1}, and pressure and temperature were 8.0 MPa and 310 K, respectively.

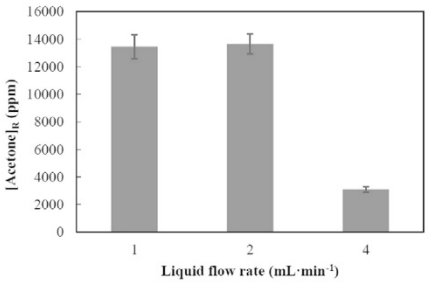

Fig. 4. Effect of liquid flow rate on acetone removal. CO_2 flow rate was kept constant at 20 g min^{-1}. Pressure and temperature were fixed at 8.0 MPa and 310 K, respectively.

It was considered that the system achieved steady state when the residual acetone concentration in the raffinate remained unchanged. A synthetic mixture of acetone and water simulating formulation A was used. For this column, it was necessary to wait 3 h at 8.0 MPa and 310 K, as shown in Fig. 2. High stabilization times to reach steady state conditions were reported by other authors for the separation of organic compounds from aqueous solutions [18,19].

Using the same synthetic mixture, the effects of liquid and CO_2 flow rates on acetone removal were also studied. Fig. 3 shows the effect of CO_2 flow rate on acetone removal keeping the liquid flow rate constant at 1 mL min^{-1}. As can be observed, no significant change in the residual acetone concentration was obtained when the CO_2 flow rate was increased from 10 to 20 g min^{-1}. However, at 30 g min^{-1} the residual acetone concentration in the raffinate was noticeably higher due to the drying of the packing, since the liquid flow rate was low.

The effect of liquid flow rate on acetone removal is shown in Fig. 4. When liquid flow rate was increased, keeping the CO_2 flow

Table 2
Characteristics of the nanoparticles produced in the high-pressure packed column using formulations A and B. EE means encapsulation efficiency; PdI, polydispersity index; $[AC]_R$, residual acetone concentration.

Formulation	EE ± SD (%)	Mean size ± SD (nm)	PdI ± SD	$[AC]_R$ ± SD (ppm)
A	72 ± 3	84 ± 1	0.39 ± 0.12	1410 ± 340
B	82 ± 4	9 ± 1	0.52 ± 0.04	279 ± 35

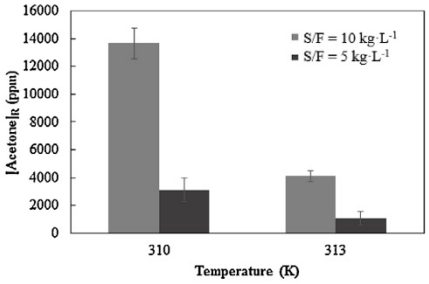

Fig. 5. Effect of the operating temperature on acetone removal at different solvent to feed ratio (S/F). Operating pressure was 8.0 MPa.

rate constant at 20 g min^{-1}, no significant reduction in the residual acetone concentration in the raffinate was observed between 1 and 2 mL min^{-1}. However, at 4 mL min^{-1} much higher extraction yields were obtained. This effect was probably due to better wetting of the packing. Ruiz-Rodríguez et al. [20] also found the best liquid flow rate around 4 mL min^{-1} when performing supercritical CO_2 dealcoholization of aqueous mixtures of low ethanol concentration in a similar column (3 m high, 0.03 m of internal diameter).

Fig. 5 shows the effect of increasing the temperature at a different solvent to feed ratio. Residual acetone concentration in the raffinate was reduced by one third when increasing the temperature from 310 K to 313 K. This important impact of the temperature seems not to be fully explained by the increment of the vapor pressure of acetone. For example, the vapor pressure of acetone increases 6 kPa by raising 3 K. Recently, Lévai demonstrated that the extraction of the organic solvent from the emulsion was kinetically controlled by the CO_2 mass transfer through the water phase [21]. Consequently, the highest removal rate of acetone at higher temperatures could be related to the influence of temperature on transport properties; in fact, the diffusivity coefficient of CO_2 in water considerably increased with slight changes in temperature [22].

The best extraction yield was obtained at 313 K using a solvent to feed ratio of 5 kg L^{-1} (20 g min^{-1} of CO_2 and 4 mL min^{-1} of emulsion), for which the residual acetone concentration was decreased to 1080 ± 480 ppm. Consequently, 8.0 MPa, 313 K, 20 g min^{-1} of CO_2 and 4 mL min^{-1} of emulsion were the operating conditions used for the production of nanoparticles. In order to enhance extraction yield, packing type, packing height and hydrodynamics should be improved. The impact of the increase in the number of theoretical stages, i.e., the increase in packing height, is analyzed in Section 3.4.

3.3. Production of vitamin E nanoparticles in a packed column

Using the best operating conditions, 8.0 MPa, 313 K, 20 g min^{-1} of CO_2 and 4 mL min^{-1} of emulsion, nanoparticles of vitamin E in PCL were produced by continuous SFEE in the high-pressure packing column using the formulations shown in Table 1. Although the presence of solids is not recommended in packed columns due to the blockage of the packing, no problem was observed. Della Porta et al. [4] also had no trouble with the presence of solid when producing PLGA microparticles by SFEE in a packing column. It may be due to the small size of the solid particles and to the presence of the surfactant in the aqueous particle suspension, which prevented the particles from sticking on the packing surface.

The characteristics of the produced nanoparticles are shown in Table 2. Nanoparticles obtained from formulation A had a high encapsulation efficiency and nanometer size. Compared to the particles obtained from the same formulation in a batch bubble column [2], particle size highly decreased (from 153 to 84 nm) because of the different operating mode. In the bubble column, the emulsion in the vessel came into contact with CO_2 at 6.0 MPa, the temperature was adjusted to 313 K and finally pressure was increased to 8.0 MPa; whilst in the column the first contact between the emulsion and the supercritical CO_2 occurred at 8.0 MPa and 313 K. According to the phase equilibrium diagram of the CO_2–acetone mixture [15], while in the bubble column the first contact between phases took place in the expanded liquid region; in the column, the first contact between phases took place in the supercritical region. This generates particles of different sizes similarly to how it occurs in SAS technology [23,24]. This phenomenon, by which smaller particles were produced, can be also the reason for the lower encapsulation efficiency in the particles obtained in the column (a reduction from 90 to 72%), favoring the migration of vitamin E to the water phase outside the particle.

The residual acetone concentration in the particle suspension was slightly higher when working with the emulsion, 1410 ± 340 ppm, compared to 1080 ± 480 ppm when the synthetic acetone–water mixture was treated, maybe due to the greater difficulty in removing the acetone from the interior of the colloid. A similar residual acetone concentration (1075 ppm) was obtained by Della Porta et al. [3] for the encapsulation of retinoids in PLGA (poly(lactic-co-glycolic)acid), using a packing column (1 m long and 0.01 m of internal diameter), packed with Propak, at a gas-to-liquid ratio of 10, at 8 MPa and 309 K. PCL and PLGA nanoparticles with a residual acetone concentration of 967 ppm were obtained by Campardelli et al. [25], working with a Propak packed column (1.7 m long and 0.01 m of internal diameter) with a gas-to-liquid ratio of 10, at pressures between 8 and 14 MPa and 311 K.

The obtained nanoparticles had a residual acetone concentration much lower than 5000 ppm so they are suitable for use in the pharmaceutical industry [26]. However, a residual concentration of 50 ppm required for food applications [27] could not be reached with this column.

Formulation B produced nanoparticles with a mean size of 9 nm, an encapsulation efficiency higher than 80% and a residual acetone concentration around 300 ppm. The reduction in the residual acetone concentration was due to an initial lower amount of acetone in the starting emulsion, and consequently a higher CO_2/acetone ratio, 46 kg CO_2 kg $acetone^{-1}$, compared to 19 kg CO_2 kg $acetone^{-1}$ for formulation A. This formulation contained a high surfactant concentration (10% by mass), which could provoke flooding of the column due to the formation of foam; nevertheless, no problem was observed in the operation of the column at this surfactant concentration and at the liquid and CO_2 flow rates used.

Regarding morphology, both formulations generated non-aggregated spherical nanoparticles as shown in Fig. 6.

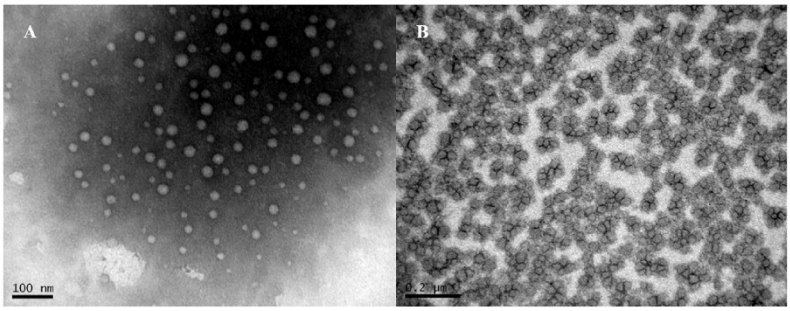

Fig. 6. TEM images of the nanoparticles obtained in the high-pressure packed column. A nanoparticles obtained from formulation A; B nanoparticles obtained from formulation B.

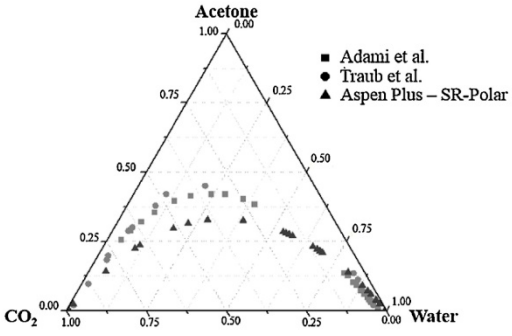

Fig. 7. Comparison of the CO_2–acetone–water phase equilibrium data from Adami et al. [28], Traub et al. [27] and the data provided by Aspen Plus using the model SR-Polar, at 10 MPa and 313 K.

3.4. Process simulation

The CO_2–acetone–water system shows a peculiar phase behavior. Several scientific papers discuss the salting out effect of CO_2 in acetone–water mixtures [28,29], but only two of them provide phase equilibrium data in the two-phase region over the upper critical solution pressure at 313 K [30,31]. A comparison was made between the available experimental equilibrium data and that provided by the simulation software using the implemented thermodynamic models indicated in Section 2.8. The best models were SR-Polar and PSRK. Of the two, SR-Polar represented the literature data slightly better than PSRK did (results not shown). Fig. 7 shows a comparison between available phase equilibrium data and data generated by Aspen Plus with the SR-Polar thermodynamic model. At molar fractions of acetone below 12% the fitting was good, and it is in this range of low concentrations of acetone where the column operated.

Once the thermodynamic model was selected, the block Extract was used to model the supercritical extraction column. The column was operated in countercurrent flow without reflux, where upper inlet stream (Feed) was the dispersed phase entering at the top of the column and the solvent stream (CO_2) was the continuous phase entering at the bottom of the column. The vapor phase containing the CO_2 and the acetone left the column as the top product stream (Extract) and the liquid phase exhausted in acetone was obtained as the bottom product (Raffinate). Conditions of the operating unit and inlet streams were supplied. The model Extract required data on number of stages, key components, position of inlet and outlet streams, pressure and estimated operating temperature. The key component for the first liquid phase was water and for the second liquid phase, it was carbon dioxide. The Feed stream entered the column at first stage and CO_2 at the last stage. The Extract stream left the column by the first stage. The Raffinate left the column by the last stage. Pressure in the column was kept constant at 8.0 MPa. Estimated temperature in the first stage was 318 K. It was also necessary to define pressure, temperature, flow rate and composition of the inlet streams to proceed to the simulation. These conditions are summarized in Table 3.

The only unknown parameter was the number of theoretical stages. This parameter was determined iteratively in order to find the value that reproduced the experimental results. When the composition of the Feed stream was formulation A, four theoretical stages were required to obtain a residual acetone concentration in the Raffinate stream close to the experimental value

Table 3
Simulation results of the SFEE column using Aspen Plus with the SR-Polar model and the Extract block.

	CO_2	Feed	Extract	Raffinate
Formulation A – 4 theoretical stages				
T (K)	313	313	320	312
P (MPa)	8.5	8.0	8.0	8.0
Flow rate (g min^{-1})	20.0	3.7	21.1	2.6
Composition (by mass)				
CO_2	100%	0	946,923 ppm	10,589 ppm
Acetone	0	28.4%	49,704 ppm	936 ppm
Water	0	71.6%	3373 ppm	988,475 ppm
Formulation B – 5 theoretical stages				
T (K)	313	313	315	311
P (MPa)	8.5	8.0	8.0	8.0
Flow rate (g min^{-1})	20.0	3.9	20.4	3.5
Composition (by mass)				
CO_2	100%	0	976,604 ppm	10,545 ppm
Acetone	0	11.1%	21,143 ppm	314 ppm
Water	0	88.9%	2252 ppm	989,140 ppm

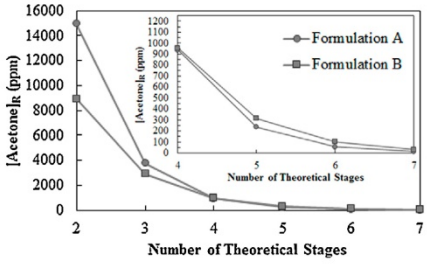

Fig. 8. Dependence of the composition of the raffinate stream on the number of theoretical stages.

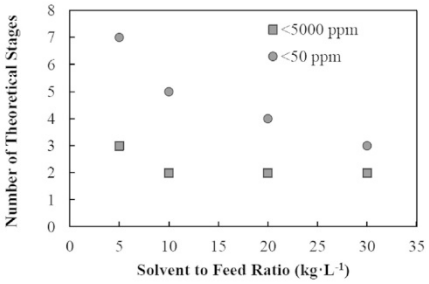

Fig. 9. Influence of the solvent to feed ratio on the required number of theoretical stages for a desired residual acetone concentration in raffinate.

of 1410 ± 340 ppm. Two theoretical stages produced a Raffinate stream of 15,000 ppm; this value was consistent with the experimental residual acetone concentration in the Raffinate stream (15,400 ± 310 ppm) obtained when the emulsion was introduced in the column at the second inlet of the column where only 1 m of packing height was used.

When using formulation B, five theoretical stages were required to reach a residual acetone concentration in the Raffinate close to the experimental value of 279 ± 35 ppm. The stream summary of both simulations is shown in Table 3. Similar results were obtained with the flash cascade, which also needed the same number of theoretical stages to reach the experimental residual acetone concentration in the raffinate (results not shown).

The height of the theoretical stage (HETP) could be estimated through the comparison between the simulation and the experimental data. It varied between 0.4–0.5 m depending on the composition of the Feed stream. These values are consistent with those reported in the literature for aqueous mixtures [7]. Budich *et al.* [18] obtained HETP between 0.25 and 1 m for the supercritical fluid extraction of ethanol from aqueous solutions using Sulzer CY packing.

In order to reach the residual acetone concentration of 50 ppm required for food applications [27] at these operating conditions, it was necessary to increase the number of theoretical stages. Fig. 8 shows the evolution of the residual acetone concentration in the Raffinate stream with the number of theoretical stages. Both formulations required seven theoretical stages to reach an acetone concentration in the Raffinate stream lower than 50 ppm. Therefore, it would be necessary to increase the packing height to 3.5 m.

A sensitivity analysis was also done studying the variation of the raffinate composition with the number of stages at different solvent to feed ratios. The calculation was carried out at a constant feed flow rate of 4 mL min^{-1} and with various CO_2 flow rates. Results are shown in Fig. 9. Similar results were obtained for both formulations. By increasing the solvent to feed ratio, acetone extraction increased and consequently it would be possible to reduce the required number of theoretical stages. Indeed, by increasing the CO_2 flow rate to 60 g min^{-1}, it would be feasible to obtain a residual acetone concentration in the Raffinate stream lower than 50 ppm using the same column.

4. Conclusions

The scope of the present work was to determine the technical feasibility of using a countercurrent high-pressure packed column to carry out the SFEE process to continuously produce nanoparticles of vitamin E in PCL. The use of a packing column for SFEE offers the possibility of a high production capacity of nanocapsules with a small volume plant, along with greater product homogeneity by eliminating differences between batches. As a result of the use of the emulsion, particles with a high encapsulation efficiency and sizes at the nanoscale could be obtained. The particle size could be reduced from 84 nm to 9 nm by tuning the starting emulsion formulation. The encapsulation efficiency, as well as the size of the nanoparticles obtained in the column decreased with respect to those obtained in the batch bubble column due to the variation in the operating mode. In contrast, they were not affected by the presence of the packing, which provided a large contact area between CO_2 and the emulsion to obtain nanoparticles with a low residual acetone concentration, suitable for pharmaceutical applications. However, a residual concentration of 50 ppm required for food applications could not be reached with the apparatus used.

Using Aspen Plus, the process was successfully simulated and analyzed. The simulations showed that increasing the solvent to feed ratio as well as the number of the theoretical stages of the column favored acetone removal. According to the simulations, it would be necessary to increase the packing height to 3.5 m or to increase the CO_2 flow rate to 60 g min^{-1} to get a Raffinate stream with a residual acetone concentration below 50 ppm. The height of the column or the CO_2 flow rate could be reduced using another type of packing which provides better contact between phases.

Acknowledgments

The authors would like to thank to Professor M. Ladero for his support on HPLC analysis, Centro Nacional de Microscopía Electrónica (CNME) for its support on TEM analyses. Cristina Prieto thanks the Universidad Complutense de Madrid for an UCM predoctoral grant and a mobility grant (EB64/15).

References

[1] P. Chattopadhyay, R. Huff, B.Y. Shekunov, Drug encapsulation using supercritical fluid extraction of emulsions, J. Pharm. Sci. 95 (2006) 667–679, http://dx.doi.org/10.1002/jps.20555.
[2] C. Prieto, L. Calvo, Supercritical fluid extraction of emulsions to nanoencapsulate vitamin E in polycaprolactone, J. Supercrit. Fluids 119 (2017) 274–282, http://dx.doi.org/10.1016/j.supflu.2016.10.004.
[3] G. Della Porta, R. Campardelli, N. Falco, E. Reverchon, PLGA microdevices for retinoids sustained release produced by supercritical emulsions extraction: continuous versus batch operation layouts, J. Pharm. Sci. 100 (2011) 4357–4367, http://dx.doi.org/10.1002/jps.22647.
[4] G. Della Porta, N. Falco, E. Reverchon, Continuous supercritical emulsions extraction: a new technology for biopolymer microparticles production, Biotechnol. Bioeng. 108 (2011) 676–686, http://dx.doi.org/10.1002/bit.22972.
[5] R. Ruivo, M.J. Cebola, P.C. Simões, M. Nunes da Ponte, Fractionation of edible oil model mixtures by supercritical carbon dioxide in a packed column. 2. A mass-transfer study, Ind. Eng. Chem. Res. 41 (2002) 2305–2315, http://dx.doi.org/10.1021/ie0106579.
[6] J.D. Seader, E.J. Henley, D.K. Roper, Separation Process Principles, 3rd ed., John Wiley & Sons, New York, 2010, pp. 207–213.
[7] G. Brunner, Counter-current separations, J. Supercrit. Fluids 47 (2009) 574–582, http://dx.doi.org/10.1016/j.supflu.2008.09.022.
[8] G. Brunner, Gas Extraction. An Introduction to Fundamentals of Supercritical Fluids and the Application to Separation Processes, Steinkopff/Springer, Darmstadt/New York, 1994, http://dx.doi.org/10.1007/978-3-662-07380-3.
[9] R. Ruivo, M.J. Cebola, P.C. Simões, M. Nunes da Ponte, Fractionation of edible oil model mixtures by supercritical carbon dioxide in a packed column. Part

1: experimental results, Ind. Eng. Chem. Res. 40 (2001) 1706–1711, http://dx.doi.org/10.1021/ie000747y.
[10] T.K. Sherwood, G.H. Shipley, F.A.L. Holloway, Flooding velocities in packed columns, Ind. Eng. Chem. 30 (1938) 765–769, http://dx.doi.org/10.1021/ie50343a008.
[11] R. Stockfleth, G. Brunner, Film thickness, flow regimes, and flooding in countercurrent annular flow of a falling film at high pressures, Ind. Eng. Chem. Res. 40 (2001) 6014–6020, http://dx.doi.org/10.1021/ie0100885.
[12] W.E. Lobo, L. Friend, F. Hashmall, F. Zenz, Limiting capacity of dumped tower packings, Trans. Am. Inst. Chem. Eng. 41 (1945) 693.
[13] N. Falco, E. Reverchon, G. Della Porta, Continuous supercritical emulsions extraction: packed tower characterization and application to poly(lactic-co-glycolic acid) + insulin microspheres production, Ind. Eng. Chem. Res. 51 (2012) 8616–8623, http://dx.doi.org/10.1021/ie300482n.
[14] R. Stockfleth, G. Brunner, Holdup, pressure drop, and flooding in packed countercurrent columns for the gas extraction, Ind. Eng. Chem. Res. 40 (2001) 347–356, http://dx.doi.org/10.1021/ie000466q.
[15] H.Y. Chiu, M.J. Lee, H.M. Lin, Vapor–liquid phase boundaries of binary mixtures of carbon dioxide with ethanol and acetone, J. Chem. Eng. Data 53 (2008) 2393–2402, http://dx.doi.org/10.1021/je800371a.
[16] J. Chrastil, Solubility of solids and liquids in supercritical gases, J. Phys. Chem. 86 (1982) 3016–3021, http://dx.doi.org/10.1021/j100212a041.
[17] R. Wiebe, The binary system carbon dioxide–water under pressure, Chem. Rev. 29 (1941) 475–481, http://dx.doi.org/10.1021/cr60094a004.
[18] M. Budich, G. Brunner, Supercritical fluid extraction of ethanol from aqueous solutions, J. Supercrit. Fluids 25 (2003) 45–55, http://dx.doi.org/10.1016/S0896-8446(02)00091-8.
[19] J.S. Lim, Y.W. Lee, J.D. Kim, Y.Y. Lee, H.S. Chun, Mass-transfer and hydraulic characteristics in spray and packed extraction columns for supercritical carbon dioxide–ethanol–water system, J. Supercrit. Fluids 8 (1995) 127–137, http://dx.doi.org/10.1016/0896-8446(95)90025-X.
[20] A. Ruiz-Rodríguez, T. Fornari, L. Jaime, E. Vázquez, B. Amador, J.A. Nieto, M. Yuste, M. Mercader, G. Reglero, Supercritical CO_2 extraction applied toward the production of a functional beverage from wine, J. Supercrit. Fluids 61 (2012) 92–100, http://dx.doi.org/10.1016/j.supflu.2011.09.002.
[21] G. Lévai, Bioproducts Processing by SFEE: Application for Liquid and Solid Quercetin Formulations, in: Dissertation, Universidad de Valladolid, Valladolid, 2016.
[22] S.P. Cardogan, G.C. Maitland, J.P. Martin Trusler, Diffusion coefficients of CO_2 and N_2 in water at temperatures between 298.15 K and 423.15 K at pressures up to 45 MPa, J. Chem. Eng. Data 59 (2014) 519–525, http://dx.doi.org/10.1021/je401008s.
[23] E. Reverchon, I. De Marco, Mechanisms controlling supercritical antisolvent precipitate morphology, Chem. Eng. J. 169 (2011) 358–370, http://dx.doi.org/10.1016/j.cej.2011.02.064.
[24] E. Reverchon, Supercritical antisolvent precipitation of micro- and nano-particles, J. Supercrit. Fluids 15 (1999) 1–21, http://dx.doi.org/10.1016/S0896-8446(98)00129-6.
[25] R. Campardelli, G. Della Porta, E. Reverchon, Solvent elimination from polymer nanoparticle suspensions by continuous supercritical extraction, J. Supercrit. Fluids 70 (2012) 100–105, http://dx.doi.org/10.1016/j.supflu.2012.06.005.
[26] Guidance for Industry QC3 – Tables and List, U.S. Department of Health and Human Services, Food and Drug Administration Center for Drug Evaluation and Research (CDER), Center for Biologics Evaluation and Research (CBER), ICH, Revision 2, 2012.
[27] Spain 2011. Real Decreto 1101/2011, de 22 de Julio, por el que se aprueba la lista positiva de los disolventes de extracción que se pueden utilizar en la fabricación de productos alimenticios y de sus ingredientes, Boletín Oficial del Estado 208 (August) (2011) 94132–94137.
[28] M. Wendland, H. Hasse, G. Maurer, Multiphase high-pressure equilibria of carbon dioxide–water–acetone, J. Supercrit. Fluids 7 (1994) 245–250, http://dx.doi.org/10.1016/0896-8446(94)90011-6.
[29] A.Z. Panagiotopoulos, R.C. Reid, High-pressure phase equilibria in ternary fluid mixtures with a supercritical component, in: T. Squires, M.E. Paulatis (Eds.), Supercritical Fluids. Chemical and Engineering Principles and Applications, ACS Symposium Series, American Chemical Society, Washington, 1987, pp. 115–129, http://dx.doi.org/10.1021/bk-1987-0329.ch010.
[30] P. Traub, K. Stephan, High-pressure phase equilibria of the system CO_2–water–acetone measured with a new apparatus, Chem. Eng. Sci. 45 (1990) 751–758, http://dx.doi.org/10.1016/0009-2509(90)87016-L.
[31] R. Adami, J. Schuster, S. Liparoti, E. Reverchon, A. Leipertz, A. Braeuer, A Raman spectroscopic method for the determination of high pressure vapour liquid equilibria, Fluid Phase Equilib. 300 (2013) 265–273, http://dx.doi.org/10.1016/j.fluid.2013.09.046.

Publication V:

"The encapsulation of low viscosity omega-3 rich fish oil in polycaprolactone by supercritical fluid extraction of emulsions"

Cristina Prieto, Lourdes Calvo

Submitted for publication.

Impact Factor: -

Citations: -

The encapsulation of low viscosity omega-3 rich fish oil in polycaprolactone by supercritical fluid extraction of emulsions

Cristina Prieto and Lourdes Calvo*

Departamento de Ingeniería Química, Facultad de Ciencias Químicas, Universidad Complutense de Madrid, Av. Complutense s/n, 28040 Madrid, Spain

crisprie@ucm.es, lcalvo@ucm.es

Correspondence should be addressed to Lourdes Calvo,

lcalvo@ucm.es,

Tf: (+34) 91 394 4185

ABSTRACT

Supercritical fluid extraction of emulsions technology (SFEE) was used for the encapsulation of a liquid lipophilic compound, specifically fish oil rich in ω-3 polyunsaturated fatty acids. Three different emulsion formulations containing stabilizing agents were tested using Tween 80 as a surfactant, polycaprolactone as coating polymer and acetone as organic solvent. Spherical and non-aggregated nanoparticles with sizes ranging from 6 to 73 nm were obtained depending on the formulation. The encapsulation efficiency of the nanoparticles produced by SFEE was around 40%, similar to that generated by conventional solvent evaporation. Operating at 8.0 MPa and 313 K, less than 25 kg CO_2·kg acetone^{-1} were required to reduce the acetone concentration in the nanoparticle suspension to 5000 ppm (pharmaceutical requirements). However, to obtain nanoparticles for use in the food industry (maximum acetone concentration of 50 ppm), CO_2 consumption required being increased to 127 kg CO_2·kg acetone^{-1}.

KEYWORDS

Supercritical fluid extraction of emulsions, fish oil rich in ω-3 PUFAs, polycaprolactone, encapsulation, nanoparticles.

1. Introduction

Fish oil is the most important source of ω-3 polyunsaturated fatty acids (PUFAs), such as eicosapentaenoic acid (EPA, C20:5) and docosahexaenoic acid (DHA, C22:6) [1]. EPA and DHA are important functional ingredients due to their documented health benefits. These bioactive compounds can reduce the risk of certain chronic diseases, such as inflammation, cardiovascular disease, immune response disorders, mental disorders and poor infant development [2]. The ω-3 fatty acids EPA and DHA cannot be synthesized in the human body, and their supply relies on dietary intake. Seafood, fish, marine and algal oils, nuts and seeds are the dietary sources of these compounds [3]. The levels reported to promote health benefits are > 250 mg per day [2]. However, average current intake is far below the recommendations, around 100 mg per day [3], hence, the great interest in the incorporation of PUFAs into foods, supplements and pharmaceuticals.

Nevertheless, the direct incorporation of PUFAs presents several limitations. First, PUFAs are highly lipophilic molecules, explaining their poor absorption and limited bioavailability [2]. Second, PUFAs are highly susceptible to oxidation, which involves a loss of nutritional value, formation of toxic products such as peroxides, and formation of volatile degradation products that have an unpleasant smell and taste, reducing consumer acceptability [4]. For these reasons, the development of special delivery systems is needed to overcome these challenges. So far, two different strategies have been used: emulsion-based delivery systems [3] and encapsulation techniques [5]. However, encapsulation techniques enhance stability against oxidation, bioavailability, mask undesirable odor, flavor and color, and provide a controlled release of these bioactive compounds as a result of the polymeric wall [6, 7]. Spray-drying, freeze-drying, coacervation, inclusion

complexation, emulsion-diffusion, and solvent evaporation are conventional encapsulation techniques that have been used for fish oil encapsulation until now [4, 5]. Among them, spray-drying is the main encapsulation method due to the low production costs and the scale-up difficulty of the other techniques [5]. However, spray-drying requires high operating temperatures and high air flow rates which could contribute to oil oxidation. Furthermore, during the drying process, some oil may adhere to the particle surface, which exhibits potential for oxidation and changes in the organoleptic properties of the product [8]. Furthermore, particle size is in the range of microns [4].

The emerging encapsulation techniques with supercritical fluids represent an alternative to conventional encapsulation processes. In addition to promoting the effective removal of organic solvents resulting from the high solubility of small organic molecules, the use of CO_2 limits the oxidation of PUFAs present in fish oil because the process occurs under an inert atmosphere and at moderately low temperatures [9]. Several processes have been used for the encapsulation of essential oils: Solution Enhanced Dispersion by Supercritical Fluids (SEDS) [10], Particles from Gas Saturated Solutions (PGSS) [11], PGSS-drying [12], Rapid Expansion from Supercritical to Surfactant Solution (RESSS) [13], and Supercritical Solvent Impregnation (SSI) [14]. Only PGSS and PGSS-drying were used for the encapsulation of fish oil [15, 16]. In both cases, the oil was encapsulated in water-soluble polymers with a particle size of microns.

Supercritical fluid extraction of emulsions (SFEE) is a novel encapsulation technology [17] that combines conventional emulsion processes with the unique properties of supercritical fluids to produce tailor-made micro- and nanoparticles. The basis of this process relies on the use of supercritical CO_2 to rapidly extract the organic phase of an

emulsion in which a bioactive compound and its coating polymer have been previously dissolved. By removing the solvent, both compounds precipitate, generating a suspension of particles in water. The produced particles have controlled size and morphology [17] due to the use of the emulsion and the fast kinetics of supercritical CO_2 extraction. Particle agglomeration in the aqueous phase is avoided since the particles are stabilized by a surfactant. In addition, this technology is very versatile. It is possible to encapsulate hydrophilic and lipophilic compounds by changing the starting emulsion. An oil-in-water (O/W) emulsion can be used to encapsulate lipophilic compounds, while a water-in-oil-in-water (W/O/W) emulsion can be used to encapsulate hydrophilic compounds. Previous studies have demonstrated that this process is easily scalable by means of a countercurrent packed column [18]. Most existing research conducted in this field has involved the encapsulation of solid pharmaceutical compounds in poly(lactic-co-glycolic acid) (PLGA). However, this method may also represent a promising technique for encapsulating nutraceuticals for the food industry. One example is the nanoencapsulation of vitamin E in polycaprolactone [19], in which core-shell structures in the nanometer scale with high encapsulation efficiency and high long-term stability were obtained.

The possibility of encapsulating fish oil using SFEE was tested using the system made up of acetone (O) and water (W), Tween 80 as a surfactant, and polycaprolactone (PCL) as the encapsulating polymer, which generated nanoparticles with very good characteristics in the encapsulation of vitamin E [19]. PCL is a synthetic, biocompatible, and fully biodegradable polymer, which has a semicrystalline nature (glass transition temperature of 213 K). It is approved by the FDA (Food and Drug Administration) for drug delivery. It has high hydrophobicity, high *in vitro* stability and is low-cost. Due to its slow

degradation, PCL is ideally suited for long-term delivery, or when a targeted delivery to the intestinal tract is intended [20]. Acetone was selected as the organic solvent because of its low toxic potential (Class 3), which is in line with ICH guidelines [21]. Tween 80 was used as the surfactant because it is a particularly attractive non-ionic surfactant that is non-toxic, environmentally-friendly and biocompatible. It is commercially inexpensive and is approved for pharmaceutical and food use [22].

The aim of this work was the application of SFEE for the nanoencapsulation of fish oil with a high content in ω-3 PUFAs in polycaprolactone. Several formulations to prepare stable fish oil enriched emulsions were first studied. The best formulations were subjected to SFEE and the obtained nanoparticles were compared in terms of encapsulation efficiency, particle size distribution and morphology. Finally, a comparison with the particles produced by conventional solvent evaporation was also made to analyze the potential improvements generated by the use of supercritical technology.

2. Materials and methods

2.1 Materials

Fish oil with high content in EPA and DHA was kindly donated by Biomega Natural Nutrients (Spain), and its composition is shown in Table 1. Tween 80, α-tocopherol (≥95%), polycaprolactone (PCL) (MW=10000), acetone (≥99.5%), chloroform (≥99%), n-hexane (≥99%) and potassium hydroxide (85%) were all from Sigma Aldrich (Spain). Glycerol (PRS-CODEX) was from Merck (Spain). Methanol LC Optima was obtained from Fisher Scientific (Spain). Xanthan gum was provided by Manuel Riesgo (Spain).

Sodium phosphotungstic acid solution (1%) was from Panreac (Spain). Carbon dioxide (>99.95%) was from Carburos Metálicos (Air Products, Spain). All materials were used as received. Millipore water was used throughout the study.

Table 1. Fatty acid profile of the fish oil used.

Fatty acids	Proportion (%)
C14:0	2.70 ± 0.04
C15:0	0.61 ± 0.01
C16:0	16.06 ± 0.09
C16:1	4.23 ± 0.04
C17:0	1.39 ± 0.00
C17:1	0.65 ± 0.00
C18:0	4.34 ± 0.01
C18:1	20.00 ± 0.08
C18:2	0.82 ± 0.00
C18:3	0.29 ± 0.00
C18:4	0.40 ± 0.00
C20:0	0.19 ± 0.00
C20:1	7.08 ± 0.07
C20:4	1.65 ± 0.01
C20:5	4.50 ± 0.02
C22:5	2.29 ± 0.01
C22:6	20.98 ± 0.03
Saturated Fatty Acids	25.30 ± 0.10
Monounsaturated Fatty Acids	31.96 ± 0.11
Polyunsaturated Fatty Acids	30.94 ± 0.04
EPA+DHA	25.49 ± 0.04

2.2 Preparation of the emulsion.

PCL was dissolved in acetone at 313 K, followed by addition of fish oil and α-tocopherol when required. The aqueous continuous phase was prepared by mixing the water and the surfactant, Tween 80. A thickener, glycerol or xanthan gum, was added to the water phase in some formulations. The organic phase was added to the water phase and

stirred in the vortex (Heidolph REAX top) for 5 min to guarantee a homogeneous dispersion.

2.3 Determination of phase behavior

The first step in determining phase behavior involved visually inspecting the samples. Samples in the entire composition range were classified: first, according to turbidity, since in colloidal dispersions this parameter could be an indicator of the size of the colloid. In general terms, samples with colloids ranging from 2 to 50 nm in diameter are transparent, while samples with colloids larger than 100 nm are opaque [23]. Second, they were classified according to phase separation, and third, according to PCL flocculation or precipitation, which is a symptom that the nanoparticles are not correctly formed [24]. Finally, they were also classified according to their fishy smell. All samples were analyzed in triplicate.

2.4 SFEE nanoparticle formation

The SFEE apparatus consisted of a 10 mL cylindrical stainless steel extractor with a length-to-diameter (L/D) ratio of nine. Liquid-cooled CO_2 at 263 K was delivered using a head-cooled piston pump (Jasco, PU-2080) and bubbled through the emulsion. The temperature in the extractor was regulated by a heating jacket and recorded within ± 0.1 K through the use of a type T thermocouple that was positioned inside the vessel. The pressure inside the extractor was regulated by a backpressure regulator (BPR, TESCOM) and read via a digital internal pump manometer within ± 0.1 MPa and via an external online Bourbon manometer. A mass flow meter (Alicat Scientific, M-10SLPM-D) was used to measure the total amount of CO_2 used. A scheme of the equipment is shown in Figure 1.

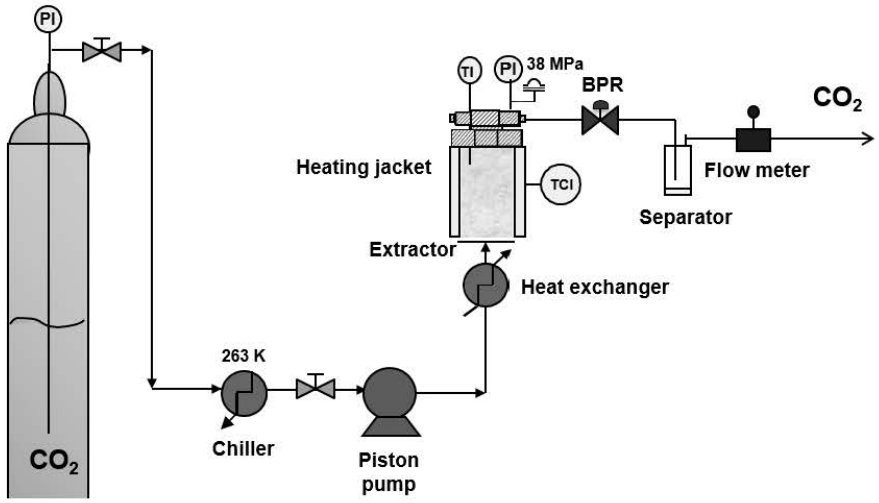

Figure 1. Scheme of the equipment used for supercritical fluid extraction of emulsions process (SFEE).

In order to carry out the process, five grams of the emulsion were placed inside the extractor before the vessel was closed. CO_2 was added, and the temperature was adjusted. The vessel was then pressurized to 8.0 MPa. Finally, the BPR was opened and the flow adjusted. The operation was deemed to be complete when the selected operating time was reached. The vessel was then slowly depressurized. A suspension of nanoparticles in water was recovered and stored in screw cap glass vials in the refrigerator until the time of analysis.

2.5 Formation of nanoparticles through conventional solvent evaporation

The acetone was extracted from 100 g of emulsion by solvent evaporation using a hotplate with temperature control (MST-Digital, IKA) at 313 K for 8 h inside a fume hood, under constant magnetic stirring (400 rpm).

2.6 Encapsulation efficiency

Encapsulation efficiency was determined as the percentage of fish oil entrapped inside the particle with respect to the theoretical content. Quantitative measurements of fish oil were performed by gas chromatography coupled to mass spectrometry (GC-MS).

First, nanoparticle suspensions were centrifuged (Digicen 21, Orto Arlesa) at 15000 rpm for 10 min. The liquid phase was removed, and the pellet was washed with Milli-q water and centrifuged to recover the pellet. The polymeric wall of the particles was opened in 2 mL of chloroform. Chloroform was evaporated from the sample via a SpeedVac concentrator (Thermo Electron Corporation – Savant SPD131 DDA).

For the derivatization of the fish oil contained in the nanoparticles, 50 µl of methanol were first added and mixed in an ultrasound bath for 15 min to resuspend the oil. Then, 1 mL of KOH 2 M in methanol was added. The mixture was stirred in the vortex for 1 min and incubated for 5 min at room temperature. Five milliliters of hexane were added and the mixture was stirred in the vortex for 1 min. The mixture was incubated for 15 min at room temperature to facilitate phase separation. A volume of 4.5 mL of the supernatant was collected and concentrated in the SpeedVac concentrator for later injection into the gas chromatograph.

GC-MS analysis for fatty-acid methyl esters was performed on Varian CP-3800 gas chromatography instrument coupled with a Varian Saturno 2200 ion trap mass selective detector. The capillary column Equity (diphenyl polysiloxane) with dimensions of 30 m x 0.25 mm i.d., 0.25 µm film thickness (Supelco) was used for the separation of fatty-acid methyl esters. Oven temperature increased from 333 K to 373 K at 4 $K \cdot min^{-1}$, from 373 K

to 508 K at 2 $K \cdot min^{-1}$ and from 508 K to 533 K at 20 $K \cdot min^{-1}$. The split ratio was 1:100, and helium was used as the carrier gas at a flow rate of 1 $mL \cdot min^{-1}$ in constant flow mode. Injector temperature was 523 K. The mass spectrometer was operated in electron impact mode at 70 eV in the scan range of 25-600 m/z. The injection sample volume was 1 µl. Fatty acid identification was done by comparing the retention time for each peak with those of the standard mixture of 37 fatty acid methyl esters (Supelco 37 Component FAME Mix). Quantification of the fish oil inside the nanoparticles was performed based on the C18:1 peak of a sample of known fish oil concentration.

The loading capacity was calculated as the mass percentage ratio between the encapsulated fish oil and the total mass of the particle (encapsulated fish oil, vitamin E and polymer).

2.7 Particle size distribution

Particle size distribution was measured by photon correlation spectroscopy using a Zetasizer Nano Zs (Malvern). A dilution of the sample with Milli-q water was required to achieve suitable optical density. All measurements were performed at 298 K.

2.8 Residual acetone concentration

The amount of acetone in the nanoparticle suspension was measured using headspace gas chromatography. In order to generate the headspace, 2 mL of nanoparticle suspension were introduced into a 20 mL vial and stabilized for 1 h at 333 K. At this temperature, the polymer melts and acetone is enriched in the vapor phase. Then, 0.5 mL of the vapor phase of this vial were extracted with a gas-tight syringe and injected manually into a gas chromatograph (Shimazdu, GC-2010-Plus) that was connected to a flame ionization

detector. Acetone was separated using a fused-silica capillary column: 20 m long, 0.18 mm internal diameter and 0.18 μm film thickness (Zebron-ZB-1HT inferno). The oven temperature was set to 313 K for 6 min. The injector temperature was maintained at 453 K in split mode (ratio 19.5) and nitrogen was employed as the carrier at 7 $mL \cdot min^{-1}$ at 40.9 kPa. Each sample was measured in triplicate.

2.9 Nanoparticle morphology

Aqueous suspensions of nanoparticles were centrifuged at 15000 rpm for 10 min. After that, 70% of the supernatant was removed. A drop of concentrated aqueous suspension was negatively stained for 60 s with a 1% sodium phosphotungstic acid solution, and placed on a carbon-coated copper grid. Transmission Electron Microscopy (TEM) images were taken using a JEOL JEM 1010.

2.10 Statistical analysis

The experiments were repeated three times. Analyses were performed in duplicate for each replicate (n=3 x 2). Means and standard deviations were calculated for all data.

3. Results and discussion

The purpose of this research is the encapsulation of fish oil in PCL using the SFEE process. First, the best emulsion formulation to be subjected to SFEE was sought using the acetone-water-Tween 80 system. Thickening agents were tested to improve stability of the emulsions. Second, the effect of the initial formulation was evaluated in terms of encapsulation efficiency, particle size, particle size distribution, and morphology. Third,

CO_2 consumption to obtain nanoparticles with a residual organic solvent concentration suitable for the pharmaceutical and food industries was studied. Finally, nanoparticles obtained by SFEE were compared with those generated by solvent evaporation in terms of nanoparticle characteristics and acetone residual concentration.

3.1 Selection of the emulsion formulation

The initial step in the fish oil encapsulation process was to select the emulsion formulation to be subjected to SFEE. Since the emulsion acts as a template for the nanoparticles during the SFEE process, an O/W emulsion, with small colloid size and narrow distribution of the organic phase droplets, and stable to agglomeration and coalescence, is required. The system used for the encapsulation of fish oil consisted of acetone and water, Tween 80, PCL, due to the good characteristics of the vitamin E nanoparticles generated with this system by SFEE [19]. However, it was not possible to obtain a stable O/W emulsion with the fish oil. This behavior could be due to the complete miscibility of acetone in the aqueous phase. In the case of vitamin E, its high viscosity allowed the formation of stable emulsions [19]. However, the viscosity of the fish oil is around 40 times lower than that of vitamin E. Therefore, it was necessary to increase the viscosity of one of the phases in order to limit acetone diffusion. Thickening agents are known to increase viscosity and improve emulsion stability [25]. Consequently, glycerol and xanthan gum were selected as water-soluble thickeners as they are approved by the FDA as food additives. Vitamin E was selected as an oil-soluble weighting agent which, in addition to providing viscosity, is the main natural antioxidant found in fish oils [5].

Besides being a thickener, glycerol also acts as a salting-out agent for the acetone-water mixture, being able to generate immiscibility regions at low water concentrations, ≤ 20% [26]. In this region, acetone is not miscible in the aqueous phase, leading to the formation of stable emulsions. To begin with, the acetone-water-Tween 80 ratio that provided a stable O/W emulsion was sought. For this reason the concentration of glycerol in the aqueous phase (80% by mass of glycerol) and the concentrations of fish oil and PCL in the organic phase (0.51 and 0.63% by mass, respectively) were maintained constant. Twenty-two compositions were selected to completely cover the pseudo-ternary phase diagram in which the behavior of each sample was represented. The visual observation of each sample resulted in the triangular diagram depicted in Figure 2. Samples 1, 2, 21 and 22 were slightly turbid, samples 3 and 4 were transparent, and sample 20 was turbid. The rest of the samples were highly unstable to phase separation. Only samples 20, 21 and 22 might have an O/W structure based on composition. However, they were not very stable, and after a short time, they showed phase separation and fishy smell. Therefore, an improvement in the emulsion formulation was required. For that purpose, the amounts of Tween 80, glycerol and PCL were varied. Moreover, addition of vitamin E was also considered in order to enhance stabilization of the fish oil in the organic phase. Tables 2, 3 and 4 show the results of these variations from sample 20, shown as formulation A. Same variations were done with samples 21 and 22 (results not shown), but no stable emulsions were found in any condition.

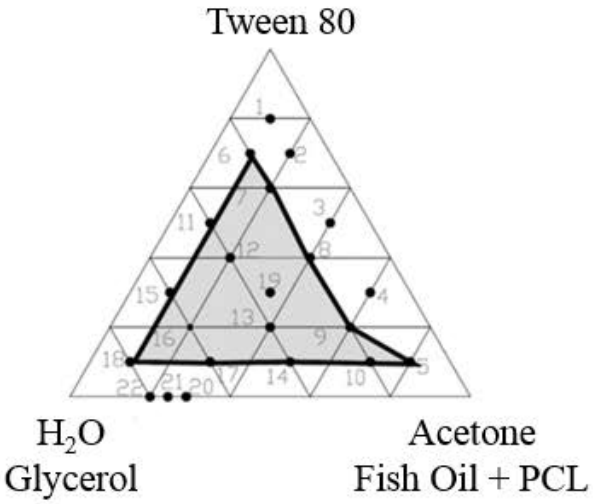

Figure 2. Phase map of the Tween 80 / water + glycerol / acetone + fish oil + PCL system. The light shaded area depicts the samples where phase separation occurred. The rest of the samples consisted of a single phase.

Table 2. The stability and smell of several formulations for the encapsulation of fish oil rich in ω-3 PUFAs by SFEE using glycerol as aqueous phase thickener. Formulation A corresponds to sample 20. Gly means glycerol; T80, Tween 80; AC, acetone; PCL, polycaprolactone; ω-3, fish oil rich in ω-3 PUFAs; Vit E, vitamin E.

Formulation	M H_2O+GLY (g)	[GLY] (% by mass)	M T80 (g)	M AC (g)	M PCL (g)	M ω-3 (g)	M Vit E (g)	Turbidity	Phase separation	PCL precipitation	Fishy smell
Effect of the Amount of Tween 80											
A	3.580	80	*0.004*	1.420	0.009	0.007	--	YES	YES	NO	YES
B	3.580	80	*0.090*	1.420	0.009	0.007	--	YES	YES	NO	YES
C	3.580	80	*0.180*	1.420	0.009	0.007	--	YES	YES	NO	YES
D	3.580	80	*0.270*	1.420	0.009	0.007	--	YES	YES	NO	YES
E	3.580	80	*0.360*	1.420	0.009	0.007	--	YES	NO	NO	YES
Effect of the Fish Oil:Vitamin E Ratio											
F	3.580	80	0.360	1.420	0.009	*0.014*	*0.007*	YES	NO	NO	YES
G	3.580	80	0.360	1.420	0.009	*0.007*	*0.007*	YES	NO	NO	YES
H	3.580	80	0.360	1.420	0.009	*0.007*	*0.014*	YES	NO	NO	NO
Effect of the Amount of Glycerol											
I	3.580	*70*	0.360	1.420	0.009	0.007	0.014	NO	NO	NO	NO
J	3.580	*60*	0.360	1.420	0.009	0.007	0.014	YES	NO	YES	NO
K	3.580	*50*	0.360	1.420	0.009	0.007	0.014	YES	NO	YES	NO
Effect of the Amount of PCL											
L	3.580	70	0.360	1.420	*0.018*	0.007	0.014	YES	NO	YES	NO
M	3.580	70	0.360	1.420	*0.027*	0.007	0.014	YES	NO	YES	NO

Table 3. The stability and smell of several formulations for the encapsulation of fish oil rich in ω-3 PUFAs by SFEE using xanthan gum as aqueous phase thickener. XG means xanthan gum; T80, Tween 80; AC, acetone; PCL, polycaprolactone; ω-3, fish oil rich in ω-3 PUFAs; Vit E, vitamin E.

Formulation	M H_2O+XG (g)	[XG] (% by mass)	M T80 (g)	M AC (g)	M PCL (g)	M ω-3 (g)	M Vit E (g)	Turbidity	Phase separation	PCL precipitation	Fishy smell
Effect of the Amount of Xanthan Gum											
N	3.580	*0.100*	0.360	1.420	0.009	0.007	0.014	YES	NO	YES	YES
O	3.580	*0.250*	0.360	1.420	0.009	0.007	0.014	YES	NO	NO	NO
Effect of the Amount of PCL											
P	3.580	0.250	0.360	1.420	*0.018*	0.007	0.014	YES	NO	YES	NO
Q	3.580	0.250	0.360	1.420	*0.027*	0.007	0.014	YES	NO	YES	NO

Table 4. The stability and smell of the formulation without thickener for the encapsulation of fish oil rich in ω-3 PUFAs by SFEE. T80, Tween 80; AC, acetone; PCL, polycaprolactone; ω-3, fish oil rich in ω-3 PUFAs; Vit E, vitamin E.

Formulation	M H_2O (g)	M T80 (g)	M AC (g)	M PCL (g)	M ω-3 (g)	M Vit E (g)	Turbidity	Phase separation	PCL precipitation	Fishy smell
R	3.580	0.004	1.420	0.009	0.007	0.014	YES	NO	NO	NO

In the first place, the amount of Tween 80 was varied, as denoted by formulations A-E in Table 2. It was necessary to increase the amount of surfactant to 0.360 g to avoid phase separation. Despite being a high surfactant concentration, which may affect manufacturing costs, it is within the concentration ranges used in the pharmaceutical and food industries. Indeed, the U.S. Food and Drug Administration (FDA) puts a legal limit on the use of Tween 80 in special dietary foods of < 360 mg per day. In these conditions, the emulsion was turbid. However, the fishy smell persisted. Therefore, different fish oil:vitamin E ratios corresponding to formulations F-H in Table 2 were tested. Nevertheless, fish odor masking was only achieved with formulation H, in which the amount of vitamin E was twice that of fish oil.

The concentration of glycerol in the aqueous phase was also studied, as reflected by formulations I-K in Table 2. A glycerol concentration below 60% provoked PCL precipitation. At a glycerol concentration of 70%, the emulsion became transparent. This phenomenon could be due to a droplet size reduction, but also due to the effect of glycerol on the refractive index of the aqueous phase [27]. Finally, the amount of PCL was increased for the purpose of enhancing encapsulation efficiency. However, precipitation of the polymer was observed.

In second place, glycerol was substituted with xanthan gum. Table 3 shows the stability of the emulsions formed using this thickener and varying the other components. 0.25% by mass of xanthan gum in water was enough to stabilize the emulsion. In comparison with the 70% by mass of glycerol, this could lead to savings in raw materials. This is one of the reasons xanthan gum is frequently used in the food industry, since it

presents great solubility in cold water and high thickening properties at a very low concentration [26], in addition to antioxidant activity [28]. The amount of PCL was studied in formulations P-Q. Again, the increase in PCL concentration caused its precipitation.

Finally, the option of adding only vitamin E as a thickener (formulation R in Table 4) was explored. The emulsion generated with this formulation was stable, turbid and achieved odor masking.

Therefore, three formulations, I, O and R, were selected to be subjected to SFEE. All of them were stable O/W emulsions for at least 5 h and achieved odor masking. Formulation I was transparent, whilst formulations O and R were turbid.

3.2 Nanoparticle formation by SFEE

The formation of fish oil in PCL nanoparticles by SFEE was based on polymer precipitation once the organic solvent was extracted from the emulsion by supercritical CO_2. Operating conditions were selected to reach complete acetone extraction without extracting the fish oil. Therefore, according to the high-pressure vapor-liquid equilibrium diagram of the CO_2-acetone mixture [29], temperature and pressure were set at 313 K and 8.0 MPa, respectively, because in these conditions supercritical CO_2 and acetone were completely miscible and fish oil solubility in supercritical CO_2 was rather low (0.73 mg fish oil · g CO_2^{-1}) [30]. The solubility of the other compounds of the system under such conditions was also low or negligible, that is, 0.30 mg vitamin E · g CO_2^{-1} [31], 0.05 mg glycerol · g CO_2^{-1} [32], 0.20 mg water · g CO_2^{-1} [33].

Compared to other encapsulation technologies, such as spray drying, SFEE requires moderately low temperatures. This helps to avoid bioactive compound degradation, but also

the loss of stability of the emulsion because of the change of the hydrophilic character of the surfactant with temperature. Temperature can also affect the polymeric wall porosity if the organic solvent boiling temperature is reached, as well as the compound permeability if the glass transition temperature of the polymer is exceeded [19].

Other parameters affecting acetone extraction were extractor design and CO_2 flow rate. For a 10 mL extractor with an L/D=9, the best flow rate to maximize acetone extraction, avoiding entrainment of the emulsion, was 2 $mL \cdot min^{-1}$ [19]. The residual acetone concentration versus the required amount of CO_2 for each formulation is shown in Table 5. Acetone extraction was initially very fast because high amounts of acetone were available. Under these conditions, less than one hour was required to reduce residual acetone concentration to 5000 ppm, as required for pharma products [21]. However, as the acetone concentration decreased (less driving force) and nanoparticles were formed, the extraction rate rapidly decreased. Some of the acetone was entrapped inside the particles. Consequently, higher CO_2 ratios and longer operating times were required to reduce the acetone concentration to 50 ppm, which is the maximum acetone concentration allowed in the food industry [34]. Indeed, 240 min and 101 kg $CO_2 \cdot kg\ acetone^{-1}$ were required to reach the legally permitted level of acetone in food in the case of formulation R, whilst 300 min and 127 kg $CO_2 \cdot kg\ acetone^{-1}$ were needed when using formulations I and O, as shown in Table 5. As demonstrated by Lévai [35], extraction of the organic solvent from the emulsion is kinetically controlled by the dissolution of supercritical CO_2 in the organic solvent and in the water phase, and the extraction of the organic phase by the supercritical CO_2 through the water phase boundary. Hence, the increase in aqueous phase viscosity due to thickeners slowed down the extraction rate.

Table 5. Acetone removal in a bubble column at 8.0 MPa and 313 K with a CO_2 flow rate of 2 mL·min^{-1}.

Time	CO_2/acetone ratio	[Acetone]$_R$ ± SD (ppm)		
(min)	(kg·kg^{-1})	Formulation I	Formulation O	Formulation R
30	13	14300 ± 5300	10840 ± 450	19300 ± 1300
60	25	951 ± 76	1980 ± 150	1170 ± 150
120	51	651 ± 45	568 ± 68	117 ± 19
180	76	400 ± 31	303 ± 67	63 ± 2
240	101	136 ± 8	142 ± 4	54 ± 5
300	127	30 ± 3	63 ± 14	--

3.3 Nanoparticle characterization

The impact of the initial formulation on the characteristics of the nanoparticles (particle size distribution, encapsulation efficiency, and morphology) obtained by SFEE was investigated. Table 6 shows the characteristics of the nanoparticles from formulations, I, O and R.

Table 6. Characteristics of the nanoparticles produced in the bubble column using formulations I, O and R. EE means Encapsulation Efficiency; PdI, Polydispersity Index; LC, Loading Capacity.

Formulation	EE ± SD (%)	Mean diameter ± SD (nm)	PdI ± SD	LC ± SD (%)
I	38 ± 5	8 ± 1	0.29 ± 0.02	10 ± 1
O	12 ± 1	6 ± 1	0.44 ± 0.09	3 ± 1
R	43 ± 12	73 ± 1	0.40 ± 0.03	15 ± 6

All formulations resulted in encapsulation efficiencies of less than 50%, the formulation with xanthan gum yielding the worst results. This could be because of the solubility of fish oil in supercritical CO_2, which could be increased by the presence of acetone. However, no significant amounts of fish oil were collected in the vial. Another explanation could be the loss of stability of the emulsion during SFEE treatment, which

could release the fish oil to the water phase. Low encapsulation efficiency is not advisable from the economic point of view, but also because external oil becomes oxidized more rapidly than the encapsulated oil, affecting product acceptability. One possible strategy would be to remove the non-encapsulated fish oil by introducing a washing step after encapsulation [1].

Similar efficiencies were obtained in the encapsulation of bioactive oils with other supercritical fluid technologies. Dubbert *et al.* [15] obtained low encapsulation efficiency for the encapsulation of fish oil in chitosan by PGSS-drying. Varona *et al.* [11] got an encapsulation efficiency between 13-45% for the encapsulation of lavandin oil in PCL by PGSS. Regarding conventional techniques, higher encapsulation efficiencies were reported. Sanguansri *et al.* [36] achieved an encapsulation efficiency of 90% for the encapsulation of tuna oil in sodium caseinate by spray-drying. Velasco *et al.* [37] obtained an encapsulation efficiency of 71% for the encapsulation of fish oil in sodium caseinate by freeze-drying. The higher encapsulation efficiency may be explained by a higher polymer:oil ratio; however, for this system that was not possible because of the polymer precipitation, as shown above.

Due to the low encapsulation efficiency, the loading capacity was also low, below 20%, but remained within the loading capacity range obtained in the encapsulation of oils by supercritical fluids [11]. Although higher values were obtained (between 60-100%) by means of impregnation techniques [14], values ranging between 30 and 60% were achieved through conventional evaporation techniques [38].

Regarding particle size, nanometer scale particles were obtained. Whilst formulations I and O generated particles with a size under 10 nm, formulation R produced particles having a size of 73 nm. As the operating conditions were the same, the difference in size can only be explained by the difference in the emulsion formulation. In the encapsulation of vitamin E in PCL using the same system, it was observed that particle size could be reduced by increasing the amount of vitamin E [19]. The smaller size of the nanoparticles obtained with the I and O formulations can be related to the presence of the thickener. In the case of both glycerol and xanthan gum, an effect of decreasing the droplet size of the emulsion was reported as the amount of thickener increased [2, 39]. Glycerol was also able to reduce the polydispersity index [2].

Compared to other supercritical fluid techniques, the nanoparticle size achieved was much lower than that obtained using techniques such as PGSS or PGSS-drying. Only sizes smaller than 1 μm of nanoparticles encapsulating oils were reported in research conducted with SEDS [10] or RESSS [13]. Conventional techniques generated particles with sizes around 20 μm [4]. Lower sizes of particles encapsulating fish oil have only been achieved by the emulsion-diffusion technique (90 nm) [38].

3.4 Morphology

The morphology of the nanoparticles produced by SFEE was characterized by TEM. A comparison of the nanoparticles obtained from each formulation is shown in Figure 3. All formulations provided spherical and non-aggregated nanoparticles. In the case of formulation I, the TEM image confirms the size, 8 nm, and the low polydispersity index measured by photon correlation spectroscopy (Table 6). The clustered appearance of the

nanoparticles could be due to the presence of glycerol in the concentrated nanoparticle suspension. In relation to the particles obtained from formulation O, greater size variability was observed, which was also reported in the photon correlation spectroscopy analysis, since the polydispersity index was 0.44. Finally, the nanoparticles obtained by formulation R were larger than the previous ones with a high polydispersity index, as reflected in the observed size variability.

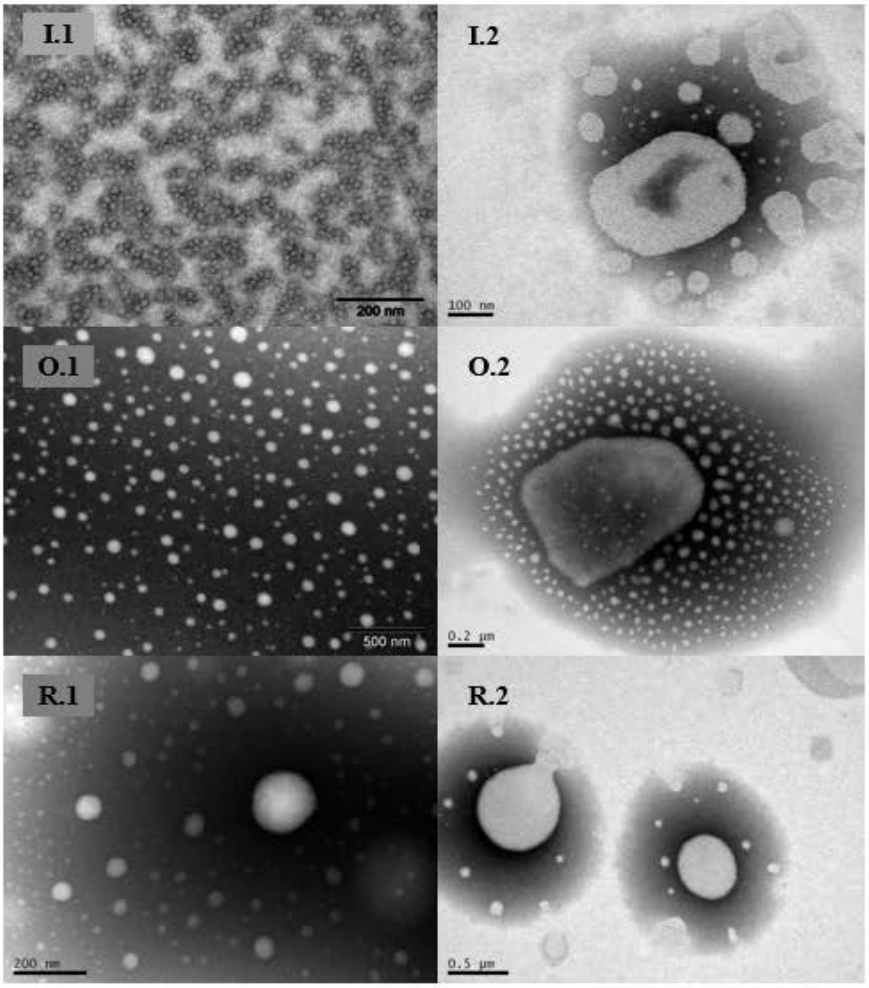

Figure 3. TEM image of fish oil-loaded nanoparticles obtained by SFEE (left) and conventional solvent evaporation (right) from formulations I, O and R.

3.5 Formation of nanoparticles through conventional solvent evaporation

Fish oil-loaded nanoparticles were formed by conventional solvent evaporation using the three selected formulations, i.e., I, O and R, in order to compare results with those nanoparticles obtained by SFEE. The characteristics of the nanoparticles obtained by solvent evaporation are shown in Table 7.

Table 7. Characteristics of the fish oil-loaded nanoparticles produced by solvent evaporation from formulations I, O and R. EE means Encapsulation Efficiency; LC, Loading Capacity.

Formulation	EE ± SD (%)	LC ± SD (%)	$[Acetone]_R$ ± SD (ppm)
I	49 ± 7	13 ± 2	758 ± 101
O	19 ± 12	5 ± 4	6295 ± 804
R	10 ± 5	3 ± 1	34 ± 4

Similar encapsulation efficiency and loading capacity were obtained by SFEE and conventional solvent evaporation for formulations I and O. However, formulation R showed a much lower encapsulation efficiency in nanoparticles obtained by conventional solvent evaporation. During experiments conducted with formulation R, a yellowish substance was observed covering the magnetic stirrer when the process finished. This could be due to low stability of the emulsion or because the nanoparticles did not resist the mechanical stress of the magnetic stirrer. This yellowish substance was also observed in formulation O. In addition, large, white, round particles (around 2 mm in diameter) were observed on the surface of the beaker in formulations I and O. The presence of large particles was also reflected in the TEM images (Figure 3). This suggests that particle aggregation has occurred. On the other hand, both formulations I and R showed a strong fishy smell after 8 h of process; however, for this smell was less intense for formulation O.

Contact with air, the temperature of the conventional process or the loss of stability of the organic phase droplets could be the reason behind the fishy odor. On the other hand, particle suspensions obtained by SFEE showed no odor at the end of the process.

Residual acetone concentration after 8 h of solvent evaporation was different for each formulation. While formulation R provided a particle suspension with less than 50 ppm, formulations I and O still contained important quantities of acetone. The thickener of formulations I and O delayed acetone removal, which was much slower for the sample with xanthan gum.

4. Conclusions

This research demonstrates that it is possible to encapsulate liquid lipophilic compounds with low viscosity, such as fish oil, by SFEE. Although encapsulation efficiency was around 50%, spherical and non-aggregated nanoparticles with a size smaller than 100 nm were obtained. Particle size could be reduced to 8 nm when thickeners were added to the aqueous phase. Resulting from the use of PCL as a coating polymer, these nanoparticles could be used in aqueous-based products. Furthermore, as PCL is a slow-degrading polymer, it provides great stability to the nanoparticles for up to one year [19], so they could be used in controlled delivery systems. These characteristics are of interest in applications for food, pharmaceutical and cosmetic products. On the other hand, the process occurs under a CO_2 inert atmosphere and at low temperatures, which limits PUFA oxidation. Furthermore, it can be easily scaled by means of a high-pressure packing column having an adequate length run in countercurrent mode, increasing production capacity and

reducing the amount of CO_2 required to obtain nanoparticles with a residual acetone concentration suitable for commercial application [18].

Acknowledgments

The authors gratefully acknowledge the financial support for this work provided by the Ministry of Economy and Competitiveness, project ref. CTQ2013-41781-P. The authors would also like to thank Biomega Natural Nutrients for kindly providing the fish oil rich in omega 3, and Centro Nacional de Microscopía Electrónica (CNME) for its support in TEM analysis. Cristina Prieto thanks the Universidad Complutense de Madrid for a UCM predoctoral grant.

References

[1] S. Drusch, An industry perspective on the advantages and disadvantages of different fish oil delivery systems, in: N. Garti, D.J. McClements (Eds.), Encapsulation technologies and delivery systems for food ingredients and nutraceuticals, Woodhead Publishing Limited, Cambridge, 2012, 488-504.

[2] A. Gulotta, A.H. Saberi, M.C. Nicoli, D.J. McClements, Nanoemulsion-based delivery systems for polyunsaturated (ω-3) oils: formation using a spontaneous emulsification method, Journal of Agricultural and Food Chemistry 62 (2014) 1720-1725, http://dx.doi.org/10.1021/jf4054808.

[3] L.A. Shaw, H. Faraji, T. Aoki, D. Djordjevic, D.J. McClements and E.A. Decker, Emulsion droplet interfacial engineering to deliver bioactive lipids into functional foods, in:

N. Garti (Ed.), Delivery and controlled release of bioactives in foods and nutraceuticals, Woodhead Publishing Limited, Cambridge, 2008, pp. 184-206.

[4] J. Rodríguez, M.J. Martín, M.A. Ruíz, B. Clares, Current encapsulation strategies for bioactive oils: from alimentary to pharmaceutical perspectives, Food Research International 83 (2016) 41-59, http://dx.doi.org/10.1016/j.foodres.2016.01.032.

[5] S.J. Lee, D.Y. Ying, Encapsulation of fish oils, in: N. Garti (Ed.), Delivery and controlled release of bioactives in foods and nutraceuticals, Woodhead Publishing Limited, Cambridge, 2008, pp. 370-403.

[6] S. Torres-Giner, A. Martínez-Abad, M.J. Ocio, J.M. Lagaron, Stabilization of a nutraceutical omega-3 fatty acid by encapsulation in ultrathin electrosprayed zein prolamine, Journal of Food Science 75 (2010) N69-N79, http://dx.doi.org/10.1111/j.1750-3841.2010.01678.x.

[7] M.A. Augustin, L. Sanguansri, Challenges in developing delivery systems for food additives, nutraceuticals and dietary supplements, in: N. Garti, D.J. McClements (Eds.), Encapsulation technologies and delivery systems for food ingredients and nutraceuticals, Woodhead Publishing Limited, Cambridge, 2012, 19-48.

[8] W. Kolanowski, M. Ziolkowski, J. Weiβbrodt, B. Kunz, G. Laufenberg, Microencapsulation of fish oil by spray drying - impact on oxidative stability. Part 1, European Food Research & Technology 222 (2006) 336-342, http://dx.doi.org/10.1007/s00217-005-0111-1.

[9] W. Eltringham, O. Catchpole, Processing of fish oils by supercritical fluids, in: J.L. Martínez (Ed.), Supercritical fluid extraction of nutraceuticals and bioactive compounds, CRC Press, Boca Raton, 2008, pp. 141-188, http://dx.doi.org/10.1201/9781420006513.ch5.

[10] D.L. Boschetto, I. Dalmolin, A.M. de Cesaro, A.A. Rigo, S.R.S. Ferreira, M.A.A. Meireles, E.A.C. Batista, J. Vladimir Oliveira, Phase behavior and process parameters effect on grape seed extract encapsulation by SEDS technique, Industrial Crops and Products 50 (2013) 352-360, http://dx.doi.org/10.1016/j.indcrop.2013.07.044.

[11] S. Varona, A. Martín, M.J. Cocero, C.M.M. Duarte, Encapsulation of lavandin essential oil in poly-(ε-caprolactone) by PGSS process, Chemical Engineering & Technology 36 (2013) 1187-1192, http://dx.doi.org/10.1002/ceat.201200592.

[12] S. Varona, S. Kareth, A. Martín, M.J. Cocero, Formulation of lavandin essential oil with biopolymers by PGSS for application as biocide in ecological agriculture, Journal of Supercritical Fluids 51 (2010) 369-377, http://dx.doi.org/10.1016/j.supflu.2010.05.019.

[13] Z. Wen, B. Liu, Z. Zheng, X. You, Y. Pu, Q. Li, Preparation of liposomes entrapping essential oil from *Atractylodes Macrocephala Koidz* by modified RESS technique, Chemical Engineering Research and Design 88 (2010) 1102-1107, http://dx.doi.org/10.1016/j.cherd.2010.01.020.

[14] S. Varona, S. Rodríguez-Rojo, A. Martín, M.J. Cocero, C.M.M. Duarte, Supercritical impregnation of lavandin (*Lavandula Hybrida*) essential oil in modified starch, Journal of Supercritical Fluids 58 (2011) 313-319, http://dx.doi.org/10.1016/j.supflu.2011.06.003.

[15] K. Dubbert, N. Rubio-Rodríguez, S. Kareth, S. Beltrán, M. Petermann, Encapsulation of fish oil in biodegradable polymers by the PGSS process, in: Institut National Polytechnique de Lorraine (Ed.), Proceedings of the 13th European Meeting on Supercritical Fluids, The Hague, 2011, p. 176.

[16] A.S.M. Tanbirul Haque, B.S. Chun, Particle formation and characterization of mackerel reaction oil by gas saturated solution process, Journal of Food Science and Technology 53 (2016) 293-303, http://dx.doi.org/10.1007/s13197-015-2000-3.

[17] P. Chattopadhyay, R. Huff, B.Y. Shekunov, Drug encapsulation using supercritical fluid extraction of emulsions, Journal of Pharmaceutical Sciences 95 (2006) 667-679, http://dx.doi.org/10.1002/jps.20555.

[18] C. Prieto, C.M.M. Duarte, L. Calvo, Performance comparison of different supercritical fluid extraction equipments for the production of vitamin E in polycaprolactone nanocapsules by supercritical fluid extraction of emulsions, Journal of Supercritical Fluids 122 (2017) 70-78, http://dx.doi.org/ 10.1016/j.supflu.2016.11.015.

[19] C. Prieto, L. Calvo, Supercritical fluid extraction of emulsions to nanoencapsulate vitamin E in polycaprolactone, Journal of Supercritical Fluids 119 (2017) 274-282, http://dx.doi.org/10.1016/j.supflu.2016.10.004.

[20] V.R. Sinha, K. Bansal, R. Kaushik, R. Kumria, A. Trehan, Poly-ε-caprolactone microspheres and nanospheres: an overview, International Journal of Pharmaceutics 278 (2004) 1-23, http://dx.doi.org/10.1016/j.ijpharm.2004.01.044.

[21] Guidance for Industry QC3- Tables and List, U.S. Department of health and human services, food and drug administration center for drug evaluation and research (CDER), Center for Biologics Evaluation and Research (CBER), ICH, Revision 2, 2012.

[22] C. Prieto, L. Calvo, Performance of the biocompatible surfactant Tween 80, for the formation of microemulsions suitable for new pharmaceutical processing, Journal of Applied Chemistry, Volume 2013 (2013), Article ID 930356, 10 pages, http://dx.doi.org/10.1155/2013/930356.

[23] D.J. McClements, Nanoparticle- and microparticle based delivery systems. Encapsulation, protection and release of active compounds, CRC Press, Boca Raton, 2015, pp. 103-105, http://dx.doi.org/10.1201/b17280-4.

[24] S. Stainmesse, A.M. Orecchioni, E. Nakache, F. Puisieux, H. Fessi, Formation and stabilization of a biodegradable polymeric colloidal suspension of nanoparticles, Colloid and Polymer Science 273 (1995) 505-511, http://dx.doi.org/10.1007/BF00656896.

[25] E. Dickinson, Hydrocolloids at Interfaces and the influence on the properties of dispersed systems, Food Hydrocolloids 17 (2003) 25-39, http://dx.doi.org/ 10.1016/S0268-005X(01)00120-5.

[26] A. Matsumoto, T. Kitazawa, J. Murata, Y. Horikiri, H. Yamahara, A novel preparation method for PLGA microspheres using non-halogenated solvent, Journal of Controlled Release 129 (2008) 223-227, http://dx.doi.org/10.1016/j.jconrel.2008.04.008.

[27] W. Chantrapornchai, F.M. Clydesdale, D.J. McClements, Influence of relative refractive index on optical properties of emulsions, Food Research International 34 (2001) 827-835, http://dx.doi.org/10.1016/S0963-9969(01)00105-3.

[28] D.J. McClements, E.A. Decker, Lipid Oxidation in oil-in-water emulsions: impact of molecular environment on chemical reactions in heterogeneous Food Systems, Journal of Food Science 65 (2000) 1270-1282, http://dx.doi.org/10.1111/j.1365-2621.2000.tb10596.x.

[29] H.Y. Chiu, M.J. Lee, H.M. Lin, Vapor-liquid phase boundaries of binary mixtures of carbon dioxide with ethanol and acetone. Journal of Chemical Engineering Data 53 (2008) 2393-2402, http://dx.doi.org/10.1021/je800371a.

[30] C. Borch-Jensen, J. Mollerup, Phase equilibria of fish oil in sub- and supercritical carbon dioxide, Fluid Phase Equilibria 138 (1997) 179-211, http://dx.doi.org/10.1016/S0378-3812(97)00155-6.

[31] J. Chrastil, Solubility of solids and liquids in supercritical gases, Journal of Physical Chemistry 86 (1982) 3016-3021, http://dx.doi.org/10.1021/j100212a041.

[32] H. Sovová, J. Jez, M. Khachaturyan, Solubility of squalane, dinonyl phthalate and glycerol in supercritical CO_2, Fluid Phase Equilibria 137 (1997) 185-191, http://dx.doi.org/10.1016/S0378-3812(97)00102-7.

[33] R. Wiebe, The binary system carbon dioxide-water under pressure, Chemical Reviews 29 (1941) 475-481, http://dx.doi.org/10.1021/cr60094a004.

[34] Spain 2011. Real Decreto 1101 /2011, de 22 de Julio, por el que se aprueba la lista positiva de los disolventes de extracción que se pueden utilizar en la fabricación de productos alimenticios y de sus ingredientes. Boletín Oficial del Estado, 30 de Agosto de 2011, 208, 94132-94137.

[35] G. Lévai, Bioproducts processing by SFEE: application for liquid and solid quercetin formulations, Dissertation, Universidad de Valladolid, Valladolid, 2016.

[36] L. Sanguansri, L. Day, Z. Zhen, P. Fagan R. Weerakkody, L. Jiang Cheng, J. Rusli, M.A. Augustin, Encapsulation of mixtures of tuna oil, tributyrin and resveratrol in spray dried powder formulation, Food & Function 4 (2013) 1794-1802, http://dx.doi.org/10.1039/c3fo60197h.

[37] J. Velasco, F. Holgado, C. Dobarganes, G. Márquez-Ruíz, Influence of relative humidity on oxidation of the free and encapsulated oil fractions in freeze-dried microencapsulated oils, Food Research International 42 (2009) 1492-1500, http://dx.doi.org/10.1016/j.foodres.2009.08.007.

[38] M.J. Choi, U. Ruktanonchai, A. Soottitantawat, S.G. Min, Morphological characterization of encapsulated fish oil with β-cyclodextrin and polycaprolactone, Food Research International 42 (2009) 989-997, http://dx.doi.org/10.1016/j.foodres.2009.04.019.

[39] V. Krtonošić, L. Dokić, P. Dokić, T. Dapčević, Effects of xanthan gum on physicochemical properties and stability of corn oil-in-water emulsions stabilized by polyoxyethylene (20) sorbitan monooleate, Food Hydrocolloids 23 (2009) 2212-2218, http://dx.doi.org/10.1016/j.foodhyd.2009.05.003.

Appendices

Appendix A:

Conventional encapsulation processes

In the following pages, the fundamentals of the main conventional encapsulation processes are explained.

- ***Interfacial polymerization***
- ***Coacervation***
- ***Solvent evaporation***
- ***Solvent diffusion***
- ***Nanoprecipitation***
- ***Salting out***
- ***Ionic gelation***
- ***Spray drying***
- ***Spray cooling/chilling***
- ***Freeze drying***
- ***Fluid bed coating***
- ***Coextrusion***
- ***Electrospinning***

Interfacial polymerization

In this process, the polymerization reaction occurs at the interface of an emulsion [1]. The core material and the monomer (isocyanate, acid chlorides or a combination of both), are dissolved in the organic phase, and dispersed in an aqueous phase to form an O/W emulsion. An initiator (usually an amine), is then added to the aqueous phase. This produces a rapid polymerization reaction at the interface, generating the capsules.

This process has not a big interest in the pharmaceutical or food industries due to the presence of residual toxic monomers and the non-biodegradability of the polymer [2]. An alternative procedure has been developed for the pharmaceutical industry. In this case, the monomer is dissolved in the continuous aqueous phase. The polymerization starts when the monomer is excited by high-energy radiation (gamma-radiation, ultraviolet or strong visible light) or by enzymatic action [1].

This process can generate nanocapsules with high encapsulation efficiency. However, the use of organic solvents and the additional washing step may hinder its industrial application [1].

Coacervation

Encapsulation takes place by deposition of the polymer around the core material [2]. To do this, the core material is first dispersed in a polymer solution. Subsequently, the deposition of the coating takes place by a variation of pH, or by the addition of a non-solvent, a salt or an incompatible polymer. Once deposition is performed, it is necessary to cure the capsule using crosslinking agents such as glutaraldehyde or transglutaminase [3].

Coacervation is an efficient, expensive and rather complex process [4]. The spheres are produced with core-shell structure, although the wall thickness is not uniform. It is difficult to generate particles in the nanoscale. Although it is possible to treat heat sensitive compounds since the process takes place at room temperature, the presence of solvents and coacervating agents on the particles limits its application.

Solvent evaporation

The wall and the core materials are dissolved in a volatile organic solvent. The organic phase is then dispersed in the aqueous phase, which contains an appropriate surfactant, to form an O/W emulsion. Once the emulsion is formed, the organic solvent is evaporated by raising temperature, under vacuum pressure or continuous stirring. The result is the creation of a suspension of solid particles that can be recovered by filtration or centrifugation [1]. Figure A.1 shows a schematic mechanism of this process. Although the concept of the process is simple, physicochemical phenomena are very complex.

The particle size can be controlled by adjusting the emulsion formulation (type and amount of dispersing agent, viscosity of the organic and aqueous phases, stirring energy, among others), and/or the operating parameters (temperature, vacuum pressure, etc.). However, limitations are imposed in the scale-up and in the high-energy requirements in homogenization [5].

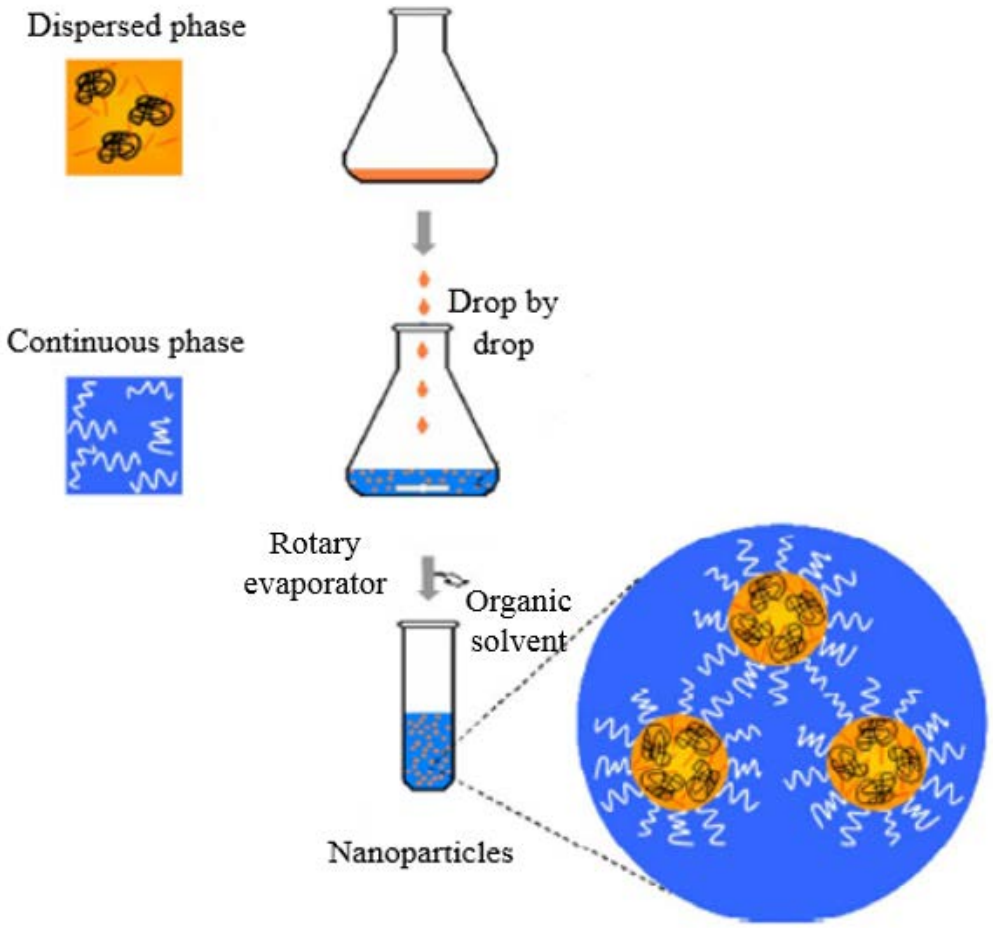

Figure A.1. Schematic mechanism of the solvent evaporation process. (Adapted from Ribeiro *et al*. [6]).

Solvent diffusion

The encapsulating polymer and the core material are dissolved in a partially water-soluble solvent, which is saturated with water to ensure the thermodynamic equilibrium between both liquids [1]. Subsequently, the organic phase is dispersed in the aqueous phase to form an emulsion. Thereafter, an excess of aqueous phase is added to produce the precipitation of the polymer by causing the diffusion of the solvent from the disperse phase to the continuous phase. Finally, the solvent is

eliminated by evaporation [7]. Figure A.2. shows an scheme of the mechanism of the process.

This technique allows obtaining particles in the nanoscale, with narrow size distribution. Capsules can be produced, and the encapsulation efficiency is high. However, the main drawbacks are the requirement of high temperatures and the use of organic solvents and high volumes of water [8].

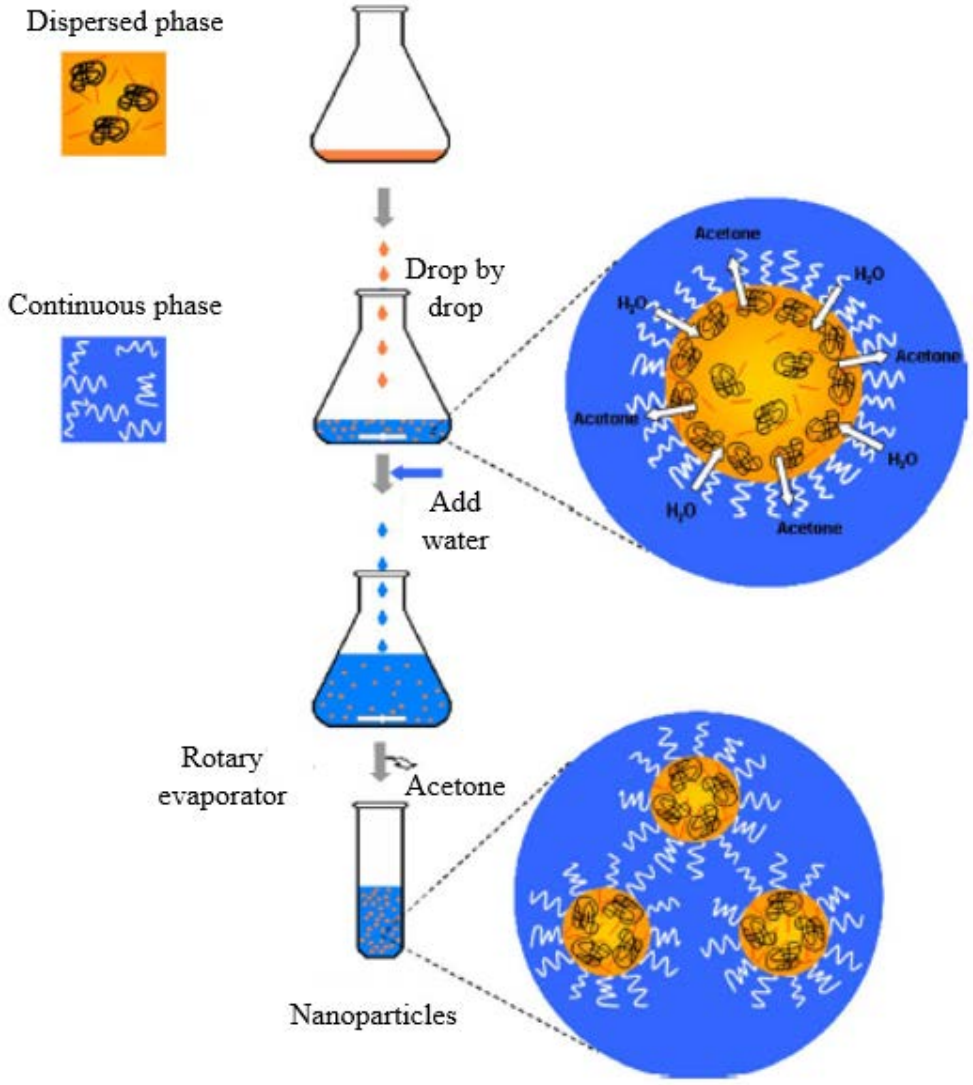

Figure A.2. Schematic mechanism of the solvent diffusion process. (Adapted from Ribeiro *et al*. [6])

Nanoprecipitation

The nanoprecipitation method is also called solvent displacement or interfacial deposition [7]. First, the polymer and the bioactive compound are dissolved in a water-miscible organic solvent (ethanol or acetone). Then, the organic phase is slowly added to the aqueous phase under moderate stirring to produce the spontaneous emulsification and the rapid diffusion of the organic solvent to the aqueous phase, provoking the polymer precipitation and the formation of a particle suspension [1].

Particle characteristics are influenced by the nature and concentration of the components of the emulsion, and by the conditions of addition of the organic phase to the aqueous phase (method of addition, injection and agitation rate) [7]. Nanoprecipitation can form capsules at the nanoscale, achieving high encapsulation efficiencies with lipophilic compounds [9]. However, the use of organic solvents is one of the main limitations of this technology.

Salting out

This method is based on the separation of a water miscible solvent from the aqueous solution via a salting out effect [8].The core and the coating material are dissolved in a water miscible organic solvent. The aqueous phase consists of water, an emulsifier and a salting out agent (sodium chloride, magnesium acetate, magnesium chloride, sucrose) [8], which provokes the immiscibility between the organic and aqueous phases. The organic phase is dispersed in the aqueous phase under vigorous stirring to form an O/W emulsion. This emulsion is diluted with a volume of water to break the stability of the emulsion and cause the diffusion of the organic solvent into the

aqueous phase, thereby inducing the formation of particles. The salting out agent can be removed by cross-flow filtration. This technique leads to high encapsulation efficiencies. However, the greatest disadvantage is the requirement of extensive particle washing steps [1].

Ionic gelation

In this process, the formation of the coating wall takes place by an ionic gelation reaction between a polysaccharide and an ion with opposite charge [2]. Sodium alginate is the most widely used polyanion. This method consists of dropping a bioactive-loaded alginate solution into an aqueous calcium chloride solution. Calcium ions diffuse into the alginate drops, forming an ionically crosslinked alginate. This membrane is insoluble in water but permeable. Particles with a diameter between 0.2 and 5 mm are obtained (known as beads). It is a simple process, it does not require extreme conditions of heat or pH, or the use of organic solvents, but the release of the bioactive is very fast (burst release) [10]. A few new processes have been proposed to facilitate the large-scale production of alginate beads [11]. Figure A.3. shows the different dripping tools available for the commercial application of this technology.

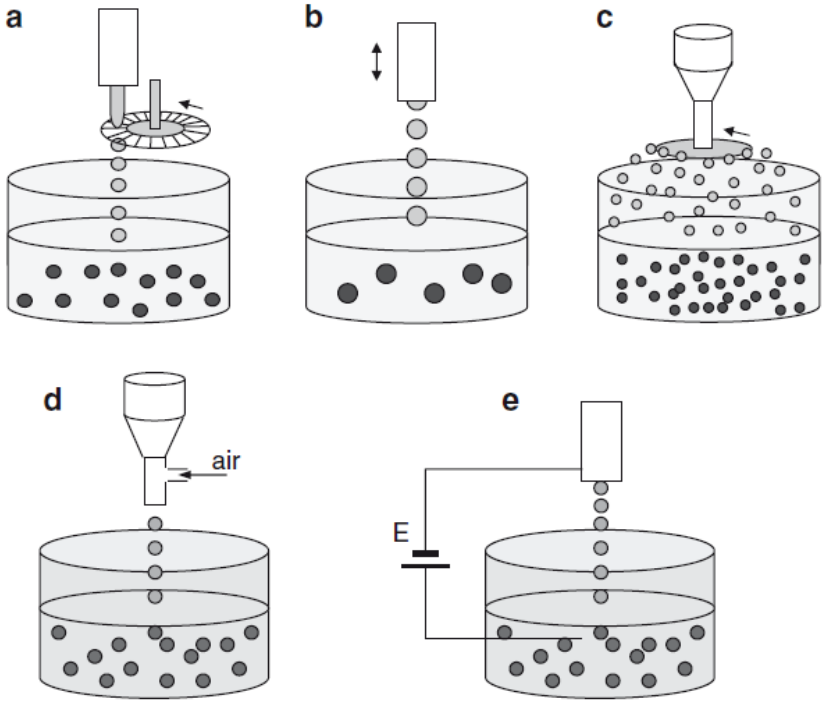

Figure A.3. Different dripping tools available for the commercial application of the ionic gelation encapsulation technology: a) jet cutter, b) vibrating nozzle, c) spinning disk, d) coaxial air-flow, e) electrostatic potential controlled nozzles [11].

Spray drying

Spray drying is an economical, flexible and fast commercial process, capable of continuous operation and produces a dry powdered product [12].

In this method, the core and the coating materials are mixed with the solvent to form a solution, an emulsion or a suspension. Then, the mixture is atomized via a nozzle or spinning wheel to form a mist of fine drops. The outlet of the nozzle is located in a chamber supplied with hot air, so that the solvent rapidly evaporates [12]. The powder particles are then separated from the drying air by means of a cyclone or a bag-filter and collected in powder form. Figure A.4. shows a scheme of the spray-drier.

Spray drying is an efficient method. The obtained particles generally have a matrix or polynuclear structure with a typical spherical shape, although fibers can also be obtained. The particle size may vary 10-400 µm. However, the porosity of the wall is high, consequently the release of the bioactive is very fast (burst release) [2].

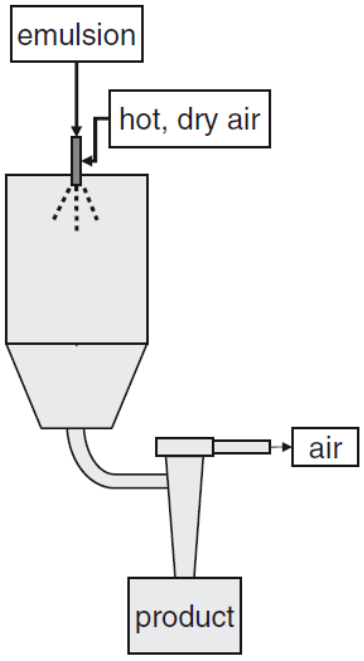

Figure A.4. Set-up of a spray-drier [11].

Spray cooling/chilling

In this method, the active ingredient is dissolved or dispersed into a molten coating material. The hot mixture is atomized into a cooled or chilled air stream, making the coating material to solidify. Waxes, fats, lipids or gelling hydrocolloids, which are solid at room temperature but meltable at reasonable temperature, are used in this process [2]. The particles obtained are matrix type or polynuclear, so some of the bioactive ingredient may be lying on the surface of the particle [13]. Particle size is

difficult to control and range between 20-200 μm. It is the least expensive encapsulation technology; however, special handling and storage conditions could be required.

Freeze drying

Freeze drying, also known as lyophilization, is a multi-stage encapsulation operation throughout the four main stages: freezing, sublimation, desorption stage and storage [5]. This method is useful for heat-sensitive compounds that would degrade under the temperatures used for spray drying. The solvent is removed from a frozen solution by vacuum sublimation, maintaining the drying chamber pressure and temperature below the triple point of the solvent. However, long processing time (>20 h), high cost (30 to 50 times higher than spray drying), the requirement of special storage and transport, and the open porous structure of the particle are the main drawbacks [14]. Currently, freeze drying is a widely used technique to remove water from particles suspensions without changing shape and structure.

Fluid bed coating

In this process, the particles are fluidized by means of a gas stream in a controlled temperature and humidity chamber. The molten or dissolved coating is atomized through a nozzle. Particles, individually accessible to the shell material, are covered by a layer that adheres to their surface [2]. The coating material precipitates or hardens by the effect of the hot/cold gas stream. To ensure the complete coating of the particles, several cycles have to be done, which enormously increases the operation

time and the consumption of the coating material [15]. Fats, emulsifiers, waxes, starches, gums, maltodextrins or synthetic polymers can be used as carriers [10]. Different types of fluid-bed coaters are shown in Figure A.5.

Optimal results are obtained with particle sizes between 50-500 microns. The main drawback of this technique is related to the particles irregularity in terms of shape and size [2].

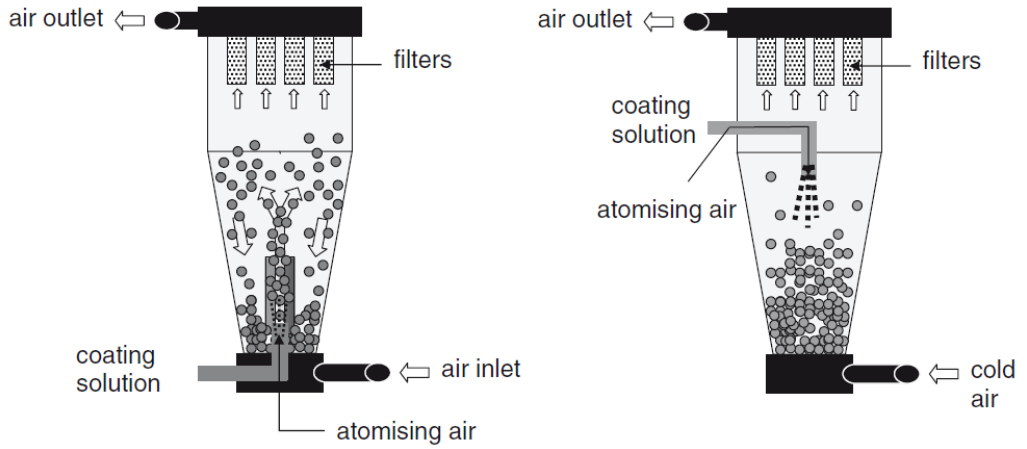

Figure A.5. Fluid bed coating set-up. Wüster's coater is shown on the left and top-spray coater is shown on the right [11].

Coextrusion

Coextrusion technology is a physical encapsulation technique used for the formation of core-shell liquid-filled particles [16]. Core materials can be water or oil soluble liquids, slurries and gases. Stationary, centrifugal, vibrating or submerged coaxial nozzles are used to form concentric droplets that harden when the outer liquid shell solidifies through congealing, gelation or precipitation. Coextrusion technology is capable of producing particles from 150 microns to 8 mm with a loading capacity up to 90%.

Electrospinning

It is an emerging method, which permits producing flat fibers, ribbon-like fibers or particles (in this particular case, this technique is also known as electrospraying) [17].

In an electrospinning process, the polymer solution is delivered to a spinneret with high voltage. The electrical potential causes the pendant droplet to elongate towards a grounded collector [18]. As the polymer solution takes flight in the air, it stretches into ultrafine fibers, or particles depending on the properties of the polymer solution (viscosity, conductivity, surface tension) and process parameters (spinneret-collector distance, temperature, humidity). The evaporation of solvent causes the polymer solution to solidify, with the fiber finally depositing on the collector as a nonwoven mat [19].

It is a rapid and easy method. Its versatility for forming submicron polymeric fibers and particles (fiber diameter 40-2000 nm), and the absence of heat have captivated a lot of interest. However, bioactive functionality may be affected by exposure to organic solvents, as well as by the electric charge and mechanical stress during the process [20].

References

[1] C. Pinto Reis, R.J. Neufeld, A.J. Ribeiro, F. Veiga, Nanoencapsulation I. Methods for preparation of drug-loaded polymeric nanoparticles, Nanomedicine: Nanotechnology, Biology, and Medicine 2 (2006) 8-21, http://dx.doi.org/10.1016/j.nano.2005.12.003.

[2] C. Remuñán López, M.J. Alonso Fernández, Microencapsulación de medicamentos, in: J.L. Vila Jato, Tecnología Farmacéutica vol. 1: Aspectos Fundamentales de los Sistemas Farmacéuticos y Operaciones Básicas, Editorial Síntesis, Madrid, 2008, pp. 577-608.

[3] M.A. Augustin, Y. Hemar, Nano- and micro-structured assemblies for encapsulation of food ingredients, Chemical Society Reviews 38 (2009) 902-912, http://dx.doi.org/10.1039/b801739p.

[4] D.T. Santos, M.AA. Meireles, Carotenoid pigments encapsulation: Fundamentals, techniques and recent trends, The Open Chemical Engineering Journal 4 (2010) 42-50, http://dx.doi.org/10.2174/1874123101004010042.

[5] P.N. Ezhilarasi, P. Karthik, N. Chhanwal, C. Anandharamakrishnan, Nanoencapsulation techniques for food bioactive components: a review, Food and Bioprocess Technology 6 (2013) 628-647, http://dx.doi.org/10.1007/s11947-012-0944-0.

[6] H.S. Ribeiro, B.S. Chu, S. Ichikawa, M. Nakajima, Preparation of nanodispersions containing β-carotene by solvent displacement method, Food Hydrocolloids 22 (2008) 12-17, http://dx.doi.org/10.1016/j.foodhyd.2007.04.009.

[7] C.E. Mora-Huertas, H. Fessi, A. Elaissari, Polymer-based nanocapsules for drug delivery, International Journal of Pharmaceutics 385 (2010) 113-142, http://dx.doi.org/10.1016/j.ijpharm.2009.10.018.

[8] D. Quintanar-Guerrero, E. Allémann, H. Fessi, E. Doelker, Preparation techniques and mechanisms of formation of biodegradable nanoparticles from preformed polymers, Drug Development and Industrial Pharmacy 24 (1998) 1113-1128, http://dx.doi.org/10.3109/03639049809108571.

[9] U. Bilati, E. Allémann, E. Doelker, Development of a nanoprecipitation method intended for the entrapment of hydrophilic drugs into nanoparticles, European Journal of Pharmaceutical Sciences 24 (2005) 67-75, http://dx.doi.org/10.1016/j.ejps.2004.09.011.

[10] S. Gouin, Microencapsulation: industrial appraisal of existing technologies and trends, Trends in Food Science & Technology 15 (2004) 330-347, http://dx.doi.org/10.1016/j.tifs.2003.10.005.

[11] N.J. Zuidam, E. Shimoni, Overview of microcapsulates for use in food products or processes and methods to make them, in: N.J. Zuidam, V.A. Nedovic (Eds.), Encapsulation Technologies for Active Food Ingredients and Food Processing, Springer, New York, 2010, pp. 3-29, http://dx.doi.org/10.1007/ 978-1-4419-1008-0_2.

[12] Z. Fang, B. Bhandari, Spray drying, freeze drying and related processes for food ingredient and nutraceutical encapsulation, in: N. Garti, D.J. McClements, Encapsulation Technologies and Delivery Systems for Food Ingredients and Nutraceuticals, Woodhead Publishing Limited, Cambridge, 2012, pp. 73-109.

[13] J.D. Oxley, Spray cooling and spray chilling for food ingredient and nutraceutical encapsulation, in: N. Garti, D.J. McClements, Encapsulation Technologies and Delivery Systems for Food Ingredients and Nutraceuticals, Woodhead Publishing Limited, Cambridge, 2012, pp. 110-130.

[14] G. Bonat Celli, A. Ghanem, M. Su-Ling Brooks, Bioactive encapsulated powders for functional foods - a review of methods and current limitations, Food and Bioprocess Technology 8 (2015) 1825-1837, http://dx.doi.org/10.1007/s11947-015-1559-z.

[15] N. Venkata Naga Jyothi, P. Muthu Prasanna, Suhas Narayan Sakarkar, K. Surya Prabha, P. Seetha Ramaiah, G.Y. Srawan, Microencapsulation techniques, factors influencing encapsulation efficiency, Journal of Microencapsulation 27 (2010) 187-197, http://dx.doi.org/10.3109/02652040903131301.

[16] Z. Knezevic, D. Gosak, M. Hraste, I. Jalsenjak, Fluid-bed microencapsulation of ascorbic acid, Journal of Microencapsulation 15 (1998) 237-352, http://dx.doi.org/10.3109/02652049809006853.

[17] S. Torres-Giner, A. Martinez-Abad, M.J. Ocio, J.M. Lagaron, Stabilization of a nutraceutical omega-3 fatty acid by encapsulation in ultrathin electrosprayed zein prolamine, Journal of Food Science 75 (2010) N69-N79, http://dx.doi.org/10.1111/j.1750-3841.2010.01678.x.

[18] L.T. Lim, Encapsulation of bioactive compounds using electrospinning and electrospraying technologies, in: C.M. Sabliov, H. Chen, R.Y. Yada, Nanotechnology and Functional Foods: Effective Delivery of Bioactive Ingredients, John Wiley & Sons, Chichester, 2015, pp. 297-317, http://dx.doi.org/10.1002/9781118462157.ch18.

[19] K. Moomand, L.T. Lim, Effects of solvent and n-3 rich fish oil on physicochemical properties of electrospun zein fibres, Food Hydrocolloids 46 (2015) 191-200, http://dx.doi.org/10.1016/j.foodhyd.2014.12.014.

[20] R. Pérez-Mariá, M.J. Fabra, J.M. Lagarón, A. López-Rubio, Use of electrospinning for encapsulation, in: V. Mittal (Ed.), Encapsulation Nanotechnologies, John Wiley & Sons, Hoboken, (2013) pp. 107-135, http://dx.doi.org/10.1002/9781118729175.ch4.

Appendix B:

Supercritical fluid encapsulation processes

In the following pages, the fundamentals of the main supercritical fluid encapsulation processes are explained.

- ***Rapid Expansion of Supercritical Solutions (RESS)***
- ***Supercritical Antisolvent Precipitation (SAS)***
- ***Particles from Gas Saturated Solutions (PGSS)***
- ***Concentrated Powder Form (CPF)***
- ***Supercritical Solvent Impregnation (SSI)***
- ***Supercritical Fluid Extraction of Emulsions (SFEE)***

Rapid Expansion of Supercritical Solutions (RESS)

In this process, the bioactive compound and the coating are first solubilized in the supercritical fluid at high pressure in the extractor. This is followed by a rapid depressurization of the solution through a heated nozzle into an expansion vessel. Decrease in supercritical fluid density due to decompression, results in loss of the solvation power, causing a rapid supersaturation. The precipitation of the coating (and the bioactive) via nucleation and/or growth leads to the formation of particles [1]. A scheme of the RESS process is shown in Figure B.1.

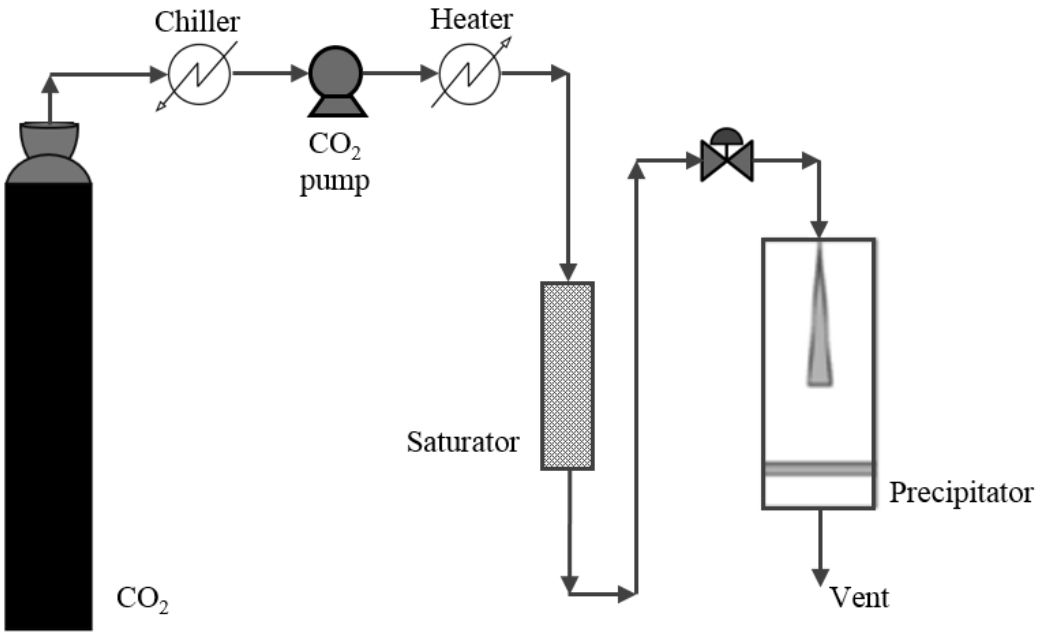

Figure B.1. Schematic diagram of the RESS process.

Particle size and particle size distribution can be controlled with process parameters (pressure, temperature, concentration, flow rate, nozzle design…). This process is able to produce very small particles with regular particle size distributions, although agglomeration between particles may happen [2]. However, since the

precipitation is extremely fast, it is very difficult to control morphology and loading of the bioactive compound in the particle [3]. RESS is an attractive process due to its simplicity, low cost and the absence of organic solvents; but it can be applied only to materials soluble in CO_2 [4].

An interesting variation of the RESS process is the RESOLV (Rapid Expansion of a Supercritical solution into a Liquid Solvent) or RESAS (Rapid Expansion of an Aqueous Solution) that consist of spraying the supercritical solution into a liquid or aqueous solvent, often containing a stabilizer, to avoid particle agglomeration [4].

RESS could also be coupled with a fluid bed coating process to encapsulate solid particles. Hence, the coating is dissolved in CO_2 and then the solution is depressurized via a nozzle at the center of the gas distributor of the fluidized bed of particles [5].

Supercritical Antisolvent Precipitation (SAS)

In this process, supercritical CO_2 is not used as solvent but antisolvent. The bioactive compound and the coating material are dissolved in an organic solvent and the solution is mixed in the precipitation chamber with CO_2. When the supercritical CO_2 dissolves in the organic solvent, the solvation power of the organic solvent is reduced because of the antisolvent effect, causing a supersaturated solution from which the coprecipitation of coating and core materials occurs [1]. A scheme of the SAS set up is shown in Figure B.2.

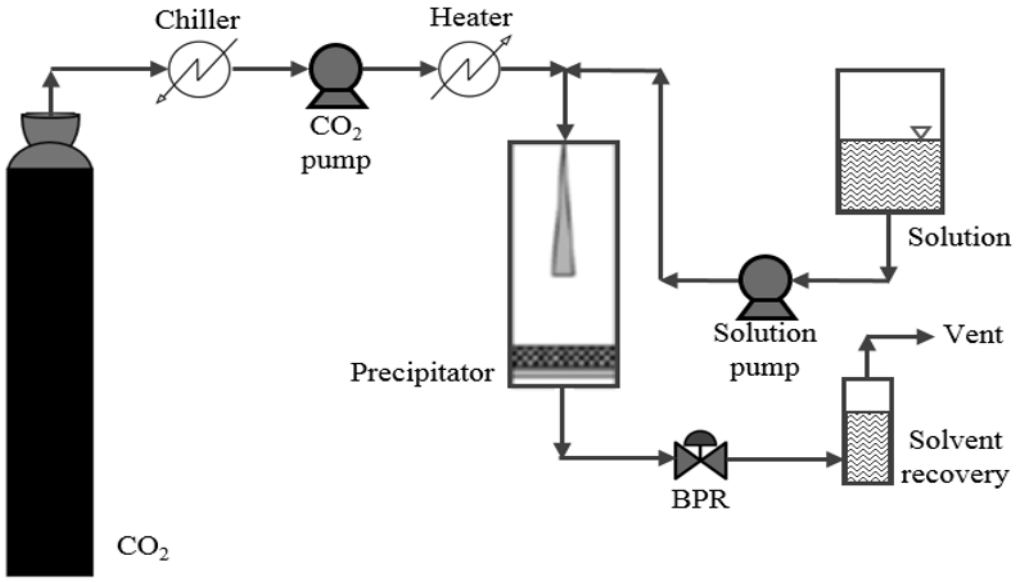

Figure B.2. Schematic diagram of the SAS process.

With respect to RESS, SAS is a much versatile technology, since it can be applied to a much wider range of materials [2]. However, the use of organic solvents is one of its major drawbacks, which may lead to organic solvent residues in the product and may difficult the purification process of CO_2. Thermolabile products can be treated with this process since mild conditions of temperature close to the critical point are usually used [4]. On the other hand, different morphologies can be obtained depending on the process temperature and the initial concentrations of core and coating materials [3].

Several variants of the SAS process have been developed which main difference is the design of the device [2]. In this sense, SEDS uses a coaxial nozzle to improve the dispersion of the solution into the antisolvent for increased mass-transfer [1]. In the case of ASES, an aerosol of solution is formed to maximize the contact area between the solution and the antisolvent [5].

In similar fashion to the RESS process, SAS can also be coupled to fluid bed coating to coat solid spherical particles of the bioactive with coating materials that are not soluble in CO_2 [5].

Particles from Gas Saturated Solutions (PGSS)

The PGSS method requires neither the bioactive compound nor the coating to be dissolved in supercritical CO_2. The supercritical fluid is dissolved into a molten or plasticized mixture of the bioactive and the coating, leading to a gas saturated solution. The high concentration of CO_2 in the liquid phase leads to a considerable reduction of melting point, viscosity and interfacial tension, helping to render substances sprayable [6]. The rapid expansion of the solution through a nozzle results in the formation of solid particles due to the intense cooling effect caused by the release of CO_2 [1]. The consumption of CO_2 in this method is lower than RESS method. In addition, no organic solvent is used in contrast with SAS technique [1]. This process can be operated in continuous mode and is easily scalable. A scheme of the process is shown in Figure B.3.

Particle size and morphology depend on polymer properties and expansion conditions. Thus, particle size control can be difficult due to the high melt viscosities, which may suppress the formation of fine particles [7]. On the other hand, depending on expansion conditions particles with a porous structure can be obtained.

PGSS process can be used to encapsulate liquid bioactive compounds [3] and it is applicable to produce particles from aqueous solutions, which in that particular case is known as PGSS-drying. In this case, the principle is the same with the only

modification that the operating conditions inside the spray tower are chosen to avoid condensation, so all the water is evaporated [1].

DELOS process is a variant of the PGSS technique. The key difference with respect to the PGSS process is the use of a liquid solvent, which enables the processing of materials that cannot be melted [2]. As well as in the previous processes, PGSS can also be coupled to fluid bed coating [5].

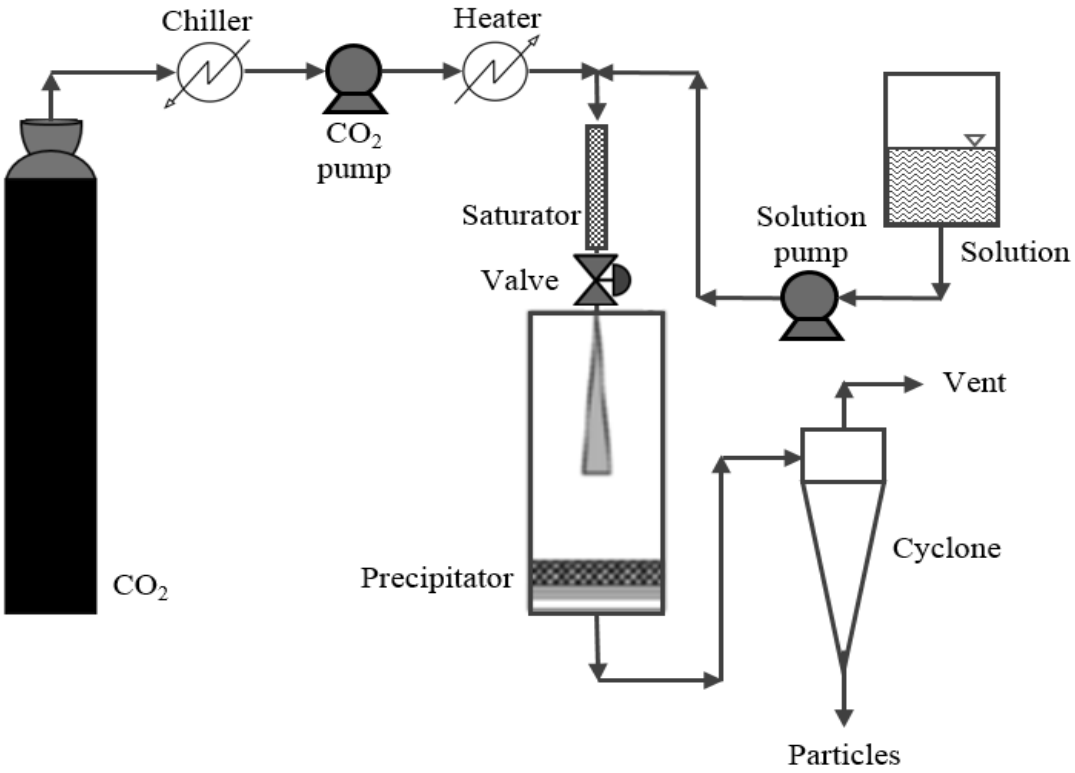

Figure B.3. Schematic diagram of the PGSS process.

Concentrated Powder Form (CPF)

The CPF technique is a continuous spray agglomeration technique that allows the production of liquid-loaded composites. The liquid to be powderized is contacted with a pressurized gas and expanded in a nozzle, generating a fine spray of liquid droplets. A solid coating material is blown into that spray by means of an inert gas. The mixing of the droplets with the stream of solid carrier, forms solid free-flowing agglomerates with loadings up to 90 % by weight [6]. Figure B.4 illustrates the flow scheme of this process.

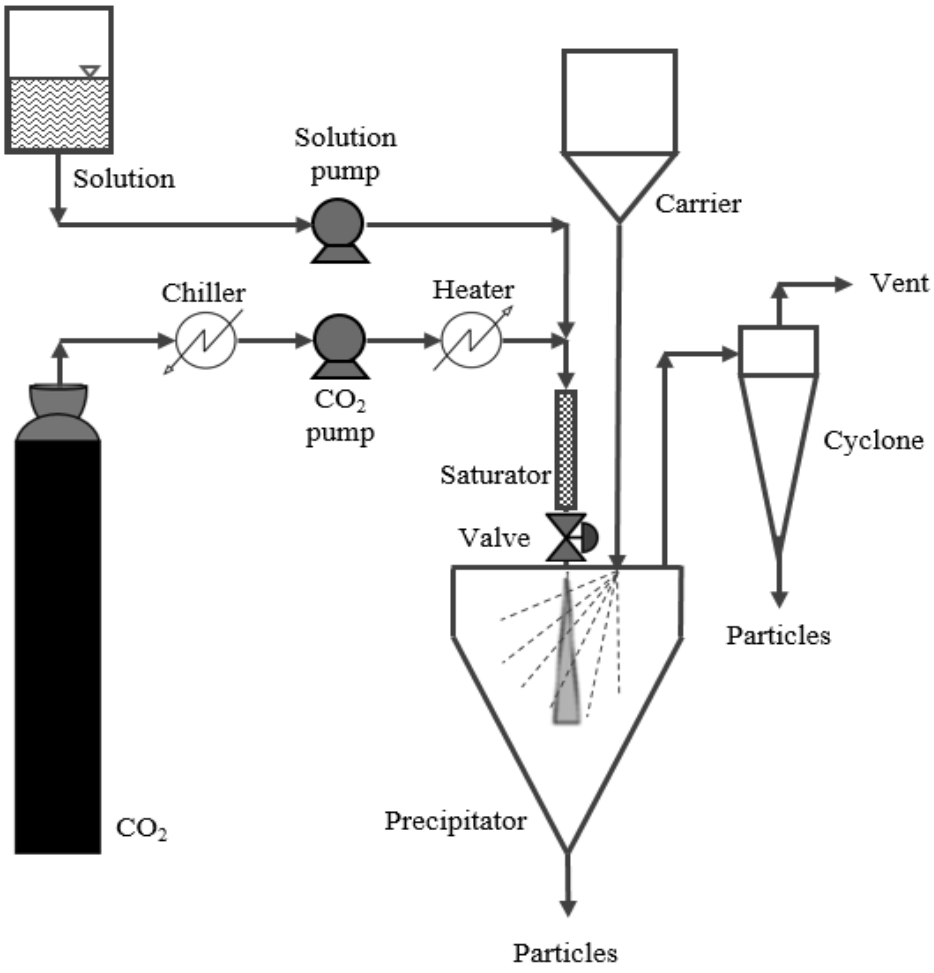

Figure B.4. Schematic diagram of CPF process.

Supercritical Solvent Impregnation

Impregnation consists of introducing the core material inside the coating polymer matrix with the aid of supercritical CO_2. Basically, the impregnation process includes three major steps: first, to expose the polymer to supercritical CO_2 for a period of time in order to alter and swell the microstructure of the polymer; second, to solubilize the core material in CO_2 and transfer the solute from the CO_2 to polymer; third, release the CO_2 in a controlled manner to trap the solutes in the polymer [3]. The scheme of the set-up is shown in Figure B.5. Drug loading depends on the rate of the depressurization step, time of impregnation, and CO_2 density [3].

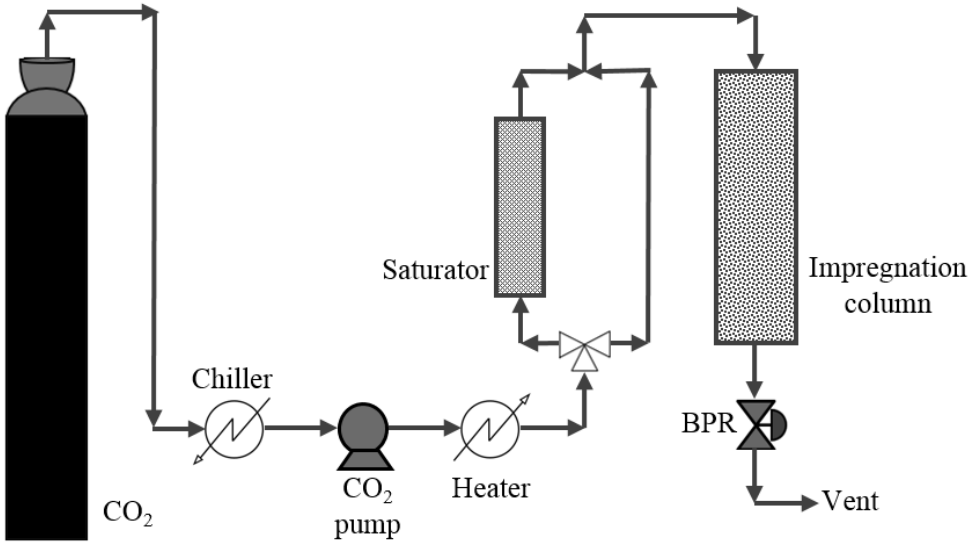

Figure B.5. Schematic diagram of the impregnation process.

Supercritical Fluid Extraction of Emulsions (SFEE)

SFEE is a combination of the conventional emulsion precipitation technology with the supercritical antisolvent processes. The basis of the SFEE process relies on the use of supercritical CO_2 to rapidly extract the organic phase of an emulsion, in which a bioactive compound and its coating polymer have been previously dissolved. By removing the solvent, both compounds precipitate, generating a suspension of particles in water. The produced particles have controlled size and morphology [8], due to the use of the emulsion and to the fast kinetics of the supercritical CO_2 extraction. Particle agglomeration in the aqueous phase is avoided since the particles are stabilized by a surfactant. In addition, this technology is very versatile. It is possible to encapsulate hydrophilic and lipophilic compounds by changing the starting emulsion. An oil in water (O/W) emulsion, water-free emulsions (O/O), different multiple emulsions (W/O/W) or suspensions, can be used to encapsulate bioactive compounds [7].

One of the key parameters of the process is the formulation of the emulsion (components, composition and preparation procedure). As the emulsion acts as a template, it must be stable and provide a suitable droplet size and structure.

So far, the process has been carried out in bubble [9], spray [8] or packed columns [10]. Figures B.6 shows the schematic set-up of a bubble column. Pressure, temperature, and emulsion and CO_2 flow rates should be selected to maximize organic solvent extraction without extracting the bioactive compound.

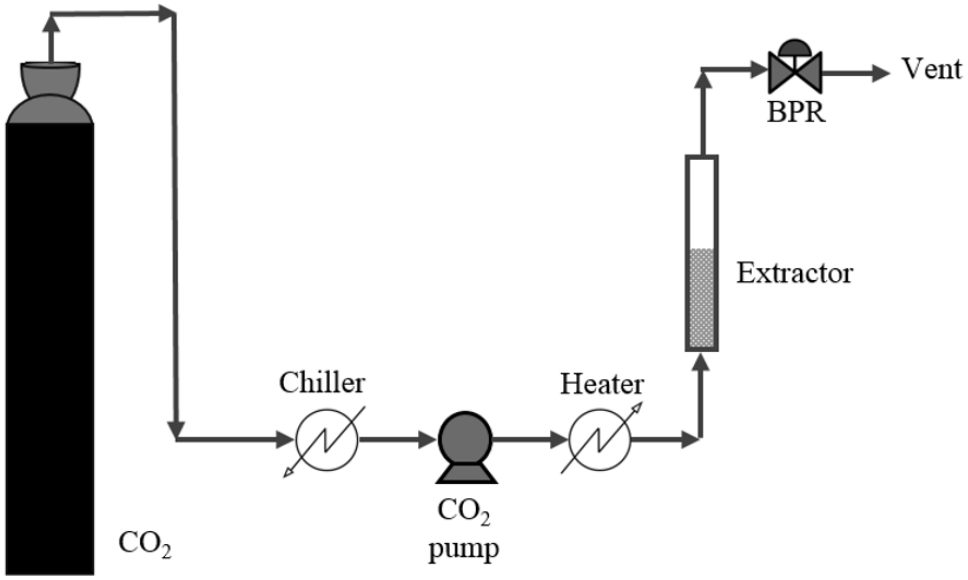

Figure B.6. Schematic set-up of the SFEE process in a bubble column.

Through this process, particles of nanometric size and controlled morphology can be obtained. However, an additional drying step may be required to obtain the particles in powder-form [7].

References

[1] M. Bahrami, S. Ranjbarian, Production of micro- and nano-composite particles by supercritical carbon dioxide, Journal of Supercritical Fluids 40 (2007) 263-283, http://dx.doi.org/10.1016/j.supflu.2006.05.006.

[2] A. Martín, M.J. Cocero, Precipitation processes with supercritical fluids: patents review, Recent Patents on Engineering 2 (2008) 9-20, https://doi.org/10.2174/187221208783478561.

[3] M.J. Cocero, A. Martín, F. Mattea, S. Varona, Encapsulation and co-precipitation processes with supercritical fluids: Fundamentals and applications, Journal of Supercritical Fluids 47 (2009) 546-555, http://dx.doi.org/10.1016/j.supflu.2008.08.015.

[4] R. Campardelli, L. Baldino, E. Reverchon, Supercritical fluids applications in nanomedicine, Journal of Supercritical Fluids 101 (2015) 193-214, http://dx.doi.org/10.1016/j.supflu.2015.01.030.

[5] J. Jung, M. Perrut, Particle design using supercritical fluids: Literature and patent survey, Journal of Supercritical Fluids 20 (2001) 179-219, http://dx.doi.org/10.1016/S0896-8446(01)00064-X.

[6] E. Weidner, High pressure micronization for food applications, Journal of Supercritical Fluids 47 (2009) 556-565, http://dx.doi.org/10.1016/j.supflu.2008.11.009.

[7] B.Y. Shekunov, P. Chattopadhyay, J. Seitzinger, Engineering of composite particles for drug delivery using supercritical fluid technology, in: S. Svenson (Ed.), Polymeric Drug Delivery II. Polymeric Matrices and Drug Particle

Engineering, ACS Symposium Series, Vol. 924, 2006, pp. 234-249, http://dx.doi.org/10.1021/bk-2006-0924.ch015.

[8] P. Chattopadhyay, R. Huff, B.Y. Shekunov, Drug encapsulation using supercritical fluid extraction of emulsions, Journal of Pharmaceutical Sciences 95 (2006) 667-679, http://dx.doi.org/10.1002/jps.20555.

[9] G. Della Porta, E. Reverchon, Nanostructured microspheres produced by supercritical fluid extraction of emulsions, Biotechnology and Bioengineering 100 (2008) 1020-1033, http://dx.doi.org/10.1002/bit.21845.

[10] G. Della Porta, R. Campardelli, N. Falco, E. Reverchon, PLGA microdevices for retinoids sustained release produced by supercritical emulsion extraction: continuous versus batch operation layouts, Journal of Pharmaceutical Sciences 100 (2011) 4357-4367, http://dx.doi.org/10.1002/jps.22647.

Curriculum Vitae

Curriculum Vitae

Cristina Prieto López

03/06/1986

Education

Chemical Engineering
Specialty: *Process Control* and *Chemical and Biochemical Processes*
University of Santiago de Compostela
February 2010

Master in Industrial Processes Engineering
Specialty: *Industrial Process Technology*
Complutense University of Madrid
July 2011

Participation in research projects

Extraction of impurities from natural polymers with supercritical mixtures
Amorim
December 2010 - July 2012
Principal Investigator: Lourdes Calvo and Albertina Cabañas

Preparation of nanomaterials with supercritical CO_2 and their application in catalysis and pharmacology (CTQ2013-41781-P)
Ministry of Economy and Competitiveness
December 2014-present
Principal Investigator: Albertina Cabañas and Concepción Pando García Pumarino

Research stays

Nutraceuticals and Controlled Delivery Lab
Instituto de Biologia Experimental e Tecnológica (IBET) and
Instituto de Tecnologia Química e Biológica António Xavier (ITQB).
Universidade Nova de Lisboa (Portugal).
2015 3.5 months
Topic: "*Scale-up of the supercritical fluid extraction of emulsions (SFEE) technology to produce nanoparticles with application in the food and pharmaceutical industries*"

Publications

C. Prieto, L. Calvo, ***The encapsulation of low viscosity omega-3 rich fish oil in polycaprolactone by supercritical fluid extraction of emulsions***, (submitted for publication)

C. Prieto, L. Calvo, C.M.M. Duarte, ***Continuous supercritical fluid extraction of emulsions to produce nanocapsules of vitamin E in polycaprolactone***, Journal of Supercritical Fluids 124 (2017) 72-79, http://dx.doi.org/10.1016/j.supflu.2017.01.014.

C. Prieto, C.M.M. Duarte, L. Calvo, ***Performance comparison of different supercritical fluid extraction equipments for the production of vitamin E in polycaprolactone nanocapsules by supercritical fluid extraction of emulsions***, Journal of Supercritical Fluids 122 (2017) 70-78, http://dx.doi.org/10.1016/j.supflu.2016.11.015.

C. Prieto, L. Calvo, ***Supercritical fluid extraction of emulsions to nanoencapsulate vitamin E in polycaprolactone***, Journal of Supercritical Fluids 119 (2017) 274-282, http://dx.doi.org/10.1016/j.supflu.2016.10.004. **Editor-in-Chief's Featured Article, January 2017.**

M. Viguera, A. Marti, F. Masca, C. Prieto, L. Calvo, ***The process parameters and solid conditions that affect the supercritical CO_2 extraction of the lipids produced by microalgae***, Journal of Supercritical Fluids 113 (2016) 16-22, http://dx.doi.org/10.1016/j.supflu.2016.03.001.

C. Prieto, L. Calvo, ***Performance of the biocompatible surfactant Tween 80, for the formation of microemulsions suitable for new pharmaceutical processing***, Journal of Applied Chemistry 2013 (2013) 930356, http://dx.doi.org/10.1155/2013/930356.

C. Prieto, ***Nanoencapsulation of liquid lipophilic bioactive compounds by supercritical fluid extraction of emulsions***, in: T. Gamse (Ed.) ESS-HPT 2016 The European Summer School in High Pressure Technology, Technischen Universität Graz, 2016, pp. 35-38, http://dx.doi.org/10.3217/978-3-85125-479-2, ISBN: 978-3-85125-479-2.

C. Prieto, L. Calvo, ***Supercritical fluid extraction of emulsions for the production of vitamin E nanoencapsulates***, Bioencapsulation Innovations - Bioencapsulation Research Group, September 2013, 14-15 (http://bioencapsulation.net/index2-select-newsletter-nl-BI_2013_09.html).

Congresses

Continuous production of vitamin E in polycaprolactone nanocapsules by supercritical fluid extraction of emulsions and process simulation with Aspen Plus

C. Prieto, L. Calvo, C.M.M. Duarte

EMSF 2017, 16th European Meeting on Supercritical Fluids. Lisbon (Portugal), 2017 Oral communication

Nanoencapsulation of ω-3 rich fish oil in polycaprolactone by supercritical fluid extraction of emulsions

C. Prieto, L. Calvo

EMSF 2017, 16th European Meeting on Supercritical Fluids. Lisbon (Portugal), 2017 Poster

Performance comparison of different supercritical fluid extraction equipments for nanoparticles production by SFEE

C. Prieto, L. Calvo

EMSF 2016, 15th European Meeting on Supercritical Fluids. Essen (Germany), 2016

Oral communication

Supercritical fluid extraction of emulsions for the production of vitamin E nanoencapsulates

C. Prieto, L. Calvo

VII Reunión de Expertos en Tecnologías de Fluidos Comprimidos (FLUCOMP 2014). Barcelona (Spain), 2014

Oral communication

Supercritical CO_2 extraction of the lipids produced by microalgae Chlorella protothecoides under heterothrophic growth

M. Viguera, A. Marti, C. Prieto, A. Martín, J. Casas, L. Calvo

X International Conference on Renewable Resources & Biorefineries.

Valladolid (Spain), 2014

Oral communication

Heterotrophic growth of microalgae Chlorella Prototecoides for lipid production using wastes

A. Martín, A. Marti, M. Viguera, J. Casas, C. Prieto, L. Calvo

X International Conference on Renewable Resources & Biorefineries. Valladolid (Spain), 2014

Poster

Supercritical fluid extraction of emulsions for the production of vitamin E nanoencapsulates

C. Prieto, L. Calvo

XXI International Conference on Bioencapsulation. Berlin (Germany), 2013

Oral communication

Formación y estabilidad de emulsiones con surfactantes biocompatibles para aplicaciones en nanotecnología

C. Prieto, J. Roland, L. Calvo

VI Reunión de Expertos en Tecnologías de Fluidos Comprimidos (FLUCOMP 2012). Madrid (Spain), 2012

Poster

Formation and stability of macro and microemulsions with a biocompatible surfactant

C. Prieto, L. Calvo

9th Green Chemistry Conference. An international event.

Alcalá de Henares (Spain), 2011

Poster

Courses, seminars & workshops

ESS-HPT 2016. "The European Summer School in High Pressure Technology"
University of Maribor (Slovenia) and University of Graz (Austria)
July 3-17, 2016.

Eudragit & Eudraguard Advanced Workshop
Evonik Industries
May 18-19, 2016

Winesense Spring School
High Pressure Processes Group, University of Valladolid
April 18-21, 2016

7th Training School on Microencapsulation
Bioencapsulation Research Group
February 23-26, 2015

Innovations in Encapsulation 2014
Formulation Science & Technology Group, Royal Society of Chemistry, IChemE, Ashland, P&G
December 12, 2014

Analysis of Industrial Risks in Chemical and Petrochemical Plants
IMAES, University of Castilla-La Mancha
February 14 – March 14, 2014

Practical Course in Process Engineering Design
IMAES, University of Castilla-La Mancha
March 17 – April 17, 2014

Workshop of Nanotechnology in the Food Industry
University of Burgos
September 27, 2012

International Symposium: Drugs, Nanomedicine and Biomaterials: A common goal
Royal Academy of Pharmacy and Areces Foundation
April 24-25, 2012

Green Product Design
University of Valladolid
May 27-31, 2011

Workshop on Design and Execution of Industrial Installations
University of Santiago de Compostela
July 2010

Teaching activity

Collaboration in teaching activities

Separation Processes
BSc in Chemical Engineering, Complutense University of Madrid
Academic year: 2015/2016, 20 h.

Separation Processes II
BSc in Chemical Engineering, Complutense University of Madrid
Academic years: 2014/2015 and 2015/2016, 30 h.

Advanced Separation Processes
Master in Chemical Engineering, Complutense University of Madrid
Academic years: 2014/2015 and 2015/2016, 30 h.

Thermal Engineering
BSc in Chemical Engineering, Complutense University of Madrid
Academic year: 2015/2016, 20 h.

Fundamentals in Chemical Engineering
BSc in Biochemistry, Complutense University of Madrid
Academic year: 2014/2015, 20 h.

Publications

L. Calvo, C. Prieto, ***The teaching of enhanced distillation processes using a commercial simulator and a project based learning approach***, Education for Chemical Engineers Journal 17 (2016) 65-74, http://dx.doi.org/10.1016/j.ece.2016.07.004.

C. Prieto, L. Calvo, ***Simulación mediante Aspen Plus de un proceso de destilación reactiva para la producción de MTBE***, in: P. Marzal Doménech (Ed.) CIDIQ, II Congreso de Innovación Docente en Ingeniería Química, Coddiq & Universitat de Valéncia, Valencia, 2014, pp.54, ISBN: 978-84-370-9271-3.

C. Prieto, L. Calvo, ***Simulación en Aspen Plus del fraccionamiento del sistema acetona-metanol mediante procesos de destilación avanzada***, in: P. Marzal Doménech (Ed.), CIDIQ, II Congreso de Innovación Docente en Ingeniería Química, Coddiq & Universitat de Valéncia, Valencia, 2014, pp.117, ISBN: 978-84-370-9271-3.

C. Prieto, L. Calvo, ***The teaching of advanced separation processes using the chemical process simulator Aspen Plus***, in: P. Membiela, N. Casado, M.I. Cebreiros (Eds.), Presente y futuro de la docencia universitaria, Educación Editora, Ourense, 2016, pp. 383-388, ISBN: 978-84-15524-28-1.

Congresses

The teaching of advanced separation processes using the chemical process simulator, Aspen Plus
C. Prieto, L. Calvo
IV Congreso Internacional de Docencia Universitaria. Vigo (Spain), 2015
Oral communication

Simulación mediante Aspen Plus de un proceso de destilación reactiva para la producción de MTBE

C. Prieto, L. Calvo

II Congreso de Innovación Docente en Ingeniería Química. Valencia (Spain), 2014

Oral communication

Simulación en Aspen Plus del fraccionamiento del sistema acetona-metanol mediante procesos de destilación avanzada

C. Prieto, L. Calvo

II Congreso de Innovación Docente en Ingeniería Química. Valencia (Spain), 2014

Poster

Honors & awards

"Emprendedor Universitario UCM", in the category of Projects of Technological base, University Complutense of Madrid, V edition.

"Winner of the Best Contributions" at the XXI International Conference on Bioencapsulation" held August 2013 in Berlin (Germany), for the oral communication: "Supercritical fluid extraction of emulsions for the production of vitamin E nanoencapsulates".

UCM predoctoral grant (BE43/11) and ***UCM mobility grant*** (EB64/15).

One of the five best academic records of the XII promotion of Chemical Engineering at the University of Santiago de Compostela

Business practice

Corporación del Noroeste: Grupo Cimpor

June- September 2008, 500 h.

Languages

Spanish	Native proficiency
Galician	Native proficiency
English	Level C1-CAE. University of Cambridge (2013)
French	Level C1. Ministère de l'Éducation Nationale. République Française (2013)
Italian	Elementary proficiency. University of Santiago de Compostela (2006)
Portuguese	Elementary proficiency